Mechanisms of Resistance to MAPK Pathway Inhibition in RAS-Mutant Cancers

Mechanisms of Resistance to MAPK Pathway Inhibition in *RAS*-mutant Cancers

A dissertation presented

by

Belinda Wang

to

The Division of Medical Sciences

in partial fulfillment of the requirements

for the degree of

Doctor of Philosophy

in the subject of

Biological and Biomedical Sciences

Harvard University

Cambridge, Massachusetts

April 2016

Mechanisms of Resistance to MAPK Pathway Inhibition

in *RAS*-mutant Cancers

Abstract

The *RAS* family of genes are among the most frequently mutated genes in human cancers, including nearly all pancreatic cancers, ~40% of colorectal cancers, and ~30% of lung cancers. Although most *RAS*-mutant cancers depend on RAS signaling for proliferation and survival, direct RAS inhibitors have not yet been developed for clinical use. An alternative approach to treating *RAS*-mutant cancers is to inhibit RAS effector pathways, such as the RAS-RAF-MEK-ERK (MAPK) pathway. However, while some patients with *RAS*-mutant cancers benefit clinically from MAPK pathway inhibition (MAPKi), most do not respond to this regimen. Moreover, of the patients who do respond, nearly all progress to secondary therapeutic resistance.

In this work, we applied systematic gain- and loss-of-function (GOF and LOF) screening approaches to identify modifiers of MAPK pathway dependence. Using *RAS*- or *BRAF*-mutant pancreatic and lung cancer cell lines, we performed a genome scale open reading frame (ORF) screen and six genome scale CRISPR-Cas9 knockout screens to investigate mechanisms of resistance to MEK or BRAF inhibition. We found that the most potent GOF mediators of resistance were overexpression of components of the RTK-RAS-MAPK pathway, which restored MAPK signaling. Contrastingly, the majority of LOF events that mediated resistance to MAPKi were not direct regulators or

effectors of the MAPK pathway. From our LOF screens, we identified KEAP1 and CIC as generalizable modulators of resistance to MAPKi in *RAS*-mutant cancers. We found that *KEAP1* deletion mediates resistance through mechanisms orthogonal to the MAPK pathway, such as reducing oxidative stress and promoting anabolic metabolism. Conversely, CIC loss promotes resistance by partially restoring the transcriptional pathway downstream of ERK.

Understanding mechanisms of intrinsic resistance can enable the identification of predictive biomarkers that improve patient selection for targeted therapy. In addition, identifying mechanisms of acquired resistance can inform the development of novel agents or combination therapy strategies. Our studies highlight the ability of systematic and comprehensive *in vitro* functional screens to identify clinically relevant mediators of resistance and to provide novel insights into well-studied pathways. While we selected specific genes for detailed mechanistic studies, other genes that were identified from our screens may contribute additional biological insights.

Table of Contents

List of Figures

List of Tables

Acknowledgements

I have received invaluable support and guidance from many people. Tom Rapoport, Sol Schulman, Len Zon, and Charles Kaufman have offered me advice and encouragement since I first delved into scientific research during college and medical school. My advisor, Bill Hahn, has been an exceptional role model. He has been unfailingly supportive of diverse endeavors, granting me the freedom and resources to explore different projects while offering constructive criticism and clear feedback. Bill is unfailingly thorough and rational, with a positive attitude and reassuring presence that has been indispensible to making me a more confident, creative, and resilient scientist.

Being a member of the Hahn lab has been a wonderful experience, and I feel lucky to have interacted with and befriended such inspiring, talented, and kind people. It has been a privilege to work with Andy Aguirre, who spent an immense amount of time and energy teaching me experimental techniques and, more importantly, how to think like a scientist. He is always available to discuss ideas and give advice, and I am grateful for the unwavering support he has given me over the years. As I began investigating therapeutic resistance, I have had the pleasure of working with Elsa Beyer Krall, who has helped me become a more thoughtful and rigorous scientist. We have had countless interesting and inspiring conversations, and I feel fortunate to have had the opportunity to work closely with her.

I would also like acknowledge Eejung Kim, a fellow graduate student with whom I have had innumerable productive, commiserating, and amusing conversations over the years; and David Takeda, an immensely patient and creative scientist who took me under his wing when I was rotating in the lab. Similarly, I would like to thank Yaara

Zwang, Mik Rinne, William Kim, Andy Hong, Andrew Giacomelli, Xiaoxing Wang, Diane Shao, Sefi Rosenbluh, Barbara Weir, Nikki Spardy, Joyce O'Connell, and Nina Ilic, who have always availed themselves to discuss scientific ideas or offer their expertise since I joined the Hahn lab. I have also enjoyed the conversations I have had with newer lab members, including Gabe Sandoval, Sri Raghavan, Ji Li, Daisy Dai, Seav Huong Ly, and Mihir Doshi, who have infused the lab with their creativity and energy.

Outside of the Hahn lab, I have worked with wonderful collaborators. I learned much from members of the Genetic Perturbation Platform, including Glenn Cowley, John Doench, Federica Piccioni, Mukta Bagul, Mudra Hedge, and David Root. In addition, I appreciate the enriching discussions and advice I received from Hans Widlund. I would also like to thank the members of the Broad Cancer Program – particularly Zuzana Tothova, Mimi Bandopadhayhay, Elizabeth Stover, Quinn Sievers, Steven Corsello, Franklin Huang, Eran Hodis, and Tanaz Sharifnia – for their camaraderie, company, and insights.

I would like to recognize the members of my Dissertation Advisory Committee, Drs. Levi Garraway, Rameen Beroukhim, and Nabeel Bardeesy. Their insightful suggestions and encouragement were instrumental in moving these projects forward. I would also like to thank Drs. Robert Weinberg, Peter Hammerman, Kevin Haigis, and Levi Garraway for their willingness to serve on my Dissertation Defense Committee.

Finally, I would like to thank my family and friends for their constant support and encouragement. Throughout the years, they have been there to commiserate and laugh over failures and to celebrate even the smallest successes. I am grateful for the uplifting conversations and for the joy that they have brought me.

Abbreviations

AML	Acute myeloid leukemia
AP1	Activator protein 1
APC	Adenamatous polyposis coli
APT	Acyl-protein thioesterase
ATF	Activating transcription factor
BRAFi	BRAF inhibition
BSO	Buthionine sulfoximine
Cas9	CRISPR associated protein 9
cBioPortal	cBio Cancer Genomics Portal
CCND1	Cyclin D1
cDNA	Complementary DNA
CIC	Capicua transcriptional repressor
CML	Chronic myelogenous leukemia
COSMIC	Catalog of Somatic Mutations in Cancer
CRC	Colorectal cancer
CRISPR	Clustered regularly interspaced short palindromic repeats
DCFDA	2',7'-dichlorofluorescin diacetate
EGFR	Epidermal growth factor receptor
EGFRi	EGFR inhibitor
ERKi	ERK inhibitor
ETS	E26 transformation-specific
FTase	Farnesyltransferase
FTI	Farnesyl transferase inhibitor
GAP	GTPase activating protein
GeCKO	Genome scale CRISPR knockout
GEF	Guanine nucleotide exchange factor
GEMM	Genetically engineered mouse model
GGTase	Geranylgeranyltransferase
GOF	Gain-of-function
GPCR	G protein-coupled receptor
GSH	Glutathione (reduced)
GSSG	Glutathione (oxidized)
HAT	Histone acetyltransferase
HRAS	Harvey rat sarcoma viral oncogene homolog
ICGC	International Cancer Genome Consortium
ICMT	Isoprenylcysteine carboxyl methyltransferase
IGF1R	Insulin-like growth factor receptor
INSR	Insulin receptor
KEAP1	Kelch-like ECH associated protein 1
KO	Knockout
KRAS	Kirsten rat sarcoma viral oncogene homolog
LOF	Loss-of-function
MAF	Masculoaponeurotic fibrosarcoma
MAPK	Mitogen activated protein kinase

MAPKi	MAPK pathway inhibition
MEKi	MEK inhibition
MRP	Multidrug resistance-associated protein
NAC	N-acetyl cysteine
NADPH	Nicotinamide adenine dinucleotide phosphate
NFE2L2/NRF2	Nuclear factor (erythroid-derived 2)-like 2
NGS	Next-generation sequencing
NRAS	neuroblastoma RAS viral oncogene homolog
NSCLC	Non-small cell lung cancer
ORF	Open reading frame
p-ERK	Phospho-ERK1/2
PAT	Palmitoyl acyltransferase
PDE6δ	Phosphodiesterase 6 delta subunit
PDGFR	Platelet-derived growth factor receptor
PDK1	Phosphoinositide-dependent kinase 1
PDX	Patient-derived xenograft
PI3K	Phosphatidylinositol 3-kinase
PIP2	Phosphatidylinositol-4,5-bisphosphate
PIP3	Phosphatidylinositol-3,4,5-triphosphate
q-PCR	Quantitative PCR
RAL	RAS-like GTPase
RALBP1	RalA binding protein 1
RALGDS	RAL guanine nucleotide dissociation stimulator
RBD	RAS binding domain
RCE1	RAS converting enzyme
RGL	RALGDS-like gene
RNAseq	RNA sequencing
ROS	Reactive oxygen species
RTK	Receptor tyrosine kinase
sgRNA	Short guide RNA
SH2	Src homology 2
shRNA	Short hairpin RNA
siRNA	Small interfering RNA
SPRED	SPRY-related proteins with an EVH1 domain
TCGA	The Cancer Genome Atlas
TIDE	Tracking of Indels by DEcomposition
VEGFA	Vascular endothelial growth factor A
WGS	Whole genome sequencing

CHAPTER ONE

Introduction: Oncogenic RAS and resistance to targeted therapy

1.1 Overview

The *RAS* family of genes (*KRAS, NRAS,* and *HRAS*) are frequently mutated in human cancers, including nearly all pancreatic cancers, ~50% of colorectal cancers, ~30% of lung cancers, and ~30% of melanomas. *RAS* mutations are associated with poor prognosis, and are used to exclude patients from treatment with some targeted therapies. Most *RAS*-mutant cancers require RAS signaling for continued proliferation and survival. This phenomenon, termed “RAS addiction,” makes RAS an appealing target for therapeutic intervention. Unfortunately, pharmacologic approaches to directly target RAS proteins have not yet succeeded in clinic.

An alternative approach to target *RAS*-mutant cancers is to inhibit RAS effector pathways. One of the major signaling pathways downstream of RAS is the RAF-MEK-ERK mitogen activated protein kinase (MAPK) pathway. BRAF and MEK inhibitors are currently being tested in clinical trials for *RAS*-mutant pancreatic cancer, lung cancer, colorectal cancer, and melanoma. Early clinical data of the allosteric MEK1/MEK2 inhibitor trametinib is encouraging, achieving stable disease or partial response in a subset of patients with *RAS*-mutant pancreatic cancer or lung cancer. Although dose escalation of MEK inhibitors is limited by cutaneous and gastrointestinal toxicity, these early clinical studies support the importance of MEK as a key downstream mediator of the cellular effects of oncogenic RAS in cancer cells.

While some patients with *RAS*-mutant cancers achieve significant clinical benefit from MEK inhibition, most do not respond to this regimen. In addition, of the patients who do initially respond to therapy, nearly all progress to therapeutic resistance. Prior studies have found that a major mode of intrinsic or acquired resistance to RAF or MEK

inhibitor monotherapy in *RAS*-mutant cancers is reactivation of the RTK-RAS-MAPK pathway. However, further systematic functional characterization is necessary to broaden our understanding of mechanisms of resistance to MAPK pathway inhibition in *RAS*-mutant cancers. Understanding the molecular mechanisms of intrinsic and acquired resistance is critical to providing improved therapy. Identifying genetic alterations that promote resistance to MEK inhibition may suggest biomarkers for patient stratification, inform novel combination therapies, and increase our understanding of oncogenic RAS signaling.

Recent technological advances have provided the means to perform comprehensive gain- and loss-of-function (GOF and LOF) screens in in mammalian cells. Expression libraries enable GOF experiments to study the effects of gene overexpression. Complementary LOF studies can be conducted using clustered regularly interspaced short palindromic repeats (CRISPR)-Cas9 libraries. In this thesis, we systematically identify mechanisms of resistance to MAPK pathway inhibitor therapy in *RAS*-mutant cancers. We nominate biomarkers of intrinsic and acquired resistance to MAPK pathway inhibitor therapy and demonstrate how loss-of-function screens can contribute novel insights into well-studied pathways.

1.2 The RAS pathway

1.2.1 RAS discovery

The concept of cancer as a disease that arises from alterations in somatic genes originated from the study of cancer-inducing retroviruses isolated from animals, such as the Harvey[1] and Kirsten[2] murine sarcoma viruses. Surprisingly, the tumorigenic

sequences of these oncogenic viruses were found to have originated from the host rat genome[3,4]. These oncogenic sequences were termed *ras* (rat sarcoma). The first human oncogenes were identified by transforming NIH-3T3 mouse fibroblasts with genomic DNA isolated from human cancer cell lines[5-9]. The isolated transforming genes were found to be human counterparts of the *ras* genes previously identified in the Harvey and Kirsten sarcoma viruses, and were accordingly named *HRAS* and *KRAS*[10-12]. Subsequently, a novel human transforming gene was identified and found to be a third member of the *RAS* gene family, designated *NRAS* for its identification from neuroblastoma cells[13,14].

The three *RAS* proto-oncogenes (*HRAS, KRAS,* and *NRAS)* encode four distinct but highly homologous ~21 kDa RAS proteins: HRAS, NRAS, KRAS4A and KRAS4B, where KRAS4A and KRAS4B are alternative splice variants of the *KRAS* gene[15]. Here, 'RAS' will be used to refer generally to all isoforms.

1.2.2 RAS regulators

RAS proteins function as transducers of mitogenic signaling that link cell surface receptors to intracellular effector pathways[16-18] (**Figure 1-1**). External growth factors such as epidermal growth factor (EGF) induce cell proliferation by binding to receptor tyrosine kinases (RTKs) at the cell surface[19,20]. RAS was established as a downstream effector of RTK signaling when it was discovered that microinjection of a monoclonal antibody against RAS into cells was sufficient to abrogate oncogenic RTK signaling[18].

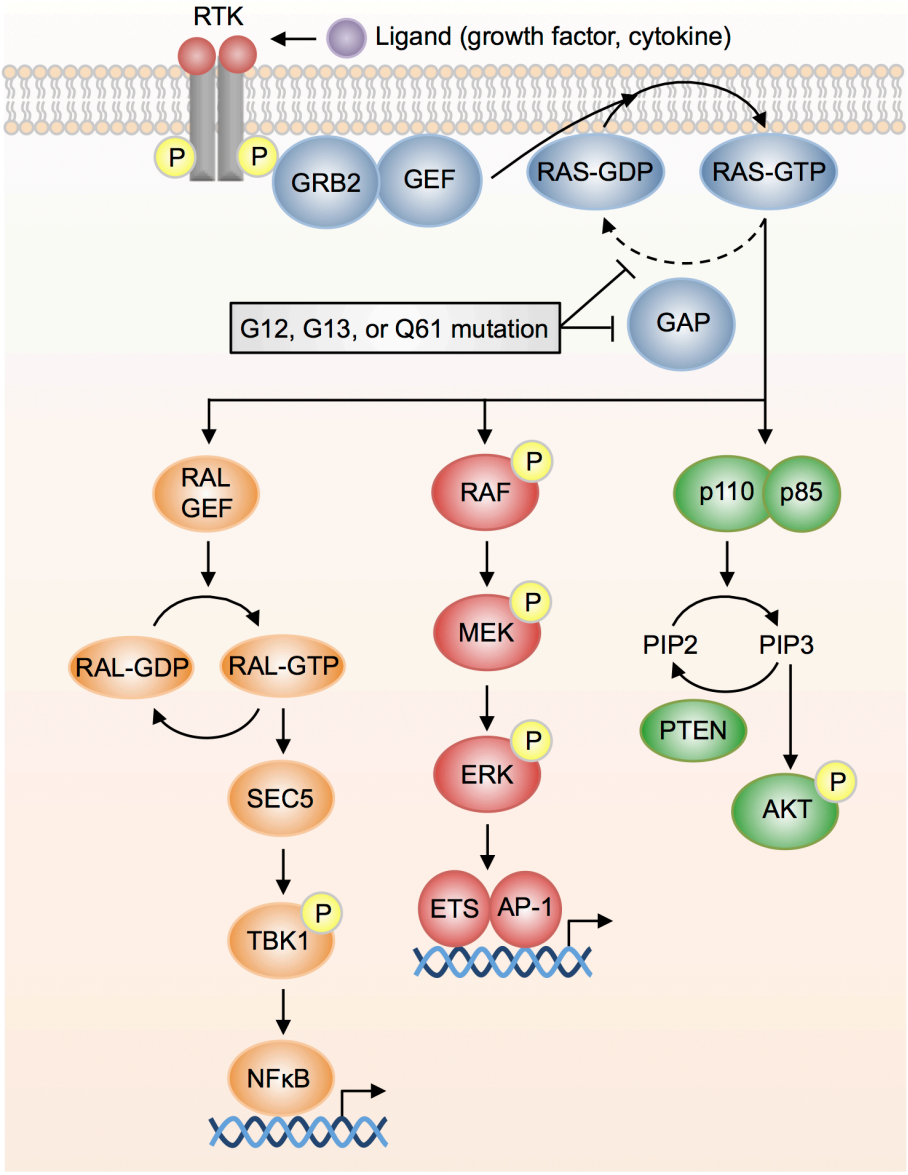

Figure 1-1. The RAS pathway. RTKs are activated by extracellular ligand binding, which induces dimerization and trans-phosphorylation of intracellular tyrosine residues. The adaptor protein GRB2 binds to the phospho-tyrosine site on RTKs and to cytosolic GEFs. RAS is activated by GEFs and inactivated by GAPs. RAS mutations in residues G12, G13, or Q61 impair intrinsic and GAP-stimulated GTPase activity. Key RAS effectors include the MAPK, PI3K, and RAL-GEF pathways.

RTKs are large glycoproteins with several conserved domains, including an extracellular ligand-binding domain, a transmembrane region, and an intracellular tyrosine-kinase domain. The epidermal growth factor receptor (EGFR) and EGFR family members ERBB2, ERBB3, and ERBB4 were the first described RTKs. Subsequently, other RTKs including the insulin receptor (INSR), insulin-like growth factor receptor (IGF1R), platelet-derived growth factor receptor (PDGFR), and KIT were identified. Thus far, over 50 RTKs have been identified, and many have been found to induce cellular proliferation when activated in cancer[21].

Signal transduction between RTKs and RAS is mediated by cytosolic adaptor proteins such as GRB2, CRKL, and IRS1. These adaptor proteins contain a Src homology 2 (SH2) domain that recognizes the tyrosine phosphorylated sites on RTKs as well as two SH3 domains that recognize proline-rich sequences on cytosolic guanine nucleotide exchange factors (GEFs)[22-30]. This RTK-adaptor protein-GEF interaction promotes RAS activation by recruiting the normally cytosolic GEFs to the plasma membrane where RAS is located[31,32].

RAS are guanine nucleotide-binding proteins[33,34] that cycle between active and inactive conformations conferred by GTP and GDP binding, respectively[35,36]. Under physiologic conditions, the transition between RAS GTP- and GDP-bound states is regulated by GEFs and GTPase-activating proteins (GAPs). GEFs, such as SOS1, SOS2, and RASGFR[37-39], accelerate the release of GDP from RAS, enabling the more abundant GTP to bind in its place. On the other hand, GAPs, such as p120[40,41] and NF1[42-45], accelerate RAS GTPase activity over 200-fold[46]. The most common oncogenic RAS mutations abrogate its interaction with GAPs[46,47] and reduce intrinsic RAS GTPase

activity ~10-fold[48-51], leading to the accumulation of active GTP-bound RAS (discussed further in Chapter 1.2.5).

1.2.3 RAS effectors

Active, GTP-bound RAS interacts with numerous downstream effectors to activate signaling pathways important for cell growth and survival[15,36]. Most RAS effectors have a RAS binding domain (RBD) or a RAS association domain[52]. The three major effectors of oncogenic RAS signaling are RAF, PI3K, and RALGDS[53-56] (**Figure 1-1**). Numerous other RAS effectors, such as PLCε[57-59], the RAC-GEF TIAM1[60], and pro-apoptotic RASSF family members[61] have been identified, but their functions are not as well studied.

The RAF serine/threonine kinases (ARAF, BRAF, CRAF) were the first RAS effectors to be identified[62-65]. RAF binds to the effector region of RAS-GTP via its RBD[62-66] at the plasma membrane. Here, RAF is phosphorylated and activated by different protein kinases[67,68]. Active RAF subsequently phosphorylates and activates the serine/threonine kinases MEK1 and MEK2 (MEK), which in turn phosphorylates and activates the serine/threonine kinases ERK1 and ERK2 (ERK)[69-72]. Active ERK can translocate into the nucleus, and has both cytosolic and nuclear protein substrates. Signaling through the RAS-RAF-MEK-ERK MAPK pathway leads to a diverse set of cellular responses, including proliferation, differentiation, inflammation, and apoptosis[15,73].

The second RAS effector pathway to be identified was the phosphatidylinositol 3-kinase (PI3K) pathway[74,75]. PI3K can be activated by RTKs[76-78], GPCRs[79,80], or RAS[75]. RAS interacts directly with the p110 catalytic subunit of type I PI3Ks, activating PI3K

through a combination of conformation change and translocation to the plasma membrane[75,81]. PI3K is a lipid kinase that converts phosphatidylinositol-4,5-bisphosphate (PIP2) into phosphatidylinositol-3,4,5-triphosphate (PIP3). PIP3 recruits phosphoinositide-dependent kinase 1 (PDK1) and the serine/threonine kinase AKT (AKT1, AKT2, and AKT3) to the plasma membrane, where PDK1 phosphorylates and activates AKT[82,83]. Subsequently, AKT phosphorylates several downstream effectors that regulate cell growth, cell cycle, and cell survival[84].

Another important class of RAS effectors are nucleotide exchange factors for the RAS-like (RAL) GTPases[85-90]. The RAL-GEF family is comprised of RAL guanine nucleotide dissociation stimulator (RALGDS), RALGDS-like gene (RGL), and RGL2. RAL-GEFs activate the RAL small GTPases RALA and RALB[91]. RALB signaling induces the SEC5 complex to associate with the atypical IκB-related protein kinase TBK1 to promote cell survival through activation of the NFκB transcription factor[92]. In addition, RAL signaling promotes filopodia formation and receptor trafficking through activation of RalA binding protein 1 (RALBP1)[93-95], and regulates epithelial cell polarity and cell motility through SEC5 and EXO84[96-100].

The relative contribution of different RAS effector arms to RAS signaling is unclear. Genetic suppression of different individual effector pathways was sufficient to prevent RAS-mediated transformation in different model systems[54,101-104]. In certain contexts, signaling through a specific effector pathway may be sufficient to induce cell transformation. For example, in a mouse model of pancreatic cancer, active BRAF, but not PIK3CA, was sufficient to mediate tumorigenesis[54]. In immortalized mouse cells, RAF activation induced transformation whereas RALGDS and PI3K activation did not[105].

Yet, in immortalized human cells, activation of RALGDS, but not RAF or PI3K, induced cell transformation[105]. It is likely that the relative importance of each RAS effector arm is context-specific.

A major downstream outcome of signaling through RAS effector pathways is the control of cell proliferation. This involves activation of the activator protein 1 (AP-1) transcription factor, a heterodimer complex composed of members of the JUN, FOS, activating transcription factor (ATF) and masculoaponeurotic fibrosarcoma (MAF) protein families[106]. ETS transcription factors, which are also activated by RAS signaling[107], cooperate with AP-1 to drive a RAS transcriptional program[108]. An important effect of RAS-induced transcriptional changes is increased expression of cell cycle regulatory proteins such as cyclin D1 (CCND1), which enable cells to progress through the G1 phase of the cell cycle[109]. In mouse models of breast cancer, deletion of *Ccnd1* abrogated the formation of Hras-induced tumors, though it had no effect on the development of Myc- or Wnt-induced tumors[110], indicating that CCND1 is an critical mediator of oncogenic RAS signaling. While regulating entry to the cell cycle is an important effect of RAS signaling, additional functions contribute to its oncogenic properties.

Aside from promoting proliferation, RAS signaling is implicated in several pro-tumorigenic properties, such as suppressing apoptosis, altering cell metabolism and promoting angiogenesis and metastasis[111]. The details of how RAS regulates these diverse pathways are still under investigation. RAS signaling has been found to upregulate both pro-apoptotic and anti-apoptotic mediators, though the balance of apoptotic regulators is maintained in favor of cell survival[111]. In addition, RAS signaling

promotes anabolic metabolism by upregulating the expression of certain rate-limiting metabolic enzymes, and induces macroautophagy, a process in which cells degrade its intracellular components to recycle metabolic substrates[112]. These metabolic changes serve to increase the availability of various metabolites to support cell proliferation. RAS signaling can mediate angiogenesis by increasing the expression of vascular endothelial growth factor A (VEGFA), which promotes endothelial cell proliferation. In addition, RAS can promote metastases by upregulating the transcriptional repressors SNAIL and SLUG, which reduce E-cadherin expression and disrupt cell-cell contact[113,114]. Moreover, ERK-mediated expression of matrix metalloproteinases and RAC-mediated effects on the cytoskeleton likely enhance cell invasiveness[115].

1.2.4 RAS post-translational modifications

RAS proteins require membrane association for their biological activity[116,117]. All RAS proteins have a carboxy-terminal CAAX tetrapeptide motif (C = cysteine, A = aliphatic amino acids, X = variable amino acid) in their C-terminal hypervariable region. This CAAX motif undergoes several post-translational modifications that enhance RAS hydrophobicity and facilitate membrane association[116]. The first step is catalyzed by cytosolic farnesyltransferase (FTase), which covalently attaches a farnesyl isoprenoid to the cysteine of the CAAX motif[118,119]. In the presence of an FTase inhibitor (FTI), KRAS4B and NRAS can be alternatively prenylated by geranylgeranyltransferase (GGTase)[120-123]. Prenylated RAS travels to the endoplasmic reticulum, where it is further modified by RAS converting enzyme (RCE1) and isoprenylcysteine carboxyl methyltransferase (ICMT). RCE1 proteolytically removes the AAX amino acids[124,125], and the newly C-terminal farnesylcysteine is methylesterified by ICMT[126-128]. This three-

step modification of the RAS CAAX motif enhances the hydrophobicity of the RAS C-terminus, increasing its affinity for lipid membranes.

The CAAX- modifications are required for RAS membrane association. However, RAS localization to the inner leaflet of the plasma membrane requires an additional motif to facilitate its integration into lipid membranes[118]. For KRAS4B, this motif is a polybasic domain of lysine residues. For the remaining RAS proteins, it consists of one or two cysteine residues in the hypervariable region that are modified by addition of the fatty acid palmitoyl by palmitoyl acyltransferase (PAT) at the Golgi complex[129]. Palmitoyl groups can be removed by acyl-protein thioesterase (APT), which allows RAS to traffic between the plasma membrane and the Golgi complex[129]. Together, these post-translational modifications enable RAS to associate with the negatively charged head groups of phosphatidylserine and phosphatidylinositol in the plasma membrane[130].

1.2.5 RAS mutations in cancer

RAS is the most frequently mutated oncogene in human cancers[36,131]. *RAS* mutations occur in nearly all pancreatic cancers, ~50% of colorectal cancers, and ~30% of lung cancers[131] (**Table 1-1**). The involvement of RAS signaling in cancer is evident not only by the high incidence of *RAS* mutations, but also by the high frequency of mutations in RAS regulators (such as RTKs and NF1) and RAS effectors (such as members of the MAPK and PI3K pathways)[132,133].

Over 95% of oncogenic *RAS* mutations involve point mutations in codons 12, 13, or 61 (analysis of the Catalog of Somatic Mutations in Cancer (COSMIC) database[134]). These G12, G13, or Q61 mutations decrease RAS intrinsic GTPase activity, reduce GAP binding affinity, and abrogate the ability of GAPs to stimulate RAS GTPase

activity[135]. This causes RAS to accumulate in the active GTP-bound state, signaling to downstream effectors even in the absence of extracellular stimuli.

Table 1-1. Frequency of *RAS* mutations in human cancers.

Cancer	% *KRAS*	% *NRAS*	% *HRAS*	% *RAS*
Pancreatic ductal adenocarcinoma	97.7	0	0	97.7
Colorectal adenocarcinoma	44.7	7.5	0	52.2
Multiple myeloma	22.8	19.9	0	42.6
Lung adenocarcinoma	30.9	0.9	0.3	32.2
Skin cutaneous melanoma	0.8	27.6	1	29.1
Uterine corpus endometrioid carcinoma	21.4	3.6	0.4	24.6
Uterine caricinosarcoma	12.3	1.8	0	14.3
Thyroid carcinoma	1	8.5	3.5	12.5
Acute myeloid leukemia	3.1	6.7	1.6	11.4
Bladder urothelial carcinoma	3.1	1.4	5.9	10.6
Gastric adenocarcinoma	11.4	0.9	0	10
Cervical adenocarcinoma	8.3	0	0	8.3
Head and neck squamous cell carcinoma	0.5	0.3	4.7	5.5
Diffuse large B cell lymphoma	5.2	0	0	5.2

Adapted from Cox et al. 2014[131], where data were compiled from a variety of sources, including but not limited to The Cancer Genome Atlas, the International Cancer Genome Consortium, and cBioPortal[136,137].

Oncogenic *RAS* cooperates with other oncogenes or loss of tumor suppressors to initiate transformation[138-140] and mediate cancer progression[141-145]. KRAS is a major driver of lung adenocarcinoma and pancreatic cancer, and KRAS mutations are likely an initiating event in these tumors. In pancreatic cancer, mutant *KRAS* is detected in the earliest pre-malignant lesions, and is present during all stages of disease progression[141,146]. Contrastingly, mutant KRAS is likely not a primary initiating event in CRC, though it contributes to tumor progression[142,144,147].

RAS mutations are associated with worse outcome in some cancers. *NRAS* mutations in melanoma[148] and *KRAS* mutations in NSCLC[149] have been found to be negative prognostic makers for overall survival. In addition, RAS mutations predict

intrinsic resistance to certain targeted therapies, and are used as an exclusionary criterion (discussed in Chapter 1.3.1).

1.2.6 Functional differences among RAS proteins and *RAS* mutations

Historically, the different RAS proteins were thought to be functionally equivalent due to their sequence homology and similar behavior in biochemical assays. RAS proteins are highly conserved, and the first 85 amino acids (GTP/GDP-, regulator-, and effector-binding regions) are identical in all four proteins. In addition, all RAS isoforms are able to induce cancer in model systems and all are expressed in adult tissues and in most tumors[36,111]. However, there is now accumulating evidence that the four RAS isoforms – and even specific RAS mutations – are not functionally equivalent.

A striking difference among RAS proteins is their mutation frequency in human cancers. *RAS* mutations more commonly arise in *KRAS* (86%) than in *NRAS* (11%) or *HRAS* (3%) and the frequency of RAS gene mutations varies widely in cancers originating from different tissues[131,134]. Nearly all pancreatic cancers have *KRAS* mutations, whereas *NRAS* mutations are more common in melanoma and *HRAS* mutations are predominant in bladder cancer (**Table 1-1**). The prevalence of specific missense mutations also varies among RAS proteins. *KRAS* and *HRAS* predominantly harbor mutations in codon G12, whereas *NRAS* typically has mutations in codon Q61[131,134]. The frequency of specific mutant alleles vary by cancer-type[131]. For example, $KRAS^{G12D}$ is the most common mutation in pancreatic and colorectal cancers, while $KRAS^{G12C}$ is most common in lung cancer[131,135]. The forces driving the varying frequencies of *KRAS*, *HRAS*, and *NRAS* mutation in human cancers remains poorly understood. It is likely that many factors are involved, including differences in RAS

effectors, RAS expression level[150,151], RAS genomic loci[152], environmental exposures[153,154], and cellular context[135,155-157].

There is some evidence that RAS isoforms have distinct functions. KRAS has enhanced tumor-initiating properties compared to HRAS and NRAS. In a mouse model of colorectal cancer, $Kras^{G12D}$ promoted tumor formation when expressed in adenamotous polyposis coli (APC)-deficient colonic epithelial cells, but $Nras^{G12D}$ did not[158]. In a mouse model of tumor initiation and differentiation, $Kras^{G12V}$, but not $Hras^{G12V}$ or $Nras^{G12V}$, was able to initiate tumors via a mechanism involving stem cell expansion[159]. A difference in calmodulin binding may underlie the unique tumorigenic phenotype of mutant KRAS. It has been demonstrated that KRAS binds calmodulin, while NRAS and HRAS do not[160]. The interaction between KRAS and calmodulin has been found to contribute to tumorigenesis and tumor maintenance by inhibiting calmodulin kinase activity and suppressing FZD8-mediated non-canonical WNT signaling[161]. This unique property of KRAS may contribute to the relatively high frequency of KRAS mutations in human cancers.

The differences in frequency of *KRAS*, *NRAS*, and *HRAS* mutations may also reflect differences in gene expression. *KRAS* is enriched for rare codons, which results in reduced protein expression[150]. This may enable cells expressing oncogenic KRAS to avoid oncogene-induced senescence[151], facilitating the accumulation of further genetic events to drive cancer progression. However, this rationale is at odds with the fact that *NRAS* and *HRAS* are preferentially mutated in some cancer types. In addition, the existence of germline $HRAS^{G12S/A}$ mutations in individuals with Costello syndrome suggests that activated HRAS does not cause senescence in normal tissue[162].

The RAS gene locus may contribute to differences in mutation frequency among RAS isoforms. For example, Kras is essential during mouse development[163,164], though Kras4a[165], Nras[166], and Hras[167] are not, and mice lacking both Nras and Hras are viable[168]. However, mice expressing Hras from the endogenous *Kras* genomic locus are viable, indicating that Kras can be functionally replaced by Hras during embryogenesis[152]. Moreover, in a mouse model of lung cancer in which the genomic *Kras* locus was genetically engineered to express Hras, the lung tumors that arose were predominantly driven by mutant Hras rather than Kras[169]. These observations suggest that the RAS genetic locus may have more influence on the observed mutation frequency than the isoform of RAS that is expressed.

The reason behind the different frequencies of specific RAS activating mutations are similarly poorly understood[135]. Some of these differences are influenced by the environment in which the tumor develops. For example, the G12C mutation, which is the most common *KRAS* mutation in lung cancer, arises from a cytosine to adenine (C > A) nucleotide transversion, which is a hallmark of exposure to tobacco smoke[40,41,135,153,170]. Differences in biochemical and functional properties of mutant proteins may also affect mutation frequency. The commonly occurring mutant forms of KRAS differ in certain biochemical properties, such as rate of nucleotide exchange, intrinsic and GAP-stimulated GTP hydrolysis, and binding affinity to the RAF RBD[157]. In lung adenocarcinomas, $KRAS^{G12C}$ and $KRAS^{G12V}$ preferentially activate the RAL effector pathway, while other KRAS alleles such as $KRAS^{G12D}$ preferentially activate the MAPK and PI3K effector pathways[156].

Consistent with the idea that specific *RAS* mutations have unique biologic

properties, some *RAS* mutations may have prognostic[171,172] or predictive[173-176] value in certain clinical settings. In patients with *KRAS*-mutant colorectal cancer, $KRAS^{G13}$ mutations were associated with increased risk of relapse or death[171]. Interestingly, a study found that patients with $KRAS^{G13D}$ mutant colorectal cancer demonstrated clinical benefit from treatment with the EGFR inhibitor cetuximab whereas patients with $KRAS^{G12}$ mutations did not[173,177]. In a study of NSCLC, it was found that tumors with $KRAS^{G12C}$ or $KRAS^{G12V}$ mutations correlated with worse progression-free survival compared to tumors with other *KRAS* mutations, possibly because of differential activation of downstream effectors[156]. Currently, the majority of drug discovery efforts and clinical trials assume that all RAS isoforms and mutations are equivalent. Increasing evidence suggests that each may require distinct therapeutic approaches. Going forward, it will be important to examine the functional differences and prognostic/predictive value of different RAS isoforms and mutant alleles.

Much remains unknown about the factors that drive the differences in RAS mutation frequency across human cancers. Variations in protein function, gene loci, expression level, and carcinogen exposure likely play a role, though the relative importance of these contributing factors remains unclear and it is likely that many remain unidentified.

1.2.7 Oncogene addiction in *RAS*-mutant cancers

Cancer cells with mutant oncogenes are frequently dependent on continued signaling from the activated signaling pathways. This phenomenon, termed “oncogene addiction,” provides a therapeutic opportunity because it renders cancer cells sensitive to drugs targeting these pathways. Importantly, cancer cells are often more dependent

on the oncogenic gene than normal cells, conferring a large therapeutic window[178,179]. Targeting oncogene addiction has been successful in treating many cancers, such as chronic myelogenous leukemia (CML) with the *BCR-ABL* fusion oncogene treated with ABL kinase inhibitors, *EGFR*-mutant lung cancer treated with EGFR inhibitors, and *BRAF*-mutant melanoma treated with BRAF inhibitors[180,181].

RAS-mutant cells are dependent on continued RAS signaling for sustained survival/proliferation. An analysis of *KRAS*-mutant cancer cell lines suggested that there is a spectrum of RAS dependency[182]. However, the majority of human cancer cell lines[53,182-184] and tumors from genetically engineered mouse models (GEMMs) harboring a mutant *RAS* allele demonstrate RAS addiction[185-191]. Indeed, removing Kras from established *Kras*-mutant tumors in mouse models results in dramatic tumor regression[186,188,190]. As the majority of *RAS*-mutant cancers are addicted to RAS, there has been much interest in inhibiting RAS for cancer therapy.

1.3 Strategies to target mutant RAS

Several approaches have been taken to therapeutically target *RAS*-mutant cancers, including: 1) inhibiting RAS activators, 2) directly inhibiting RAS, 3) preventing RAS from associating with the plasma membrane, 4) inhibiting RAS effector pathways, and 5) inhibiting tumor-specific vulnerabilities that are induced by oncogenic RAS signaling (non-oncogene addictions or synthetic lethal interactions)[192] (**Figure 1-2**).

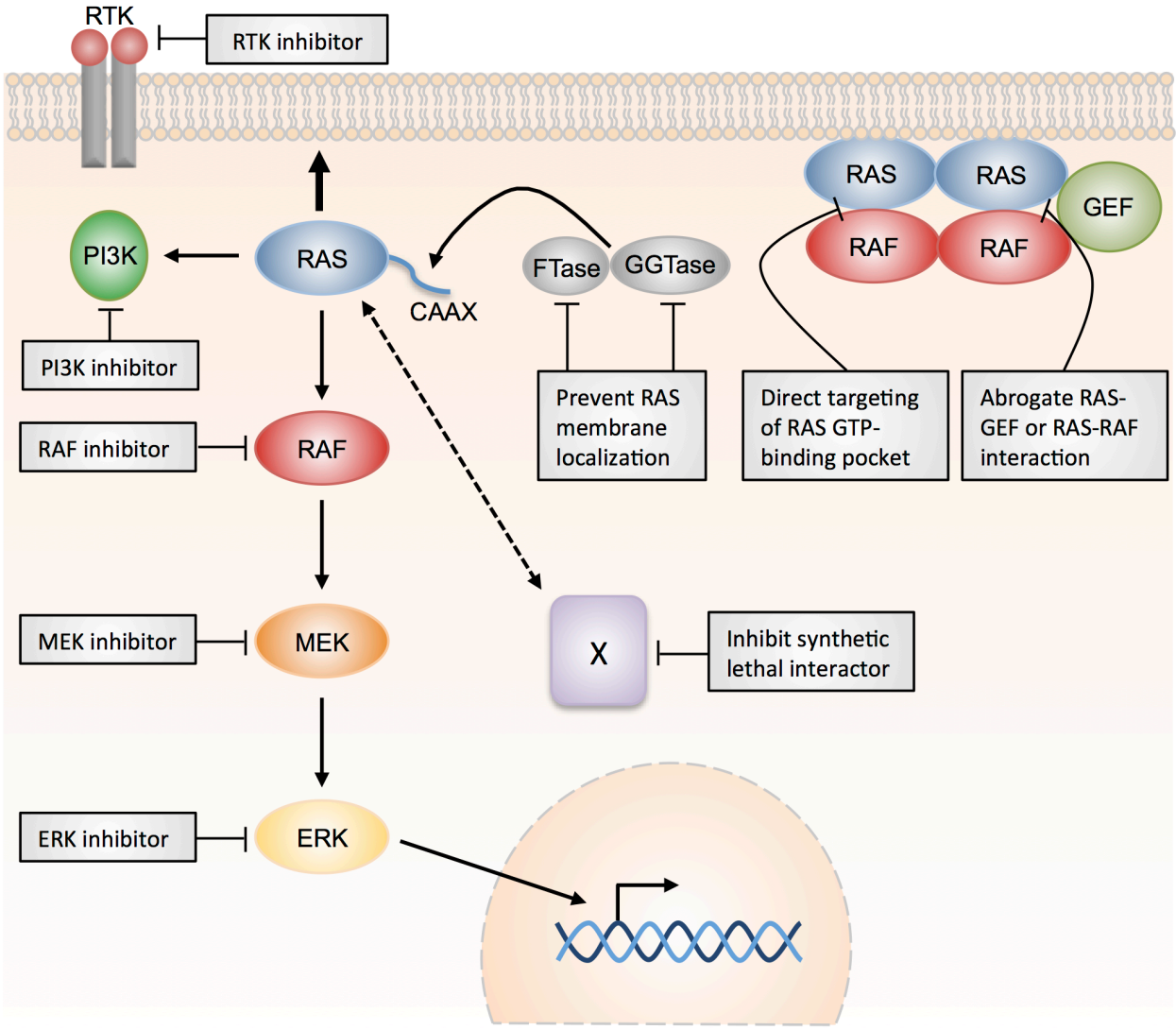

Figure 1-2. Strategies to target mutant RAS. Pharmacologic approaches to inhibit oncogenic RAS include inhibiting upstream RAS activators, such as RTKs; directly targeting RAS at its GTP-binding pocket or interfering with the RAS–GEF or RAS–RAF interaction; preventing RAS membrane localization of by inhibiting RAS prenylation with FTIs or GGTIs, or by inhibiting PDEδ; inhibiting downstream RAS effectors using RAF, MEK, ERK, or PI3K pathway inhibitors; and inhibiting RAS synthetic lethal interactors. Figure adapted from Samatar et al. 2014[193].

1.3.1 Inhibiting upstream RAS activators

Inhibiting upstream RTKs could be effective in treating *RAS*-mutant cancers because these cells produce autocrine growth factors, such as EGF[194]. Indeed, an *in vivo* study demonstrated that autocrine EGFR activation is important for tumorigenesis in cancers driven by constitutively active SOS, a GEF that activates RAS[195]. However, subsequent clinical studies indicated that *KRAS* mutations predict insensitivity to EGFR inhibitor therapy. Currently, *RAS* mutation is an exclusionary criterion for EGFR inhibitor treatment in patients with colorectal cancer[196,197] because EGFR inhibitor treatment is ineffective for *RAS*-mutant tumors. Similarly, patients with *RAS*-mutant NSCLC are likely insensitive to EGFR inhibitor therapy[175,176,198,199].

Accumulating data suggests that not all individual *RAS* mutations are functionally equivalent (discussed in Chapter 1.2.6). Patients with $KRAS^{G13D}$ mutant colorectal cancer may derive modest benefit from EGFR inhibitor treatment[173,177,200]. However, the effect was not sufficiently robust to indicate EGFR inhibitor treatment in this patient population[201]. Additional studies are necessary to determine the predictive value of specific *RAS* mutations for response to EGFR inhibitor treatment.

1.3.2 Direct RAS inhibition

As the majority of *RAS*-mutant cancers are addicted to RAS, there has been much interest in developing RAS inhibitors. Unfortunately, RAS has proven to be a challenging target. RAS has a picomolar affinity for GTP/GDP and the millimolar cytosolic concentration of guanine nucleotides makes it unlikely that a competitive inhibitory nucleotide analogue will be developed[202]. Additionally, RAS activation and

signaling is mediated by transient protein-protein interactions that are difficult to target using small molecules[203].

Despite these challenges, several groups have identified compounds that bind to RAS non-covalently and either abrogate the RAS-RAF interaction[204-208] or inhibit GEF-mediated nucleotide exchange[209-214]. However, these early-stage compounds have low RAS-binding affinity and potency, and will have to be improved before clinical application. More recently, covalent inhibitors targeting $KRAS^{G12C}$ have been developed[215,216]. These mutation-specific electrophilic compounds irreversibly bind to the reactive cysteine in $KRAS^{G12C}$, blocking KRAS nucleotide exchange[215,216]. While $KRAS^{G12C}$ mutations occur in ~15% of lung adenocarcinomas[170], it arises infrequently in other cancer types. It is possible that other compounds will be identified that specifically target RAS^{G12D} and RAS^{G13D}, but it will be difficult to selectively target other common RAS mutations due to their less reactive side chains. While the advances in efforts to directly target oncogenic RAS are encouraging, these approaches have yet to produce clinically usable agents.

1.3.3 Targeting RAS post-translational modifications

Another approach to inhibiting RAS is to target its post-translational modifications. As discussed in Chapter 1.2.4, post-translational lipid modification is necessary for RAS membrane association and biological activity[116,117]. RAS farnesylation by FTase is the first, irreversible, and rate-limiting step of the RAS post-translational modifications that increase RAS hydrophobicity and enable membrane association[130,217]. The identification of FTase and the discovery that its catalytic activity could be inhibited by short CAAX tetrapeptides[218] encouraged efforts to develop FTIs[219].

Preclinical mouse studies showed that FTIs effectively suppressed the proliferation of *HRAS*-driven tumors with little general toxicity[220,221]. This motivated the development of FTIs that advanced to Phase III clinical trials. Unfortunately, these FTIs did not demonstrate significant clinical benefit in patients with advanced NSCLC[222], pancreatic cancer[223,224], colon cancer[225], or acute myelogenous leukemia (AML)[226]. The mode of action of FTIs is unclear, as the ability of FTIs to inhibit cancer cell growth did not correlate with *RAS* mutation status[227-229].

The discrepancy between pre-clinical and clinical data for FTIs in *RAS*-mutant cancers may be attributable to the fact that KRAS4B and NRAS can be alternatively prenylated by GGTase in the context of FTI treatment[120-123]. The addition of a geranylgeranyl modification in place of farnesyl enables KRAS4B and NRAS to remain fully functional. The phenomenon of alternative prenylation was not discovered in FTI preclinical studies because HRAS, which does not undergo alternative prenylation, was the RAS isoform examined[220,221]. NSCLC and pancreatic cancer are associated with mutations in *KRAS* or *NRAS* rather than *HRAS*, which could explain the lack of efficacy of FTIs in these cancer types[222-224].

Although FTIs are not effective in treating cancers with oncogenic KRAS or NRAS, which are the most frequently mutated RAS isoforms in human cancers, it remains possible that they will be effective for *HRAS*-mutant cancers such as thyroid, bladder, and head and neck cancers[230] (**Table 1-1**). A potential solution to the problem of alternative prenylation of KRAS and NRAS is combined FTase and GGTase inhibition[231]. However, although dual inhibitors have been developed, their use in clinic may be limited by toxicity in normal tissues[232-234]. There is ongoing interest in inhibiting

other RAS CAAX-processing enzymes such as RCE1 and ICMT1, palmitoyl transferases, or proteins that mediate RAS trafficking to and from the plasma membrane[36,131]. Recently, an inhibitor that disrupts the association between farnesylated KRAS4B and the chaperone protein phosphodiesterase 6 delta subunit (PDE6δ), which augments RAS localization to the plasma membrane, was found to reduce oncogenic KRAS signaling[235]. However, these efforts remain far from clinical implementation.

1.3.4 Inhibiting RAS effector pathways

Targeting RAS proteins or RAS modifier proteins directly has proven difficult. Hence, efforts have shifted towards alternative ways of selectively targeting *RAS*-mutant cells, such as inhibiting RAS effector pathways. While many RAS effector families have been identified, the RAF serine/threonine kinases likely play a key role in *RAS*-mediated oncogenesis[54,102]. As described in Chapter 1.2.3, RAF activates the MEK kinases, for which the only known substrates are the ERK kinases. However, because the MAPK signaling pathway involves multiple feed-forward and feedback mechanisms that dynamically modulate ERK activity, pharmacological inhibition of the MAPK pathway at the level of RAF and MEK have not demonstrated equivalent outcomes[131,236,237].

Vemurafenib and dabrafenib are ATP-competitive RAF inhibitors that have been approved for treatment of *BRAF*-mutant melanoma[238,239]. However, in *NRAS*-mutant melanoma, treatment with these first-generation BRAF inhibitors paradoxically activates the MAPK pathway through RAF dimerization and consequent CRAF trans-activation[240-243]. However, a second generation of ‘paradox-breaking’ BRAF inhibitors that do not

promote RAF dimerizaton[244] or pan-RAF inhibitors that inhibit all three RAF proteins[245] have been generated and may have improved efficacy in treating *RAS*-mutant cancers.

Several MEK inhibitors are currently being tested in clinical trials for *RAS*-mutant pancreatic cancer, colorectal cancer, lung cancer, and melanoma. Although MEK inhibition has been successful in treating *BRAF*-mutant melanoma[239,246], it has had limited success in *RAS*-mutant NSCLC[247-249], pancreatic cancer[248], and melanoma[250]. As discussed in Chapter 1.4.3, a major mode of intrinsic or acquired resistance to MEK inhibitor monotherapy in *RAS*-mutant cancers is the reactivation of the RTK-RAS-MAPK pathway[236]. It was thought that ERK inhibition would overcome this mode of resistance. However, it has been shown that ERK inhibitors alleviate feedback inhibition of RAF, resulting in enhanced MEK activation[251]. Combined inhibition of RAF, MEK, and ERK may be necessary for more effective MAPK pathway inhibition, though overlapping toxicities could be limiting in patients.

The p110 catalytic subunits (α- γ- and δ-subunits) of class I PI3Ks are also important effectors of oncogenic RAS[55,101,252]. A *Kras*-driven mouse model of lung cancer suggested that PI3K signaling was essential for tumorigenesis and tumor maintenance[253]. However, in a later study, small molecule inhibition of the PI3K pathway in a mouse model of lung cancer demonstrated little effect on *Kras*-driven tumor growth[254], and subsequent *in vitro* studies suggested that oncogenic *RAS* confers resistance to PI3K inhibition[255]. It is not clear whether *RAS*-mutant cancers demonstrate greater dependence on PI3K signaling than cells driven by other oncogenes[77].

There is some evidence that the PI3K pathway may not be a key RAS effector in certain contexts. For example, while *BRAF* and *RAS* mutations are mutually exclusive in

human cancers, *PIK3CA* and *RAS* mutation frequently co-occur, suggesting that oncogenic *RAS* alone does not fully activate the PI3K pathway. In addition, while depletion of *KRAS* in *KRAS*-mutant colorectal cancer cell lines reduced levels of ERK signaling, AKT signaling remained intact via elevated RTK signaling[76]. Several inhibitors of the PI3K-AKT-mTOR signaling pathway are currently under clinical evaluation in *RAS*-mutant cancers. In addition, efforts to target other effectors of oncogenic RAS, such as RALGDS and RAC1 are ongoing. However, similar to RAS, neither are considered tractable drug targets[36,131].

Oncogenic RAS signals through multiple signaling pathways, and it is possible that inhibition of a single effector arm will not be sufficient to induce tumor regression. In pre-clinical studies, combined MAPK and PI3K inhibition effectively induced regression of *KRAS*-mutant tumors[254]. There are several clinical trials assessing the efficacy of combined MAPK (MEK or ERK) plus PI3K pathway (PI3K, AKT, or mTOR) inhibition in *RAS*-mutant cancers. The results of most of these trials are not yet available. However, while this dual-targeting strategy has the potential of being more effective than inhibition of either pathway alone, there may not be a wide enough therapeutic window to effectively suppress both pathways in human cancers[256]. In a recent trial that combined the AKT inhibitor MK-2206 with the MEK inhibitor selumetinib, no patient achieved over 70% inhibition of both targets at the maximum tolerated drug dose[257].

In summary, while RAS effector inhibition has been the most promising strategy to target oncogenic RAS, several challenges endure. Inhibition of effector pathways are complicated by compensatory feedback mechanisms, which necessitate inhibition at multiple levels of the pathway. In addition, as several effectors pathways are important

in oncogenic RAS signaling, concurrent inhibition of multiple pathways may be critical. However, while combination inhibition of more than one effector pathway may be more effective in inducing tumor regression, the resulting increase in toxicity to normal cells may reduce the therapeutic window. Nevertheless, it remains possible that combined inhibition of different nodes of these effector pathways (RAF, MEK, or ERK and PI3K, AKT, or mTOR) will yield different toxicities, with greater therapeutic windows in specific combination strategies.

1.3.5 Synthetic lethality

An alternative strategy of targeted drug development for *RAS*-mutant cancers involves identifying signaling pathways that become essential for cancer cell survival in the context of oncogenic RAS signaling. These “synthetic lethal” interactions (also known as induced essentiality, non-oncogene addiction, or co-dependency) provide opportunities for rational drug development to treat *RAS* mutant malignancies[178,179,258] (**Figure 1-3**). Breast and ovarian cancers with mutations in the tumor suppressor genes *BRCA1* or *BRCA2* are a paradigm for exploiting synthetic lethal interactions in targeted cancer therapy. These tumors are dependent on the DNA repair enzymes PARP1 and PARP2, and respond to treatment with PARP inhibitors[259,260].

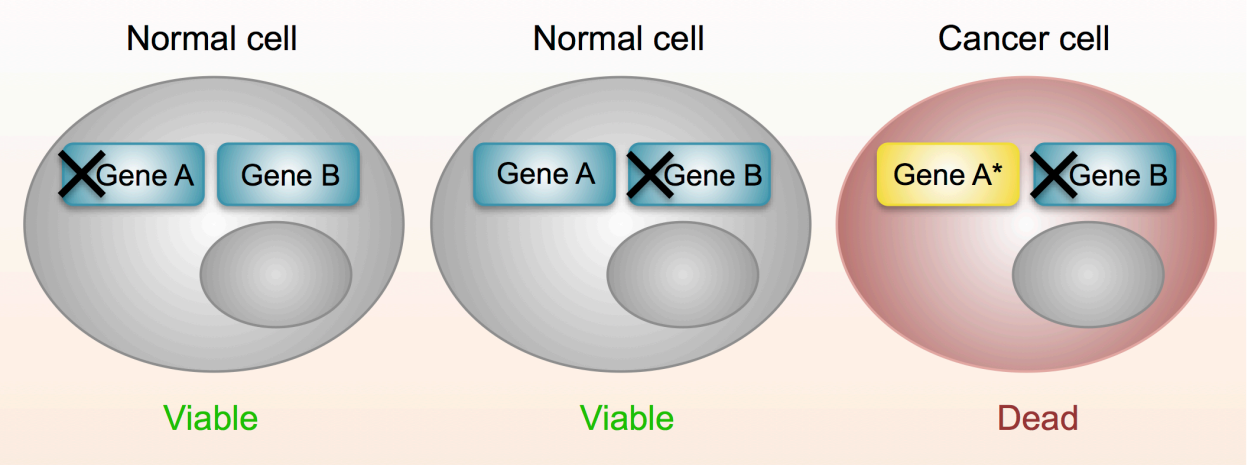

Figure 1-3. Synthetic lethality in cancer. Gene B is considered to be synthetic lethal to gene A if mutation (or inhibition) of gene B is lethal only to cells harboring mutant gene A. For cancer relevant genes such as RAS, synthetic lethal interactors represent potential drug targets. * Indicates mutation, X indicates inhibition.

Several systematic genetic screens have been performed in human cancer cell lines to identify synthetic lethal interactors with mutant RAS. These studies have employed different screening modalities (cell line selection, time frame, pooled versus arrayed screening) and reagents (siRNA or shRNA)[261]. Screens have typically been performed using pairs of isogenic cell lines or a panel of cancer cell lines that differ in *RAS* mutation status. These screens have confirmed that many *RAS*-mutant cell lines are addicted to RAS, and identified many genes that may be synthetic lethal with oncogenic RAS (**Table 1-2**). These genes are involved in diverse processes, including cell cycle (*BIRK5, PLK1,* and *APC/C*), cell survival (*BCL2L1* and *WT1*), transcription (*GATA2* and *SNAIL1*), and proliferation (*TAK1* and *TBK1*) (**Table 1-2**).

Table 1-2. RAS synthetic lethal genes.

Synthetic lethal genes or pathways	Library (assay and format)	Cells in primary screen	Drug inhibition	References
RAN, TPX2, SCD1	~3,700 druggable genes, siRNA, arrayed cell death	NCIH1299 (*NRAS*^{Q61K} NSCLC)	Not tested	Morgan Lappe et al. 2007[262]
BIRC5 (survivin), *CDK1, RBCK1*	~4,000 genes, siRNA, arrayed cell death	Isogenic DLD1 (CRC, *KRAS*^{G13D})	Not tested	Sarthy et al. 2007[263]
PLK1, APC/C, proteosome	Genome scale, shRNA, pooled proliferation screen with microarray readout	Isogenic DLD1 (CRC, *KRAS*^{G13D})	BI-2536	Luo et al. 2009[264]
STK33, AKT3, CPNE1, CAMPK1, MLKL, FLT3LG, and *DGKZ*	~1,000 druggable genes, shRNA, arrayed proliferation	Pan-cancer cell line panel (4 *KRAS*-mutant, 4 *KRAS*-wildtype) and 2 immortalized cell lines	STK33 kinase inhibitor, failed to suppress proliferation in *KRAS*-mutant cells[265-267]	Scholl et al. 2009[268]
TBK1, PSKH2, PTCH2, CPNE1, MAP3K8, proteasome	~1,000 druggable genes, shRNA, arrayed proliferation	Pan-cancer cell line panel (7 *KRAS*-mutant, 10 *KRAS*-wildtype) and 2 immortalized cell lines	CYT387 (TBK1 and JAK inhibitor), assessed in[269]	Barbie et al. 2009[184]
WT1, RAC1, PHB2	162 KRAS related genes, shRNA, *in vitro* and *in vivo* pooled proliferation screens with bead array readout	LKR10 and LKR13 (*Kras;Trp53* mutant mouse lung tumor derived cell lines)	Not tested	Vicent et al. 2010[270]
SNAI2 (SNAIL2)	~2,500 druggable genes, shRNA, pooled proliferation with microarray readout	Isogenic HCT116 (CRC, *KRAS*^{G13D})	Not tested	Wang et al. 2010[271]
GATA2, CDC6, proteasome	~8,000 druggable genes, siRNA, arrayed apoptosis and cell proliferation	Isogenic HCT116 (*KRAS*^{G13D}) and pan-cancer cell line panel (14 *KRAS*-mutant, 12 *KRAS*-wildtype)	Bortezomib with fasudil (GATA2)	Kumar et al. 2012[272], Steckel et al. 2012[273]
MAP3K7 (TAK1)	17 kinases highly expressed in *KRAS*-dependent CRC, shRNA, arrayed proliferation	KRAS-dependent SW620 and KRAS-independent SW837 (CRC, *KRAS*-mutant)	5Z-7-oxozeaenol	Singh et al. 2012[274]
Cttnb1 (β-catenin), *Mllt6*	Genome scale, shRNA, pooled *in vivo* proliferation with NGS readout	Mouse keratinocytes (*Hras*^{G12V})	Not tested	Beronja et al. 2013[275]
COP1 coatomer	Genome scale, siRNA, arrayed proliferation	17 *KRAS*- and *LKB1*-mutant lung cancer cell lines, matched tumor (*KRAS*-mutant) and normal NSCLC cell line pair	Saliphenylhala-mide A	Kim et al. 2013[276]
ARHGEF2 (GEFH1)	Genome scale, shRNA, pooled proliferation with NGS readout	Pan-cancer panel (72 cell lines).	Not tested	Marcotte et al. 2012[277], Cullis et al. 2014[278]

Table 1-2 (Continued).

Synthetic lethal genes or pathways	Library (assay and format)	Cells in primary screen	Drug inhibition	References
BCL2L1 (BCLXL)	~1,200 druggable genes in presence of MEK inhibitor (selumetinib), shRNA, pooled proliferation with NGS readout, synergistic death with MEK inhibitor	HCT116 and SW620 (CRC, *KRAS*-mutant)	Selumetinib and navitoclax	Corcoran et al. 2013[279]

Abbreviations: NSCLC (non-small cell lung cancer), CRC (colorectal cancer), NGS (next-generation sequencing).

Thus far, none of the proposed RAS synthetic lethal interactors have been able to discriminate between *RAS*-mutant and *RAS*-wildtype cells as well as RAS itself[261]. Notably, there has been a striking lack of overlap in RAS synthetic lethal genes identified from different screens. The only genes to score across multiple screens were proteasome complex members[184,264,272,273]. Oncogenic *RAS* has been reported to increase rates of protein synthesis, which may render cells more dependent on the proteasomal degradation of mutated or misfolded proteins[280]. However, it remains unclear whether *RAS* mutation status predicts clinical response to proteasome inhibitor therapy[281].

The first generation of *RAS* synthetic lethal screens have uncovered interesting biology in *RAS*-mutant cancers. However, the lack of overlap in identified synthetic lethal interactors with oncogenic *RAS* have raised concerns about the applicability of these findings. There are multiple possible explanations for the low overlap across different screens. Studies have employed different reagents (siRNA or shRNA), screening modalities (time frame, pooled versus arrayed and *in vitro* versus *in vivo* screening), and contexts (isogenic cell lines versus cell line panel, cell lineage)[131,261]. Each of these factors has unique limitations and likely contributes to false-negative and

false-positive rates. It is likely that many synthetic lethal partners of oncogenic KRAS remain unidentified.

While the first-generation RAS synthetic lethal screens have numerous limitations, they have led to the identification of several interesting targets, including *TBK1* and *WT1*, which continue to be the focus of ongoing investigation[184,270]. Notably, *TBK1* shows promise as a novel therapeutic target for *KRAS*-driven malignancies. Preclinical studies using a small molecule inhibitor of TBK1 achieved clear therapeutic responses in *Kras*-mutant GEMMs[282]. Additionally, studying TBK1 has led to the discovery of a novel effector pathway of oncogenic RAS, in which TBK1 promotes RAS-driven tumorigenesis by regulating an autocrine cytokine circuit. Such data support the idea that synthetic lethal genetic interactions can identify valuable therapeutic targets and broaden our understanding of critical mediators of oncogenic RAS, motivating our interest in identifying further novel candidates. Improvements in genome-scale screening technology, such as improved RNAi libraries or CRISPR-Cas9 knockout libraries, and the use of expanded collections of cancer cell lines could lead to the discovery of novel synthetic lethal targets.

1.4 Resistance to targeted therapy

1.4.1 Modes of resistance to targeted therapy

Therapies targeting oncogenically activated kinases have achieved impressive clinical responses in oncogene-addicted tumors, such as CML harboring the *BCR-ABL* fusion oncogene treated with an ABL kinase inhibitor[283], *EGFR*-mutant NSCLC treated with an EGFR kinase inhibitor[284], *BRAF*-mutant melanomas treated with a BRAF

inhibitor[246], *HER2*-amplifed breast cancers treated with HER2-targeting antibodies[285,286], and *EML4-ALK* fusion-containing NSCLCs treated with an ALK kinase inhibitor[287]. However, while single-agent targeted therapies can be highly effective, they are rarely curative. Drug resistance, which can be separated into intrinsic and acquired resistance, limits the therapeutic benefit of targeted drug therapy.

In cancers with intrinsic resistance, tumors are refractory to targeted therapy despite possessing the genetic alteration that predicts sensitivity because the majority of cancer cells harbor resistance-mediating factors. Contrastingly, acquired drug resistance develops in tumors that were initially sensitive to treatment either from positive selection of a small subpopulation of cells that possess a mechanism of resistance[288] or from the outgrowth of cells that acquire *de novo* resistance alterations during the course of treatment. Understanding intrinsic and acquired resistance mechanisms can lead to the identification of predictive biomarkers that inform patient selection and the design of rational therapeutic approaches to overcome these resistance mechanisms.

The phenomena of oncogene addiction and therapeutic resistance are closely related. For an oncogene-addicted cancer cell to be resistant to targeted therapy, it must either maintain oncogene activity, or, if the oncogene is successfully inhibited, activate pathways with overlapping functional effects. Hence, studying mechanisms of resistance to oncogene inhibition can provide insight to oncogenic signaling pathways and to important mediators of cancer cell survival and proliferation.

In cancers driven by kinase oncogenes, resistance mechanisms most frequently involve pathway reactivation (**Figure 1-4**). There are three major mechanisms of

resistance to kinase-targeted therapy[289]. These include 1) *target reactivation* through mutation or amplification of the target oncogene, loss of feedback inhibition ("feedback activation"), or activation of upstream regulators; 2) *activation of downstream effectors* through genetic alteration, feedback activation, or activation of an associated pathway; and 3*) oncogene bypass,* which can be mediated by activation of an "associated pathway" that reactivates the target gene pathway, or by activation of an "orthogonal pathway" that mediates resistance by an independent mechanism. Examples of these different mechanisms of resistance that have been identified in *KRAS*- or *BRAF*-mutant cancers treated with MEK or BRAF inhibitors are discussed in Chapter 1.4.3.

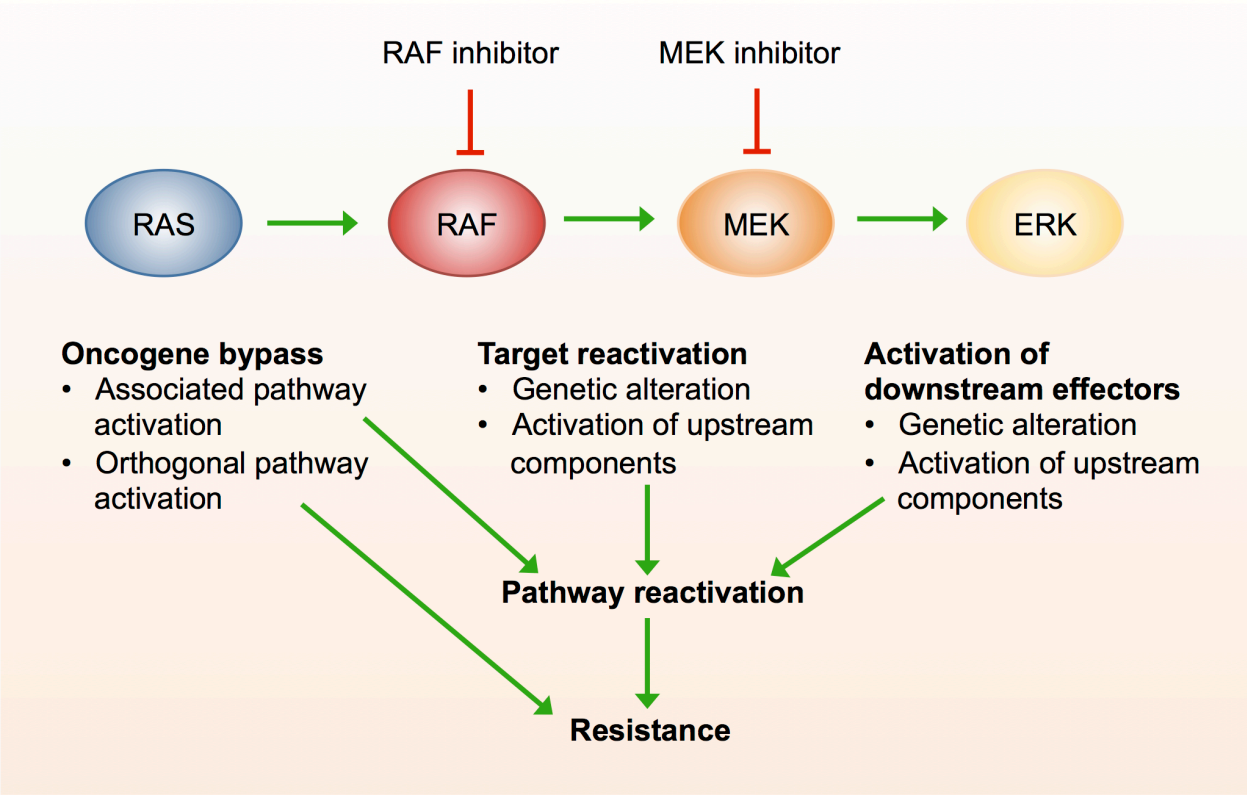

Figure 1-4. Mechanisms of resistance to targeted therapy. Adapted from Garraway et al. 2012[289].

1.4.2 Experimental approaches to study resistance to targeted therapy

The main experimental systems used to identify and investigate resistance mechanisms to targeted therapies are human cancer cell lines, genetically engineered mouse models, and human tumor samples (**Figure 1-5)**. Regardless of the experimental method used, a *bona fide* mechanism of resistance is 1) necessary and sufficient for drug resistance, and 2) clinically operant in unresponsive or relapsing tumors.

Figure 1-5. Experimental approaches to study cancer drug resistance. (A) *In vitro* resistance studies introduce mutagenized target cDNAs to a sensitive cell line or expose the cell line to a mutagen and subsequently treat with drug to select for drug-resistant clones **(Ai)**; culture sensitive cell lines in the presence of drug until drug-resistant clones emerge **(Aii)**; or perform systematic gain-of-function (ORF) or loss-of-function (RNAi and CRISPR-Cas9) screens in arrayed **(Aiii)** or pooled **(Aiv)** format by introducing screening libraries to sensitive cell lines and treating cells with drug to identify the genetic perturbations that confer drug resistance. **(B)** *In vivo* resistance studies using GEMMs, patient-derived xenografts (PDXs), or cell line xenografts. Mice harboring a genetically defined tumor or xenograft are treated with drug until a drug-resistant population emerges. Tumors with intrinsic or acquired resistance are subjected to genomic and/or molecular characterization and subsequent experimental validation studies. **(C)** Characterization of patient tumor samples obtained before treatment, during treatment, and after relapse, with matched normal tissue samples. Unbiased or candidate-driven genetic and molecular analyses are performed to identify or to confirm the existence of candidate mediators of resistance, respectively. Abbreviations: ORF (open reading frame), GEMM (genetically engineered mouse model), WGS (whole genome sequencing), RNAseq (RNA sequencing). Figure adapted from Garraway et al. 2012[289].

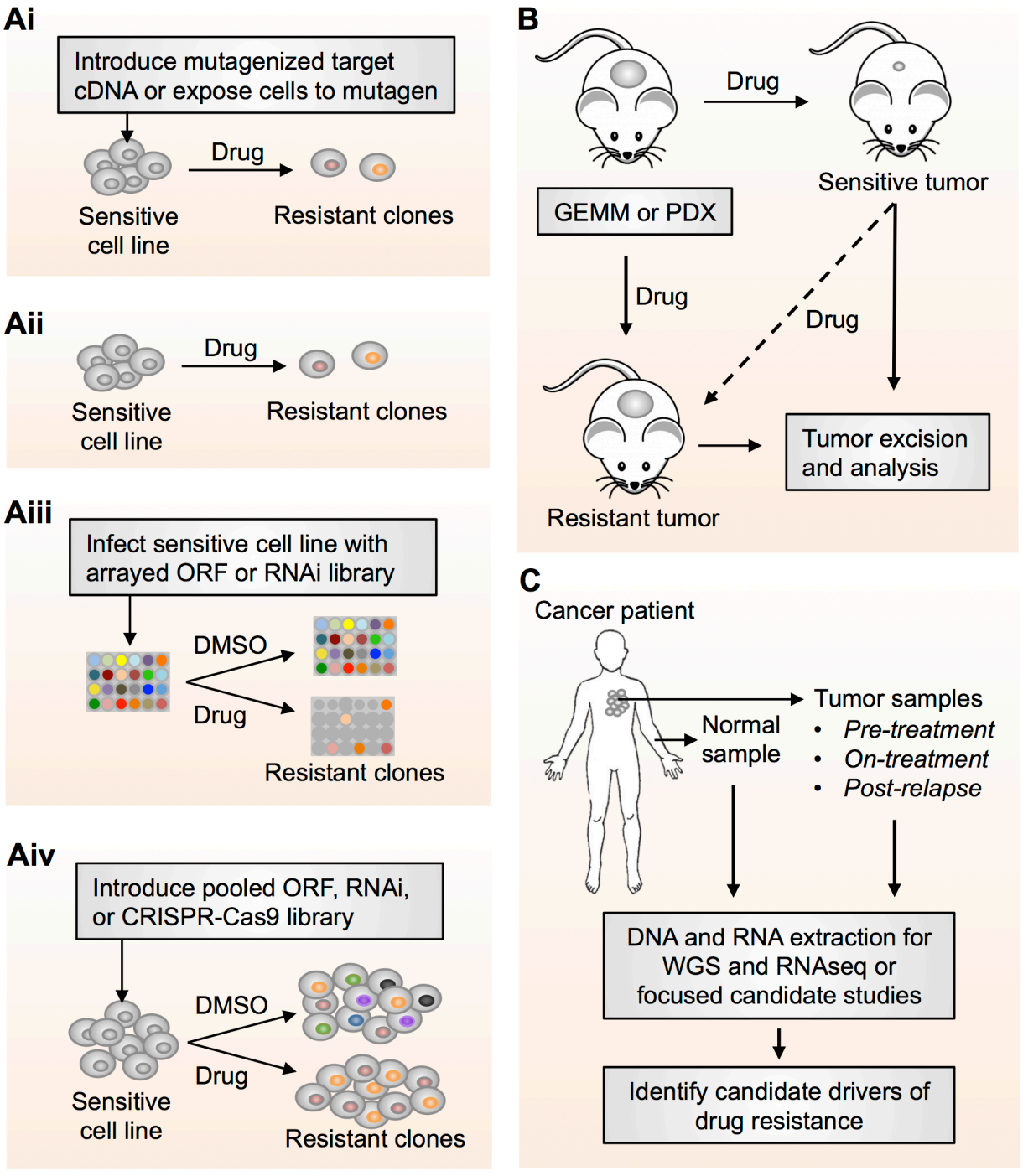

Figure 1-5 (Continued).

Human cancer cell lines enable relatively low-cost and feasible experiments to identify resistance mechanisms. Acquiring a secondary mutation within the target protein is a common mechanism of resistance to targeted agents. This mode of resistance was initially described in patients with CML containing the *BCR-ABL* translocation treated with imatinib, where "gatekeeper" mutations in the kinase domain of ABL block the interaction of imatinib with the ATP-binding pocket of ABL[290]. To identify mutations in the drug target that can confer resistance, different groups have introduced randomly mutagenized target cDNA to a sensitive cell line or induced mutations in the endogenous target gene by exposing the cell line a mutagen[291,292] (**Figure 1-5Ai**). Cells are subsequently grown in the presence of drug to positively select for those that have acquired drug resistance, and the target gene cDNA or endogenous locus of these cells are sequenced to identify mutations that conferred resistance.

Cell lines have also been used to identify mechanisms of resistance in a more unbiased manner. A common approach is to culture drug-sensitive cancer cell lines in the presence of drug and analyze the drug-resistant clones that emerge[293-296] (**Figure 1-5Aii**). The drug-resistant populations are compared to the drug-sensitive parental cell line to identify genetic or molecular alterations that drive the resistance phenotype. This approach has identified several clinically relevant mechanisms of drug resistance. However, identifying the spectrum of alterations that mediate resistance requires comprehensive genetic analysis and functional studies, and for many drug-resistant clones, the mechanism of resistance remains undetermined[293-296]. More recently, the generation of genome-scale open reading frame (ORF), RNAi, and CRISPR-Cas9

libraries[297-300] have enabled the systematic identification of gain- or loss-of-function events that mediate drug resistance[297,300-303] (**Figure 1-5Aiii-iv**). These unbiased functional screens have the potential to uncover diverse resistance mechanisms, many of which could have immediate clinical relevance.

Cell line findings do not always validate *in vivo,* and the clinical relevance of results obtained from *in vitro* experiments is not always clear. In order to interrogate resistance mechanisms in the context of an intact organism/microenvironment, several groups have used genetically engineered mouse models (**Figure 1-5B**). In these experiments, autochonous tumors or xenografts are treated with drug until resistant tumors emerge[133,304,305]. Mutations may be induced by retroviral insertional mutagenesis to accelerate the rate at which resistant tumors arise[305]. The molecular and genetic profiles of the resistant tumors are analyzed to identify potential resistance mechanisms. These efforts have demonstrated the value of mouse models as a discovery effort to identify novel mechanisms of resistance. However, as with resistance experiments conducted in cancer cell lines, the causal mechanism of resistance can be challenging to identify and remains unclear in some resistant tumors[133,304,305].

While *in vitro* and *in vivo* experimental approaches are powerful and scalable ways to identify putative mediators of resistance, these candidate resistance mechanisms may not be operant in clinic. For example, BRAF gatekeeper mutations can confer resistance to BRAF inhibitors *in vitro* and *in vivo*[306], but have not been observed as a mechanism of resistance in patients. Studying patient tumors that became resistant to targeted therapy is a powerful method to identify relevant mechanisms of resistance. These studies can be conducted in a candidate-based or

unbiased approach. In a candidate-based approach, the presence of a specific mechanism of resistance, typically identified from *in vitro* or *in vivo* studies, is assessed in human tumor samples[294-296,301,307-311]. In an unbiased approach, genome scale technologies are applied to analyze the genetic and molecular profiles of tumor samples to identify putative mechanisms of resistance[312-315] (**Figure 1-5C**). Ideally, matched pre-treatment, post-relapse, and matched normal samples are available for these studies to help identify drivers of resistance, which should be present only in the post-relapse resistant sample. However, obtaining adequate sample numbers and sufficient material for thorough molecular studies can be challenging. A major difficulty in both candidate-based and unbiased studies is in distinguishing correlation from causation. Discoveries should be coupled with functional studies to validate whether the proposed alterations are necessary and sufficient for resistance.

The study of resistance mechanisms to targeted therapies have led to the identification of predictive biomarkers that improve patient selection[196,316-318]. In addition, it has contributed to the discovery of novel agents[316,319-321] and suggested therapeutic combinations to overcome these resistance mechanisms[236,237,294-296,318].

1.4.3 Mechanisms of resistance to MAPK pathway inhibition in *RAS*- or *BRAF*-mutant cancers

The major modes of intrinsic or acquired resistance to RAF or MEK inhibitor therapy in *RAS*- and *RAF*- mutant cancers that have been identified involve reactivation of the RTK-RAS-MAPK pathway (**Table 1-3**). A common drug resistance mechanism involves genetic alterations involving the target gene itself. In patients with *KRAS*- or *BRAF*-mutant cancers treated with MEK inhibitors, MEK1 or MEK2 mutations that

enhance intrinsic MEK activity or abrogate drug binding frequently arise[322]. In *BRAF*-mutant cancers treated with a BRAF inhibitor, BRAF amplification[323] or alternatively spliced BRAF[296] are a common mechanism of resistance, though secondary mutations of BRAF itself have not been identified.

Beyond mutations of the drug target itself, the target gene can remain active in resistant tumors through activation of upstream regulators. For cells treated with BRAF or MEK inhibitors, this can occur by *NF1* deletion[297,302,313,335,336], *NRAS* or *KRAS* mutation[294,313-315,323,326,327,329,331], or BRAF amplification (in the context of MEK inhibition)[312-315,323,328,330,331]. Resistance to BRAF or MEK inhibition in *RAS*- or *BRAF*-mutant cancers can also arise from alterations in downstream effectors. Examples include gain-of-function MEK mutations (in the context of BRAF inhibition)[308,312-314,331], elevated CDK4 activity through *CDKN2A* deletion[329,331,341], and *CCND1* amplification[340].

Other mechanisms of resistance include oncogenic bypass, which is achieved by activation of compensatory signaling pathways through associated pathway activation or orthogonal pathway activation (**Figure 1-4**). In associated pathway activation, signaling through the MAPK pathway is restored, typically by increased signaling through RTKs. Heightened RTK activity can be due to stromal[345,346] or autocrine[337,342-344] ligands, RTK feedback activation[311,343,347-349,355] or upregulated RTK expression[294,295,310,314,323,327,342,344]. Associated pathway activation may also be achieved through increased COT[307] or MLK1-4[350] expression, which also reactivate the MAPK pathway. In *KRAS*-mutant cancers treated with a BRAF inhibitor, MAPK pathway activity can also be restored through CRAF activation[240-242,337-339]. Contrastingly, in resistance mediated by orthogonal pathway activation, signaling through the MAPK

Table 1-3. Mechanisms of intrinsic and acquired resistance to RAF- and/or MEK-inhibition.

Resistance mechanism	Example	Study
Target reactivation: genetic alteration in drug target		
Mutation	*BRAF* mutation	[306]Whittaker et al. 2010[+,1,3,i]
	MEK1 or *MEK2* mutation	[324]Emery et al. 2009[*,b,1,3,4,i,iv]
		[322]Nikolaev et al. 2011[*,a,1,3]
		[325]Hatzivassiliou et al. 2012[*,b,2,3,i]
		[326]Trunzer et al. 2013[+,b,1,4,c,iv]
		[327]Morris et al. 2013[+,*,b,1,3,i]
		[328]Villanueva et al. 2013[*,#,b,1,4,i,iv]
		[315]Long et al. 2014[#,b,1,4,iv]
		[329]Moriceau et al. 2015[+,#,b,1,3,i,iv]
Amplification	*BRAF* amplification	[323]Shi et al. 2012[+,b,1,4,i,v]
		[330]Das Thakur et al. 2013[+,b,1,iii]
		[328]Villanueva et al. 2013[*,#,b,1,4,i,iv]
		[331]Shi et al. 2014[+,b,1,4,v]
		[313]Van Allen et al. 2014[+,b,1,4,v]
		[312]Wagle et al. 2014[#,b,1,4,v]
		[314]Rizos et al. 2014[+,b,1,4,iv]
		[315]Long et al. 2014[#,b,1,4,iv]
Alternative splicing	*BRAF* alternative splicing	[296]Poulikakos et al. 2011[+,b,1,3,i]
		[331]Shi et al. 2014[+,b,1,4,v]
		[312]Wagle et al. 2014[#,b,1,4,v]
		[314]Rizos et al. 2014[+,b,1,4,iv]
Target reactivation: Alteration of upstream effector		
Mutation	*KRAS* mutation	[327]Morris et al. 2013[+,*,b,3,i]
		[331]Shi et al. 2014[+,b,1,4,v]
		[329] Moriceau et al. 2015[+,#,b,1,4,i,iv]
	NRAS mutation	[294]Nazarian et al. 2010[+,b,1,3,4,i,iv]
		[323]Shi et al. 2012[+,b,1,4,i,v]
		[326]Trunzer et al. 2013[+,b,1,c,iv]
		[327]Morris et al. 2013[+,*,b,3,i]
		[331]Shi et al. 2014[+,b,1,4,v]
		[314]Rizos et al. 2014[+,b,1,4,iv]
		[315]Long et al. 2014[#,b,1,4,iv]
		[313]Van Allen et al. 2014[+,b,1,4,v]
		[329]Moriceau et al. 2015[+,#,b,1,4,i,iv]
	CRAF mutation	[332]Antony et al. 2013[+,b,1,3,i]
Amplification	*KRAS* amplification	[333]Little et al. 2011[*,b,2,3,i]
		[325]Hatzivassiliou et al. 2012[*,b,2,3,i]
	BRAF amplification	[334]Corcoran et al. 2010[*,b,1,3,i]
		[333]Little et al. 2011[*,b,1,3,i]
		[328]Villanueva et al. 2013[*,#,b,1,4,i,iv]
		[329]Moriceau et al. 2015[+,#,b,1,4,i,iv]

Table 1-3 (Continued).

Target reactivation: Alteration of upstream effector (continued)		
Deletion	*NF1* deletion	[335]Maertens et al. 2013[+,b,1,3,4,iii,iv] [302]Whittaker et al. 2013[+,a,b,1,3,4,ii,iv] [313]Van Allen et al. 2014[+,b,1,4,v] [297]Shalem et al. 2014[+,b,1,3,v] [336]Nissan et al. 2014[+,a,1,3,i]
Feedback activation	CRAF activation (BRAF:CRAF dimers)	[240]Heidorn et al. 2010[+,a,2,3,i,iii] [241]Hatzivassiliou et al. 2010[+,a,1,3,i] [296]Poulikakos et al. 2010[+,a,1,3,i] [337]Lito et al. 2012[+,a,1,3,i,iii] [338]Hatzivassiliou et al. 2013[*,a,2,3,i] [339]Lito et al. 2014[*,a,2,3,i]
Expression upregulation	Increased ARAF expression	[295]Villanueva et al. 2010[+,*,b,1,3,i]
	Increased CRAF expression	[293]Montagut et al. 2008[+,a,b,1,3,i] [295]Villanueva et al. 2010[+,*,b,1,3,i] [307]Johannessen et al. 2010[+,b,1,3,4,ii,iv] [327]Morris et al. 2013[#,b,3,i]
Alteration of downstream effector		
Mutation	*MEK1* or *MEK2* mutation	[308]et al. 2011[+,b,1,4,iv] [331]Shi et al. 2014[+,b,1,4,v] [313]Van Allen et al. 2014[+,a,b,1,4,v] [312]Wagle et al. 2014[#,b,1,4,v] [314]Rizos et al. 2014[+,b,1,4,iv]
Amplification	*CCND1* amplification	[340]Smalley et al. 2008[+,a,1,3,5]
Deletion	*CDKN2A* loss	[331]Shi et al. 2014[+,b,1,4,v] [341]Franco et al. 2014[*,a,2,,3,5] [329]Moriceau et al. 2015[+,#,b,1,4,i,iv]
Oncogene bypass: associated pathway activation		
Autocrine ligand	EGF	[342]Girotti et al. 2013[+,b,1,3,4,ii,iii,iv] [343]Duncan et al. 2012[*,a,3,ii,iii,v]
	NRG1	[344]Montero Conde et al. 2013[+,*,a,1,3,i]
Cell-extrinsic ligand	EGF, HGF, NRG, FGF	[337]Lito et al. 2012[+,a,1,3,i,iii] [345]Straussman et al. 2012[+,a,1,3,4,ii,iv] [346]Wilson et al. 2012[+,a,1,34,,i,iv]
Deletion	*DUSP4* deletion	[329]Moriceau et al. 2015[+,#,b,1,4,i,iv]
Feedback activation	EGFR	[311]Corcoran et al. 2012[+,a,1,3,i,iii] [347]Prahallad et al. 2012[+,a,1,3,ii] [348]Mirzoeva et al. 2013[*,a,2,3,i,iii]
	HER2, HER3	[349]Sun et al. 2014[*,a,2,3,ii,iii]
	PDGFRβ, DDR1, AXL	[343]Duncan et al. 2012[*,a,3,ii,iii,v]

Table 1-3 (continued).

Oncogene bypass: associated pathway activation (continued)		
Expression upregulation	EGFR	[342]Girotti et al. 2013[+,b,1,3,4,i,iii,iv] [310]Sun et al. 2014[+,⋆,b,1,4,i,iv] [300]Konermann et al. 2014[+,b,1,3,v]
	IGF1R	[295]Villanueva et al. 2010 [+,⋆,b,1,3,4,i,iv] [314]Rizos et al. 2014[+,b,1,4,iv]
	PDGFRβ	[294]Nazarian et al. 2010[+,b,1,3,4,ii,iv] [323]Shi et al. 2012[+,b,1,4,i,v] [344]Montero Conde et al. 2013[+,⋆,a,1,3,i] [327]Morris et al. 2013[#,b,3,i] [310]Sun et al. 2014[+,⋆,b,1,4,i,iv]
	HER2/HER3	[344]Montero Conde et al. 2013[+,⋆,a,1,3,i]
	COT	[307]Johannessen et al. 2010[+,b,1,3,4,ii,iv]
	MLK1-4	[350]Marusiak et al. 2014[+,b,1,3,4,i,iii,iv]
Oncogene bypass: orthogonal pathway activation		
Autocrine ligand	IL-6, IL8	[351]Bid et al. 2013[⋆,b,1,3,iii]
Mutation	*PIK3CA* mutation	[352]Halilovic et al. 2010[⋆,a,2,3,i] [313]Van Allen et al. 2014[+,b,1,4,v]
	AKT1 or *AKT3* mutation	[331]Shi et al. 2014[+,b,1,4,v] [314]Rizos et al. 2014[+,b,1,4,iv]
Deletion	*PTEN* deletion	[353]Paraiso et al. 2011[+a,1,3,i] [354]Xing et al. 2012[⋆,a,1,3,i] [331]Shi et al. 2014[+,b,1,4,v] [313]Van Allen et al. 2014[+,b,1,4,v] [329]Moriceau et al. 2015[+,#,b,1,4,i,iv]
Feedback activation	FGFR/STAT3	[355⋆,a,2,3,i,iii,iv]
Expression upregulation	YAP1	[301]Johannessen et al. 2013[+,⋆,#,b,1,3,ii] [309]Lin et al. 2015[+,⋆,#,a,1,2,3,4,ii,iii,iv]
	GPCRs	[301]Johannessen et al. 2013[+,⋆,#,b,1,3,ii]
	MITF	[313]Van Allen et al. 2014[+,b,1,4,v] [Δ301]Johannessen et al. 2013[+,⋆,#,b,1,3,4,ii,iv]
Cell state	MITF low, NFκB high	[Δ356]Konieczkowski et al. 2014[+,⋆,#,a,b,1,3,4,ii,iv]

[+]BRAFi
*MEKi
[#] BRAFi + MEKi
[a] Intrinsic resistance
[b] Acquired resistance
[1] *BRAF*-mutant cancer
[2] *KRAS*-mutant cancer
[3] Proposed on the basis of preclinical data
[4] Clinically validated
[i] Preclinical data from human cancer cell lines – candidate approach
[ii] Preclinical data from human cancer cell lines – unbiased approach
[iii] *In vivo* preclinical data – GEMM, PDX
[iv] Profiling clinical samples – candidate approach
[v] Profiling clinical samples – unbiased approach

[Δ]Endogenous MITF expression is regulated by the MAPK pathway, and low endogenous MITF levels correlates with resistance to MAPK pathway inhibition in *BRAF*-mutant cells[356]. Contrastingly, exogenous MITF expression[301] or MITF amplification[313], which are not regulated by the MAPK pathway, mediate resistance to MAPK pathway inhibition.

pathway is not restored. Mechanisms of resistance to BRAF or MEK inhibitors from orthogonal pathway activation include increased signaling through the PI3K[313,314,327,329,331,352-354,357], STAT3[351,355], or cAMP[301] pathways; or altered expression of transcription factors such as YAP1[301,309] or MITF[301,313,356].

While diverse mechanisms of intrinsic and acquired resistance to BRAF and/or MEK inhibitor therapy have been described, several remain poorly characterized. Most studies on mechanisms of resistance to BRAF or MEK inhibitor therapy have been candidate-based, and even unbiased studies have typically focused their validation efforts on known effectors or regulators of the MAPK pathway. Several resistance studies have described cell line clones or clinical samples with yet unidentified mechanisms of resistance[293,312-315], highlighting that our understanding of resistance to MAPK pathway inhibition is not yet complete. A more comprehensive understanding of the molecular basis of resistance will improve clinical assessment and rational drug combinations in stratified patient populations.

Recent technological advances have provided the means to perform comprehensive gain- and loss-of-function (GOF and LOF) screens in in mammalian cells. Validated expression libraries enable GOF experiments to study the effects of gene overexpression[298]. Complementary LOF studies can be conducted using CRISPR-Cas9 libraries[297,358]. In Chapter 2, we describe our usage of these high-throughput screening techniques to systematically identify mechanisms of resistance to MEK or BRAF inhibitor therapy.

CHAPTER TWO

Gain- and loss-of-function screens identify mechanisms of resistance to MAPKi in RAS-mutant cells

This chapter has been adapted from

Krall, E.B.*, Wang, B.*, Aguirre, A.J., Doench, J.G., Jänne, P.A., and Hahn, W.C. KEAP1 loss promotes resistance to BRAF, MEK, and EGFR inhibition in lung cancer. *In submission.*

Wang, B.*, Krall, E.B.*, Aguirre, A.J.*, Widlund, H.R., Doshi, M.B., Sicinska, E., Sulahian, R., Goodale, A., Cowley, G.S., Piccioni, F., Doench, J.G., Root, D.E., and Hahn, W.C. ATXN1L, CIC, and ETS Transcription Factors Modulate Sensitivity to MAPK Pathway Inhibition, *in submission.*

Contributions

Belinda Wang, Andrew Aguirre, Glenn Cowley, and William Hahn designed the genome scale ORF screen in PATU8902; Belinda Wang optimized and performed the screen. Andrew Aguirre, Rita Sulahian, and Federica Piccioni designed the genome scale CRISPR-Cas9 screen in PATU8988T; Amy Goodale performed the screen. Rita Sulahian contributed drug titration data for PATU8988T (**Figure 2-5A,B**). Elsa Beyer Krall, John Doench, and William Hahn designed the genome scale CRISPR-Cas9 screens in lung cancer cell lines; Elsa Beyer Krall and Belinda Wang optimized and performed the screens. Elsa Beyer Krall contributed drug titration data for the lung cancer cell lines (**Figure 2-6**). Belinda Wang, Andrew Aguirre, and William Hahn designed the genome scale CRISPR-Cas9 screen in PATU8902; Belinda Wang, Andrew Aguirre, Amy Goodale, and Glenn Cowley performed the screen. Elsa Beyer Krall and John Doench designed the candidate mini-pool CRISPR-Cas9 screens; Elsa Beyer Krall and Belinda Wang optimized and performed the screens. Elsa Beyer Krall contributed SKMEL2 drug optimization data (**Figure 2-8B**). Belinda Wang, Elsa Beyer Krall, Andrew Aguirre, John Doench, Glenn Cowley, and Federica Piccioni analyzed screening data. Belinda Wang performed enrichment analyses on all screening data.

2.1 Introduction

Targeted kinase inhibitors have significantly improved response and survival in cancers driven by a dominant oncogene, such as *EGFR*-mutant lung cancer and *BRAF*-mutant melanoma[238,284]. However, despite initial success, resistance mechanisms to therapy quickly arose[308,316]. As discussed in Chapter 1.4.1, tumors may be intrinsically resistant to targeted therapy, in which cells never respond to therapy, or acquire resistance after an initial period of response. Maximizing the potential of targeted therapies requires a thorough understanding of the resistance mechanisms that limit their efficacy.

The recent development of genome scale open reading frame (ORF)[298], RNAi[299], and CRISPR-Cas9[297,300,358] libraries have enabled the systematic identification of GOF or LOF events that confer drug resistance[301,302]. These comprehensive and scalable functional screens have the potential to uncover diverse resistance mechanisms. An improved understanding of the molecular pathways that mediate resistance to targeted therapy could nominate predictive biomarkers of intrinsic resistance to stratify patient populations and inform rational drug combinations that delay or prevent acquired resistance.

Several MEK and BRAF inhibitors are currently in clinical trials for *RAS*- and *RAF*-mutant cancers. Early results suggest that, while a subset of patients respond to therapy, MAPK pathway inhibition confers limited clinical benefit to many patients with *RAS*-mutant pancreatic or colorectal cancer[248,249] or *BRAF*-mutant lung and colorectal cancer[359]. As described in Chapter 1.4.3, preclinical and clinical studies have shown that a major mode of intrinsic and acquired resistance to MEK or BRAF inhibitor

monotherapy in *RAS*- or *BRAF*-mutant cancers is reactivation of the RTK-RAS-MAPK pathway by diverse mechanisms[236,237]. These mechanisms include loss of feedback inhibition[311,343]; upregulated RTK signaling[294,295]; *NF1* inactivation[302]; or increased NRAS[294], RAF[240,241,295,296,330], COT[307], or MEK activity[308,322]. These studies, discussed in Chapter 1.4.3 and detailed in **Table 1-3** highlight a major role for sustained RTK/MAPK signaling in mediating resistance to pharmacologic inhibition of this pathway in *RAS*- or *BRAF*-mutant cancers.

The majority of BRAF and MEK inhibitor resistance studies have been conducted in the context of *BRAF*-mutant melanoma cell lines or clinical samples. Indeed, to our knowledge, the only genome scale GOF and LOF resistance screens have been performed in A375, a *BRAF*-mutant melanoma cell line[297,301,302]. This limits the scope of our understanding, for lineage and mutational context likely influence response to MAPK pathway inhibition and accompanying resistance mechanisms. For example, while BRAF inhibition induces cell death in *BRAF*-mutant melanoma, most *BRAF*-mutant colon cancer cells are resistant due to feedback activation of EGFR[311,347], and *RAS*-mutant cells are resistant due to CRAF-mediated reactivation of the MAPK pathway[240-242].

Here, we performed a genome scale ORF screen and six genome scale CRISPR-Cas9 knockout screens to study mechanisms of resistance to MAPK pathway inhibitor therapy in *RAS*- or *RAF*-mutant pancreatic cancer or lung cancer cell lines. In addition, candidate genes identified from one of the genome scale CRISPR-Cas9 screens were further screened in *NRAS*-mutant melanoma cell lines treated with a MEK inhibitor.

2.2 Results

2.2.1 Genome scale ORF screen in a *KRAS*-mutant pancreatic cancer cell line

We performed a genome scale ORF screen to identify genes that confer resistance to MEK inhibition in the *KRAS*-mutant pancreatic cancer cell line PATU8902. We screened PATU8902 cells using two different doses of the allosteric MEK1/2 inhibitor trametinib (50 nM and 100 nM) that robustly inhibit ERK phosphorylation and induce proliferative arrest or cell death (**Figure 2-1**). Screening was performed using a lentivirally delivered pooled ORF library containing ~16,000 ORFs[298]. PATU8902 cells were infected with the ORF library, passaged for 5 days in puromycin, and treated with trametinib for 7, 14, or 21 days (**Figure 2-2A**). Levels of phospho-ERK1/2 (p-ERK) were assessed at different time points in the screen to determine the efficiency of MAPK pathway inhibition (**Figure 2-2B).** At early stages of the screen (Days 2 and 7), p-ERK was robustly suppressed by trametinib treatment. However, by Day 21 of the screen, p-ERK levels had surpassed pre-treatment expression levels, suggesting that a sub-population of cells with restored MAPK pathway signaling had overtaken the cell population. The increase in p-ERK expression corresponded to an increase in cell proliferation during the course of the screen, suggesting that a population of cells resistant to trametinib treatment was selected for over time (**Figure 2-2C**).

We identified ORFs that became enriched in the trametinib-treated samples compared to the pre-treatment (Day -1) samples. ORFs that more than tripled in representation ($\log_2$(fold change) > 1.58) on average across all replicates at any time point were considered to be “hits” (**Figure 2-3**). Using this metric, hits have an average $\log_2$(fold change) at least 4 standard deviations above the mean ($p < 10^{-4}$). We

examined the genes that scored in this screen to determine if they grouped into particular functional categories. As expected, many genes in the MAPK pathway scored, including several RTKs (EGFR, FGFR2, NTRK2, and RET), KRAS, and all three RAF paralogs (ARAF, BRAF, and RAF1/CRAF). TCL1B, an AKT co-activator, was also a hit. This is in agreement with prior observations that increased signaling through the PI3K pathway can compensate for loss of MAPK signaling[295,327,331,353,354]. The transcriptional co-activator WWTR1/TAZ was also significantly enriched. TAZ is a paralog of YAP1, whose overexpression has previously been shown to promote resistance to MAPK pathway inhibition[309] or KRAS depletion[360,361] in *KRAS*-mutant cells. In addition to these expected pathways, several of the genes that scored are involved in metabolic pathways (OSTC, PCMTD1, HY1, and NCSTN), DNA repair (MLH1 and APTX), or RNA polymerase function (GPN1, and POLR2F).

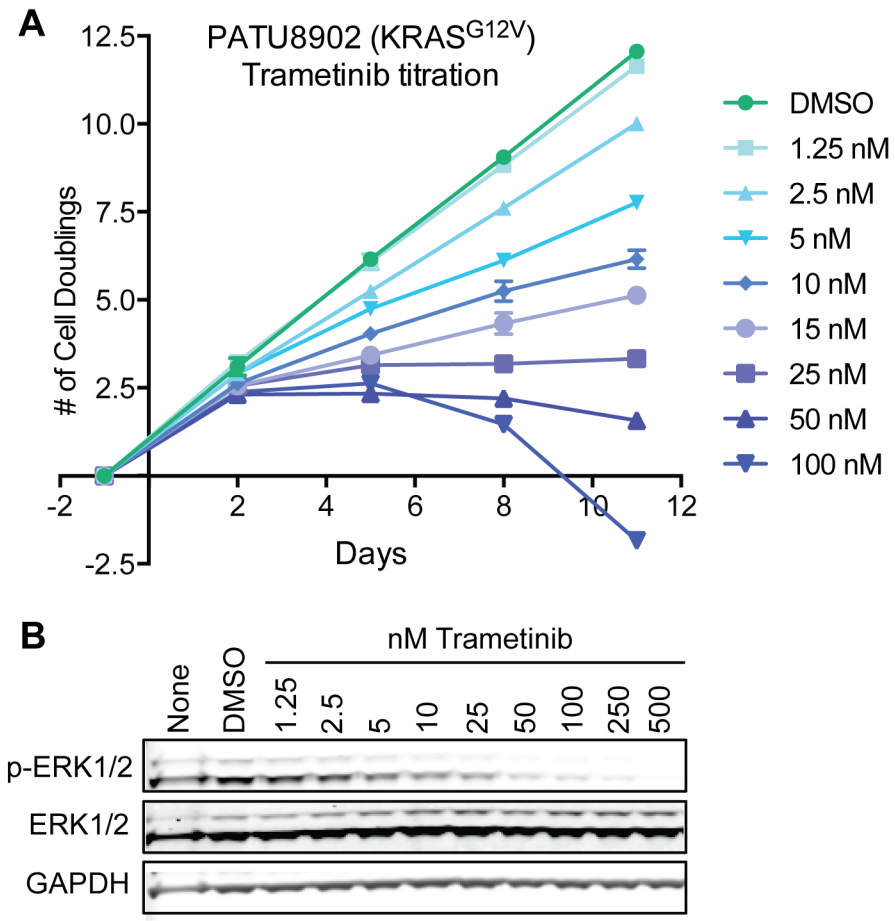

Figure 2-1. Optimization of screening conditions in PATU8902. (A) Proliferation of PATU8902 cells treated with the indicated concentration of trametinib, *n* = 2 replicates. **(B)** Immunoblot analysis of PATU8902 cells treated with the indicated concentration of trametinib for 24 hours.

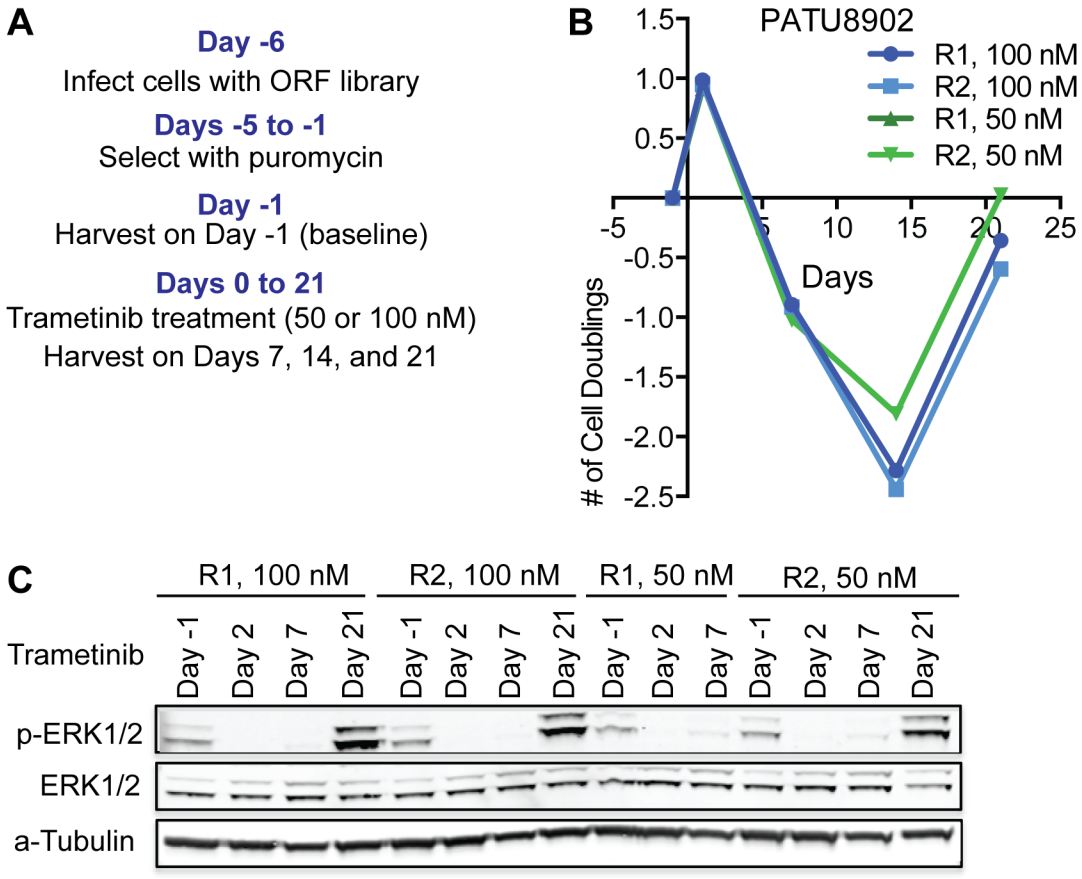

Figure 2-2. Genome scale ORF screen in a *KRAS*-mutant pancreatic cancer cell line. (A) Outline of genome scale ORF screen in PATU8902 cells treated with trametinib. **(B)** Immunoblot analysis of p-ERK expression on the indicated days of the screen. R = replicate. **(C)** Proliferation of PATU8902 cells infected with the ORF library during the 21 days of trametinib treatment in the screens. R = replicate.

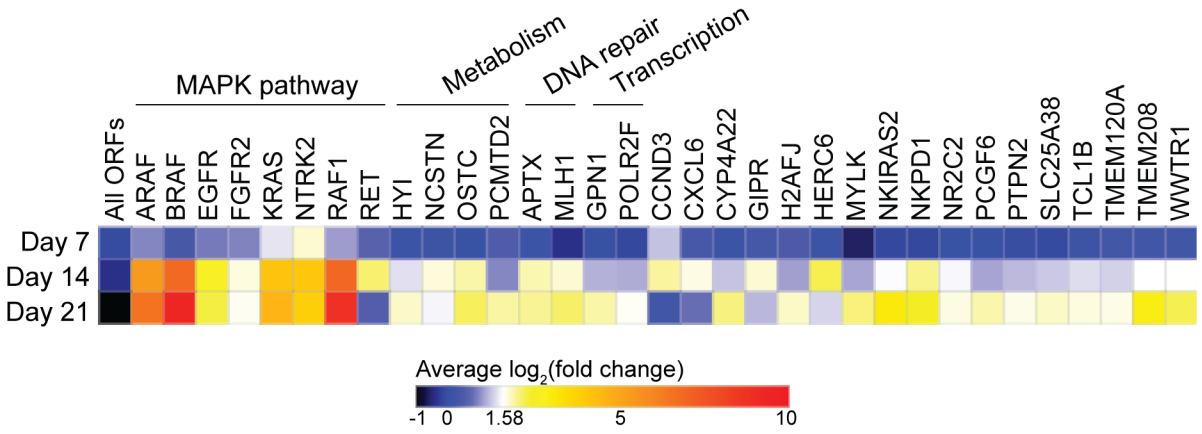

Figure 2-3. Functional grouping of genes that mediate trametinib resistance. Average $\log_2$(fold-change) in ORF representation across all replicates at the indicated time points. ORFs that were significantly enriched ($\log_2$(fold-change) ≥ 1.58) in at least one time point are shown. “All ORFs” indicates the average $\log_2$(fold-change) of all the ORFs included in the screen. *N* = 4 biological replicates (2 treated with 50 nM trametinib and 2 with 100 nM trametinib) for Day 7, *n* = 3 biological replicates (1 treated with 50 nM trametinib, 2 treated with 100 nM trametinib) for Days 14 and 21.

2.2.2 Genome scale CRISPR-Cas9 screens in *RAS*- and *RAF*-mutant pancreatic and lung cancer cell lines

To identify genes whose deletion promotes proliferation/survival in the context of MEK and BRAF inhibition in lung cancer cell lines with different *RAS* or *BRAF* mutations, we performed six genome scale CRISPR-Cas9 knockout screens (**Figure 2-4**). We screened two $KRAS^{G12V}$ pancreatic cancer cell lines (PATU8902 and PATU8988T) in the context of trametinib treatment. We screened PATU8902 cells with a relatively high dose of 100 nM trametinib, which robustly inhibits ERK phosphorylation and induces proliferative arrest or cell death (**Figure 2-1A,B**). For PATU8988T, we performed the screen using a moderate dose of 10 nM trametinib, which modestly suppresses ERK phosphorylation and decreases the rate of cell proliferation by approximately 50% (**Figure 2-5A-B**). We used these different doses of trametinib to increase the dynamic range of the screens (**Figure 2-5C,D**). We also used different genome scale sgRNA libraries with <5% overlapping sgRNA sequences for the PATU8902 (GeCKOv2 library[297]) and PATU8988T (Avana library[358]) screens to mitigate the possibility that genes identified in these experiments were the consequence of off-target effects.

In addition, we performed genome scale CRISPR-Cas9 screens in three lung cancer cell lines (Figure 2-4). We performed three screens with the MEK inhibitor trametinib in NCIH1299 ($NRAS^{Q61K}$), HCC364 ($BRAF^{V600E}$), and CALU1 ($KRAS^{G12C}$). One additional screen was performed using HCC364 cells treated with the BRAF inhibitor vemurafenib. For these screens, we used the lowest concentration of drug that inhibited ERK phosphorylation and resulted in proliferative arrest (**Figure 2-6**).

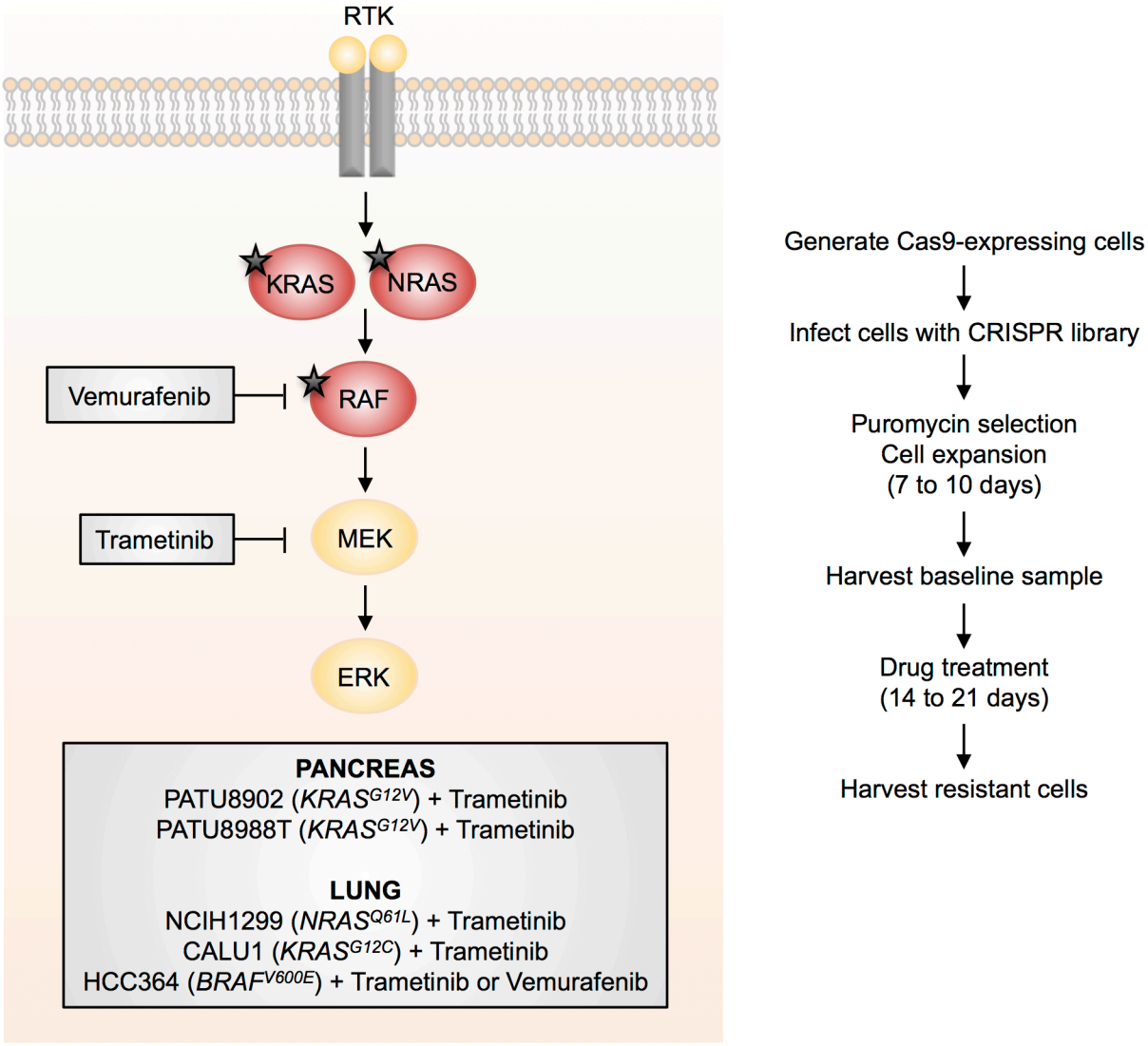

Figure 2-4. Screening strategy for genome scale CRISPR-Cas9 screens.

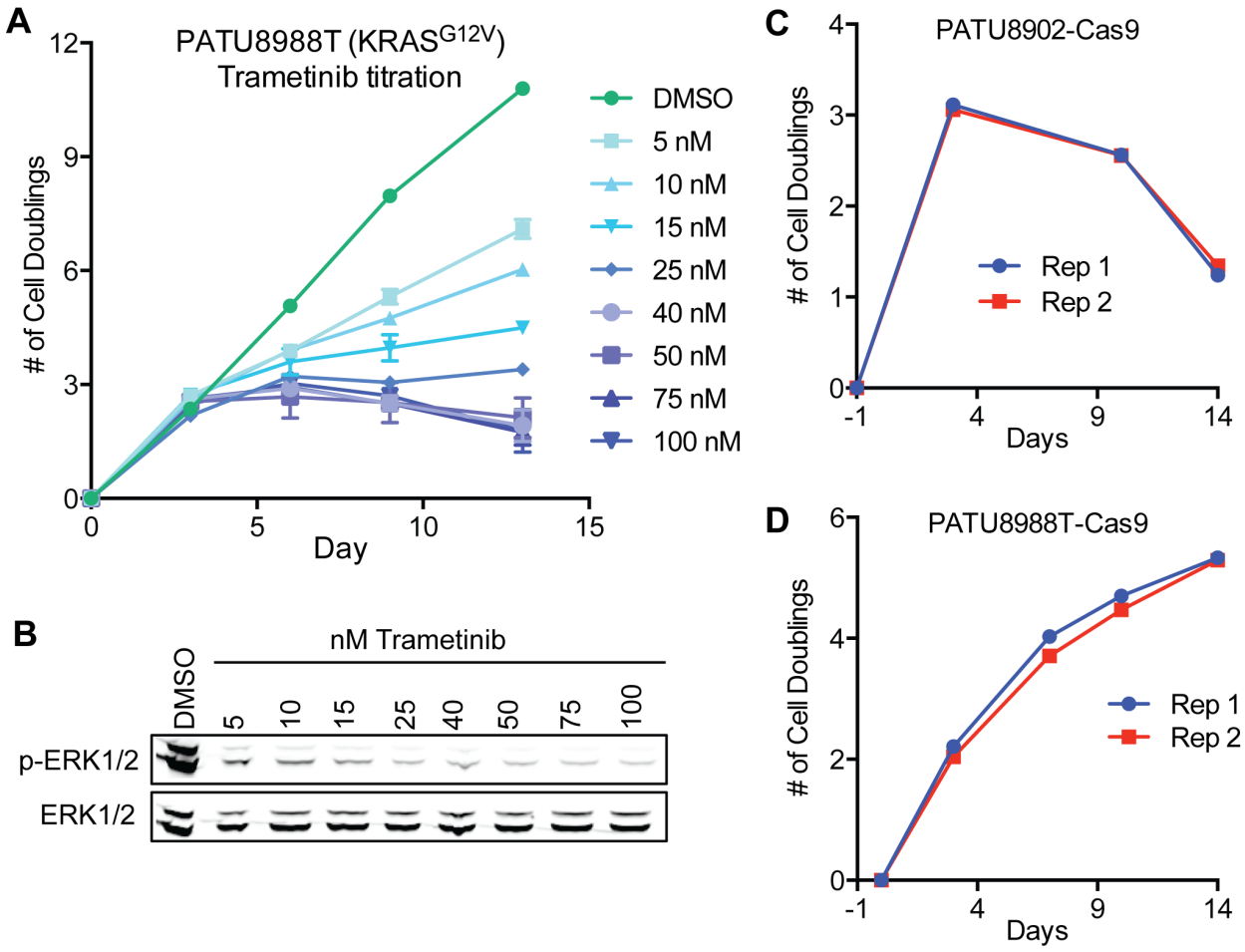

Figure 2-5. Genome scale CRISPR-Cas9 screens in *KRAS*-mutant pancreatic cancer cell lines. (A) Proliferation of PATU8988T-Cas9 cells treated with the indicated concentration of trametinib, *n* = 2 replicates **(B)** Immunoblot analysis of PATU8988T cells treated with the indicated concentration of trametinib for 17 days. **(C,D)** Proliferation of PATU8902-Cas9 **(C)** or PATU8988T-Cas9 **(D)** cells infected with the CRISPR library during the 14 days of trametinib treatment in the screens. Rep = replicate. Rita Sulahian performed the experiments in **(A)** and **(B).** Federica Piccioni and Amy Goodale contributed the data for **(D).**

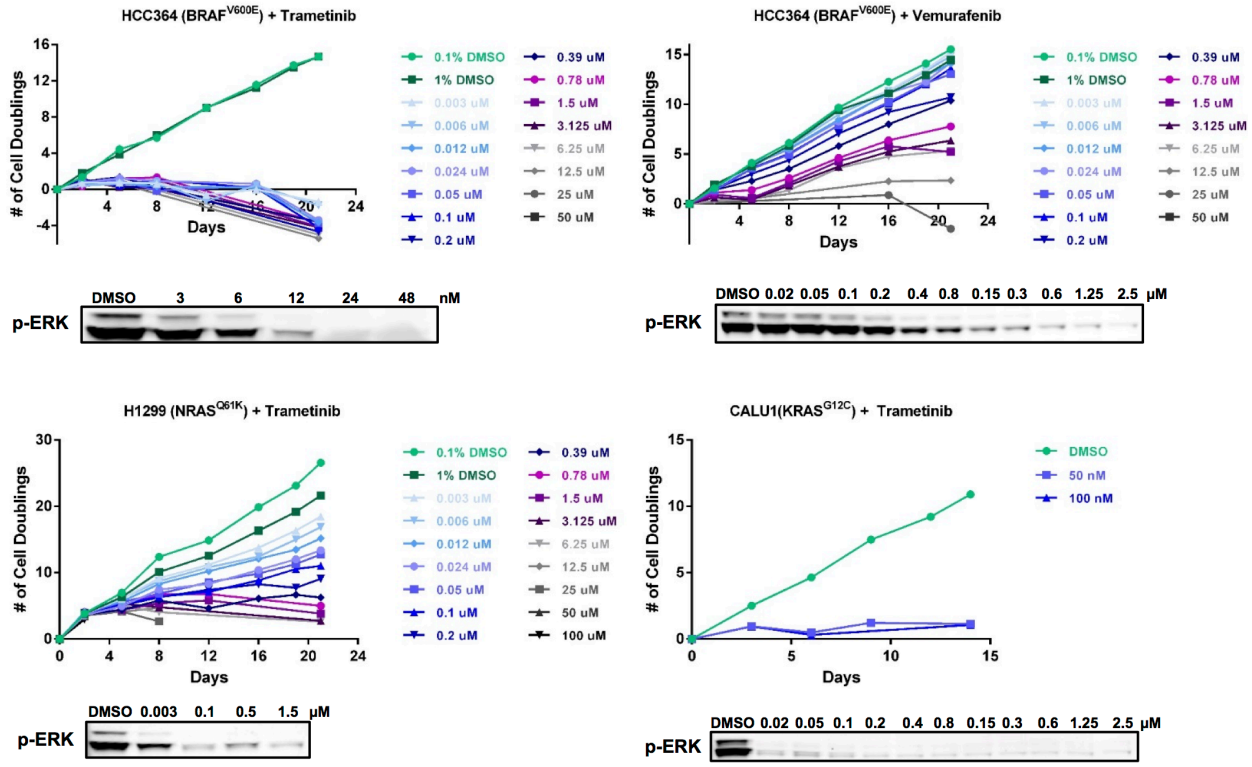

Figure 2-6. Optimization of screening conditions in lung cancer cell lines. Cell counting or immunoblot analysis of NSCLC cells treated with the indicated amount of drug. For immunoblot analysis, cells were treated with the indicated concentration of trametinib for 90 minutes. Experiments were performed by Elsa Beyer Krall.

Screening was performed using a lentivirally delivered two-vector CRISPR-Cas9 system[297,358] (**Figure 2-4**). Specifically, Cas9-expressing cells were infected with either the genome scale CRISPR-Cas9 knockout (GeCKOv2)[297] or Avana[358] sgRNA library and passaged for 7-10 days to allow for genomic editing. Subsequently, cells were harvested for a baseline time point or passaged in the presence of trametinib or vemurafenib. Genomic DNA was isolated after 14 or 21 days of drug treatment, and sgRNA representation was quantified by PCR and massively parallel sequencing. sgRNAs that became enriched in the drug-treated samples compared to the baseline sample were identified.

The CRISPR libraries used in these screens include multiple sgRNAs targeting each gene (6 sgRNAs per gene in GeCKOv2[297], 4 sgRNAs per gene in Avana[358]). We reduced the sgRNA-level $\log_2$(fold change) data to a gene-level "enrichment score" by calculating the probability of obtaining the observed distribution of sgRNAs targeting the gene, assuming an underlying binomial distribution, and re-scaling it by taking the negative logarithm (further details in Materials and Methods section). Using this metric, high enrichment scores indicate genes whose sgRNAs were consistently and/or robustly enriched in the screen. We defined "hits" as genes whose enrichment score was greater than 5 in any one of the screens, and identified 90 hits (**Figure 2-7**).

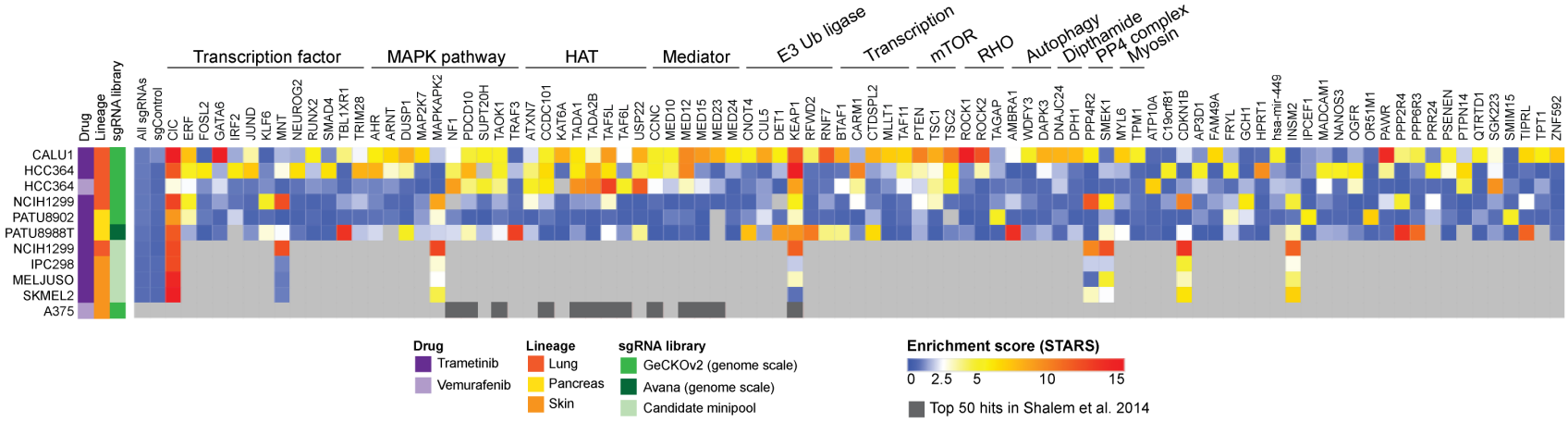

Figure 2-7. Candidate genes whose knockout confers resistance to MAPKi segregate into different functional groups. Enrichment score (STARS score) of genes whose knockout confer resistance to MAPKi in the genome scale CRISPR-Cas9 screens and the candidate mini-pool CRISPR-Cas9 screens. Genes that had an enrichment score ≥ 5 in at least one genome scale screen are displayed. Light gray boxes indicate that the gene was not assessed. In addition, hits from a previously described genome scale CRISPR-Cas9 screen performed in A375 (*BRAF*^{V600E} melanoma)[297] are indicated with dark gray boxes. Enrichment scores were calculated from $n \geq 2$ replicates. Abbreviations: E3 Ub ligase (E3 ubiquitin ligase), HAT (histone acetyltransferase).

2.2.3 Mini-pool CRISPR-Cas9 screens in *NRAS*-mutant lung cancer and melanoma cell lines

We were interested in determining whether genes whose deletion conferred resistance to MEK inhibitor therapy in the *NRAS*-mutant lung cancer cell line NCIH1299 would also confer resistance to MEK inhibitor therapy in three *NRAS*-mutant melanoma cell lines (IPC298, MELJUSO, and SKMEL2). We created a candidate mini-pool sgRNA library that contained 10-11 sgRNAs targeting each of the 8 most significant gene hits from the NCIH1299 screen (CIC, CKN1B, INSM2, KEAP1, MAPKAPK2, MNT, PPP4R2, and SKMEK1). We also used a control mini-pool library containing ~1000 non-targeting negative control sgRNAs. To perform the mini-pool screens, cells were separately infected with the candidate mini-pool library and the control mini-pool library. After selection, cells infected with the candidate mini-pool library were pooled with cells infected with the control mini-pool library in a 1:10 ratio. Cells were subsequently harvested for the Day 0 time point or passaged in the presence of trametinib for 14 days (**Figure 2-8**). Genomic DNA was isolated from the Day 14 and Day 0 samples, and hits were identified in the same manner as in the genome scale CRISPR-Cas9 knockout screens.

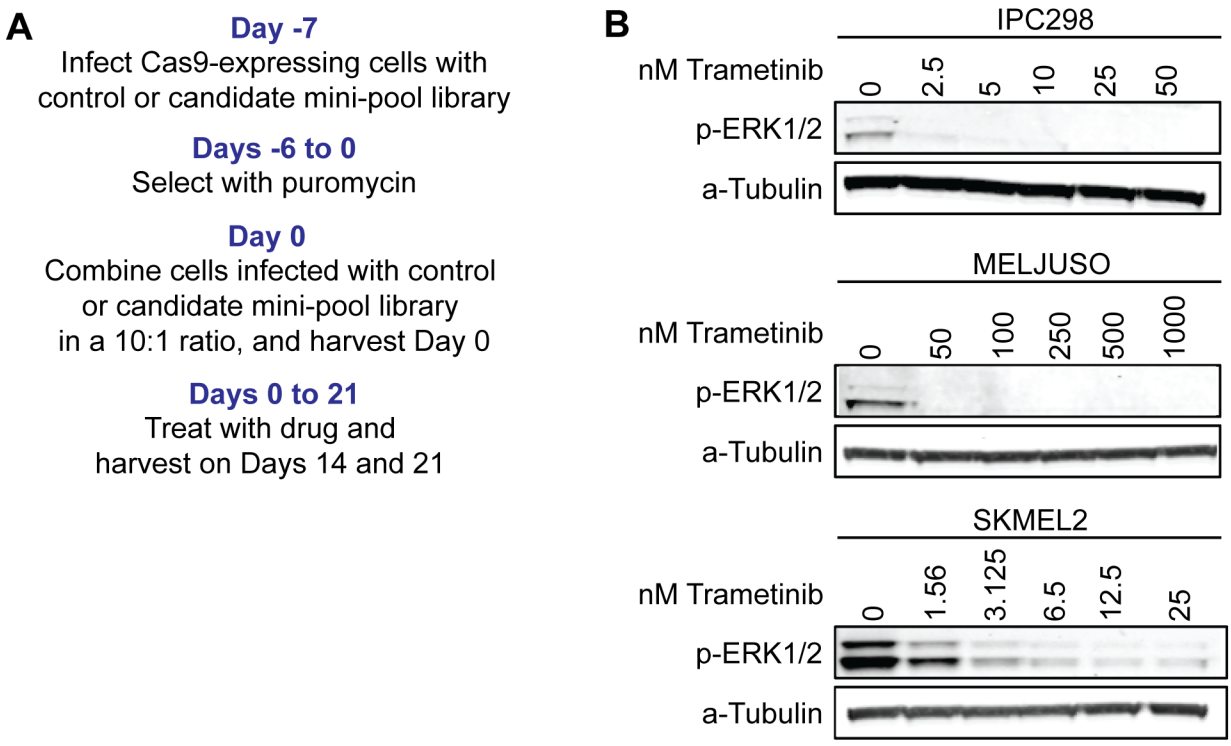

Figure 2-8. Mini-pool screens in *NRAS*-mutant melanoma cell lines. **(A)**. Outline of screening strategy. **(B)** Immunoblot analysis of cells treated with the indicated amount of trametinib for 24 hrs. The SKMEL2 immunoblot was performed by Elsa Beyer Krall.

2.2.4 CRISPR-Cas9 screen hits

The genes that scored as hits in the genome scale and mini-pool CRISPR-Cas9 resistance screens are compiled in **Figure 2-7**. Genes that scored in a previously published genome scale CRISPR-Cas9 vemurafenib resistance screen the *BRAF*^{V600E} melanoma cell line A375 are indicated[297]. We annotated the functions of each of the genes that scored in these screens to determine if particular functional categories scored repeatedly. As anticipated, several genes in the MAPK pathway scored, including NF1, a negative regulator of RAS/MAPK signaling[43], and DUSP1, a dual-specificity phosphatase that inhibits ERK[362]. We also found several positive regulators or effectors of p38/JNK MAPK signaling, suggesting that other MAPK pathways may play a pro-apoptotic or anti-proliferative role in these cells. PTEN, a negative regulator of PI3K/AKT signaling, and TSC1 and TSC2, negative regulators of mTOR signaling, also scored, indicating that increased signaling through the PI3K/AKT/mTOR pathway may compensate for loss of RAS/MAPK signaling[295,327,331,353,354]. Similarly, PTPN14, a negative regulator of YAP[363], was a hit in a subset of cell lines, confirming that YAP upregulation may promote resistance to MAPK pathway inhibition[309].

In addition to these expected pathways, several of the genes that scored are components of histone acetyltransferase (HAT) complexes or of the Mediator complex. There were also several genes whose products are members of E3 ubiquitin ligase complexes. Multiple transcription factors scored, as well as general transcription machinery genes. Other functional categories for which multiple genes scored include RHO signaling and histidine post-translational modifications. We observed that the

genes KEAP1 and CIC scored the most consistently across different screens (6 times and 9 times, respectively) (**Figures 2-7** and **2-9**).

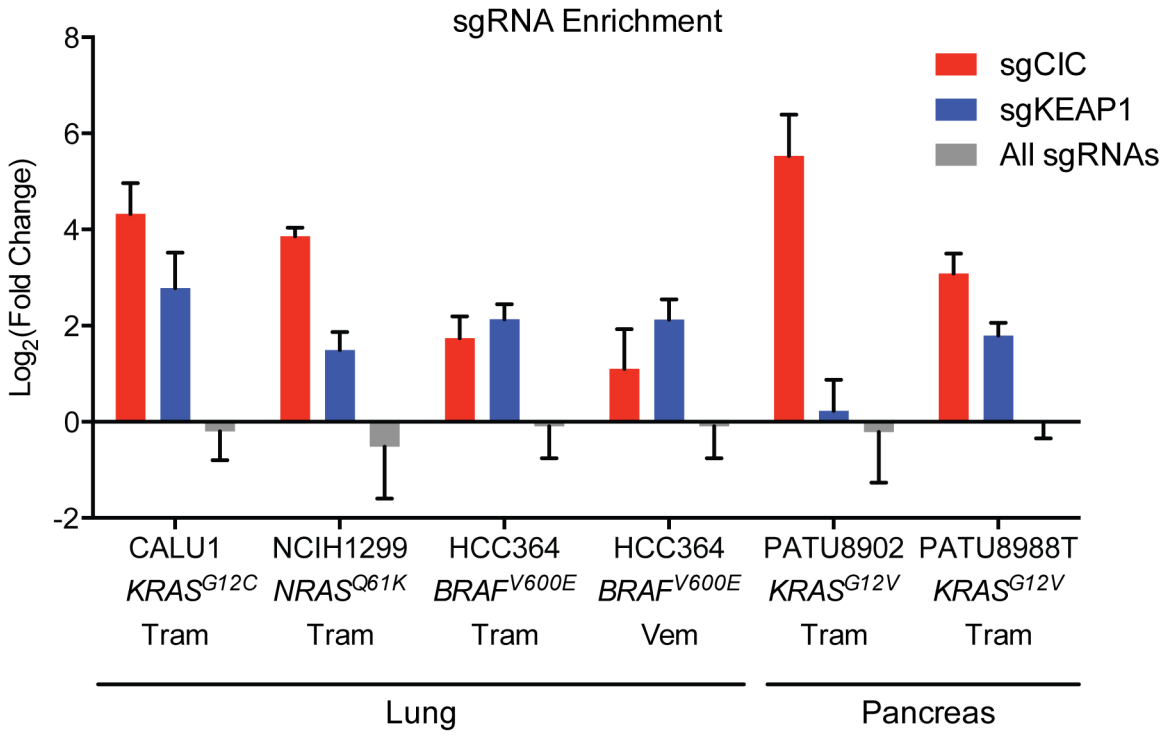

Figure 2-9. Enrichment of sgRNAs targeting *CIC* and *KEAP1* in genome scale CRISPR-Cas9 screens. Average $\log_2$(fold change) of the 3 most enriched sgRNAs targeting CIC (red) or KEAP1 (blue) on Day 14 of the indicated genome scale CRISPR-Cas9 screen. Gray bars indicate the average $\log_2$(fold change) of all the sgRNAs in the screen. Error bars represent standard deviation.

2.3 Discussion

We report the use of systematic ORF and CRISPR-Cas9 screening approaches to identify GOF and LOF events that mediate resistance to MAPKi in *RAS*- or *BRAF*-mutant pancreatic or lung cancer cell lines. To our knowledge, these represent the first instances of genome scale cDNA and CRISPR-Cas9 knockout screens in non-melanoma cancer cell lines for genes that modulate sensitivity to MAPKi. These screening approaches have identified both known and novel mediators of resistance to MAPKi. We found that the most potent GOF events that conferred resistance to MEK inhibition in a *KRAS*-mutant pancreatic cancer cell line were components of the RTK-RAS-MAPK pathway. Contrastingly, the majority of LOF events that mediated resistance to MAPKi in *RAS*- or *RAF*- mutant pancreatic and lung cancer cell lines were not direct regulators or effectors of MAPK signaling.

2.3.1 GOF mechanisms of resistance

The genome scale ORF screen identified several mediators of resistance that had been previously identified in an ORF screen for genes that complement EGFR inhibition in an *EGFR*-mutant lung cancer cell line (FGFR2, NTRK2, and RAF1/CRAF)[303] and in ORF screens for mediators of resistance to BRAF and MEK inhibition in a *BRAF*-mutant melanoma cell line (FGFR2, RAF1/CRAF, and WWTR1/TAZ)[301,307]. This suggests that GOF events that reactivate the RTK/MAPK pathway or upregulate the Hippo-YAP/TAZ pathway are generalizable mechanisms of resistance to MAPKi in cancer cells of different lineages and driver mutations.

Each of these ORF screens also identified unique GOF mechanisms of resistance to MAPKi, such as MITF, COT/MAP3K8, AXL, and PAK3 in *BRAF*-mutant melanoma cells[301,307]; MST1R, MOS, NTRK1, ITK, and FGFR1 in *EGFR*-mutant lung cancer cells[303]; and MLH1 and RET in *KRAS*-mutant pancreatic cancer cells. These differences are likely attributable to a combination of technical and biological dissimilarities. Some of the previously published ORF screens[303,307] tested only kinase libraries, which did not include several of the genes identified here. In addition, prior GOF screens[301,303,307] were conducted in arrayed format whereas the screen described here was performed in pooled format. Arrayed screens, in which each ORF is tested in individual wells, are likely better able to identify genes with autocrine effects and genes with a weaker rescue phenotype. In a pooled setting, where ORFs are competing against one another, those with the strongest pro-proliferative effect may rapidly take over the cell population, eclipsing other ORFs that confer a weaker resistance phenotype.

In addition, differences in cell lineage, co-existing genetic alterations, and drug used in the screens may underlie some of the unique GOF findings. For example, overexpression of MITF, which is a master regulator of melanocyte development and a melanoma-specific oncogene[364], was identified as a mechanism of resistance to MAPKi only in the A375 melanoma screens[301]. Beyond cell lineage, the cell lines screened here and in previous studies harbor many unique genetic alterations that likely influence the list of hits identified. Finally, each of these screens were performed using different kinase inhibitors – erlotinib (EGFRi), PLX4720 (RAFi), AZD6244 or trametinib (MEKi), or

VRT11E (ERKi), which may also contribute to differences in ORF screen findings[301,303,307].

2.3.2 LOF mechanisms of resistance

In the genome scale CRISPR-Cas9 screens, some genes appeared to be broadly generalizable modifiers of sensitivity to MAPKi. For example, CIC knockout conferred resistance in 5 of the 6 genome scale screens and in all 4 mini-pool screens, and KEAP1 deletion conferred resistance to MAPKi in all of the lung cancer cell line screens. However, the majority of hits were significant in only one or two screens. Again, these differences likely reflect both technical and biological effects.

The majority of cell lines were screened with the GeCKOv2 library[297], a first generation CRISPR library that was created prior to the identification of sgRNA sequence features that predict activity. PATU8988T was screened using the Avana CRISPR library[358], which is composed of sgRNAs designed to maximize potency and penetrance and minimize off-target effects. It is possible that some of the hits identified uniquely in PATU8988T, such as TRAF3 and AMBRA1, were not effectively knocked out by sgRNAs in the first-generation GeCKOv2 library. The dose of drug used in the screen likely also affected screen findings. While all cell lines were screened using a dose of trametinib that significantly abrogated p-ERK expression, some cell lines were able to proliferate during the course of the screen (PATU8988T, NCIH1299, HCC364/vemurafenib) whereas in other cell lines this dose of drug induced cytostasis (CALU1, HCC364/trametinib) or cytotoxicity (PATU8902). Some genes may modulate resistance to MAPKi only in certain proliferative contexts. Interestingly, the cytotoxic PATU8902 screen identified the fewest hits, suggesting that fewer genes may be able

to confer resistance to MAPKi-induced cell death than to MAPKi-induced cytostasis. In addition, the actual dose of trametinib used in the screens varied widely (from 10 nM to 1.5 μM). Although trametinib is a selective MEK1/2 inhibitor with little activity against other kinases[365], off-target effects may have contributed to idiosyncratic screen results.

Lastly, differences among cell lines, such as cell lineage and coexisting mutations, likely played a role in determining cell-line specific hits. We screened the 8 strongest hits from the genome scale screen in *NRAS*-mutant NCIH1299 lung cancer cells in 3 additional *NRAS*-mutant melanoma cell lines. While all 8 genes validated in the NCIH1299 candidate mini-pool screen, highlighting the low false-positive rate of the hits identified in our primary genome scale screen, only 1 gene (CIC) scored in the 3 *NRAS*-mutant melanoma cell lines tested (**Figure 2-7**). This suggests that the other 7 genes assessed modulate resistance uniquely in NCIH1299, possibly due to differences in lineage or in coexisting genetic alterations between NCIH1299 and the melanoma cell lines.

2.3.3 Conclusion

Overall, the ORF screen we performed suggests that the strongest GOF mechanisms of resistance to MAPK pathway inhibition involve reactivation of the RTK-RAS-MAPK pathway. This reflects previously reported mechanisms of intrinsic and acquired resistance to MAPKi from *in vitro* experiments as well as clinical specimens (**Table 1-3**). Contrastingly, the majority of genes identified in the CRISPR-Cas9 screens have not previously been identified as mechanisms of resistance to MAPKi in *RAS*- or *BRAF*-mutant cancers. To our knowledge, of our hits, only loss of NF1[302,313,336,353] or

PTEN[331] have been previously studied as a mechanism of resistance to BRAF or MEK inhibition.

Identifying mechanisms of resistance to MAPKi is of considerable clinical interest. BRAF and MEK inhibitors are currently being tested in numerous clinical trials for *RAS*-mutant pancreatic cancer, lung cancer, colorectal cancer, and melanoma and for *BRAF*-mutant lung cancer and colorectal cancer. The majority of these clinical trials are ongoing at this time. However, early phase clinical studies suggest that, while a subset of patients *KRAS*- or *BRAF*-mutant lung cancer respond to single agent MEK or BRAF inhibitor therapy[249,359], many tumors are intrinsically resistant. Moreover, for patients who do respond, acquired resistance will likely limit long-term therapeutic benefit. Understanding mechanisms of intrinsic resistance can enable the identification of predictive biomarkers that improve patient selection for targeted therapy. In addition, identifying mechanisms of acquired resistance can inform the development of novel agents or combination therapy strategies. Improving the efficacy of targeted therapies will require an expanded understanding of resistance mechanisms, the development of rationally designed targeted agents, and the translation of this information to stratify patients for therapy.

Here, we suggest a list of potential GOF and LOF mechanisms of resistance to MAPKi therapy. In Chapters 3 and 4, we study how loss of two of these genes, KEAP1 and CIC, mediate resistance to MAPKi. However, the majority of these genes have not been experimentally validated. In addition, given that *bona fide* mechanisms of intrinsic or acquired resistance should be observed in clinical specimens, it will be important to determine whether the mechanism of resistance to MAPKi proposed here arise in the

clinical setting as molecularly characterized specimens from ongoing clinical trials become available.

2.4 Materials and Methods

Cell lines and reagents

Cells were maintained in DMEM (PATU8902, PATU8988T; Corning), RPMI-1640 (HCC364, NCIH1299, MELJUSO, IPC298; Corning), or McCoy's 5A (CALU1; Gibco) supplemented with 2 mM glutamine, 50 U/mL penicillin, 50 U/mL of streptomycin (Gibco), and 10% fetal bovine serum (Sigma), and incubated at 37°C in 5% CO_2. Trametinib and vemurafenib were purchased from Selleck Chemicals.

Vectors

Cas9 in the pLX311 backbone (pXPR_BRD111) was obtained from the Genetic Perturbation Platform at the Broad Institute.

ORF library

The creation, cloning, sequencing, and production of the ORF library containing over 16,100 sequence-confirmed human ORFs has been previously described[298].

GeCKOv2 and Avana CRISPR libraries

The creation, cloning, sequencing, and production of the GeCKOv2[297] and Avana[358] CRISPR libraries have been previously described. The GeCKOv2 library contains ~120,000 barcoded guide RNAs (sgRNAs) targeting ~21,000 genes[297]. The

Avana library contains ~75,000 barcoded guide RNAs (sgRNAS) targeting ~19,000 genes[358].

Mini-pool CRISPR library

The mini-pool CRISPR libraries were created in collaboration with the Broad Genetic Perturbation Platform. The control library contains 969 negative control sgRNAs. The candidate library contains 82 sgRNAS, with 10 or 11 sgRNAs targeting each candidate gene of interest: CIC, CDKN1B, INSM2, KEAP1, MAPKAPK2, MNT, PPPAR2, and SMEK1. All sgRNAs were in the pXPR_BRD003 backbone.

Trametinib titration for genome scale ORF and CRISPR-Cas9 screens

The doses of trametinib to use in these screens were determined by propagating cells in different concentrations of trametinib to determine the effect on cell proliferation. In parallel, the level of phospho-ERK depletion in cells treated with different concentrations of trametinib was determined. For the proliferation assay**,** cells were treated with different concentrations of drug for up to 3 weeks. Cells were passaged or media was refreshed every 3-4 days. Cells were counted at east passage. For immunoblots, cells were treated with DMSO or the indicated concentrations of trametinib for 90 minutes (CALU1, HCC364, and NCIH1299), 24 hours (PATU8902) or 17 days (PATU8988T). For the lung cancer cell lines, the lowest concentration of drug that suppressed p-ERK and resulted in cell death or proliferative arrest was used in the screen (**Figure 2-6**). For PATU8902, a cytotoxic concentration of trametinib that suppressed p-ERK was used in the screen. For PATU8988T, a concentration of

trametinib that suppressed p-ERK and reduced the proliferation rate by 50% was used in the screen.

Genome scale ORF resistance screen

To titer the ORF library, 3 x 10^6 PATU8902 cells were seeded per well in a 12-well plate, and were infected with different volumes of virus (0, 50, 100, 200, 300, 500 µL), with a final concentration of 4 µg/mL polybrene. Cells were spun for 2 hours at 2000 rpm at 30°C. 2 mL of media was added to each well, and cells were incubated at 37°C overnight. The next day, each well was harvested in 2 mL of media, and 600,000 cells (400 µL) were seeded in two 10 cm plates. One plate was treated with 1 µg/mL puromycin, and one was left untreated. After 4 days of puromycin selection, cells were counted to determine the amount of virus that resulted in 30-40% infection efficiency, and this amount of virus was used in the screen

Four infection replicates were performed. For each replicate, 2 x 10^8 PATU8902 cells were infected with 30-40% infection efficiency, in order to obtain a representation of ~1,000 cells per ORF per time point after selection. After 5 days of puromycin selection, 25 x 10^6 cells were harvested for the Day -1 time point, and 80 x 10^6 cells were seeded in T225 flasks. Cells were allowed to adhere for 24 hours, and trametinib (50 nM or 100 nM) was added to the cells on Day 0. Cells were passaged in drug or fresh media containing trametinib was added every 3-4 days. One of the replicates treated with 50 nM trametinib became contaminated after 10 days of trametinib treatment, and was discarded.

Drug-treated cells were harvested 7, 14, and 21 days after initiation of trametinib treatment. To harvest cells, cells were trypsinized, spun down, washed with PBS, and the cell pellets were frozen at -80°C. Genomic DNA was extracted using the Qiagen Blood and Cell Culture DNA Maxi Kit according to the manufacturer's protocol. The ORF barcodes were PCR amplified and sequenced to quantify ORF representation at different time points. The $\log_2$(fold-change) in ORF representation between the Day 7, 14, or 21 samples and the Day -1 baseline control sample was calculated.

Genome scale CRISPR resistance screens

Blasticidin and puromycin concentrations were optimized for each cell line by treating with different concentrations of drug for 3 days (puromycin) or 7 days (blasticidin). To generate cell lines stably expressing Cas9, 200,000-400,000 cells were seeded in one well of a 6-well plate. The following day, cells were infected with 3 mL of pXPR_BRD111 (Cas9 expression vector) virus with a final concentration of 4 µg/mL polybrene. Cells were spun for 2 hrs at 2000 rpm at 30°C. 24 hrs after infection, cells were selected with blasticidin for 7 days. Cas9-expressing cells were maintained in 2-6 µg/mL blasticidin.

To determine Cas9 activity, parental cell lines and Cas9-expressing cell lines were infected with pXPR_011, a Cas9 activity reporter which expresses eGFP as well as a guide RNA targeting eGFP[366]. 200,000-400,000 cells were seeded in six wells of a 6-well plate and were infected with 25-100 µL virus with a final concentration of 4 µg/mL polybrene. Cells were spun 2 hrs at 2000 rpm at 30°C. 24 hrs after infection, each well was split into 2 wells, one of which was selected with puromycin. After 2-4 days of

puromycin selection, cells were counted and those with 30-40% infection efficiency were kept for the Cas9 activity assay. After 7 days of puromycin selection, cells were analyzed on an LSRII flow cytometer to determine the amount of GFP-positive cells. Parental cells not expressing Cas9 or pXPR_011 were used as a negative control. Cells expressing pXPR_011 but not Cas9 were used as a positive control.

To titer the GeCKOv2[297] or Avana[358] library in Cas9-expressing cells, 3 x 10^6 cells were seeded per well in a 12-well plate and were infected with different amounts of virus (0 to 500 µL), with a final concentration of 4 µg/mL polybrene. Cells were spun for 2 hours at 2000 rpm at 30°C. Approximately 6 hours after infection, 100,000 cells from each infection were seeded into duplicate wells in a 6-well plate. 24 hours after infection, one well was treated with puromycin and one with media alone. After 2-4 days of selection, cells were counted to determine the amount of virus that resulted in 30-40% infection efficiency, and this amount of virus was used in the screen.

For each screen, two infection replicates were performed. For the PATU8902, CALU1, HCC364, and NCIH1299 GeCKOv2 resistance screens, 1.5 x 10^8 cells were infected per replicate with 30-40% infection efficiency in order to obtain at least 500 cells per sgRNA after selection (60 x 10^6 surviving cells containing 120,000 sgRNAs). For the PATU8988T Avana resistance screen, 1 x 10^8 cells were infected per replicate with ~40% infection efficiency in order to obtain 500 cells per sgRNA after selection (40 x 10^6 surviving cells containing 80,000 sgRNAs). 3 x 10^6 cells per well were seeded in 12-well plates and were infected with the amount of virus determined during optimization, with a final polybrene concentration of 4 µg/mL. Plates were spun for 2

hours at 2000 rpm at 30°C. Approximately 6 hours after infection, all wells within a replicate were pooled and split into T225 flasks.

24 hours after infection, cells were selected in 2 μg/mL puromycin for 6 days and expanded in puromycin-free media for 4 days (PATU8988T) or 7 days (PATU8902, CALU1, HCC364, and NCIH1299). After puromycin selection, for CALU1, HCC364, and NCIH1299, 60 x 10^6 cells were harvested for the Day 0 time point, and 60 x 10^6 cells were treated with drug. HCC364 cells were treated with 25 nM trametinib or 6.25 μM vemurafenib; H1299 cells were treated with 1.5 μM trametinib; and CALU1 cells were treated with 50 nM trametinib. For PATU8902, 75 x 10^6 cells were seeded in T225 flasks in media without drug on Day -1. Cells were allowed to adhere for 24 hours, and 100 nM trametinib was added to the cells on Day 0. For PATU8988T, 40 x 10^6 cells were seeded in T225 flasks with 10 nM trametinib on Day 0. Cells were passaged in drug or fresh media containing trametinib was added every 3-4 days.

Drug-treated cells were harvested 14 days (all cell lines) and 21 days (CALU1, HCC364, NCIH1299, and PATU8902) after initiation of trametinib treatment. To harvest cells, cells were trypsinized, spun down, washed with PBS, and the cell pellets were frozen at -80°C. Genomic DNA was extracted using the Qiagen Blood and Cell Culture DNA Maxi Kit according to the manufacturer's protocol. PCR of gDNA and pDNA (sgRNA plasmid pool used to generate virus) was performed as previously described[358].

Sequencing and analysis of genome scale CRISPR-Cas9 knockout screens was performed as previously described[358]. The $\log_2$(fold-change) in sgRNA representation between cells treated with trametinib for 14 or 21 days and baseline sample (Day -3

sample for PATU8988T, Day -1 sample for PATU8902, and Day 0 sample for CALU1, HCC364, and NCIH1299) was calculated.

Mini-pool CRISPR screen

Cas9-expressing cell lines were generated as described above. To optimize drug concentrations for the mini-pool screens, melanoma cell lines were treated with different concentrations of trametinib for 24 hrs and then lysed in RIPA buffer. Immunoblots were performed with total and phospho-ERK antibodies to determine the concentration of inhibitor that blocked ERK phosphorylation.

The control and candidate mini-pool CRISPR libraries were titrated separately. 3 x 10^6 cells were seeded per well in a 12-well plate in 1 mL media, and were infected with different volumes of virus (0, 50, 100, 150, 200, 400 µL). Cells were spun for 2 hours at 2000 rpm at 30°C. 2 mL of media was added to each well, and cells were incubated at 37°C overnight. The next day, each well was harvested in 2 mL of media, and 600,000 cells (400 µL) were seeded in two 10 cm plates. One plate was treated with 2 µg/mL puromycin, and one was left untreated. After 4 days of puromycin selection, cells were counted to determine the amount of virus that resulted in 30-40% infection efficiency, and this amount of virus was used in the screen

Three infection replicates were performed. For each replicate, 9 x 10^6 cells were infected with the control mini-pool and 3 x 10^6 cells were infected with the candidate mini-pool at 30-40% infection efficiency. After 7 days of puromycin selection, 3 x 10^6 control mini-pool cells were mixed with 0.3 x 10^6 candidate mini-pool cells. 1 x 10^6 cells were harvested for the Day 0 time point, and 1 x 10^6 cells were seeded in T75 flasks.

Cells were treated with 10 nM (IPC298 and SKMEL2), 50 nM (MELJUSO) or 1.5 μM (NCIH1299) trametinib for 14 days. Cells were passaged in trametinib or fresh media containing trametinib was added every 3-4 days. To harvest cells, cells were trypsinized, spun down, washed with PBS, and the cell pellets were frozen at -80°C. Genomic DNA was extracted using the Qiagen Blood and Cell Culture DNA Mini Kit according to the manufacturer's protocol. Sequencing and analysis of genome scale CRISPR-Cas9 knockout screens was performed as previously described[358]. The $\log_2$(fold-change) in sgRNA representation between the Day 14 and the Day 0 sample was calculated.

Gene enrichment score for CRISPR-Cas9 screens

The GeCKOv2[297], Avana[358], and candidate mini-pool sgRNA libraries contain 6, 4, or 10-11 sgRNAs targeting each gene, respectively. To reduce sgRNA-level data to a single gene enrichment score, we used the "STARS" algorithm created by John Doench and Mudra Hedge at the Broad Genetic Perturbation Platform). The STARS Python scripts are available from the Genetic Perturbation Platform website (http://www.broadinstitute.org/rnai/public/software/stars).

The gene enrichment score is calculated using the probability mass function of a binomial distribution,

$$\Pr(X = k) = \binom{n}{k} p^k (1-p)^{n-k}$$

where *n* represents the total number of sgRNAs targeting the gene, *k* is the within-gene rank of the sgRNA, and *p* is the ratio of the rank of the *k*th sgRNA targeting the gene

over the total number of sgRNA in the experiment. An enrichment score was calculated for each gene using sgRNAs that were among the top 50% most enriched sgRNAs in the screen as determined by $\log_2$(fold change). The value of the least probable perturbation for each gene was then transformed by $-\log_{10}$ and assigned as the enrichment score (also known as STARS score). Here, we considered genes with an enrichment score ≥ 5 to be significant “hits.”

CHAPTER THREE

KEAP1 loss promotes resistance to EGFR, BRAF, and MEK inhibition in lung cancer

This chapter has been adapted from

Krall, E.B.*, Wang, B.*, Aguirre, A.J., Doench, J.G., Jänne, P.A., and Hahn, W.C. KEAP1 loss promotes resistance to BRAF, MEK, and EGFR inhibition in lung cancer. *In submission.*

Contributions

Belinda Wang, Elsa Beyer Krall, Andrew Aguirre, and William Hahn designed *in vitro* experiments. Elsa Beyer Krall contributed validation experiments (**Figures 3-1A-B, 3-3,** and **3-5A,B**), NAPDH experiments (**Figure 3-10B**), and NRF2 target gene expression experiments (**Figures 3-7, 3-8. 3-14,** and **3-15**). Belinda Wang contributed all other *in vitro* experiments. Pasi Jänne obtained patient samples and analyzed data. Data analysis was performed by Belinda Wang and Elsa Beyer Krall.

3.1 Introduction

3.1.1 Identification of *KEAP1* knockout as mechanism of resistance to MAPKi

Mutations in the RTK-RAS-MAPK pathway frequently arise in NSCLC. Data from sequenced tumors available on the cBio Cancer Genomics Portal[136] indicate that ~20% of NSCLC tumors harbor alterations in *EGFR*, ~30% in *KRAS*, ~3% in *NRAS*, and ~10% in *BRAF*. Targeted therapies have had variable clinical success in treating NSCLC. The majority of patients with *EGFR*-mutant NSCLC respond to EGFR inhibitors[284,367-369], but tumors almost invariably develop resistance[370]. MEK and BRAF inhibitors are currently in clinical trials for *RAS*- or *BRAF*-mutant lung cancer. While early results indicate that some patients respond to therapy, it is clear that both intrinsic and acquired resistance limit therapeutic efficacy[249,359].

To identify mechanisms of resistance to MEK or BRAF inhibition in *RAS*- or *BRAF*-mutant lung cancer, we performed four genome scale CRISPR-Cas9 knockout screens (described in Chapter 2.2.2). Three screens were performed with the MEK inhibitor trametinib in NCI-H1299 ($NRAS^{Q61K}$), HCC364 ($BRAF^{V600E}$), and CALU1 ($KRAS^{G12C}$) cells. One additional screen was performed using HCC364 cells treated with the BRAF inhibitor vemurafenib. *KEAP1* deletion was found to confer resistance to MAPK pathway inhibition (MAPKi) in all four screens in lung cancer cell lines (**Figures 2-7** and **2-9**).

3.1.2 KEAP1-NRF2 pathway

Kelch-like ECH-associated protein 1 (KEAP1) is the substrate adaptor protein of a CUL3 E3 ubiquitin ligase complex that targets the transcription factor nuclear factor

(erythroid-derived 2)-like 2 (NRF2) for proteosomal degradation[371]. Under normal conditions, the majority of NRF2 protein is degraded. The KEAP1-NRF2 pathway is activated in response to endogenous and exogenous cellular stress. Oxidative stress disrupts the KEAP1-NRF2 interaction, allowing NRF2 to translocate to the nucleus, where it binds to antioxidant response elements and activates transcription of cytoprotective genes[372].

NRF2 regulates the expression of genes involved in drug metabolism, antioxidant response, and cell metabolism[373]. Specifically, NRF2 induces the expression of several Phase I and Phase II drug-metabolizing enzymes, as well as multidrug resistance-associated protein (MRP) transporters. NRF2 also upregulates major endogenous antioxidant systems such as glutathione and NADPH[373,374]. Lastly, NRF2 increases the expression of rate-limiting metabolic genes in the pentose phosphate pathway[374] as well as the serine and glycine biosynthesis pathway[375]. These anabolic pathways support cell proliferation by promoting glutathione and purine nucleotide production.

3.1.3 ROS and cancer

The KEAP1-NRF2 pathway is a major regulator of oxidative stress response[372]. Reactive oxygen species (ROS) are molecules generated by the reduction of O_2 with a single electron (superoxide), two electrons (hydrogen peroxide), or three electrons (hydroxyl radical)[376]. The majority of endogenous ROS is produced at the mitochondrial respiratory chain[376]. Under normal physiological conditions, intracellular ROS is maintained at a low level. ROS detoxification and the reduction of oxidized proteins are facilitated by non-enzymatic molecules (glutathione, NADPH, flavonoids, and vitamins A, C, and E) or by antioxidant enzymes (superoxide dismutases and peroxiredoxins)[376].

Oxidative stress arises from an imbalance between the production of ROS and its elimination by protective mechanisms or antioxidants. Many cancer cells exhibit increased basal levels of oxidant stress. Oncogenic transformation is frequently associated with a shift towards a more oxidized state, which is thought to enhance proliferation[377,378]. However, this oxidative shift renders cells vulnerable to chemotherapeutic agents that act by augmenting oxidant generation[379] or inhibiting antioxidant capacity[380]. Excessive ROS generation or failure of oxidant scavenging systems can result in the accumulation of toxic amounts of ROS, leading to oxidative damage of lipids, proteins, and DNA[376,378]. ROS can induce a wide range of adaptive cellular responses depending on the level of ROS, from transient growth arrest to permanent growth arrest, apoptosis, or necrosis. Several anticancer drugs, including doxorubicin, cisplatin, taxol, and proteasome inhibitors induce ROS to a cytotoxic level[381], though the mechanisms underlying ROS increase remain poorly understood.

There have been conflicting findings regarding the role of oncogenic RAS signaling and ROS production. Mutant RAS signaling has been reported to increase endogenous ROS[377,382]. However, a recent study reported that mutant KRAS decreased ROS by increasing glutathione and NADPH synthesis, and that increased copy numbers of mutant RAS further decreased ROS levels[383]. Whether or not oncogenic RAS induces ROS, inducing high levels of oxidative stress appears to mediate *in vitro* and *in vivo* therapeutic response in models of RAS-driven cancer[384].

3.1.4 KEAP1-NRF2 alterations in cancer

The KEAP1-NRF2 pathway is activated in many cancers. The Cancer Genome Atlas (TCGA) consortium identified mutations in components of the KEAP1-NRF2

pathway (*KEAP1, CUL3,* and *NFE2L2*, which encodes NRF2) in ~35% of squamous cell lung carcinomas[385], ~25% of lung adenocarcinomas[170], and ~20% of head and neck carcinomas[132]. In addition to somatic mutations, other mechanisms may increase NRF2 activity in cancers, including DNA hypermethylation of the *KEAP1* promoter and aberrant accumulation of proteins that disrupt the KEAP1-NRF2 interaction[386]. The KEAP1-NRF2 pathway may also be indirectly activated by other oncogenic events. In cells with oncogenic KRAS and BRAF, c-Jun, which is activated by MAPK signaling, binds to the *NFE2L2* promoter and increases NRF2 expression[387]. Notably, as alterations in the KEAP1-NRF2 pathway co-occurs with mutations in the EGFR-RAS-MAPK pathway in lung cancer, *KEAP1* loss could be a biomarker of intrinsic resistance to MAPKi in these tumors.

KEAP1 loss and elevated NRF2 expression are associated with intrinsic and acquired chemoresistance, radioresistance, and poor clinical outcome[388-394]. Depleting NRF2 or inhibiting NRF2-regulated genes sensitizes cell lines to several chemotherapies *in vitro*[388,390,391,393,395]. In addition, NRF2 ablation in various tumor models results in elevated ROS and the suppression of tumor growth *in vivo*[387,392,394]. High NRF2 activity may induce chemoresistance and radioresistance by several mechanisms, such as drug efflux, drug detoxification via glutathione and other conjugating mechanisms, promoting oxidative stress relief, and increasing anabolic metabolism. However, alterations in the KEAP1-NRF2 pathway are not currently used to guide treatment decisions.

3.2 Results

3.2.1 Validation that *KEAP1*^{KO} confers resistance to MAPKi

To verify that *KEAP1* knockout (*KEAP1*^{KO}) confers resistance to MAPKi, we infected HCC364 (*BRAF*^{V600E}) and CALU1 (*KRAS*^{G12C}) cells with sgRNAs targeting KEAP1 or GFP (**Figure 3-1**). Cells were then seeded at low density in 24-well plates and treated with DMSO, trametinib, or vemurafenib. Cell viability was assessed using long-term proliferation assays. Deletion of KEAP1 conferred resistance to trametinib in both cell lines and to vemurafenib in HCC364 cells (**Figure 3-2**). Because *EGFR* mutation frequently occurs in lung cancer, we assessed the ability of KEAP1 loss to confer resistance to EGFR inhibition in *EGFR*-mutant cell lines. *KEAP1*^{KO} conferred resistance to erlotinib treatment in HCC827 (*EGFR*$^{\Delta 746\text{-}750}$) cells and to afatinib treatment in NCI-H1975 (*EGFR*$^{L858R/T790M}$) cells (**Figure 3-3**). In addition, we found that restoring wildtype KEAP1 expression in A549 cells, which are *KRAS*-mutant and *KEAP1*-null, increased their sensitivity to trametinib. In contrast, expression of the *KEAP1*^{G333C} mutant, which does not regulate NRF2, failed to alter trametinib sensitivity (**Figure 3-4**).

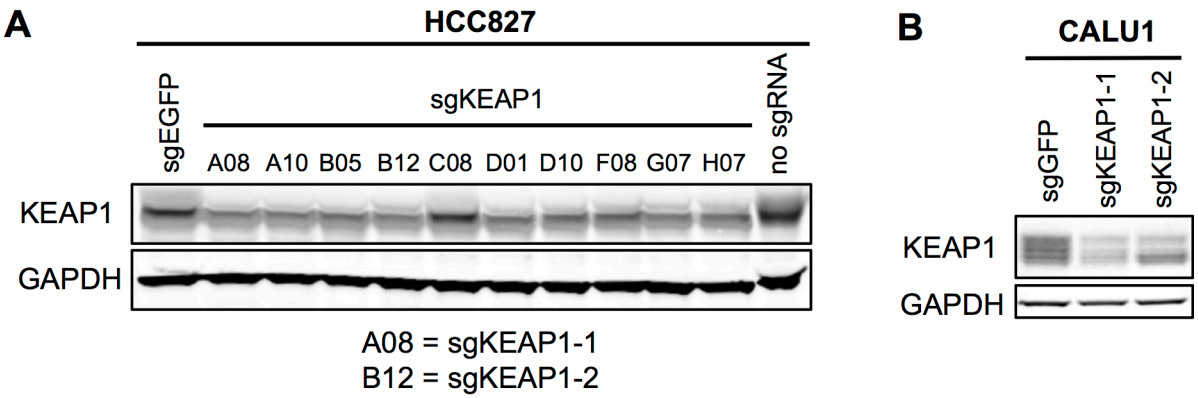

Figure 3-1. **Identification of sgRNAs that achieve robust KEAP1 knockout. (A,B)** Immunoblots showing deletion of KEAP1 by sgRNAs in HCC827 **(A)** and CALU1 **(B).** Immunoblots were performed by Elsa Beyer Krall.

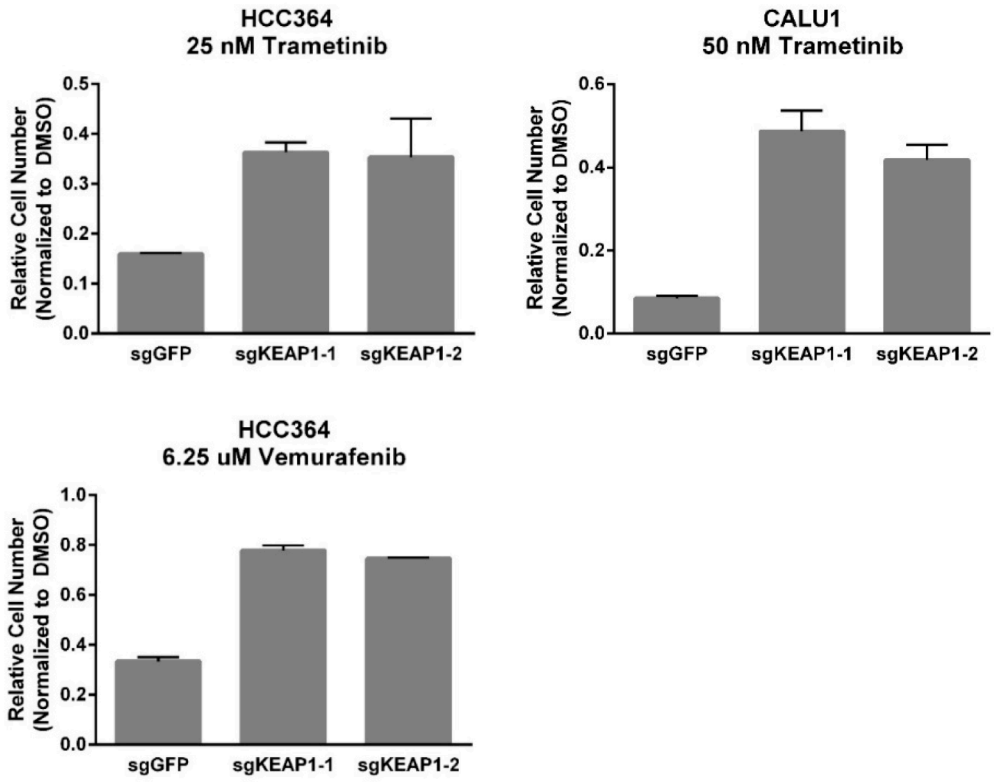

Figure 3-2. *KEAP1*^{KO} confers resistance to MEK and BRAF inhibition. Long-term proliferation assays assessing the effect of trametinib treatment in *KEAP1*^{WT} and *KEAP1*^{KO} cells. 5,000 CALU1 cells were seeded in 24-well plates and treated with 50 nM trametinib for 17 days. 2,000 HCC364 cells were treated with 25 nM trametinib or 6.25 μM vemurafenib for 21 days. *N* = 3 technical replicates representative of at least *n* = 2 independent experiments, data represented as mean ± SEM.

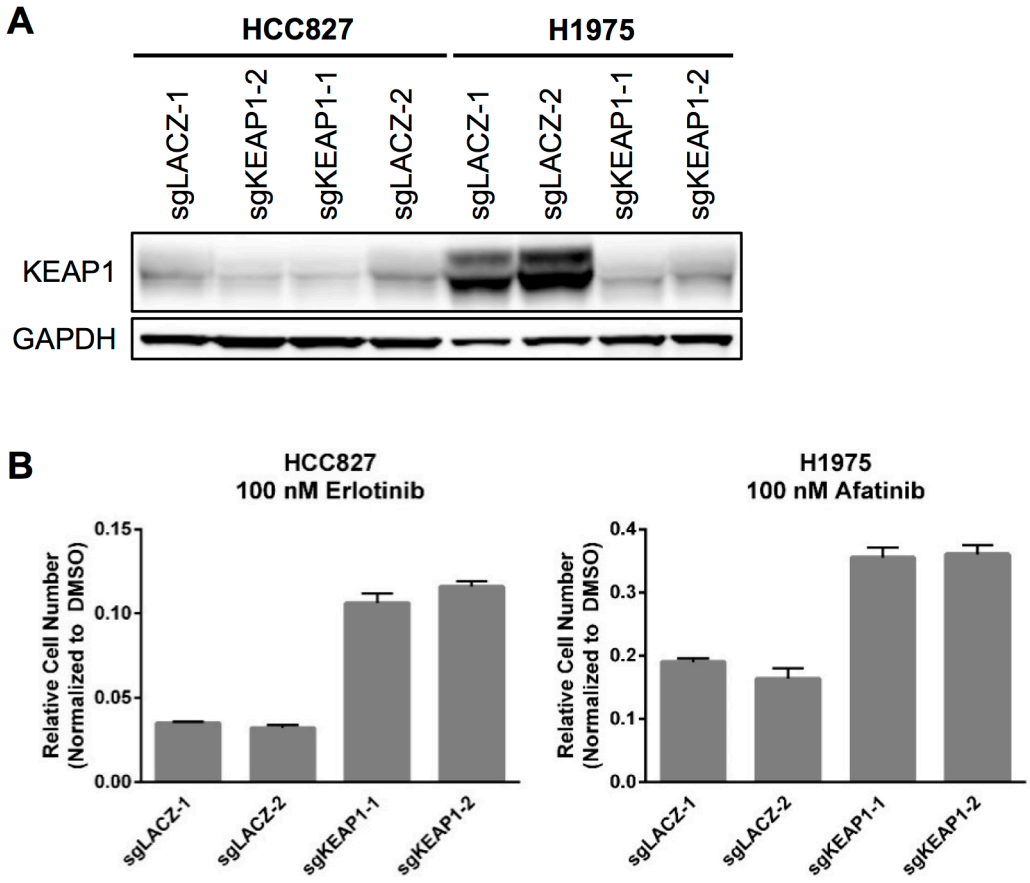

Figure 3-3. *KEAP1*^{KO} confers resistance to EGFR inhibition. (A) Immunoblot showing sgRNA mediated KEAP1 deletion in HCC827 and H1975. **(B)** Long-term proliferation assay assessing effect of trametinib treatment in *KEAP1*^{WT} and *KEAP1*^{KO} cells. 5,000 HCC827 cells were treated with 100 nM erlotinib for 10 days. 1,000 H1975 cells were treated with 100 nM afatinib for 10 days. *N* = 3 technical replicates, data represented as mean ± SEM. Experiments were performed by Elsa Beyer Krall.

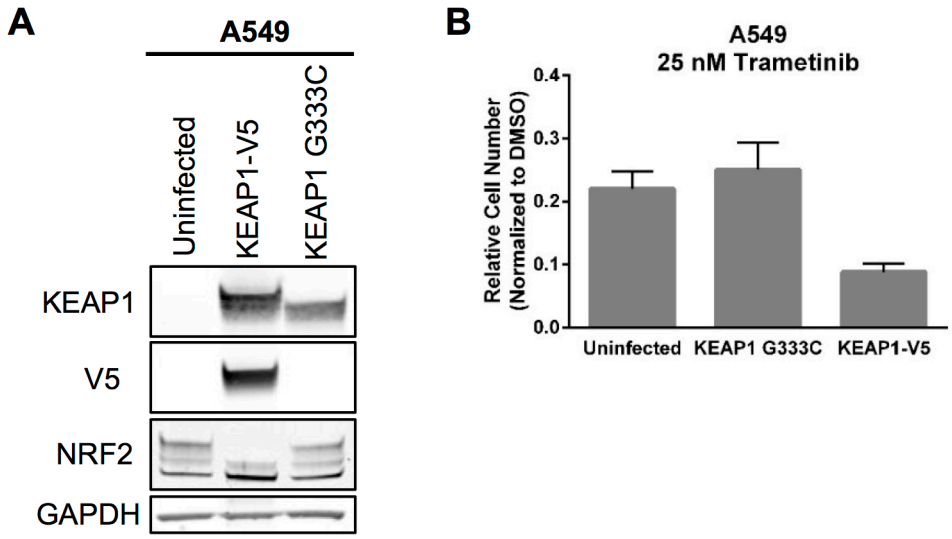

Figure 3-4. Restoration of KEAP1 expression sensitizes *KEAP1*^{KO} cells to MEK inhibitor treatment. (A) Immunoblot analysis of KEAP1 expression in A549 cells. **(B)** Long-term proliferation assay assessing effect of trametinib treatment in KEAP1-null A549 cells expressing wildtype KEAP1 or KEAP1 G333C. 5,000 cells were seeded in 24-well plates and treated with 25 nM trametinib for 12 days. Error bars represent the standard deviation of six wells. *N* = 3 technical replicates representative of *n* = 2 independent experiments, data represented as mean ± SEM.

3.2.2 *KEAP1*^{KO} confers resistance by increasing NRF2 levels

Unlike the majority of reported BRAF and MEK inhibitor resistance mechanisms (**Table 1-3**), we found that *KEAP1*^{KO} does not restore ERK activation (**Figure 3-5A,C**), suggesting that *KEAP1*^{KO} does not confer resistance by reactivating the MAPK pathway. KEAP1 is a substrate adaptor protein for the CRL3^{KEAP1} E3 ubiquitin ligase complex that targets NRF2 for proteasomal degradation[371]. As inactivating *KEAP1* and activating *NFE2L2* mutations tend to be mutually exclusive (analysis of TCGA squamous cell lung carcinoma provisional data)[136], we hypothesized that *KEAP1*^{KO} confers trametinib resistance by restoring NRF2 activity.

As expected, we found that *KEAP1*^{KO} led to increased NRF2 protein levels (**Figure 3-5B,C**). Overexpression of wildtype NRF2 or NRF2^{G31R}, which contains a mutation in the KEAP1 binding domain that that results in decreased proteosomal degradation, also conferred resistance to trametinib and vemurafenib (**Figure 3-6**). Notably, overexpression of NRF2^{G31R}, which escaped KEAP1-mediated degradation and achieved higher protein expression than wildtype NRF2 (**Figure 3-6B**), conferred more robust resistance than overexpression of wildtype NRF2 (**Figure 3-6A)**. This suggested that the elevated NRF2 levels in *KEAP1*^{KO} cells mediates resistance. Although CALU1 cells harbor a *KEAP1*^{P128L} mutation, this mutation has not been reported in cBioPortal or COSMIC[134,136], and NRF2 levels increased upon KEAP1 knockout (**Figure 3-5C**), suggesting that the regulation of NRF2 by KEAP1 is intact in these cells.

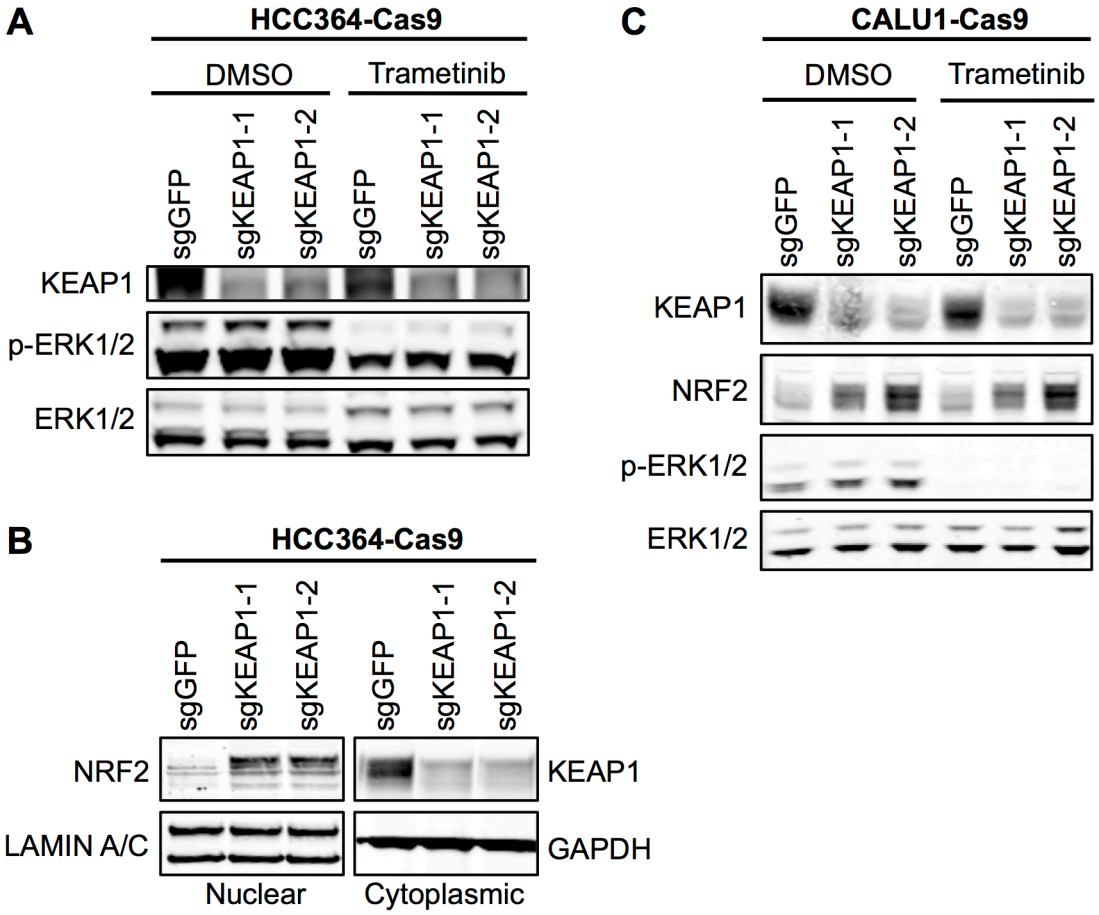

Figure 3-5. KEAP1^{KO} does not reactivate ERK but does increase NRF2 levels. (A) Whole cell lysates of HCC364-Cas9 cells with the indicated sgRNAs treated with DMSO or 25 nM trametinib for 48 hours. **(B)** Immunoblot analysis of NRF2 expression in nuclear and cytoplasmic fractions of HCC364 cells. **(C)** Whole cell lysates of CALU1-Cas9 cells with the indicated sgRNAs treated with DMSO or 50 nM trametinib for 24 hours. Immunoblots in **(A)** and **(B)** were performed by Elsa Beyer Krall.

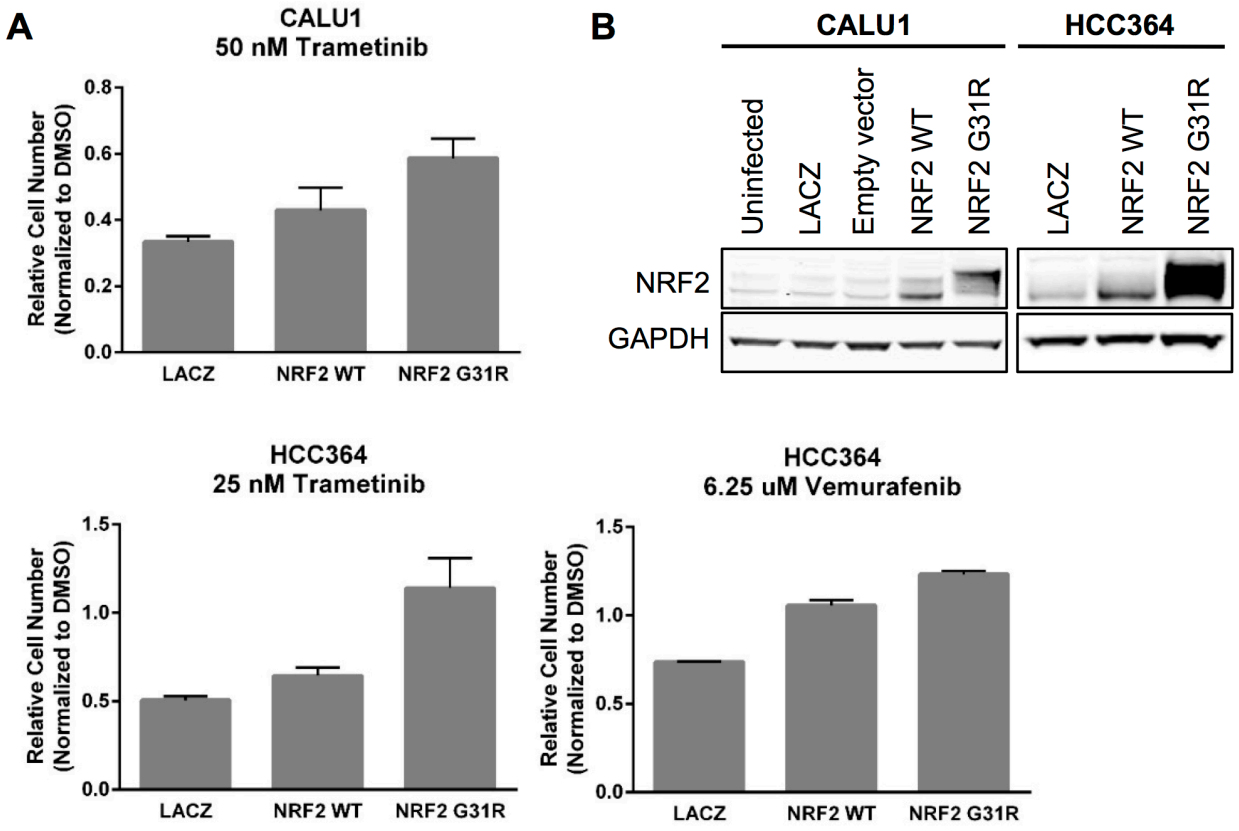

Figure 3-6. **NRF2 overexpression confers resistance to MEK or BRAF inhibition.** **(A)** Long term proliferation assays. 10,000 CALU1 cells expressing the indicated ORFs were seeded in 24-well plates and treated with DMSO for 8 days or trametinib for 10 Days. 10,000 HCC364 cells expressing the indicated ORFs were seeded in 12-well plates and treated with DMSO for 10 days or drug for 21 days. *N* = 3 technical replicates representative of at least *n* = 2 independent experiments, data represented as mean ± SEM. **(B)** Immunoblot analysis of NRF2 expression in CALU1 and HCC364.

3.2.3 Both trametinib treatment and *KEAP1*^{KO} increase NRF2 activity

To further explore the mechanism by which *KEAP1*^{KO} confers resistance to trametinib, we investigated whether trametinib treatment affected the KEAP1/NRF2 signaling axis. A prior study demonstrated that RAS-MAPK-(c-Jun) signaling increased expression of *NFE2L2* mRNA and NRF2 target genes[387]. We hypothesized that trametinib treatment would decrease expression of *NFE2L2* mRNA and NRF2-regulated target genes. Surprisingly, we found that trametinib treatment increased rather than decreased expression of *NFE2L2* mRNA and NRF2 target genes in HCC364 and CALU1 cells (**Figure 3-7**). As expected, *KEAP1*^{KO} also increased NRF2 target gene expression (**Figure 3-7**). We found that trametinib treatment increased NRF2 protein levels and induced a shift in the migration of NRF2 protein on SDS-PAGE, whereas *KEAP1*^{KO} cells maintained the expression of the higher molecular weight form of NRF2 (**Figure 3-8**). Together, these observations indicate that trametinib treatment upregulates *NFE2L2* mRNA expression and NRF2 activity, and KEAP1 knockout further increases NRF2 protein expression and NRF2 activity.

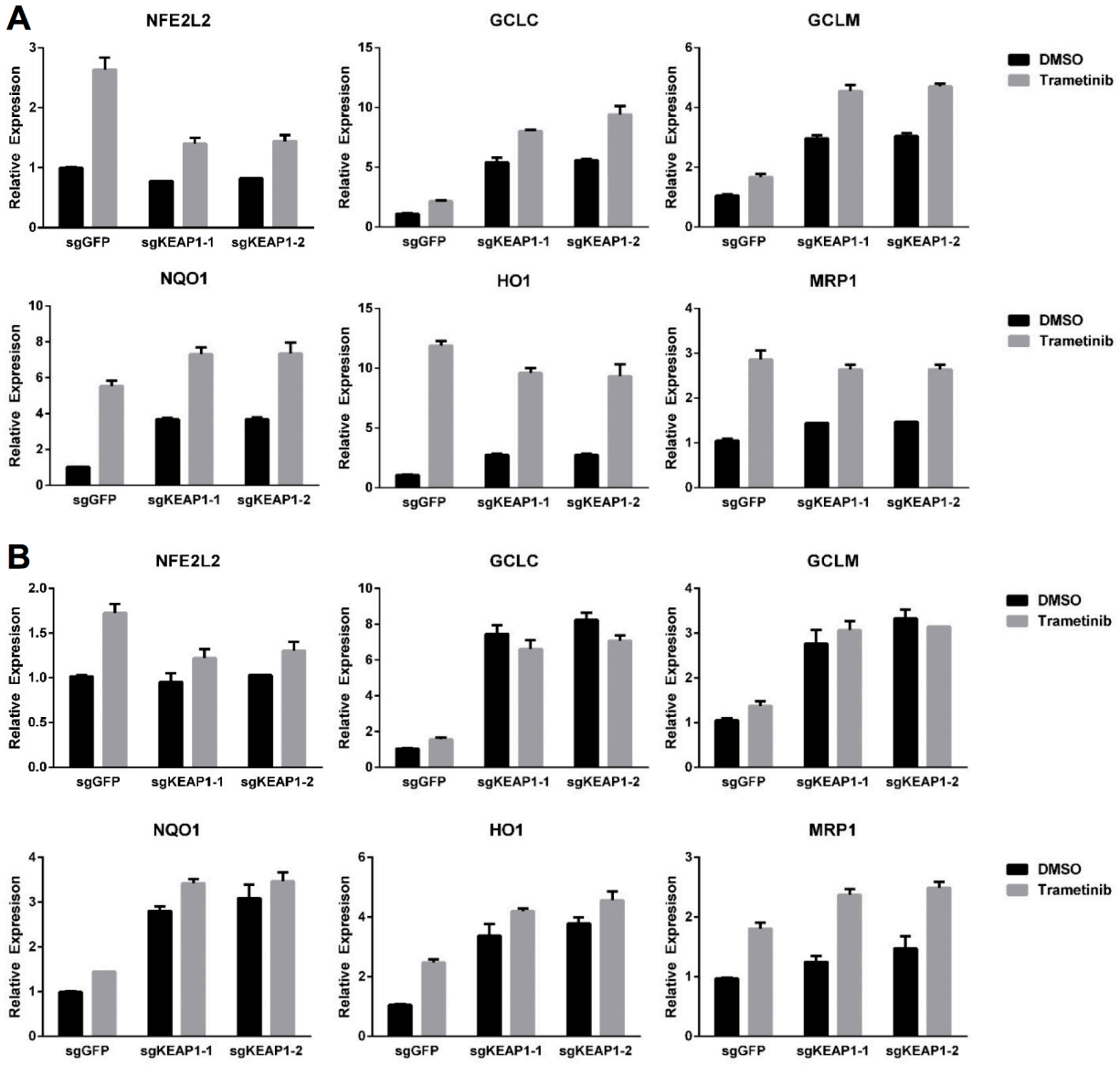

Figure 3-7. Trametinib treatment increases NRF2 activity, which is further increased by *KEAP1*^{KO}. Expression of *NFE2L2* (NRF2) mRNA and NRF2 target genes in HCC364 **(A)** or CALU1 **(B)** cells treated with DMSO or trametinib for 72 hours. *N* = 3 biological replicates, data represented as mean ± SEM. Experiment performed by Elsa Beyer Krall.

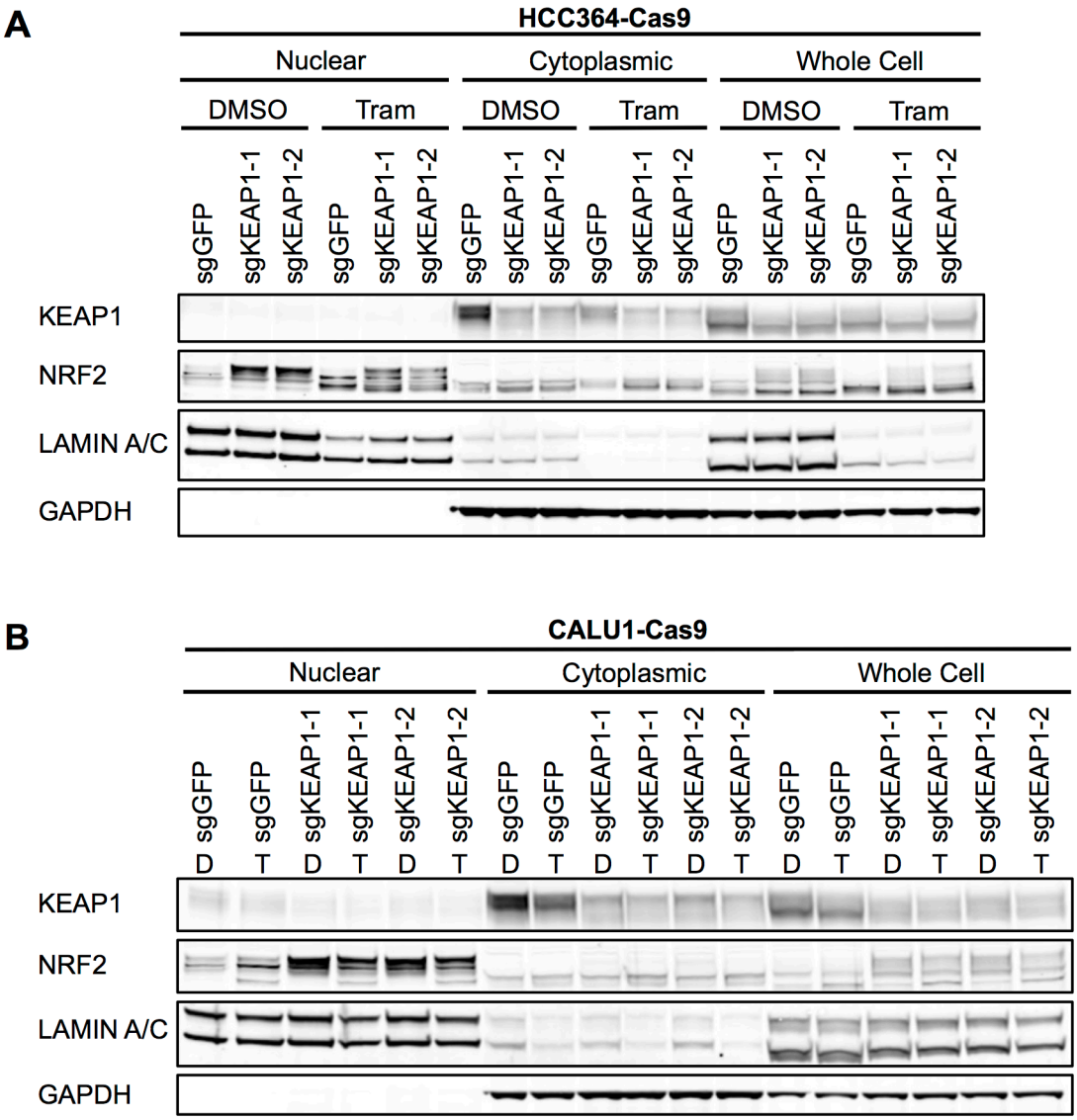

Figure 3-8. Trametinib treatment alters NRF2 migration. Immunoblot analysis of HCC364 **(A)** or CALU1 **(B)** cells treated with DMSO or trametinib for 72 hours. Tram, trametinib. Immunoblots performed by Elsa Beyer Krall.

3.2.4 *KEAP1*^{KO} reduces trametinib-induced ROS

The KEAP1/NRF2 axis responds to oxidative and electrophilic stress by regulating expression of drug efflux pumps, by scavenging reactive oxygen species (ROS), and by altering cell metabolism[373]. We investigated whether each of these functions was involved in resistance to trametinib treatment. While *KEAP1*^{KO} cells have higher expression of the transporter multidrug resistance-associated protein 1 (*MRP1*) (**Figure 3-7**), MAPK pathway inhibition is maintained in *KEAP1*^{KO} cells (**Figure 3-5A,B**), suggesting that increased drug efflux does not explain resistance.

We found that trametinib treatment induced ROS in KEAP1-intact cells (**Figure 3-9**). Reduced glutathione (GSH) and NADPH play a central role in neutralizing intracellular ROS[378,396]. Both trametinib treatment and *KEAP1*^{KO} increased the expression genes involved in synthesizing glutathione (*GCLC* and *GCLM*) and reducing NADP+ to NADPH (*NQO1*) (**Figure 3-7**). However, trametinib treatment did not affect glutathione levels (**Figure 3-10A**) or the NADPH/NADP+ ratio (**Figure 3-10B**). Trametinib-induced ROS was dramatically decreased in *KEAP1*^{KO} cells and in NRF2 overexpressing cells (**Figure 3-9**). This observation suggested that *KEAP1*^{KO} may confer resistance by reducing ROS levels. We reduced ROS in KEAP1-intact cells treated with trametinib using the ROS scavenger N-acetyl cysteine (NAC) (**Figure 3-11A**). Decreasing ROS in KEAP1-intact cells conferred trametinib resistance (**Figure 3-11B**), suggesting that ROS reduction by *KEAP1*^{KO} is important for resistance. We assessed the effect of increasing ROS on sensitivity to trametinib treatment by treating KEAP1-intact cells with trametinib and buthionine sulfoximine (BSO), which inhibits

glutathione synthesis and induces ROS[397]. We found that the combined trametinib and BSO treatment elevated ROS and decreased cell viability in CALU1 cells (**Figure 3-12**).

To further investigate whether ROS reduction was important for resistance mediated by KEAP1 loss, we treated cells with trametinib and BSO. The combination of BSO and trametinib greatly decreased viability in control cells expressing sgGFP, while *KEAP1*^{KO} prevented the BSO-induced decrease in viability (**Figure 3-13A-D**). Furthermore, combined treatment with BSO and trametinib dramatically increased ROS levels in A549 cells in which wildtype KEAP1 expression had been restored, but not in the parental cells or cells expressing KEAP1^{G333C} (**Figure 3-13E**). Together these observations suggest that trametinib treatment induces ROS, which activates NRF2 to levels that are not sufficient for resistance. Loss of KEAP1 leads to further activation of NRF2, which confers resistance in part by reducing ROS.

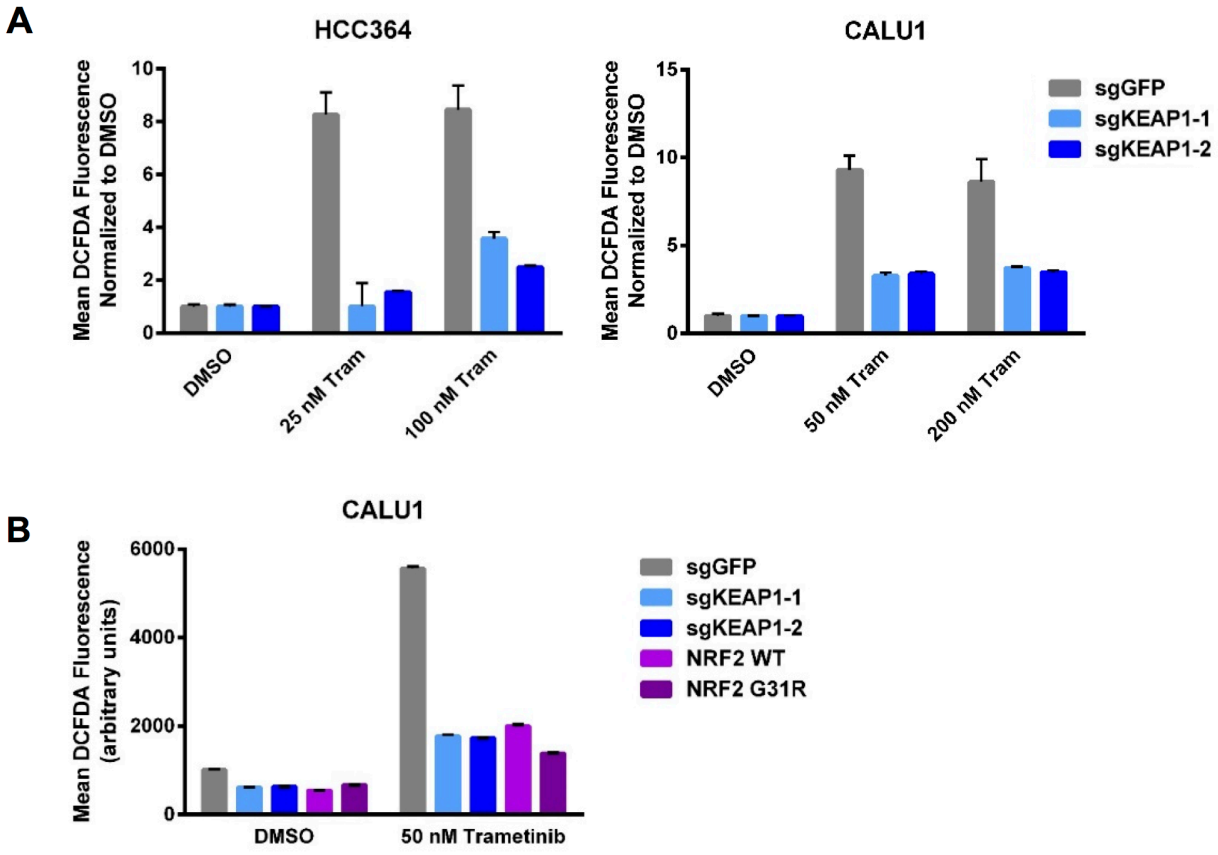

Figure 3-9. Trametinib treatment induces ROS and *KEAP1*^{KO} or NRF2 overexpression decreases ROS. (A) HCC364 or CALU1 cells were treated with DMSO or trametinib for 72 hr. ROS was measured by DCFDA fluorescence. *N* = 2 technical replicates, data represented as mean ± SEM. **(B)** NRF2 overexpression reduces trametinib-induced ROS. CALU1 cells were treated for 72 hr. *N* = 2 technical replicates, data represented as mean ± SEM.

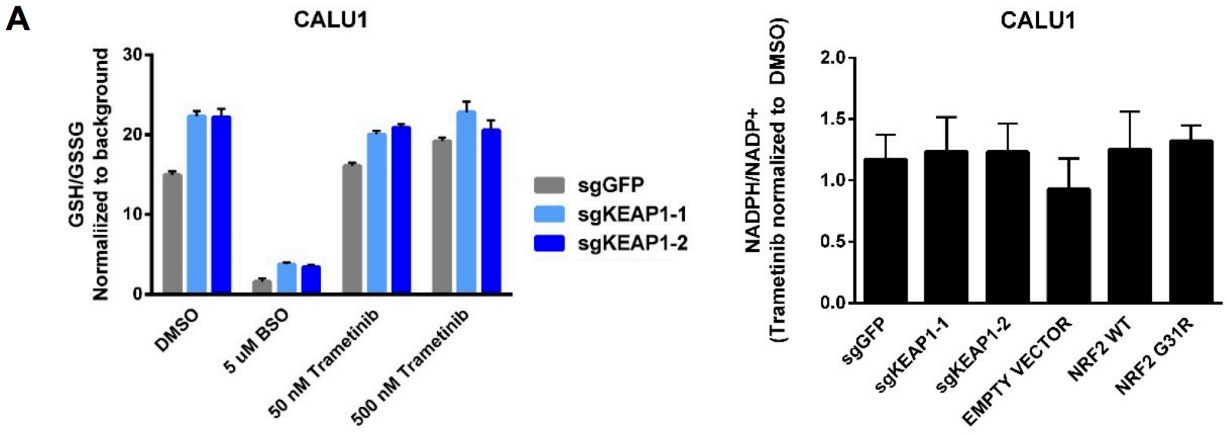

Figure 3-10. Trametinib treatment does not alter levels of reduced glutathione or NADPH. (A) Trametinib does not affect GSH/GSSG ratio. CALU1 cells were treated for 72 hr. *N* = 3 technical replicates, data represented as mean ± SEM. **(B)** NADPH/NADP+ ratio in CALU1 treated with DMSO or trametinib for 72 hours. *N* = 6 technical replicates, data represented as mean ± SEM. NADPH/NADP+ quantification was performed by Elsa Beyer Krall.

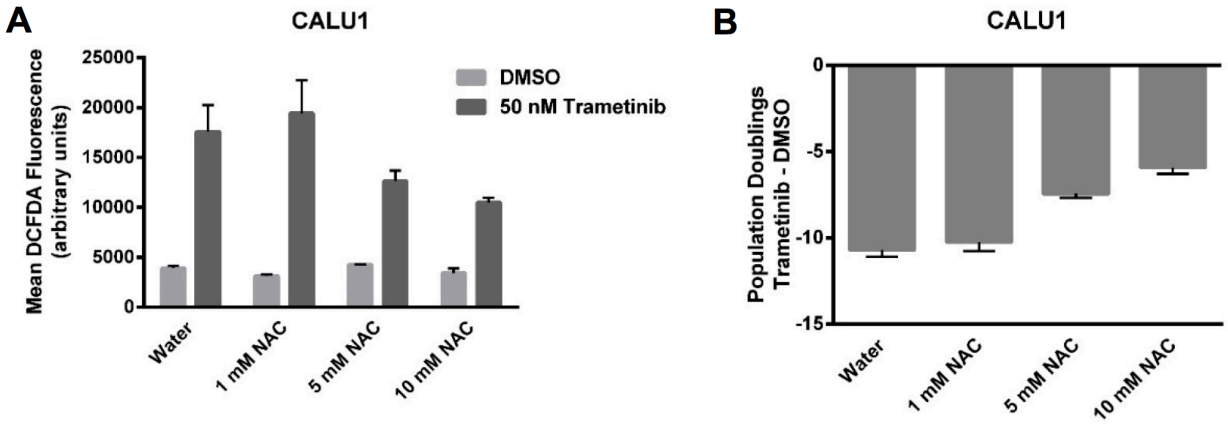

Figure 3-11. Reducing ROS confers resistance to trametinib treatment while increasing ROS reduces cell viability (A) NAC treatment reduces ROS in CALU1 cells. CALU1 cells were treated with DMSO or 50 nM trametinib and the indicated concentration of NAC for 16 days. *N* = 2 technical replicates, data represented as mean ± SEM. **(B)** Population doublings of trametinib-treated cells compared to DMSO-treated cells treated with the indicated amount of NAC. *N* = 2 technical replicates, data represented as mean ± SEM.

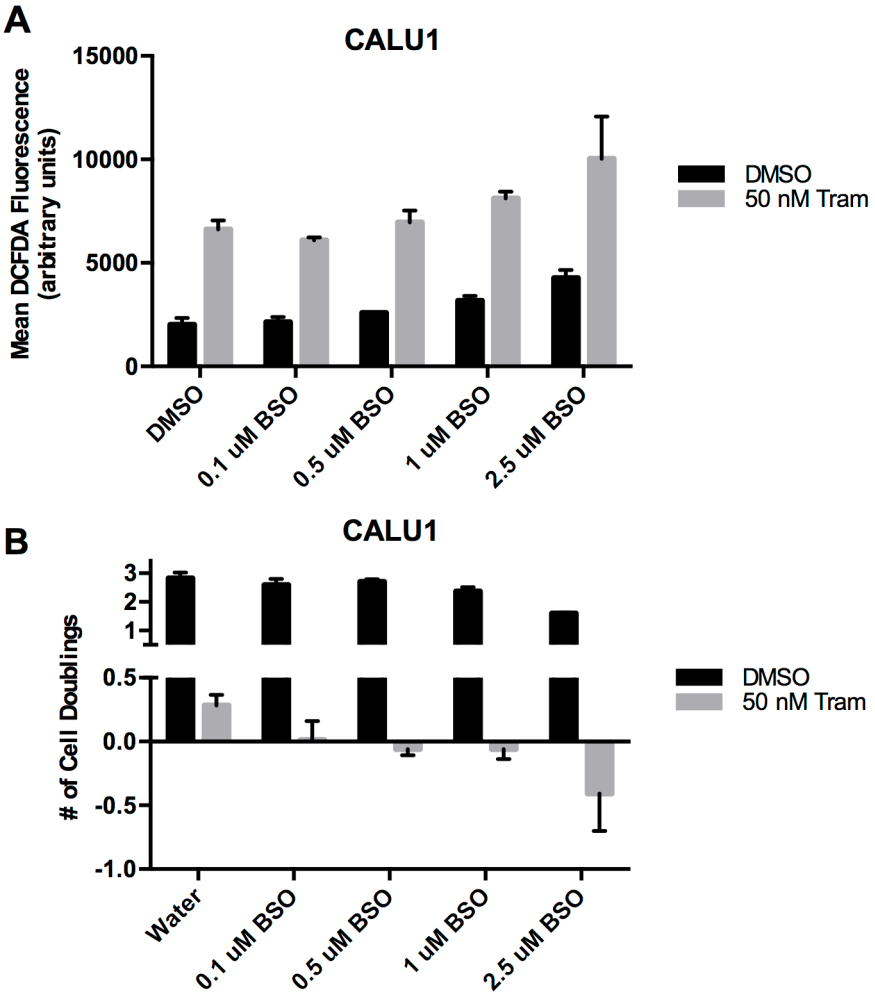

Figure 3-12. BSO increases ROS in trametinib-treated cells and decreases cell viability. (A) BSO and trametinib treatment induces ROS. CALU1 cells were treated with DMSO or 50 nM trametinib plus the indicated amount of BSO for 5 days. ROS was measured by DCFDA fluorescence. *N* = 2 technical replicates, data represented as mean ± SEM. **(B)** Cell counting assay to determine the effect of BSO plus trametinib treatment on cell viability. CALU1 cells were treated with DMSO or 50 nM trametinib plus the indicated amount of BSO for 5 days. *N* = 2 technical replicates, data represented as mean ± SEM.

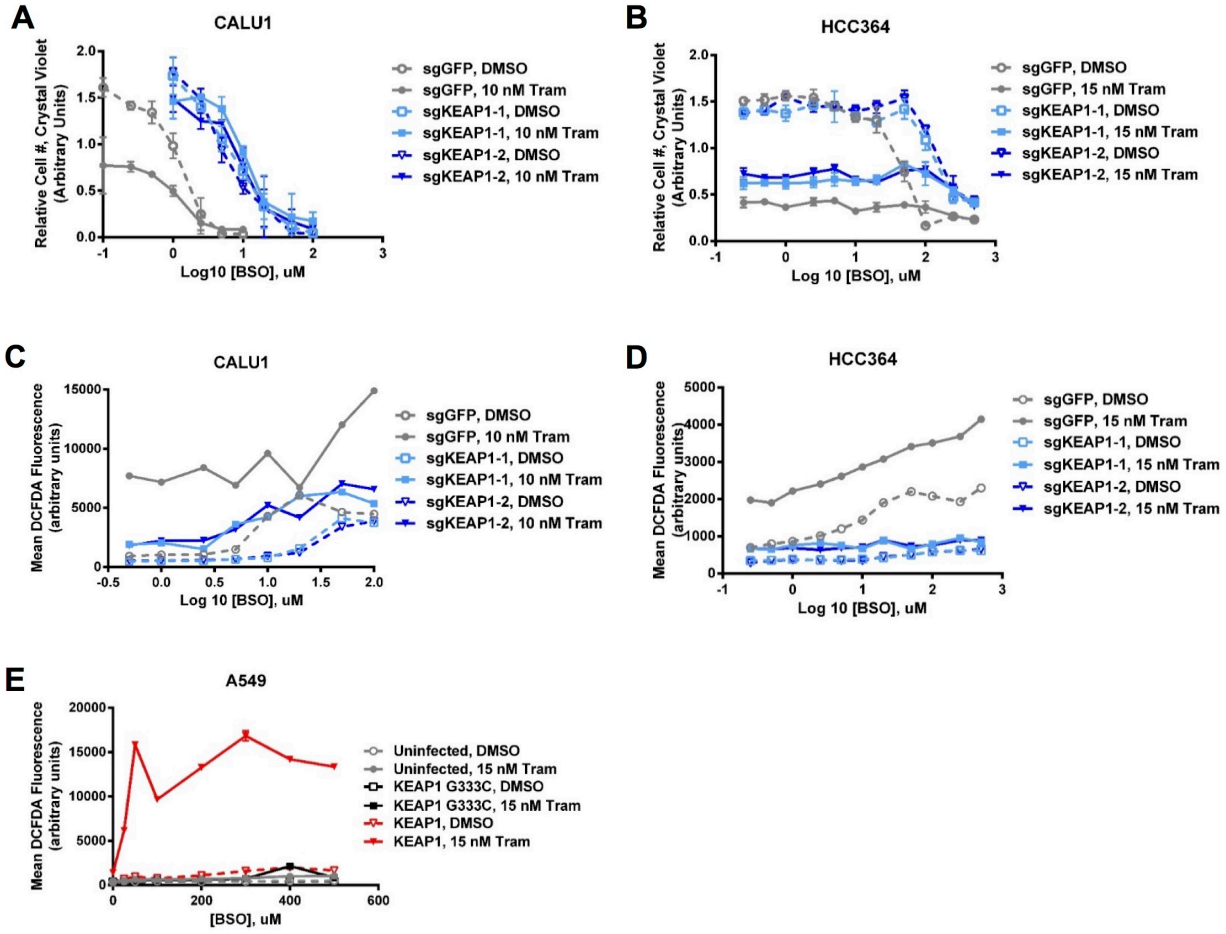

Figure 3-13. *KEAP1*^{KO} reduces ROS and increases viability in the presence of BSO. (A,B) Long-term cell proliferation assays. 20,000 CALU1 **(A)** or HCC364 **(B)** cells were seeded in 24-well plates and treated with DMSO plus BSO for 7 (CALU1) or 6 (HCC364) days or trametinib plus BSO for 12 (CALU1) or 10 (HCC364) days. **(C,D)** KEAP1^{KO} reduces trametinib- and BSO-induced ROS. CALU1 **(C)** or HCC364 **(D)** cells were treated for 72 hrs. *N* = 2 technical replicates, data represented as mean ± SEM. **(E)** Expression of WT KEAP1 but not KEAP1 G333C in KEAP1-null A549 cells increases trametinib- and BSO-induced ROS. Cells were treated for 72 hr. *N* = 2 technical replicates, data represented as mean ± SEM.

3.2.5 Trametinib treatment and *KEAP1*^{KO} alter cell metabolism

In addition to regulating ROS, NRF2 has been reported to regulate the expression of metabolic genes[374,375]. We found that trametinib induced expression of genes involved in the pentose phosphate pathway, de novo nucleotide synthesis, and NADPH synthesis (**Figures 3-14A** and **3-15A**). *KEAP1*^{KO} also increased expression of some of these genes, similar to what was observed with other NRF2 targets (**Figures 3-14A** and **3-15A**). In contrast, expression of genes involved in serine biosynthesis decreased upon trametinib treatment, and *KEAP1*^{KO} maintained higher expression (**Figures 3-14A** and **3-15B**). Together these results support a model in which trametinib treatment inhibits MAPK signaling and induces ROS, which activates NRF2 to low levels. KEAP1 loss increases NRF2 activity, which reduces ROS and alters cell metabolism, allowing cells to proliferate in the absence of MAPK signaling (**Figure 3-16**).

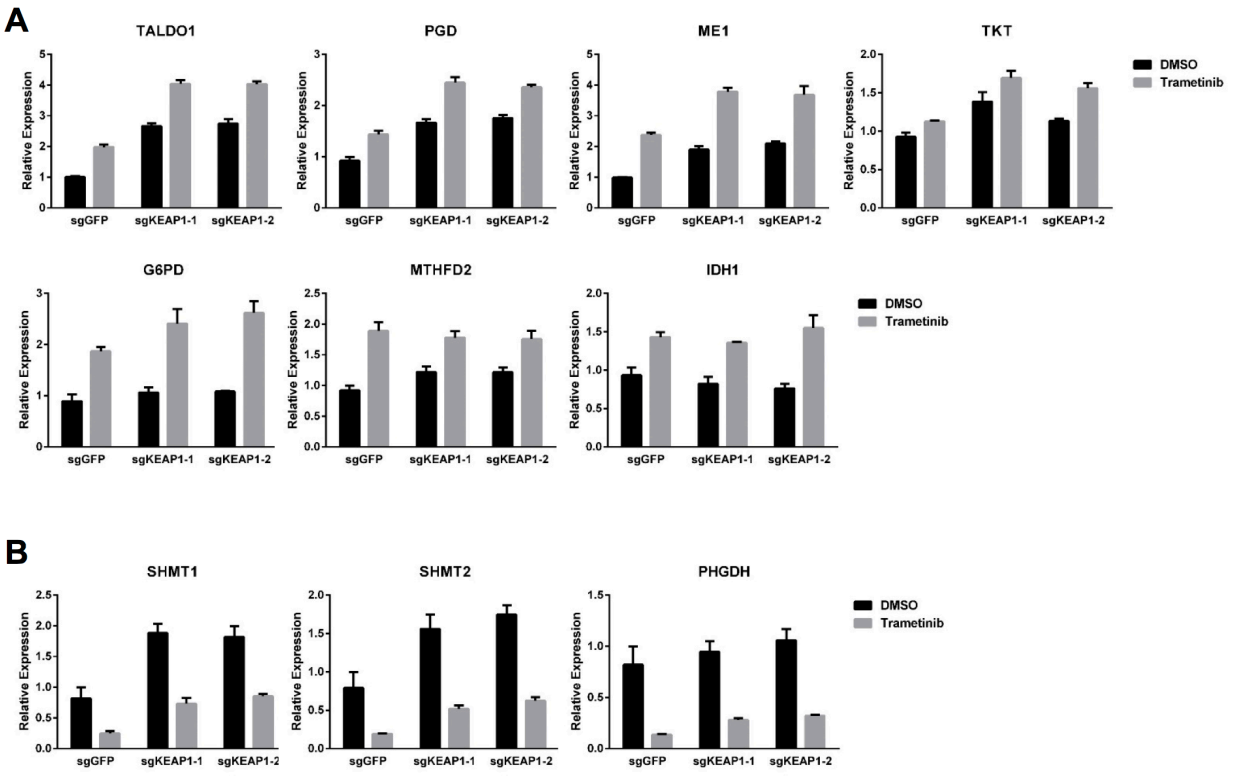

Figure 3-14. *KEAP1*^{KO} alters cell metabolism in CALU1 cells. (A,B) Expression of NRF2 metabolic target genes in CALU1 cells treated with DMSO or trametinib for 72 hours. *N* = 3 biological replicates, data represented as mean ± SEM. Experiments were performed by Elsa Beyer Krall.

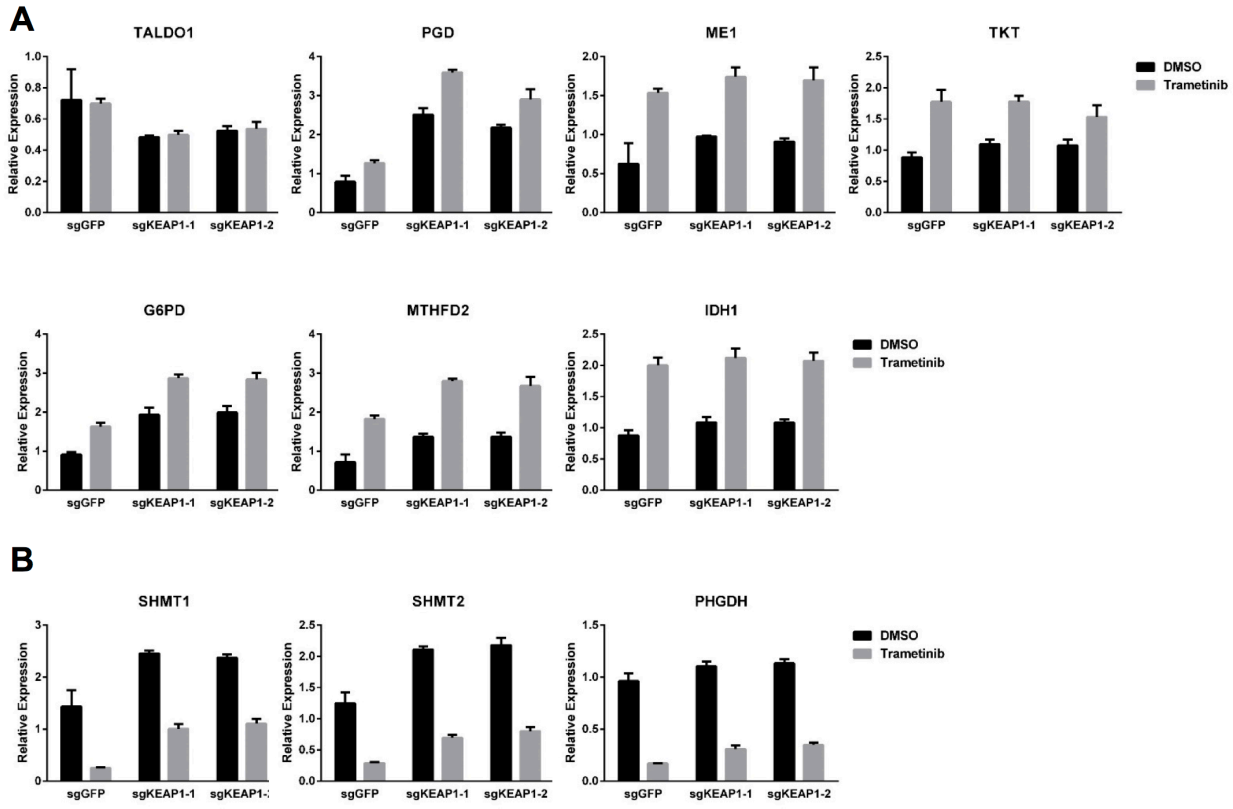

Figure 3-15. *KEAP1*^{KO} alters cell metabolism in HCC364 cells. (A,B) Expression of NRF2 metabolic target genes in HCC364 cells treated with DMSO or trametinib for 72 hours. *N* = 3 biological replicates, data represented as mean ± SEM. Experiments were performed by Elsa Beyer Krall.

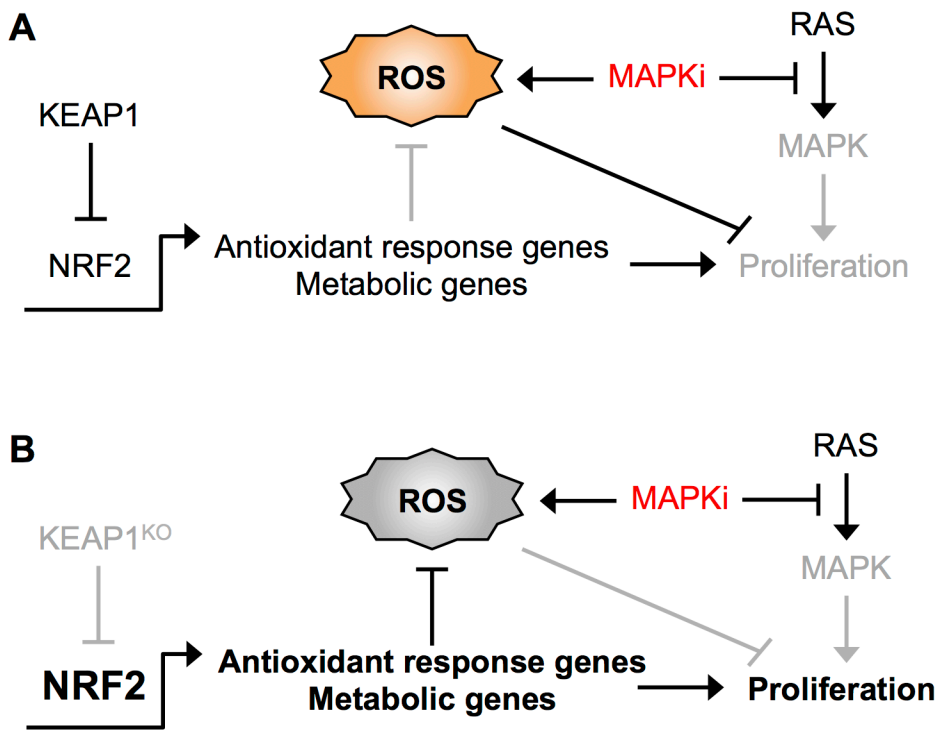

Figure 3-16. Model of resistance mediated by KEAP1 loss. (A) In KEAP1-intact cells, MAPK pathway inhibition induces ROS, which activates NRF2 to low levels. **(B)** Loss of KEAP1 leads to increased NRF2 activity, which reduces ROS levels and alters cellular metabolism, allowing cells to proliferate in the absence of MAPK signaling.

3.2.6 *KEAP1*^{KO} does not confer resistance to MEK inhibition in PATU8902

sgRNAs targeting KEAP1 were not enriched in the genome scale CRISPR-Cas9 knockout screen for mediators of trametinib resistance in the *KRAS*-mutant pancreatic cancer cell line PATU8902 (**Figures 2-7** and **2-9**). We confirmed that *KEAP1*^{KO} increased NRF2 expression in PATU8902 cells (**Figure 3-17A**). However, neither *KEAP1*^{KO} nor NRF2 overexpression conferred resistance to trametinib treatment (**Figure 3-17B**)**.** Interestingly, trametinib treatment did not induce robust levels of ROS in PATU8902 cells (**Figure 3-18A**). Indeed, ROS levels in PATU8902 cells at baseline and upon trametinib treatment were comparable to those in KEAP1-null A549 cells (**Figure 3-18B**)**.** These observations suggest that KEAP1 deletion may confer resistance only in the context where MAPKi induces ROS.

We investigated the effect of trametinib treatment on ROS in 6 *KRAS*-mutant pancreatic cell lines, and found that all 6 cell lines had lower levels of ROS induction upon trametinib treatment than the lung cancer cell lines CALU1 and HCC364 (**Figure 3-18B**)**.** It is possible that some pancreatic cancer cell lines have a lineage-specific mechanism to scavenge ROS that does not involve the KEAP1-NRF2 pathway.

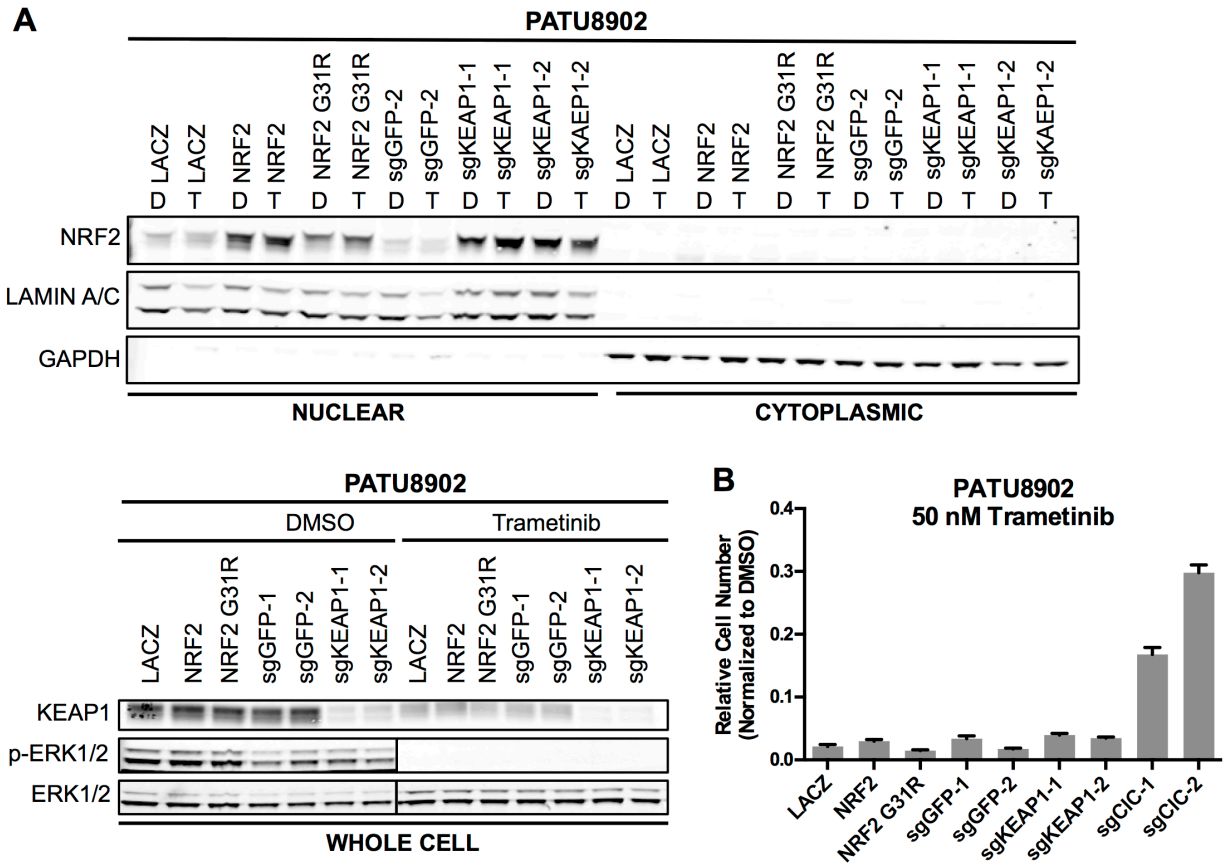

Figure 3-17. *KEAP1*^{KO} does not confer resistance to PATU8902 cells. (A) Immunoblot analysis of PATU8902 cells treated with DMSO (D) or 50 nM trametinib (T) for 48 hours (nuclear and cytoplasmic fractions) or 72 hours (whole cell). **(B)** Long-term proliferation assay assessing effect of NRF2 overexpression or *KEAP1*^{KO} on sensitivity to trametinib treatment. 20,000 PATU8902 cells were seeded in 24-well plates and treated with DMSO for 7 days or 50 nM trametinib for 12 days. *CIC*^{KO} cells (sgCIC-1 and sgCIC-2) are shown as a positive control. *N* = 3 technical replicates representative of *n* = 3 independent experiments, data represented as mean ± SEM.

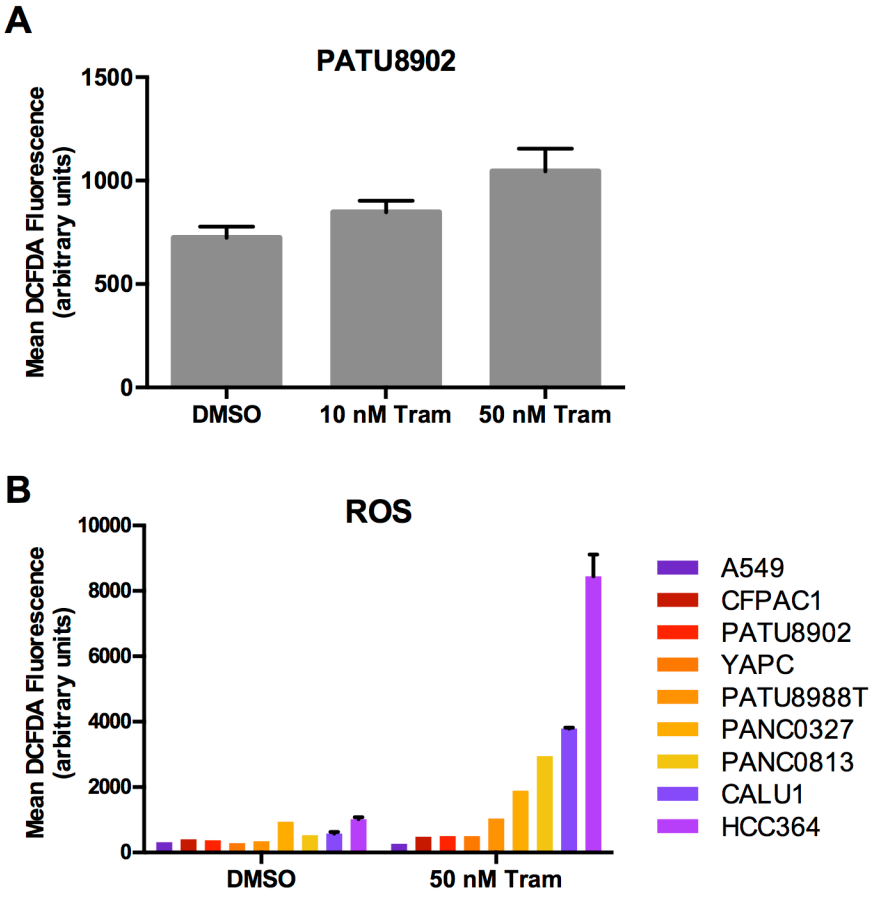

Figure 3-18. Trametinib treatment does not induce ROS in PATU8902 or other pancreatic cancer cell lines. (A) Trametinib does not robustly induce ROS in PATU8902 cells treated with trametinib for 3 days. *N* = 2 technical replicates representative of *n* = 2 independent experiments, data represented as mean ± SEM. **(B)** Effect of trametinib treatment on ROS levels in lung (purple and blue bars) or pancreatic (red, orange, and yellow bars) cancer cell lines. All cell lines have intact *KEAP1*, except A549, which are *KEAP1*-null. In addition, all cell lines except HCC364 (*BRAF*-mutant) are *KRAS*-mutant. *N* = 2 technical replicates, data represented as mean ± SEM.

3.3 Discussion

Using a systematic genetic screening approach, we identified loss of KEAP1 as a potential mechanism of resistance to MEK or BRAF inhibition in *RAS*- or *BRAF*-mutant cancer cell lines (Chapter 2.2.4). Here, we found that KEAP1 loss confers resistance to EGFR, BRAF, or MEK inhibition in lung cancer cell lines with mutant *EGFR*, *KRAS*, *NRAS*, or *BRAF*. Unlike most previously reported mechanisms of resistance, the mechanism described here does not involve reactivation of the MAPK pathway. Our findings indicate that KEAP1 loss or NRF2 overexpression restores cell proliferation in the absence of MAPK signaling by reducing ROS and altering cell metabolism.

In *RAS*- or *BRAF*-mutant lung cancer cells with intact KEAP1, MEK inhibition induced high levels of ROS. The effect of trametinib on cell proliferation was at least partly explained by elevated ROS, as reducing ROS with NAC promoted resistance while further increasing ROS with BSO decreased cell viability. BSO has been shown to be well tolerated in early clinical trials in several different cancers[398-400]. Combination treatment with a EGFR, BRAF, or MEK inhibitor plus BSO may be beneficial in treating lung cancers with *EGFR*, *RAS*, or *BRAF* mutations and intact KEAP1.

A previously published genome scale CRISPR-Cas9 resistance screen in the $BRAF^{V600E}$ melanoma cell line A375 identified $KEAP1^{KO}$ as a potential mechanism of resistance to the BRAF inhibitor vemurafenib[297]. In addition, Hugo et al. recently performed RNA-sequencing of pre-treatment and post-resistance samples from BRAF-mutant melanoma treated with MEK or BRAF inhibitors[401]. From these 29 patients, we identified one dabrafenib-treated patient in which two out of nine post-resistance biopsies had at least a two-fold decrease in KEAP1 expression compared to the pre-

treatment biopsy. One of these sites had copy number gain of BRAF and copy number loss of DUSP4, which may contribute to resistance. The other site did not have any known mechanisms of resistance, but it remains unclear whether or not decreased KEAP1 expression mediated the resistance. Together with our work, these studies suggest that KEAP1 loss may also be a mechanism of resistance to MEK and BRAF inhibition in melanoma.

A recent vemurafenib basket trial in *BRAF*^{V600E} non-melanoma cancers showed that 42% of lung cancers with the *BRAF*^{V600E} mutation responded to vemurafenib[359]. As seen with vemurafenib treatment in melanoma or with EGFR inhibitors in lung cancer, acquired resistance will likely arise. Furthermore, while MEK inhibitors only elicit responses in a small number of lung cancer patients[249], these responders are also likely to develop acquired resistance. Predicting how resistance may arise in these patients will be important for developing combination therapies. In addition, intrinsic resistance in a subset of the patients who never respond to therapy may be explained by the mechanisms we describe here.

The KEAP1/NRF2 pathway is genetically altered in ~30% of lung squamous cell carcinomas and ~20% of lung adenocarcinomas, and alterations in this pathway can co-occur with alterations in the EGFR/RAS pathway[136,137,170,385] (and P. Jänne unpublished observations). BRAF and MEK inhibitors are currently being tested in clinical trials for *RAS*- and *BRAF*-mutant lung cancer. However, for most of these trials pre-treatment and post-relapse biopsy specimens are not available for molecular analysis of resistance mechanisms. As more patients are treated with MEK and BRAF inhibitors, analyzing KEAP1 and NRF2 status in pre-treatment and post-resistance tumor samples

will determine if loss of KEAP1 or gain of NRF2 are clinically relevant mechanisms of acquired and intrinsic resistance to RTK/Ras/MAPK-targeted therapies in lung cancer. Although KEAP1/NRF2 alterations are known to confer resistance to chemotherapy, KEAP1/NRF2 mutation status is not used to make treatment decisions in lung cancer. Stratifying patients based on these findings will be important for evaluating the efficacy of these inhibitors in clinical trials and for choosing the appropriate treatment for patients.

3.4 Materials and Methods

Cell lines and reagents

Cells were maintained in RPMI-1640 (A549, CFPAC1, HCC364, HCC827, NCI-H1299, NCI-H1975, PANC0327, and PANC0813; Corning), McCoy's 5A (CALU1; Gibco), or DMEM (PATU8902, PATU8988T, and YAPC; Corning) supplemented with 2 mM glutamine, 50 U/mL penicillin, 50 U/mL of streptomycin (Gibco), and 10% fetal bovine serum (Sigma), and incubated at 37°C in 5% CO_2. Trametinib, vemurafenib, erlotinib, and afatinib were purchased from Selleck Chemicals.

Vectors

Cas9 in the pLX311 backbone (pXPR_BRD111) and sgRNAs in the pXPR_BRD003 backbone were obtained from the Genetic Perturbation Platform at the Broad Institute.

sgKEAP1 arrayed infection

500,000 cells per well were seeded in 48-well plates in 250 µL media with 4 µg/mL polybrene. 25 µL virus (sgKEAP1 or sgGFP) was added per well and plates were spun 2 hrs at 2000 rpm at 30°C. 6 hrs later, each well was split into a 6cm dish. 24 hrs after infection, cells were selected with puromycin for one week.

Long-term proliferation assays

2,000-10,000 cells were seeded in 12-well or 24-well plates in the indicated drug conditions. Media containing fresh drug was replaced every 3-5 days. After the indicated number of days, cells were washed in PBS, fixed in 10% formalin for 15 minutes, and stained with 0.1% crystal violet in 10% ethanol for 20 minutes. After acquiring images, crystal violet was extracted in 10% acetic acid for 20 minutes. The absorbance at 565 nm was determined using a Spectramax plate reader.

Cell counting assays

Cells were seeded in 10 cm (1-2 x 10^6 cells) or 15 cm (1-3 x 10^6 cells) plates and treated with drug or DMSO as indicated. Cells were propagated or media was refreshed every 3-4 days. Cells were counted at each passage, and number of cell doublings was calculated.

Quantitative PCR

RNA was harvested using a Qiagen RNeasy Kit and was reverse transcribed into cDNA using SuperScriptIII according to the manufacturer's recommendations.

Table 3-1. q-PCR primer sequences

Gene	*Forward Primer*	*Reverse Primer*
NFE2L2	TCCAGTCAGAAACCAGTGGAT	GAATGTCTGCGCCAAAAGCTG
GCLC	GTGTTTCCTGGACTGATCCCA	TCCCTCATCCATCTGGCAAC
GCLM	CATTTACAGCCTTACTGGGAGG	ATGCAGTCAAATCTGGTGGCA
HO1	CTTTCAGAAGGGCCAGGTGA	GTAGACAGGGGCGAAGACTG
NQO1	CTCACCGAGAGCCTAGTTCC	CGTCCTCTCTGAGTGAGCCA
MRP1	CTCTATCTCTCCCGACATGACC	AGCAGACGATCCACAGCAAAA
TKT	GCTGAACCTGAGGAAGATCA	TGTCGAAGTATTTGCCGGTG
TALDO1	GTCATCAACCTGGGAAGGAA	CAACAAATGGGGAGATGAGG
PGD	ATATAGGGACACCACAAGACGG	GCATGAGCGATGGGCCATA
MTHFD2	TGTCCTCAACAAAACCAGGG	TTCCTCTGAAATTGAAGCTGG
ME1	CTGCCTGTCATTCTGGATGT	ACCTCTTACTCTTCTCTGCC
IDH1	CACTACCGCATGTACCAGAAAGG	TCTGGTCCAGGCAAAAATGG
G6PD	TGACCTGGCCAAGAAGAAGA	CAAAGAAGTCCTCCAGCTTG
PHGDH	ATCTCTCACGGGGGTTGTG	AGGCTCGCATCAGTGTCC
SHMT1	TGAACACTGCCATGTGGTGACC	TCTTTGCCAGTCTTGGGATCC
SHMT2	GCCTCATTGACTACAACCAGCTG	ATGTCTGCCAGCAGGTGTGCTT
ACTIN	CAACCGCGAGAAGATGACC	ATCACGATGCCAGTGGTACG

Nuclear/cytoplasmic fractionation

5 x 10^5 cells were seeded in 10 cm dishes. The following day, cells were treated with trametinib (25 nM for HCC364 or 50 nM for CALU1) or DMSO. After 72 hrs of drug treatment, cells were lysed and fractionated using NE-PER Nuclear and Cytoplasmic Extraction Reagents (Pierce Biotechnology) according to the manufacturer's recommendations.

Antibodies and immunoblots

Cells were lysed in RIPA buffer containing protease and phosphatase inhibitors and were cleared by centrifugation. Protein was quantified using the Pierce BCA assay, and lysate concentrations were normalized. Lysates were run on SDS-PAGE gels and

were transferred to nitrocellulose membranes using the Invitrogen iBlot system. Membranes were blocked for one hour in 5% milk in Tris-buffered saline with 0.1% Tween (TBS-T). Membranes were incubated overnight at 4°C with primary antibodies in 5% BSA in TBS-T. Membranes were washed three times in TBST-T then incubated 1 hour at room temperature with secondary antibodies in 5% BSA in TBS-T. Membranes were washed in TBS-T and imaged on a Li-Cor Odyssey Infrared Imaging System. Primary antibodies were total ERK (Cell Signaling #9102), phospho-ERK (Cell Signaling #4370), total AKT (Cell Signaling #9272), phospho-AKT (Cell Signaling #4060), GAPDH (Cell Signaling #5174), LAMIN A/C (Cell Signaling #4777), KEAP1 (Proteintech 10503-3-AP), and NRF2 (Santa Cruz Biotechnology sc-13032).

ORF expression

293T cells were seeded in DMEM + 10% FBS + 0.1% Pen/Strep in 6 cm dishes. 24 hrs later, cells were transfected with 100 ng VSVG, 900 ng delta8.9, and 1 µg pLX317-ORF plasmid using OptiMEM and Mirus TransIT. 16 hrs after transfection, media was changed to DMEM + 30% FBS + 1% Pen/Strep. Virus was harvested 24 hrs later. Cell lines were seeded in 6-well plates and were infected the following day with 1:5 dilution of virus containing 4 µg/mL polybrene. 24 hrs after infection, cells were selected with puromycin.

DCFDA assays to measure ROS

Unless otherwise indicated, cells were treated with drug for 3 days. Cells were trypsinized and resuspended in media with 10 µM DCFDA (Sigma D6883) and

incubated at 37°C for 90 minutes in the dark. For a positive control, parental cells were treated with 20 μM tert-butyl hydroperoxide (Sigma Aldrich 458139) during incubation. For a negative control, parental cells were incubated in media without DCFDA. DCFDA fluorescence was detected by flow cytometry, using the FITC channel on an LSRII flow cytometer (BD Biosciences).

GSH/GSSG assays

Cells were seeded into 96-well white-walled opaque-bottom plates (Costar 3917; 5000 cells in 100 μL media per well) and allowed to adhere overnight. The following day, cells were treated with 50 μL of media containing DMSO or drug (3x desired final concentration). At the indicated amount of time after treatment, the ratio of reduced and total glutathione was determined using the GSH/GSSG-Glo Assay (Promega V6612) according to the manufacturer's protocol for adherent mammalian cells. A GSH standard curve was included to confirm that experimental readouts were within the linear range of assay detection.

NADPH/NADP+ assays

5000 cells were seeded into 96-well white-walled opaque-bottom plates in 100 μL media per well and allowed to adhere overnight. The following day, cells were treated with 25 μL of media containing 4X trametinib or DMSO. 72 hrs later, NADPH and NADP+ levels were determined using the NADP/NADPH-Glo Assay (Promega G9082) according to the manufacturer's protocol for measuring NADPH and NADP+ individually.

sgRNA Sequences

Table 3-2. sgRNA sequences

Name	*Target Sequence*
sgGFP	GGCGAGGGCGATGCCACCTA
sgLACZ-1	AACGGCGGATTGACCGTAAT
sgLACZ-2	CTAACGCCTGGGTCGAACGC
sgKEAP1-1	CTTGTGGGCCATGAACTGGG
sgKEAP1-2	TGTGTCCTCCACGTCATGAA
sgKEAP1 A10	AGTACGACTGCGAACAGCGA
sgKEAP1 B05	TCGTAGCCCCCATGAAGCAC
sgKEAP1 C08	GCCAGATCCCAGGCCTAGCG
sgKEAP1 D01	TCAAGGCCATGTTCACCAAC
sgKEAP1 D10	AGCGTGCCCCGTAACCGCAT
sgKEAP1 F08	CTACCTGGTCAAGATCTTCG
sgKEAP1 G07	GGTCAAGTACCAGGATGCAC
sgKEAP1 H07	TGACCAGGTAGTCCTTGCAG

CHAPTER FOUR

ATXN1L, CIC, and ETS transcription factors modulate sensitivity to MAPK pathway inhibition

This chapter has been adapted from

Wang, B.*, Krall, E.B.*, Aguirre, A.J.*, Widlund, H.R., Doshi, M.B., Sicinska, E., Sulahian, R., Goodale, A., Cowley, G.S., Piccioni, F., Doench, J.G., Root, D.E., and Hahn, W.C. ATXN1L, CIC, and ETS Transcription Factors Modulate Sensitivity to MAPK Pathway Inhibition, *in submission.*

Contributions

Belinda Wang, Elsa Beyer Krall, and Andrew Aguirre designed *in vitro* experiments. Elsa Beyer Krall performed validation (**Figures 4-1** and **4-2** NCIH1299), morphology (**Figure 4-4**), and q-PCR (**Figure 4-13A**) experiments. Mihir Doshi contributed **Figure 4-19B**. Andrew Aguirre and Ewa Sicinska designed and performed *in vivo* experiments with Mihir Doshi (**Figure 4-7**). Hans Widlund analyzed melanoma outcome data (**Figure 4-21**). Belinda Wang performed all other *in vitro* experiments and data analysis.

4.1 Introduction

The *RAS* family of genes (*KRAS, NRAS,* and *HRAS*) is frequently mutated in human cancers. Although the majority of cancers with mutant *RAS* are dependent on oncogenic RAS signaling for proliferation and survival, direct inhibitors of oncogenic RAS proteins have not yet been developed for clinical use[36,92,131]. An alternative approach to therapeutically target *RAS*-mutant cancers is to inhibit downstream effector pathways. The RAF-MEK-ERK MAPK pathway has been shown to be an important downstream effector of oncogenic *RAS*[54,102]*.* Early clinical trials suggest that a subset of *KRAS*- or *BRAF*-mutant cancers respond to small molecule inhibitors of MEK or BRAF, though both intrinsic and acquired resistance limit therapeutic efficacy[238,248,249,359].

We performed unbiased genome scale genetic screens to identify genes whose deletion promote resistance to MEK inhibition *KRAS*-mutant pancreatic cancer cell lines and to MEK or BRAF inhibition in *RAS*- or *BRAF*-mutant lung cancer cell lines. CIC deletion was found to confer resistance to MAPKi in five of the six genome-scale screens (**Figures 2-7** and **2-9**). Subsequently, candidate mini-pool screens demonstrated that CIC knockout confers resistance to MEK inhibition in *NRAS*-mutant melanoma cell lines. As CIC loss was found to confer resistance to MAPKi in multiple screens, we investigated how *CIC* knockout (CIC^{KO}) mediates trametinib resistance.

4.2 Results

4.2.1 CIC loss confers resistance to MEK and BRAF inhibition in multiple contexts without reactivating ERK signaling

We tested eleven *CIC*-targeting sgRNAs to identify sgRNAs that effectively eliminated CIC expression (**Figure 4-1A**). We assessed the ability of these sgRNAs to modulate trametinib sensitivity in the *NRAS*-mutant lung cancer cell line NCIH1299 using a short-term viability assay. We found that only the sgRNAs that effectively depleted CIC conferred resistance to trametinib treatment (**Figure 4-1B**). Subsequently, we verified that CIC deletion conferred resistance to trametinib treatment in four of the cell lines used in the genome scale CRISPR-Cas9 screens using a cell counting assay (**Figure 4-2**).

To determine if the observed effect of *CIC* deletion was generalizable, we assessed the ability of CIC^{KO} to confer resistance in several different lineage and mutational contexts. We found that CIC^{KO} conferred resistance to MEK inhibition in *KRAS*-mutant pancreatic, lung or colon cancer, to MEK inhibition in *NRAS*-mutant lung cancer or melanoma, and to MEK or BRAF inhibition in *BRAF*-mutant melanoma, lung cancer, and colon cancer cells (**Figure 4-3**). CIC loss restored cell proliferation in the context of trametinib treatment, and some CIC^{KO} cells treated with trametinib appeared morphologically comparable to CIC^{WT} cells treated with DMSO (**Figure 4-4**). However, CIC^{KO} did not restore signaling through the MAPK or PI3K pathways as measured by phosphorylation of ERK or AKT (**Figure 4-5**).

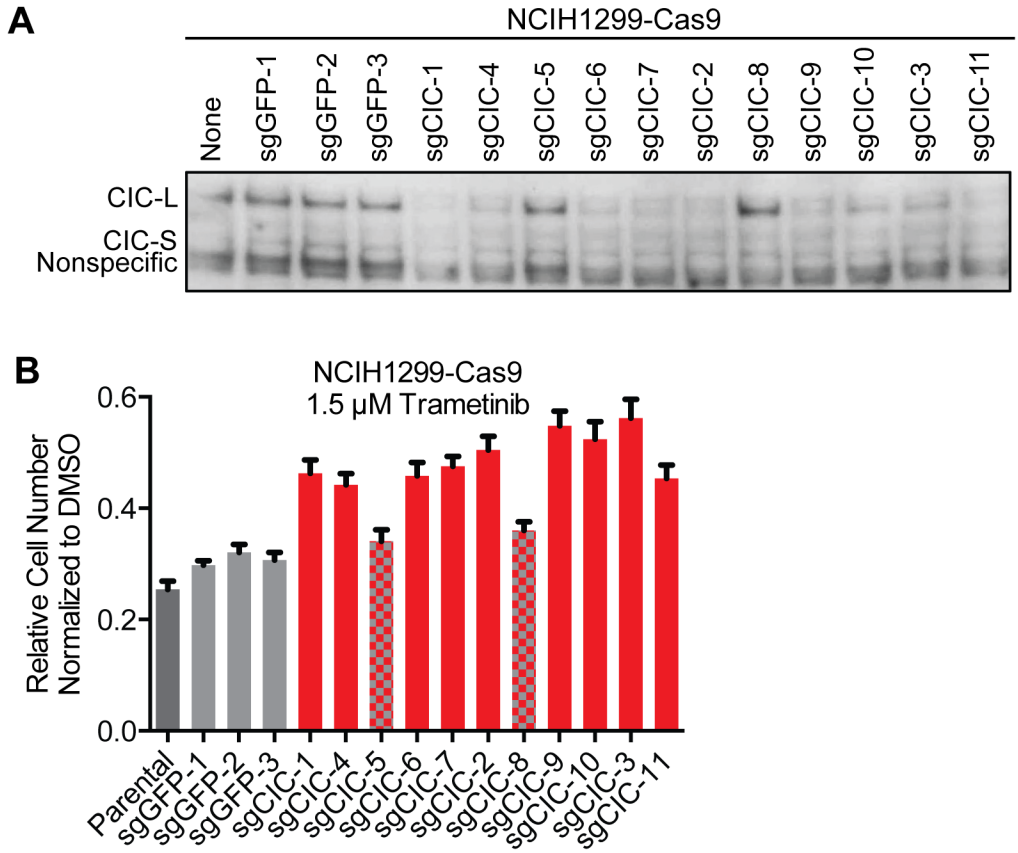

Figure 4-1. **Identification of sgRNAs that effectively knockout CIC expression.** **(A)** Immunoblot analysis of whole cell lysates of NCIH1299-Cas9 cells expressing sgRNAs targeting *GFP* (control) or *CIC*. **(B)** Short term viability assays to determine the effect of CIC^{KO} on trametinib sensitivity in NCIH1299 cells. *N = 6* technical replicates, data represented as mean ± SD. Experiment was conducted by Elsa Beyer Krall.

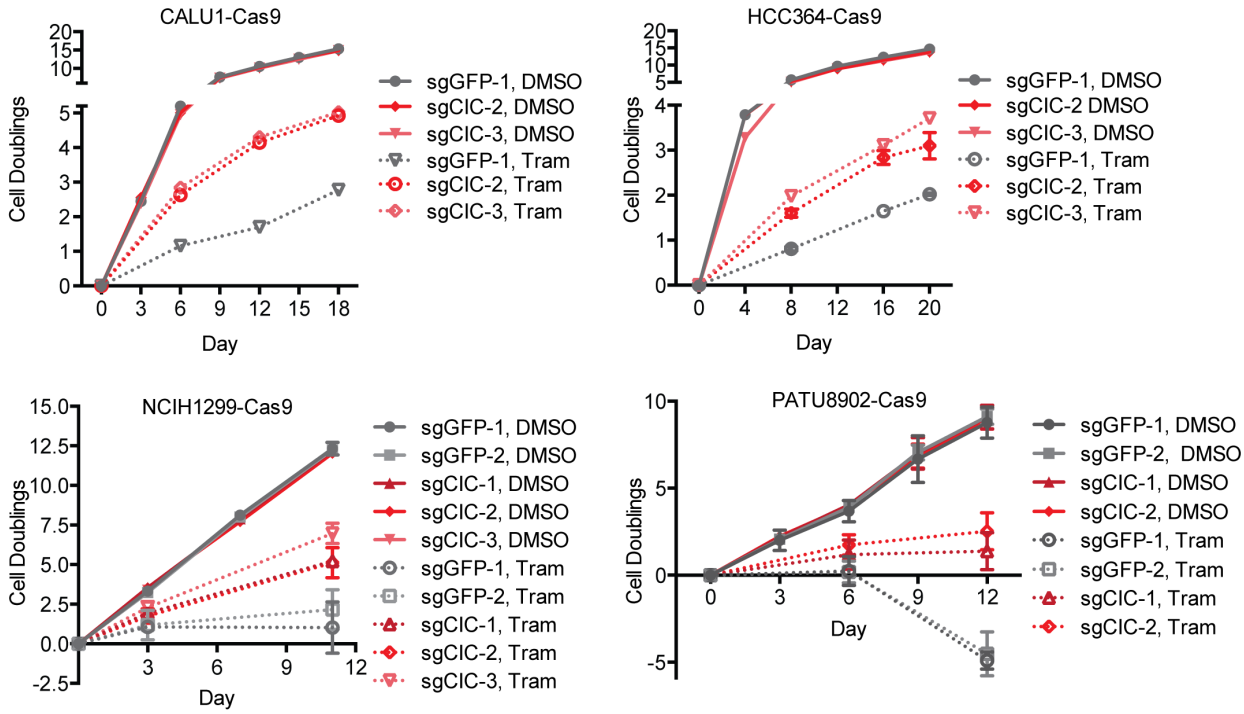

Figure 4-2. *CIC*^{KO} confers resistance to MAPK pathway inhibition. Proliferation of CALU1-Cas9, HCC364-Cas9, NCIH1299-Cas9, and PATU8902-Cas9 cells expressing sgRNAs targeting *GFP* (control) or *CIC*, and treated with DMSO or trametinib (50 nM for CALU1 and PATU8902, 25 nM for HCC364, and 1.5 μM for NCIH1299), *n* = 2 replicates, data represented as mean ± SEM. NICH1299-Cas9 cell counting assay was performed by Elsa Beyer Krall.

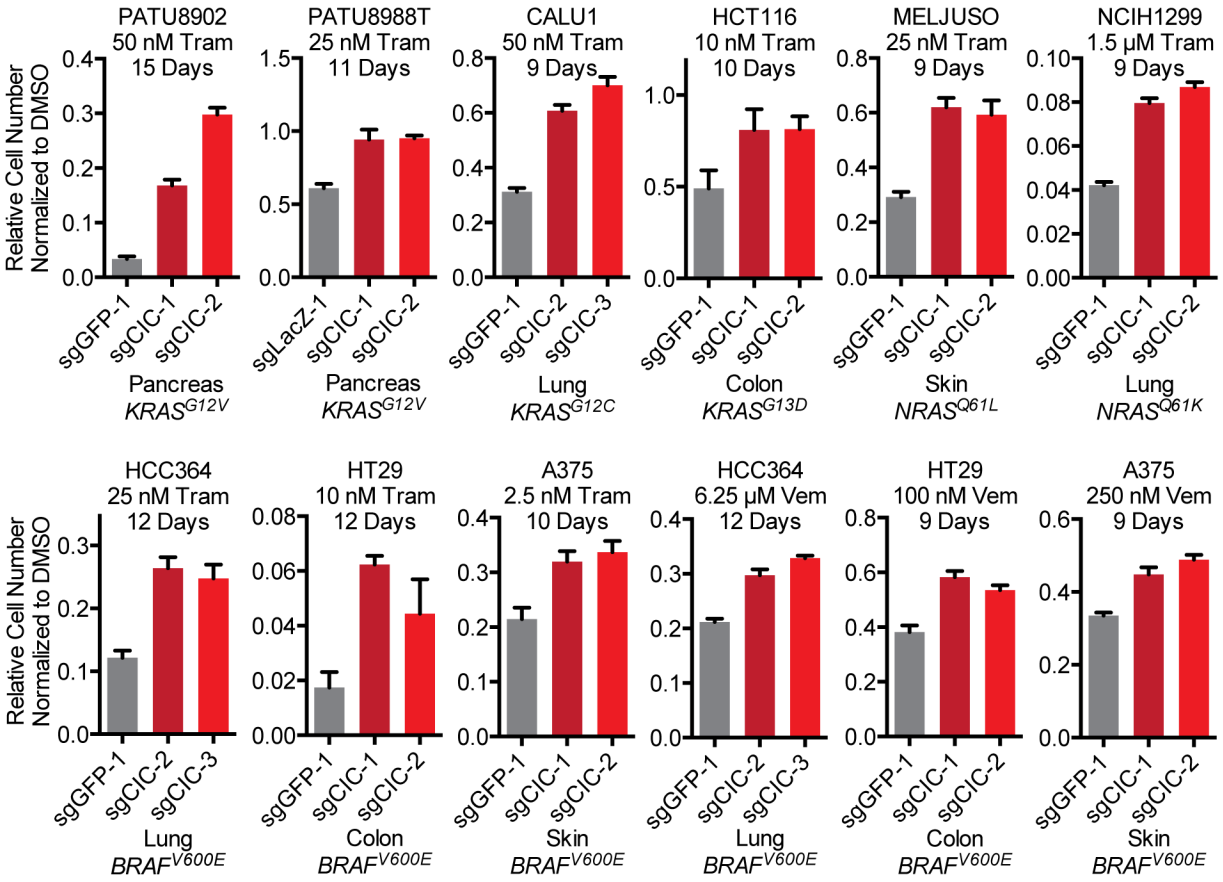

Figure 4-3. CIC loss confers resistance to MEK and BRAF inhibition in multiple contexts. Long-term proliferation assays to determine the effect of *CIC*^{KO} on trametinib (Tram) and vemurafenib (Vem) sensitivity in multiple lineage and mutation contexts. *N* = 3 technical replicates representative of at least *n* = 2 independent experiments, data represented as mean ± SEM.

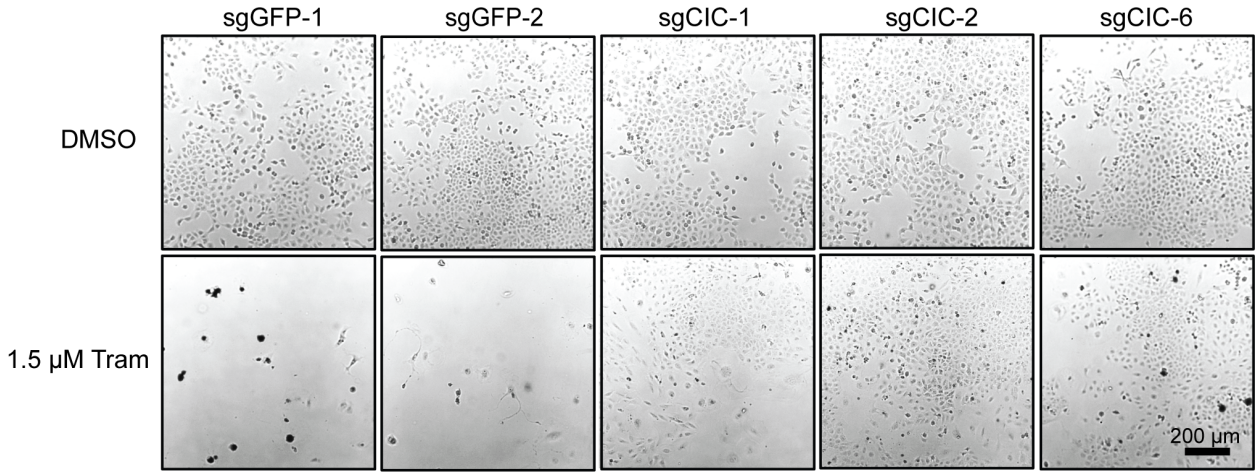

Figure 4-4. Morphology of *CIC*^{KO} cells. Morphology of NCIH1299-Cas9 cells expressing the indicated sgRNA after 4 days of treatment with DMSO or 11 days of treatment with 1.5 μM trametinib. Experiment was performed by Elsa Beyer Krall.

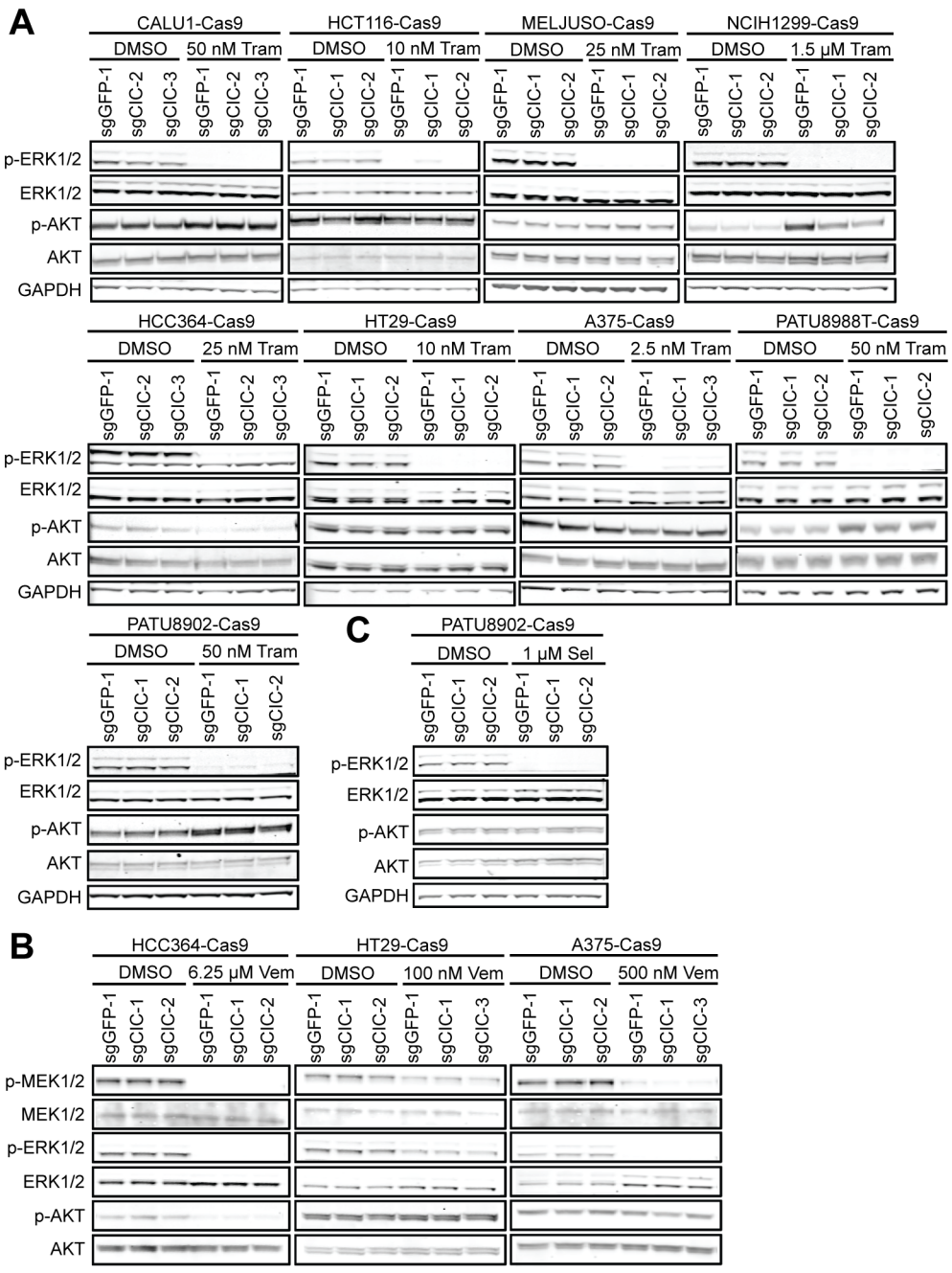

Figure 4-5. ***CIC^KO^* does not reactivate p-ERK.** Immunoblot confirmation of phospho-ERK suppression in cell lines treated with trametinib **(A)**, vemurafenib **(B)**, or selumetinib **(C)** for 24 hours. Abbreviations: trametinib (Tram), vemurafenib (Vem), selumetinib (Sel).

We next assessed whether *CIC*^{KO} confers resistance to KRAS depletion in PATU8902, a KRAS-dependent cell line. We generated the PATU8902 pTetK cell line, which harbors a doxycycline-inducible shRNA targeting *KRAS*. Subsequently, we transduced PATU8902 pTetK cells with a dual vector containing both Cas9 and an sgRNA targeting either *LacZ* or *CIC* to generate isogenic *CIC*^{WT} and *CIC*^{KO} variant cell lines (**Figure 4-6A**). We found that deleting *CIC* reduced sensitivity to KRAS depletion in PATU8902 pTetK cells in a long-term proliferation assay (**Figure 4-6B**).

To determine whether resistance mediated by *CIC* deletion was specific to inhibition of the MAPK pathway or was a more general effect, we treated *CIC*^{KO} cells with the MEK inhibitor selumetinib or three cytotoxic chemotherapeutic agents. *CIC*^{KO} conferred resistance to selumetinib (**Figure 4-6C**), but not to cisplatin, paclitaxel, or 5-FU (**Figure 4-6**). These observations indicate that CIC loss promotes proliferation/survival in the setting of suppressed KRAS or MAPK signaling in several different epithelial lineages, but does not generally promote survival to cytotoxic agents.

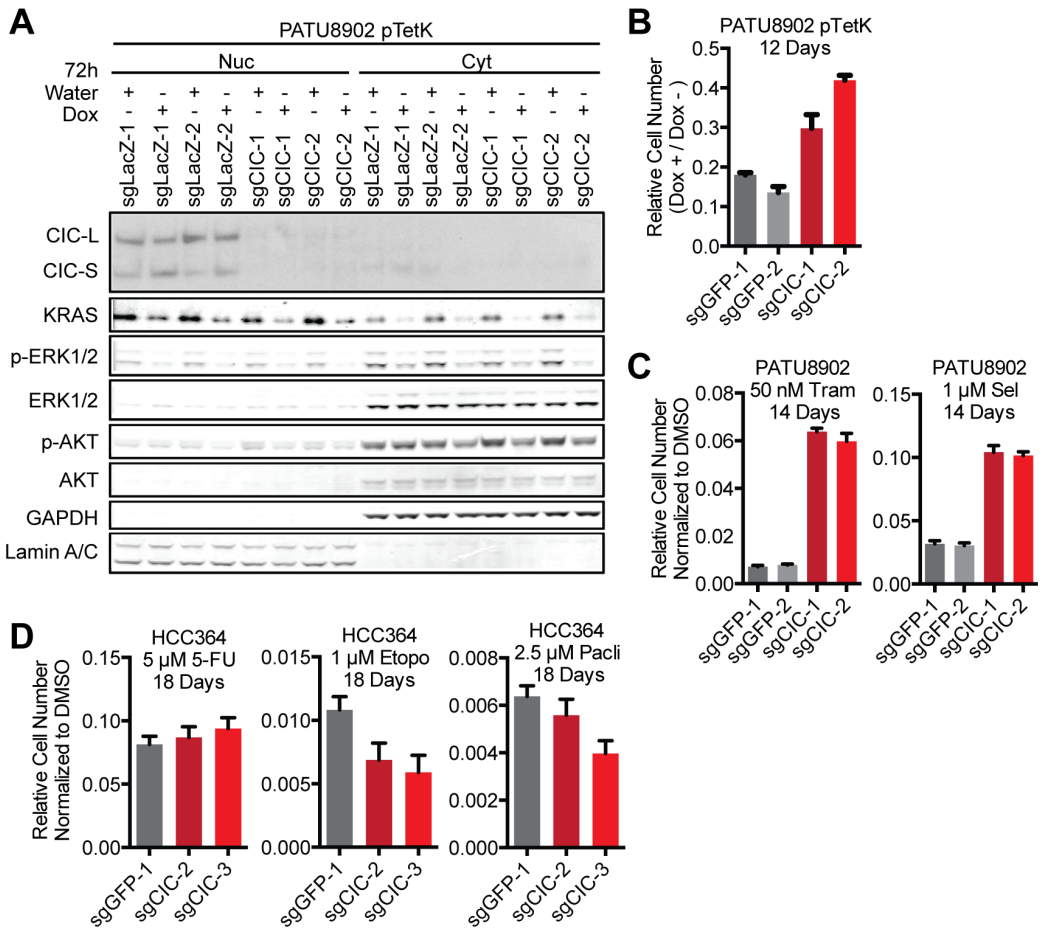

Figure 4-6. **Resistance conferred by *CIC*^{KO} is specific to RAS/MAPK pathway. (A)** Immunoblot assessment of KRAS depletion and phospho-ERK suppression in *CIC*^{WT} or *CIC*^{KO} PATU8902 pTetK cells treated with water or 1 μg/mL doxycycline (dox) for 72 hrs. **(B)** Effect of *CIC*^{KO} on sensitivity to KRAS depletion in the KRAS-dependent cell line PATU8902 pTetK. Dox = doxycycline, *n* = 3 technical replicates representative of *n* = 2 independent experiments, data represented as mean ± SEM. **(C)** Effect of *CIC*^{KO} on trametinib and selumetinib sensitivity, *n* = 6 technical replicates representative of *n* = 2 independent experiments, data represented as mean ± SEM. **(D)** Effect of *CIC*^{KO} on sensitivity to 5-FU, etoposide (etopo), or paclitaxel (pacli). *N* = 3 technical replicates, data represented as mean ± SEM.

4.2.2 CIC loss confers resistance to trametinib treatment *in vivo*

To determine whether CIC loss confers resistance to trametinib treatment *in vivo*, we injected mice with PATU8902 CIC^{WT} or CIC^{KO} cells and initiated daily trametinib treatment after tumor formation. We found that vehicle-treated CIC^{WT} and CIC^{KO} tumors grew at similar rates. Trametinib treatment decreased the growth of CIC^{WT} tumors compared to vehicle treatment ($p = 0.01$), but had no effect on CIC^{KO} tumors. Indeed, trametinib-treated CIC^{KO} tumors grew at comparable rates to vehicle-treated CIC^{WT} or CIC^{KO} tumors (**Figure 4-7**). Based on these data, we concluded that CIC^{KO} confers resistance to trametinib treatment *in vivo*.

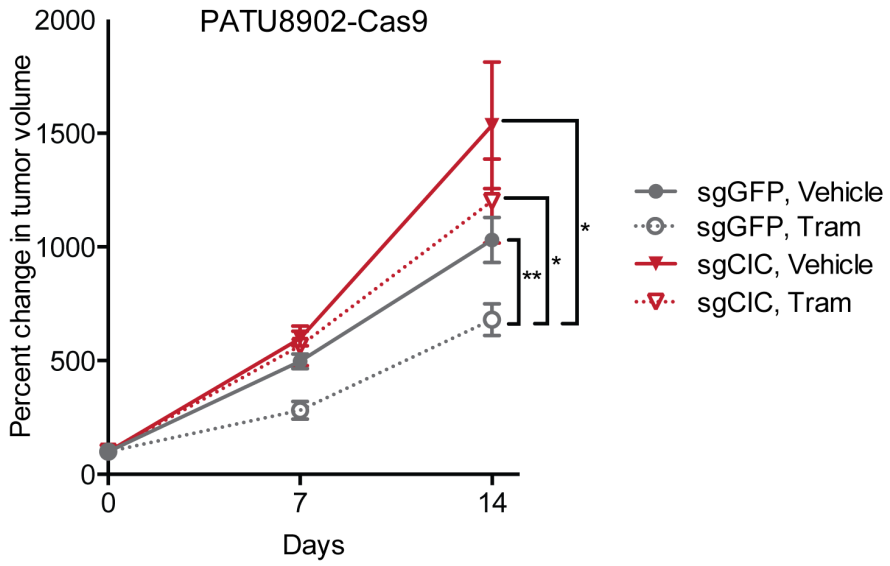

Figure 4-7. ***CIC^{KO}* confers resistance *in vivo.*** Percent change in tumor volume of CIC^{WT} (sgGFP) or CIC^{KO} (sgCIC) PATU8902 xenografts in athymic nude mice receiving daily vehicle or trametinib treatment. Average of n = 10 xenografts, data are represented as mean ± SEM, tram = 2 mg/kg trametinib. Experiment was performed by Ewa Sicinska, Andrew Aguirre, and Mihir Doshi.

4.2.3 MEK inhibition increases nuclear CIC-S and CIC-mediated repression of ETS transcription factors

CIC is a transcriptional repressor that is phosphorylated and inhibited by MAPK in *Drosophila*[402-404]. There are two CIC isoforms (CIC-S and CIC-L), which differ in size and in their N-terminal region[405]. In *Drosophila*, CIC-S fulfills most known CIC functions[406]. We found that in all the cell lines we tested, trametinib treatment induced an increase in nuclear CIC-S (**Figures 4-8, 4-9,** and **4-10**). In contrast, the effect of trametinib on CIC-L localization was inconsistent. Trametinib treatment decreased levels of nuclear CIC-L in HCC364, CALU1, and PATU8902 cells; increased levels of nuclear CIC-L in PATU8988T; and had no effect on levels of nuclear CIC-L in NCIH1299, HT29, and MELJUSO cells (**Figures 4-8, 4-9,** and **4-10**). As CIC^{KO} confers resistance to trametinib treatment in all these cell lines (**Figures 4-2** and **4-3**) and only the localization of CIC-S is consistently altered by trametinib treatment across all cell lines, we concluded that decreased CIC-S in CIC^{KO} cells may mediate resistance to trametinib.

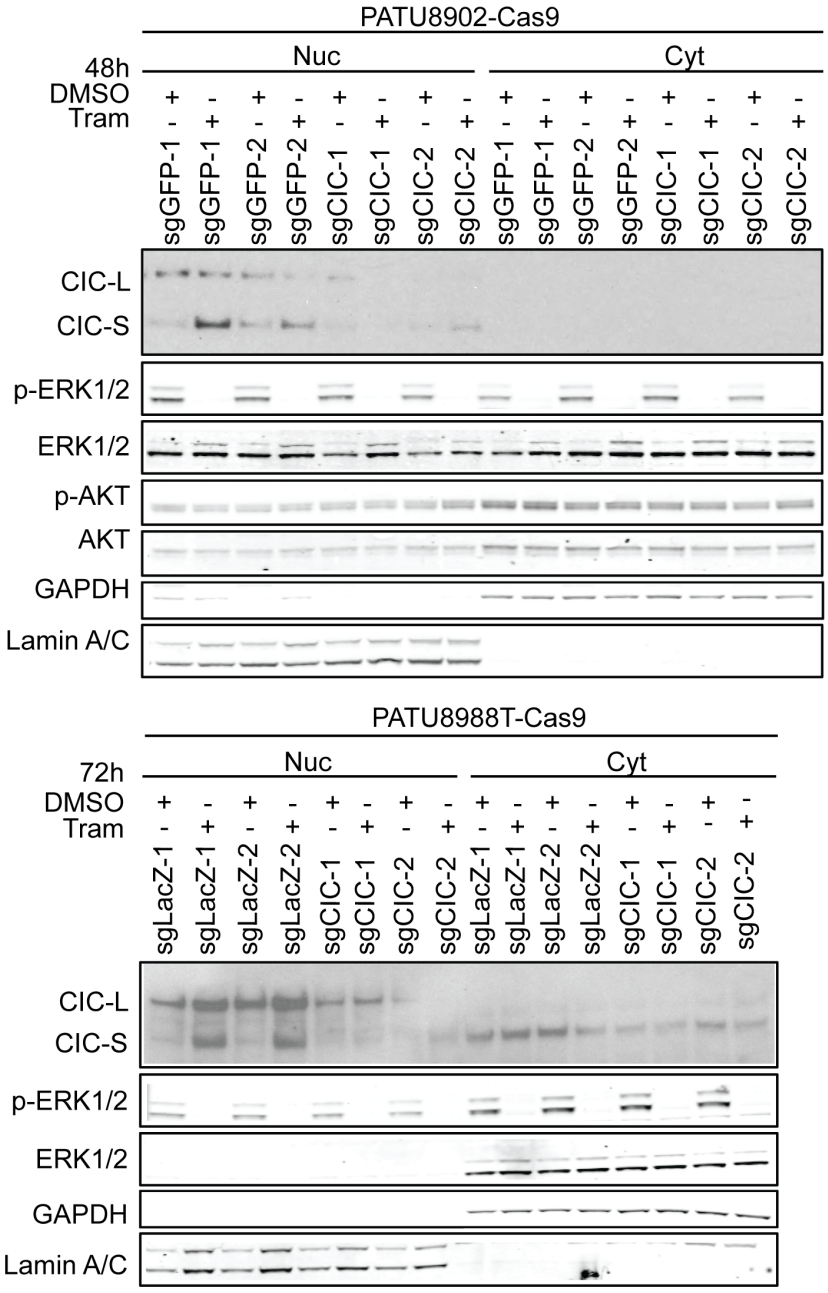

Figure 4-8. MEK inhibition increases nuclear CIC-S in pancreatic cancer cell lines. Immunoblot analysis of the effect of trametinib on CIC localization using fractionated cell lysates after 48 (PATU8902) or 72 (PATU8988T) hours of drug treatment. Nuc = nuclear, Cyt = cytoplasmic, Tram = 50 nM trametinib.

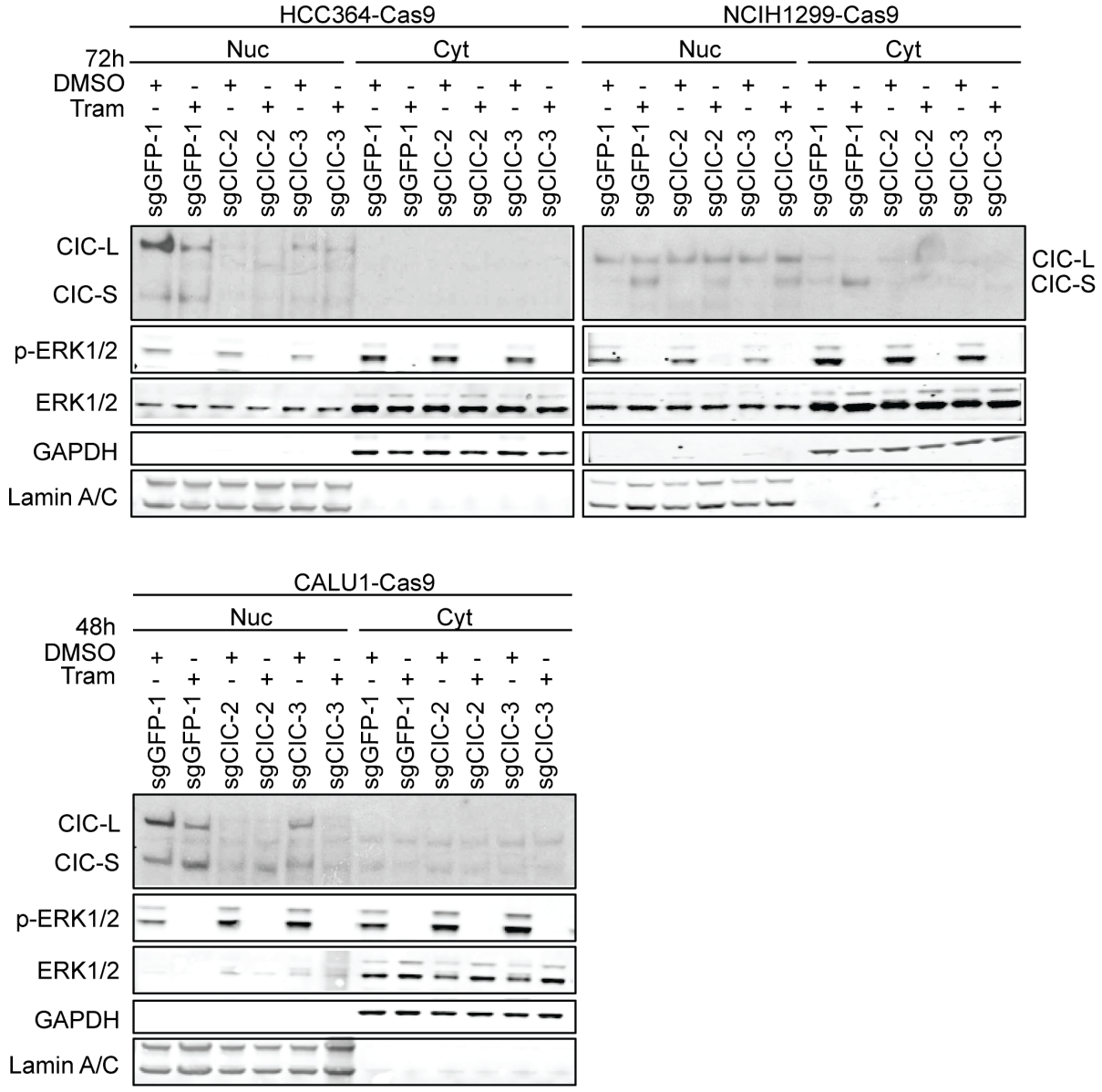

Figure 4-9. MEK inhibition increases nuclear CIC-S in lung cancer cell lines.

Immunoblot analysis of the effect of trametinib on CIC localization using fractionated cell lysates after 48 or 72 hours of trametinib treatment. Trametinib concentrations used – HCC364: 25 nM, NCIH1299: 1.5 μM, CALU1: 50 nM. Nuc = nuclear, Cyt = cytoplasmic, Tram = trametinib.

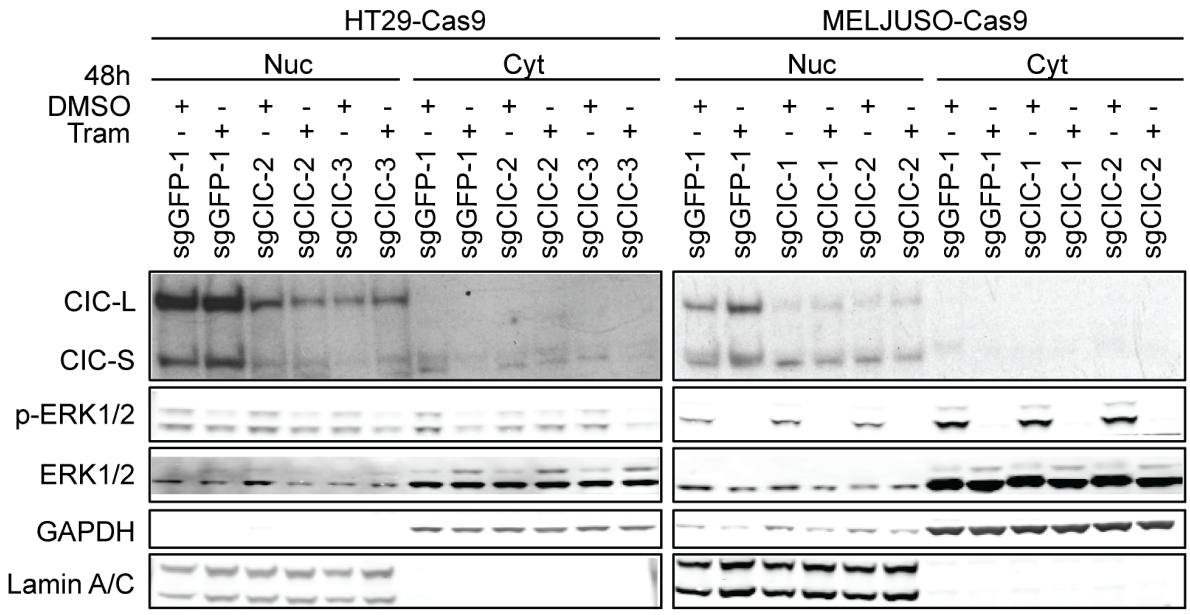

Figure 4-10. MEK inhibition increases nuclear CIC-S in colon cancer and melanoma cell lines. Immunoblot analysis of the effect of trametinib on CIC localization using fractionated cell lysates after 48 or 72 hours of trametinib treatment. Trametinib concentrations used – HT29: 10 nM, MELJUSO: 2.5 nM. Nuc = nuclear, Cyt = cytoplasmic, Tram = trametinib.

Because CIC is a transcriptional repressor whose nuclear/cytoplasmic localization is regulated by MAPK signaling[403,406], we hypothesized that MAPKi leads to active nuclear CIC and repression of pro-proliferative CIC target genes and that loss of CIC would restore expression of these genes, reducing sensitivity to MAPKi. To identify the relevant CIC target genes that mediate trametinib resistance, we treated control CIC^{WT} (sgGFP-1) or CIC^{KO} (sgCIC-1 or sgCIC-2) cells from 4 cell lines of different lineages that harbor different RAS-pathway mutations with DMSO or trametinib for 24 hours, and performed RNA-sequencing (**Figures 4-11A,B** and **4-12**). We analyzed the gene expression profiles to identify genes whose expression was suppressed in CIC^{WT} cells treated with trametinib, and restored in CIC^{KO} cells treated with trametinib. We found that trametinib treatment reduces the expression of all three members of the PEA3 family of ETS transcription factors (ETV1, ETV4, and ETV5) in all four cell lines assessed, and that loss of CIC results in maintained expression of at least one of these genes despite MEK inhibition (**Figure 4-11C,D**).

We confirmed that trametinib treatment robustly suppressed ETV1, 4, and 5 mRNA (**Figure 4-13A-D**) and protein (**Figure 4-13E**) expression in CIC^{WT} cells and that ETV 1, 4, and 5 expression was partially restored in CIC^{KO} cells. Collectively, these observations suggest that active nuclear CIC represses ETV1, 4, and 5 expression in multiple cell lineages. We concluded that signaling through the MAPK pathway induces ETV1, 4, and 5 expression by reducing nuclear CIC-S, relieving CIC-mediated gene repression. We hypothesized that elevated ETV1, 4, and 5 expression may be responsible for the resistance phenotype in CIC^{KO} cells.

Figure 4-11. MEK inhibition increases CIC-mediated repression of ETS transcription factors. (A) Overview of RNA-sequencing strategy. **(B)** Display format of RNA-sequencing data. **(C, D)** Effect of trametinib treatment and CIC^{KO} by sgCIC-1 **(C)** or sgCIC-2 **(D)** on the transcriptome. Each point represents a gene that is significantly ($q < 0.05$) differentially expressed between CIC^{KO} (sgCIC-1) and CIC^{WT} (sgGFP) cells treated with trametinib (*y*-axis), and between CIC^{WT} cells treated with trametinib versus DMSO (*x*-axis). Values represent average $\log_2$(fold-change) in expression of $n = 2$ technical replicates. Data for CALU1 sgCIC-2 is not shown because no genes were significantly differentially expressed in the contexts of interest.

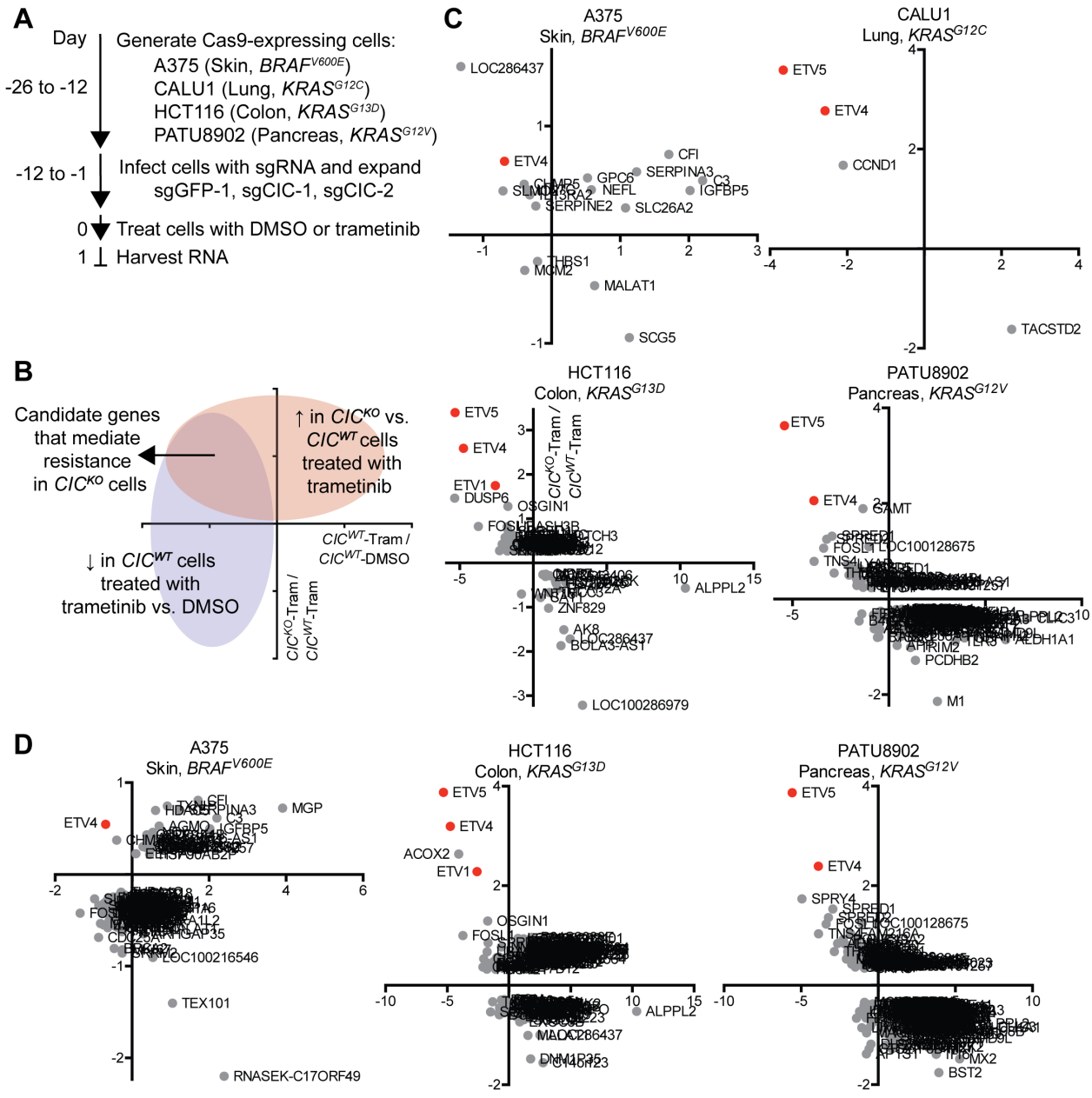

Figure 4-11 (Continued).

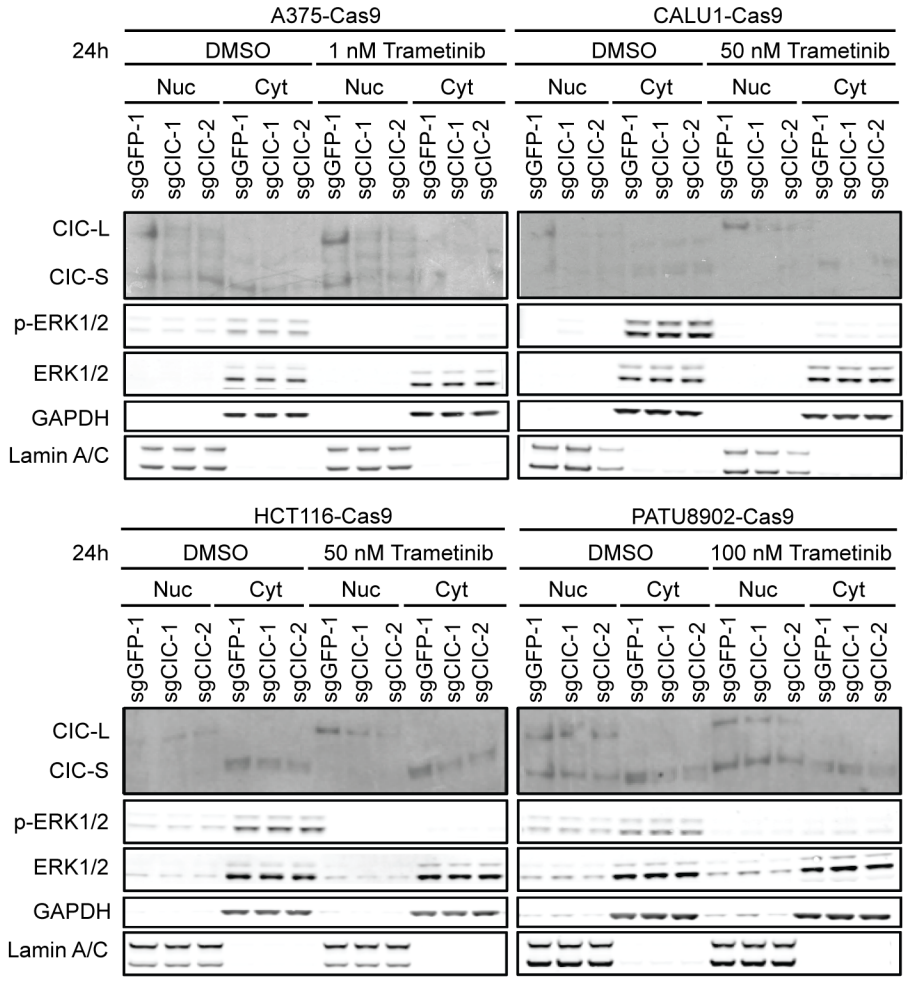

Figure 4-12. Confirmation of CIC depletion and MEK inhibition in cells used for RNA-sequencing. Immunoblot analysis of fractionated lysate from cells used for RNA-sequencing in **Figure 4-11**. Nuc = nuclear, Cyt = cytoplasmic.

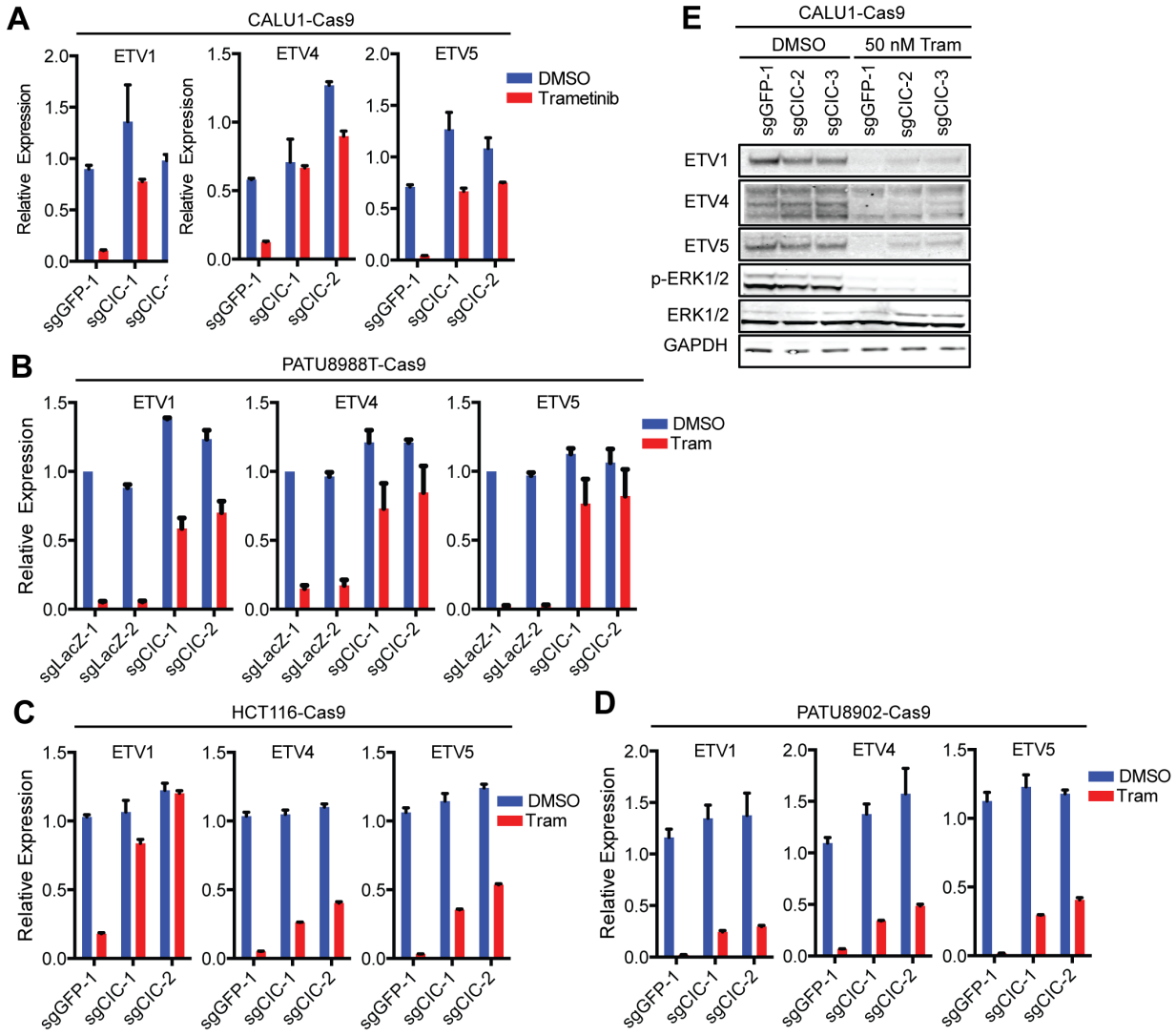

Figure 4-13. ***CIC*^{KO} restores expression of ETS transcription factors in the context of MEK inhibition. (A-D)** qRT-PCR analysis of ETV1, 4, and 5 expression in *CIC*^{WT} or *CIC*^{KO} CALU1 **(A)**, PATU8988T **(B)**, HCT116 **(C)**, or PATU8902 **(D)** cells treated with DMSO or 50 nM trametinib for 24 hrs. Average of *n* = 3 independent experiments with *n* = *3* technical replicates, data represented as mean ± SEM. **(E)** Immunoblot analysis of ETV1, 4, and 5 expression in CALU1 *CIC*^{WT} or *CIC*^{KO} cells treated with DMSO or 50 nM trametinib for 24 hours. Experiment in **(A)** was performed by Elsa Beyer Krall.

4.2.4 Increased expression of ETV transcription factors is necessary and sufficient for resistance to MEK inhibition

To assess whether expression of ETV1, 4, or 5 is necessary for the resistance conferred by *CIC* deletion, we suppressed ETV1, 4, or 5 expression in CIC^{WT} or CIC^{KO} cells (**Figure 4-14A)**. We used long-term proliferation assays to determine the effect of ETV1, 4, or 5 depletion on cell proliferation/survival in the context of trametinib treatment. We found that expression of ETV1, 4, and 5 was necessary for the full resistance mediated by CIC loss (**Figure 4-14B)**.

To determine if overexpression of the PEA3 family of ETS transcription factors was sufficient to confer drug resistance, we exogenously expressed LacZ (control), ETV1, ETV4-S (short isoform), ETV4-L (long isoform) or ETV5 and treated cells with DMSO or trametinib (**Figure 4-15A**). Overexpression of ETV1, ETV4-S, ETV4-L, or ETV5 was sufficient to confer some level of resistance in CALU1, PATU8902, and PATU8988T cells (**Figure 4-15B**). These observations extend a prior finding that ETV1 overexpression conferred resistance to MAPKi in *BRAF*-mutant melanoma[301]. Collectively, our findings suggest that increased expression of ETV1, 4, and 5 in CIC^{KO} cells is necessary for the resistance mediated by CIC^{KO}, and that overexpression of ETV1, 4, or 5 is sufficient to confer functional resistance to MEK inhibition.

Figure 4-14. Increased expression of ETS transcription factors is necessary for resistance to MEK inhibition. (A) qRT-PCR confirmation of shRNA-mediated ETV1, ETV4, and ETV5 depletion in CIC^{WT} and CIC^{KO} PATU8902 or CALU1 cells. *N* = 2 independent experiments with *n* = *3* technical replicates, data represented as mean ± SD. **(B)** Long-term proliferation assays to assess the effect of ETV1, 4, and 5 depletion on trametinib sensitivity in CIC^{WT} and CIC^{KO} cells. CIC^{WT} (sgGFP) and CIC^{KO} (sgCIC) PATU8902-Cas9 or CALU1-Cas9 cells expressing shRNAs targeting ETV1, ETV4, or ETV5 were treated with DMSO or trametinib. *N* = 3 technical replicates, representative of *n* = 2 independent experiments, data represented as mean ± SEM.

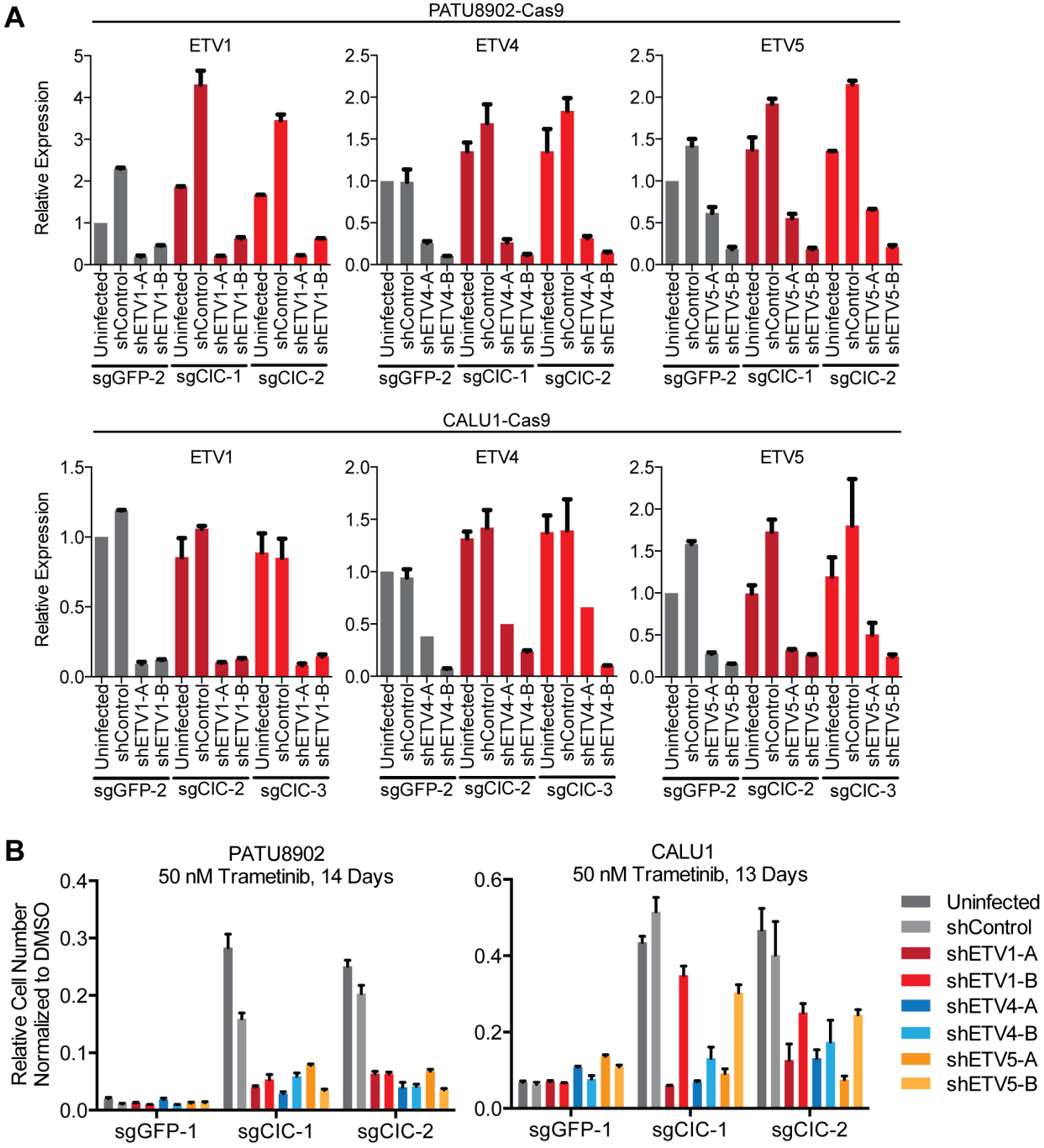

Figure 4-14 (Continued).

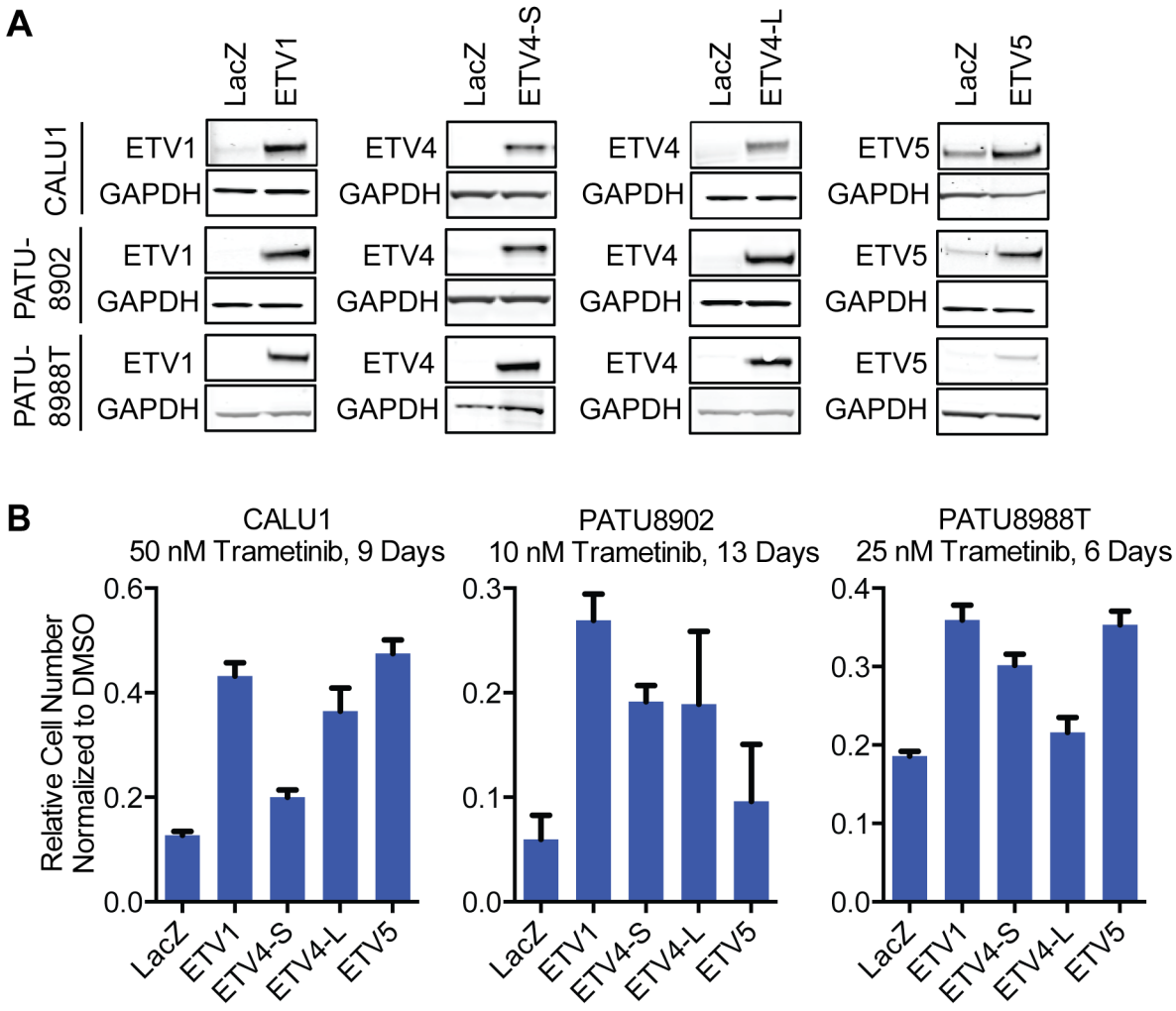

Figure 4-15. **Increased expression of ETS transcription factors is sufficient for resistance to MEK inhibition. (A)** Immunoblot analysis of CALU1, PATU8902, or PATU8988T cells expressing the indicated ORFs. **(B)** Long-term proliferation assays to determine the effect of ETV1, ETV4-S, ETV4-L, or ETV5 overexpression on trametinib sensitivity in CALU1, PATU8902, or PATU8988T cells. *N* = 3 technical replicates, representative of *n* = 2 independent experiments, data represented as mean ± SEM.

4.2.5 *ATXN1L* deletion mediates trametinib resistance by reducing CIC protein levels

In mice, ATXN1L has been shown to form a complex with CIC and increase CIC protein expression[407-409]. In addition, it has been suggested that ATXN1L acts as a co-repressor to synergistically enhance the transcriptional repressor activity of CIC[407,408]. When we examined the top scoring genes in our initial screens, we noticed that in the PATU8988T screen, all four sgRNAs targeting *ATXN1L* were enriched above two standard deviations from the mean of all sgRNAs ($p < 0.05$, **Figure 4-16A**). The PATU8988T screen was performed using the second-generation Avana CRISPR library[358], in which sgRNAs were designed to maximize potency.

The enrichment of sgRNAs targeting *ATXN1L* were not as robust in the other screens that were performed using the first-generation GeCKOv2 CRISPR library[297], in which, on average, only half of the 6 sgRNAs targeting each gene achieve effective gene knockout (J. Doench, personal communication). In all of the GeCKOv2 screens, at least one sgRNAs targeting *ATXN1L* became enriched above 2 standard deviations from the mean of all sgRNAs ($p < 0.05$, **Figure 4-16B**). We hypothesized that *ATXN1L* deletion may mediate resistance to trametinib treatment by reducing CIC expression and/or repressive function.

Figure 4-16. **sgRNAs targeting *ATXN1L* became enriched in genome scale CRISPR-Cas9 screens. (A)** Distribution of $\log_2$ fold-change in sgRNA representation on Day 14 versus the original sgRNA plasmid pool in in PATU8988T cells treated with 10 nM trametinib. Average of *n* = 2 biological replicates. Gray lines indicate average $\log_2$ fold-change (Avg) or 2 and 4 SD above average $\log_2$ fold-change of all screened sgRNAs. sgRNAs targeting *CIC* (red) and *ATXN1L* (orange) are indicated. **(B)** Distribution of $\log_2$ fold-change in representation of sgRNAs targeting *ATXN1L* on Day 14 versus the original sgRNA plasmid pool (PAT8902) or on Day 21 versus Day 0 (NCIH1299, CALU1, and HCC364) in cells treated with trametinib or vemurafenib. Average of *n* = 2 biological replicates. Gray lines indicate average $\log_2$ fold-change (solid) or 2 SD above average $\log_2$ fold-change (dashed) of all the sgRNAs in the screen. Abbreviations: Tram (trametinib), Vem (vemurafenib), Avg (average), SD (standard deviations).

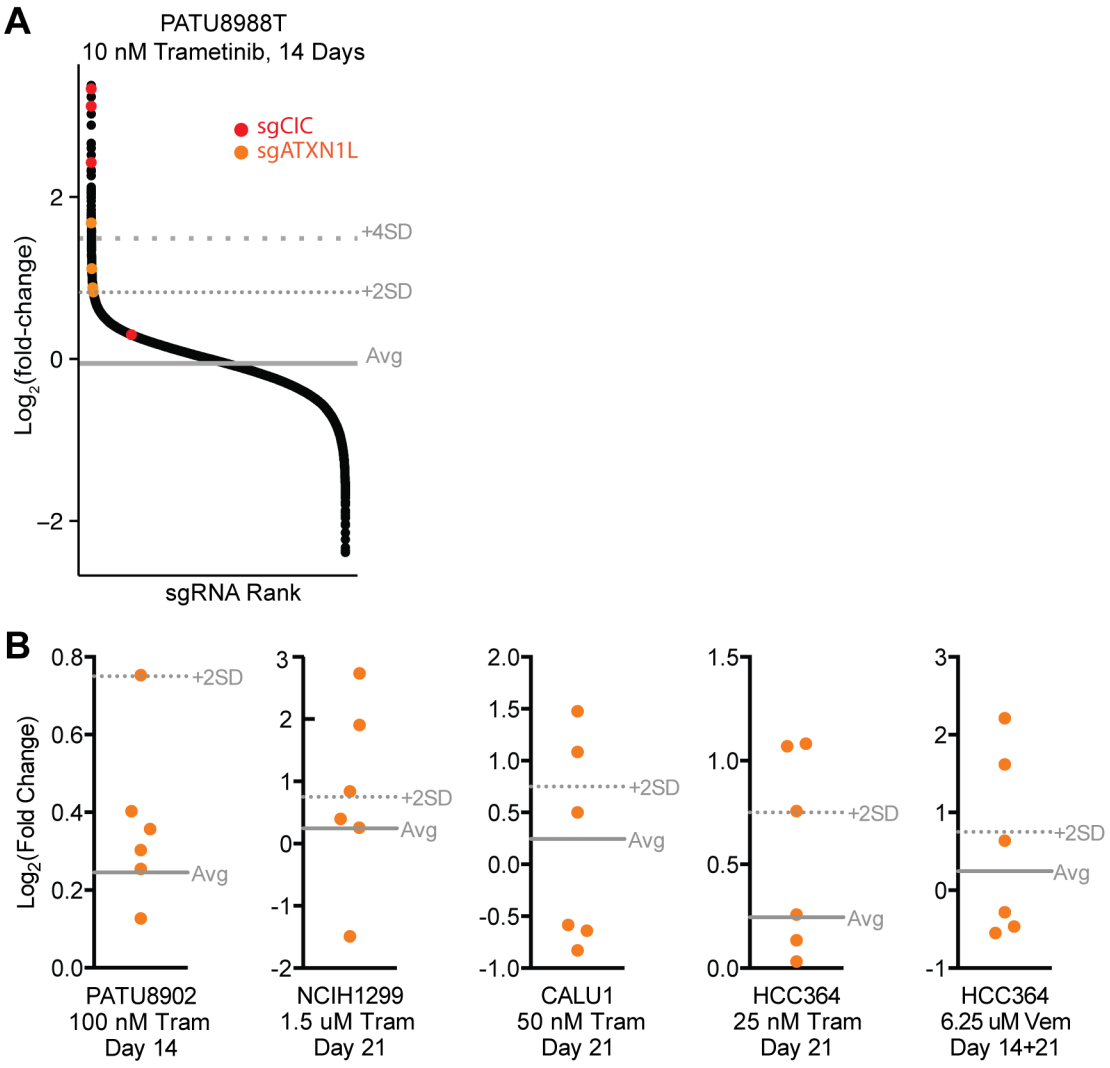

Figure 4-16 (Continued).

We generated *ATXN1L*^{KO} cells and assessed the efficiency of *ATXN1L* knockout by TIDE (Tracking of Indels by DEcomposition)[410] as we were unable to identify an ATXN1L-specific antibody for immunoblot analysis (**Figure 4-17**). TIDE is a method to quantify the frequency of mutations induced by CRISPR-Cas9. In brief, the region around the sgRNA editing site is PCR amplified from genomic DNA and sequenced. This sequencing trace is compared to one derived from a control cell line (sgLacZ-1), and the frequency of genome editing is estimated by the proportion of aberrant base signals of the test sequencing trace compared to the control sequencing trace [410]. We found that *ATXN1L* was effectively modified in >50% of PATU8988T cells expressing sgATXN1L, but in <0.5% of PATU8988T cells expressing sgLacZ (**Figure 4-17**).

ATXN1L loss had no effect on baseline *CIC* expression at the transcriptional level (**Figure 4-18A**). However, upon trametinib treatment, *ATXN1L*^{WT} cells slightly upregulate *CIC* mRNA expression while *ATXN1L*^{KO} cells do not (**Figure 4-18A**). Notably, *ATXN1L*^{KO} cells exhibited reduced expression of CIC-S protein at baseline and upon trametinib treatment (**Figure 4-18B**). These observations suggest that ATXN1L increases CIC expression post-translationally[407-409]. *ATXN1L*^{KO} partially restored ETV1, 4, and 5 mRNA expression in trametinib-treated cells, albeit not to the same magnitude as *CIC*^{KO} cells (**Figure 4-19A**). In addition, *ATXN1L* deletion conferred resistance to MEK inhibition in a long-term proliferation assay (**Figure 4-19B**). Together, these observations suggest that loss of ATXN1L mediates resistance to MEK inhibition by reducing CIC levels, which permits increased expression of ETV1, 4, and 5.

A

Control Sample	Test Sample	Efficiency
PATU8988T sgLacZ-1	PATU8988T sgLacZ-2	0.4%
PATU8988T sgLacZ-1	PATU8988T sgATXN1L-1	51.2%
PATU8988T sgLacZ-1	PATU8988T sgATXN1L-2	55.1%

B

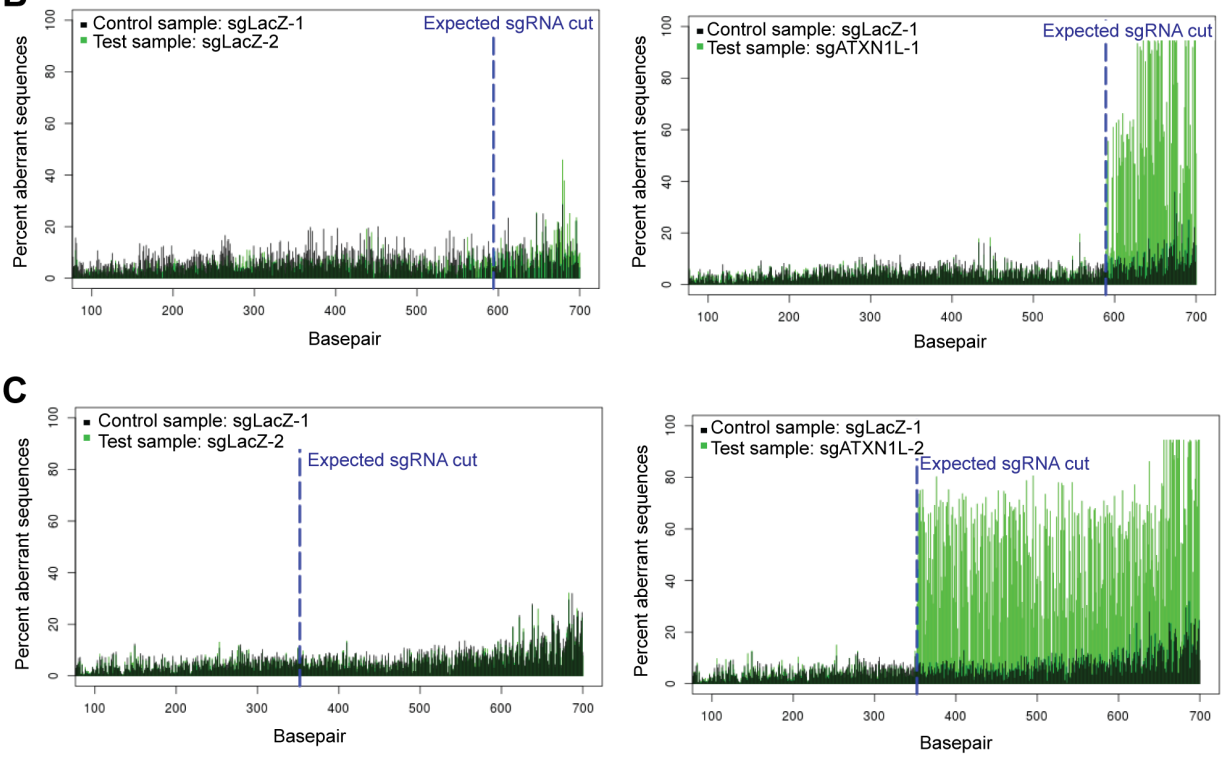

C

Figure 4-17. sgRNAs targeting *ATXN1L* effectively edit the *ATXN1L* genomic locus. (A) *ATXN1L* knockout efficiency in PATU8988T sgLacZ (control) and sgATXN1L cells, determined using TIDE. **(B-C)** *ATXN1L* knockout efficiency in PATU8988T sgLacZ-2 and sgATXN1L-1 **(B)** or sgATXN1L-2 **(C)** compared to sgLacZ-1 control samples. Graphs depict percent aberrant sequence signal of the test sample (green: sgLacZ-2, sgATXN1L-1, or sgATXN1L-2) compared to that of the control sample (black: sgLacZ-1). Blue dotted line indicates the expected sgRNA cut site.

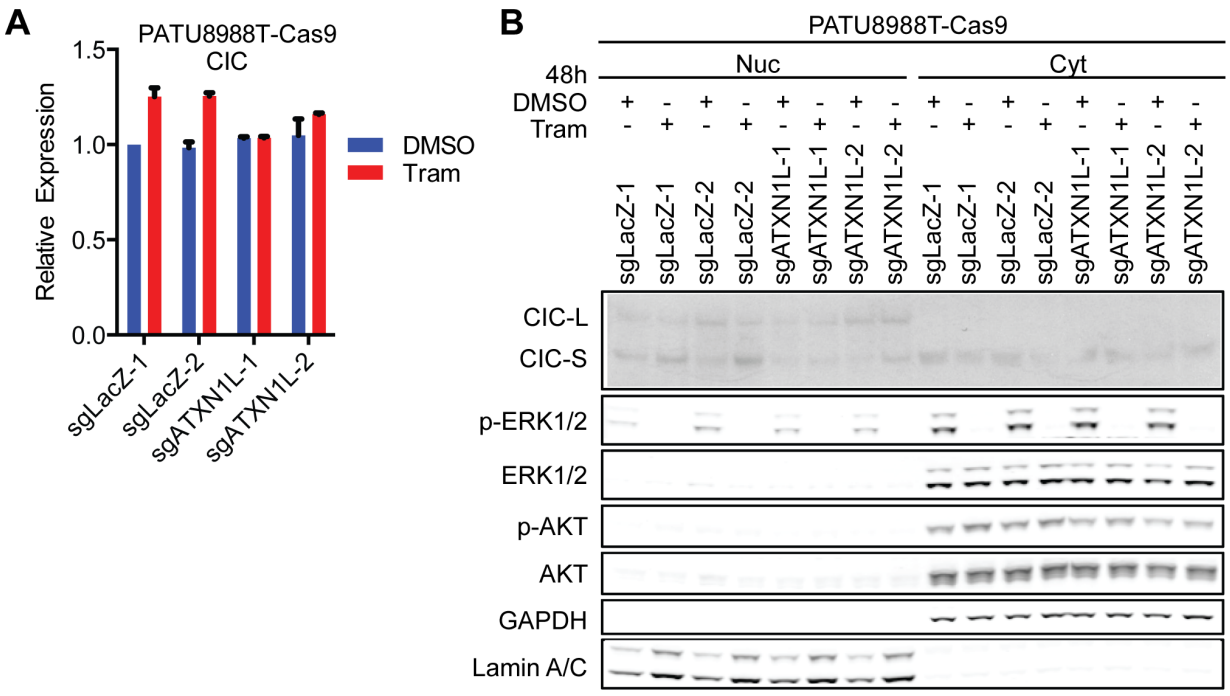

Figure 4-18. ***ATXN1L*^{KO} reduces CIC-S protein levels. (A)** qRT-PCR analysis of CIC expression in *ATXN1L*^{WT} (sgLacZ) or *ATXN1L*^{KO} (sgATXN1L) PATU8988T cells treated with DMSO or 50 nM trametinib for 24 hrs. Tram = trametinib, average of *n* = 3 independent experiments with *n* = *3* technical replicates, data represented as mean ± SEM. **(B)** Immunoblot analysis of the effect of *ATXN1L*^{KO} and trametinib treatment on CIC expression and localization using fractionated cell lysates after 48 hrs of drug treatment. Nuc = nuclear, Cyt = cytoplasmic, Tram = trametinib.

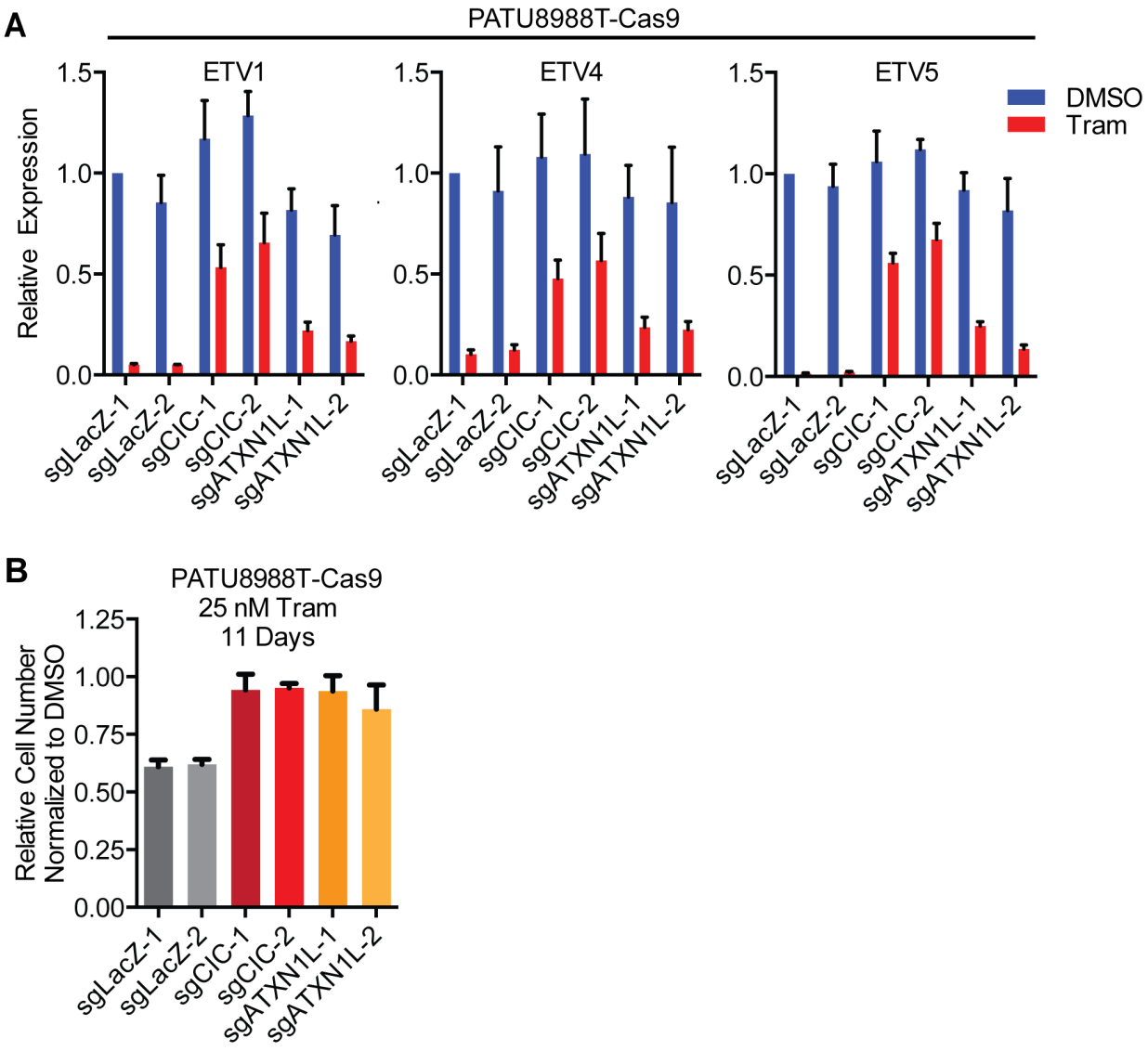

Figure 4-19. *ATXN1L*^{KO} restores ETV1/4/5 expression and confers trametinib resistance. (A) qRT-PCR of ETV1, 4, and 5 expression in control (sgLacZ), *CIC*^{KO}, or *ATXN1L*^{KO} PATU8988T cells treated with DMSO or 50 nM trametinib for 24 hrs. Tram = trametinib, average of *n* = *2* independent experiments, data represented as mean ± SEM. **(B)** Long-term proliferation assay to determine the effect of *ATXN1L*^{KO} on trametinib sensitivity. *N* = 3 technical replicates, data represented as mean ± SEM. Experiment in **(B)** was conducted by Mihir Doshi.

Based on our findings, we propose a model in which oncogenic MAPK signaling in *RAS*- or *BRAF*-mutant cells constitutively inactivates CIC. Upon MEK or BRAF inhibition, active CIC represses ETV1, 4, and 5 expression. CIC loss confers trametinib and vemurafenib resistance by restoring expression of the ETV transcription factors at a transcriptional level. Deletion of *ATXN1L* mediates resistance to MEK inhibition by reducing CIC protein levels (**Figure 4-20**).

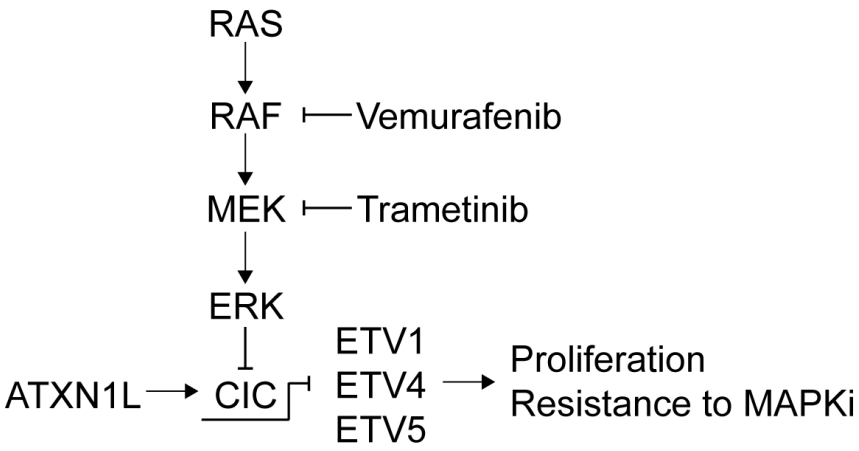

Figure 4-20. Proposed mechanism of trametinib and vemurafenib resistance mediated by CIC or ATXN1L loss. MAPKi = MAPK pathway inhibition.

4.2.6 Low *ATXN1L* expression is associated with poor overall survival in patients with *BRAF*-mutant melanoma treated with MAPK-pathway inhibitors

To determine whether the expression level of *CIC* or *ATXN1L* correlated with intrinsic resistance to MAPK pathway inhibitor therapy in cancers with mutations in the MAPK pathway, we analyzed pre-treatment microarray expression data from 30 $BRAF^{V600}$-mutant melanoma metastases derived from 21 patients subsequently treated

with dabrafenib or vemurafenib[314] and 9 patients treated with the combination of dabrafenib and trametinib[315]. We categorized the 10 tumors with lowest or highest *ATXN1L* expression as 'low' or 'high' *ATXN1L* expressers, respectively, and found that low pre-treatment *ATXN1L* expression correlated with decreased overall survival (p = 0.0375, **Figure 4-21**). This observation suggests that low *ATXN1L* expression is a biomarker of intrinsic resistance to BRAF or MEK inhibitor therapy in *BRAF*-mutant melanoma.

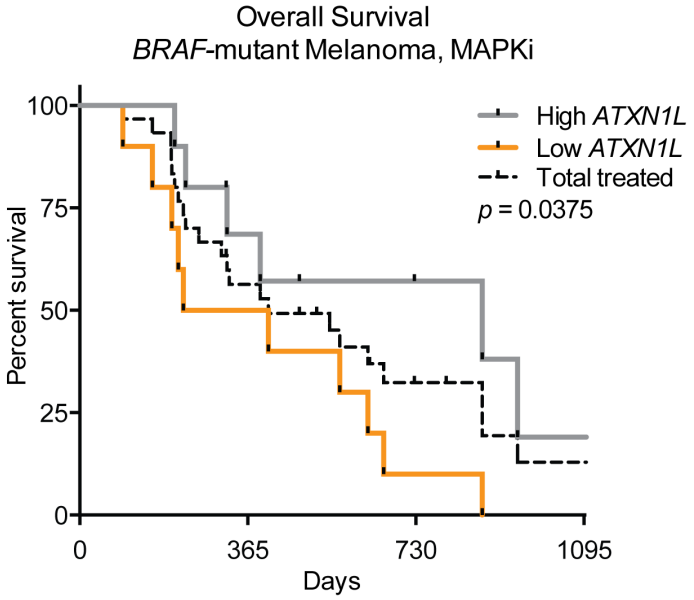

Figure 4-21. Low *ATXN1L* expression is associated with poor overall survival in patients with *BRAF*-mutant melanoma treated with MAPK pathway inhibitors. Kaplan-Meier curve depicting overall survival of 30 patients with *BRAF*-mutant melanoma[314,315] who received MAPK pathway inhibitor therapy. 'High *ATXN1L*' and 'Low *ATXN1L*' groups include the 10 patients with highest or lowest pre-treatment *ATXN1L* expression, respectively. Data analysis was performed by Hans Widlund.

4.3 Discussion

Using genome scale CRISPR-Cas9 loss-of-function screens, we identified CIC deletion as a mechanism of resistance to MEK or BRAF inhibition in *RAS*- or *BRAF*-mutant cancers (Chapter 2.2.4). Here, we demonstrate that CIC, a transcriptional repressor of ETV1, 4, and 5, is a key repressor of MAPK pathway signaling downstream of ERK in *RAS*- or *BRAF*-mutant cancer cells. *ATXN1L* deletion, which reduces CIC protein, or ectopic expression of ETV1, 4, or 5 also conferred resistance to trametinib. *ATXN1L* expression inversely correlates with response to MAPKi inhibition in clinical studies. These observations identify the ATXN1L-CIC-ETS transcription factor axis as a novel mediator of resistance to MAPK pathway inhibition.

The MAPK pathway mediates diverse cellular responses by altering gene expression through direct phosphorylation of several nuclear factors. While over 150 substrates of ERK1/2 have been identified[411], it remains unclear which of these substrates play key roles in oncogenic and treatment-related contexts. Here, we identify CIC as an important effector of MAPK in the setting of MAPKi. CIC is one of a number of regulators of MAPK signaling. ERK-dependent phosphorylation of upstream components of the pathway such as EGFR, SOS, and RAF[412-416] dampens MAPK pathway activity. In addition, ERK signaling induces the expression of SPRY and SPRY-related proteins with an EVH1 domain (SPRED) proteins[417], which inhibit MAPK signaling at multiple levels of the pathway, as well as DUSP phosphatases[362], which directly dephosphorylate and inhibit ERK1/2. The existence of multiple regulators allows for precise modulation of the magnitude and duration of MAPK signaling, enabling it to regulate diverse developmental and mitogenic functions.

In the genome scale CRISPR-Cas9 screens, we observed that deletion of several negative regulators of the MAPK pathway, such as *NF1 and DUSP1*, conferred some level of trametinib resistance to PATU8988T cells (**Figure 2-7**). However, loss of CIC conferred more robust and consistent trametinib resistance. It is possible that deletion of certain negative regulators of the MAPK pathway, such as SPRY and DUSP proteins, did not confer strong resistance in the CRISPR-Cas9 screens due to the presence of functionally redundant family members. Ultimately, we found that the CIC-ETS transcription factor axis is an important modulator of MAPK pathway output across cancer cells of multiple lineages whose proliferation is dependent on oncogenic MAPK signaling.

In *Drosophila*, Cic is a well-characterized repressor of EGFR-Ras-MAPK signaling that prevents aberrant cell proliferation by downregulating ETS factors in the absence of MAPK signaling[406,418]. A prior study suggested that this role is conserved in human CIC[403]. CIC alterations have been reported in several cancer types. The majority of oligodendrogliomas harbor inactivating mutations in CIC[419] and, consequently, overexpress the ETV transcription factors[420]. *CIC-DUX4* translocations, which encode a fusion protein that upregulates expression of ETV1 and ETV5, have been identified in Ewings family tumors[421].

Our observations indicate that the PEA3 family of ETS transcription factors, which are negatively regulated by CIC, may be principal nuclear effectors of oncogenic MAPK signaling. Indeed, a prior study suggests that ETS transcription factors may activate a RAS/MAPK transcriptional program in the absence of MAPK pathway[108]. We note that RFWD2/COP1 and DET1, substrate receptors of the $CRL4^{COP1/DET1}$ E3

ubiquitin ligase[422] that has been reported to mediate the ubiquitination and degradation of ETV1, 4, and 5[423,424] and c-Jun[425], were also hits in the PATU8988T screen (**Figure 2-7**). Interestingly, we found that while overexpression of a single ETS transcription factor could confer resistance to trametinib, suppression of any one of ETV1, 4, or 5 could strongly decrease the resistance conferred by *CIC* deletion. These observations suggest that elevated global expression of ETS transcription factors contributes to MEK inhibitor resistance. In our experiments, the exogenously expressed ETS transcription factors were overexpressed at levels greater than was achieved by CIC^{KO}. It is possible that at high levels of expression, a single ETS transcription factor is sufficient to confer resistance while at moderate levels of expression, such as that conferred by CIC^{KO}, a combination of several ETS transcription factors is necessary.

The major phenotype observed in $Atxn1l^{-/-}$ mice is defective lung alveolarization attributed to destabilization of Cic and derepression of *Etv1* and *Etv4*, which increases expression of several matrix metalloproteinase (*Mmp*) genes[408]. Several reports indicate that ATXN1L enhances CIC function by stabilizing post-transcriptional CIC expression and working as a transcriptional co-repressor with CIC[407-409]. Although ATXN1L has been reported to suppress *HEY1* expression[426], the observed phenotype in $Atxn1l^{-/-}$ mice supports the view that the major role of ATXN1L is to augment CIC-mediated gene repression.

The majority of acquired resistance mechanisms to MAPK pathway inhibitor therapy that have been identified in patients with *RAF*-mutant cancers involve upregulation of MAPK pathway signaling upstream of ERK, overcoming the effect of small molecule RAF/MEK inhibitors[308,312-315,331]. Our observations suggest that, if

RAF/MEK signaling is sufficiently suppressed in tumors with mutant *RAS* or *BRAF*, acquired resistance may arise from altered transcriptional output mediated by aberrant expression of transcription factors activated downstream of MAPK, such as ETV1, 4, and 5. Dysregulation of these transcription factors downstream of ERK may also promote intrinsic resistance to inhibition of the MAPK pathway.

Our observations suggest that low ATXN1L activity, which results in reduced CIC protein as well as elevated ETS transcription factor expression in the context of MAPKi, may be a mechanism of intrinsic resistance to MAPK inhibitor therapy in *BRAF*-mutant melanoma. We found that low *ATXN1L* expression in *BRAF*-mutant melanoma correlated with decreased overall survival in patients treated with MAPK inhibitors. However, we did not observe a correlation between low *CIC* expression and poor survival outcome. This could be attributable to technical or biological reasons. In the dataset we analyzed, gene expression in tumor samples was determined by bead-based microarrays. It is possible that the CIC probe was insufficiently sensitive to distinguish between high and low CIC expression. Alternatively, total *CIC* mRNA expression may not be reflective of nuclear CIC-S protein levels, which our findings suggest may be a more relevant marker of sensitivity to MAPKi. In addition, ETV1, 4, and 5 expression were not predictive of survival outcome, likely because oncogenic BRAF signaling inhibits CIC and induces high ETV1, 4, and 5 expression in all tumor samples, making ETV1, 4, and 5 expression an insensitive readout of ATXN1L-CIC-ETS transcription factor pathway activity in pre-treatment samples.

BRAF and MEK inhibitors are currently being tested in numerous clinical trials for *RAS*-mutant pancreatic cancer, lung cancer, colorectal cancer, and melanoma and for

BRAF-mutant lung cancer and colorectal cancer. However, pre-treatment and post-relapse biopsy specimens for molecular analysis of resistance mechanisms are not accessible for most of these trials. Moreover, most available samples from patients treated with single agent MEK or BRAF inhibitor therapies have shown only partial suppression of the MAPK signaling pathway with these agents at clinically tolerable doses. We propose that altered transcriptional output downstream of MAPK signaling may best represent an important resistance mechanism upon full suppression of the canonical kinase signaling pathway. Thus, even the limited number of available clinical samples may not be sufficient to determine whether CIC loss is an operant mechanism of intrinsic or acquired resistance in these clinical settings. However, stratifying patients for treatment based on ATXN1L-CIC-ETS transcription factor pathway activity level may also allow for the selection of patients more likely to respond to MEK and BRAF inhibitors.

4.4 Materials and Methods

Cell lines and reagents

Cells were maintained in DMEM (293T, A375, HCT116, HT29, PATU8902, PATU8988T; Corning), RPMI-1640 (HCC364, MELJUSO, NCIH1299; Corning), or McCoy's 5A (CALU1; Gibco) supplemented with 2 mM glutamine, 50 U/mL penicillin, 50 U/mL of streptomycin (Gibco), and 10% fetal bovine serum (Sigma), and incubated at 37°C in 5% CO_2. Trametinib, selumetinib, vemurafenib, 5-FU, etoposide, and paclitaxel were purchased from Selleck Chemicals. Doxycycline was purchased from Clontech.

Generation of isogenic cell lines

293T cells were seeded in 6 cm dishes. 24 hours later, cells were transfected with 100 ng VSVG, 900 ng delta8.9, and 1 µg ORF or sgRNA plasmid using OptiMEM and Mirus TransIT. Virus was harvested 48 – 72 hours after transfection. *CIC*^{WT} and *CIC*^{KO}: 500,000 cells per well were seeded in 48-well plates in 250 µL media with 4 µg/mL polybrene. 25-150 µL virus (sgGFP or sgCIC) was added per well and plates were spun for 2 hours at 2250 rpm at 30°C. 6 hours later, each well was split into a 6 cm dish. 24 hours after infection, cells were selected with 2 µg/mL puromycin for 2-3 days. *CIC* knockout was confirmed by immunoblot 8 days post infection. *ATXN1L*^{WT} and *ATXN1L*^{KO}: 200,000 cells per well were seeded in 6-well plates in 2 mL media with 8 µg/mL polybrene. 100-200 µL virus (sgLacZ or sgATXN1L) was added per well and plates were spun for 30 minutes at 2250 rpm at 30°C. 24 hours later, cells were selected with 2 µg/mL puromycin for 2-3 days. *ATXN1L* knockout was confirmed by TIDE (see below). ETV1/4/5 overexpression: Same as for *ATXN1L*^{WT} and *ATXN1L*^{KO} cell lines, using 300 µL virus (LacZ, ETV1, ETV4-S, ETV4-L, or ETV5). ETV1, 4, or 5 expression was confirmed by immunoblot 7 days after infection.

Generation of PATU8902 pTetK cells

PATU8902 cells were seeded in a 6-well plate (200,000 cells per well) in 2 mL media with 8 µg/mL polybrene. 500 µL virus (pLKO-Tet-On shKRAS-509) was added and cells were spun for 30 minutes at 2250 rpm at 30°C. 24 hours after infection, cells were selected with 1 mg/mL G418 sulfate (Thermo Fisher) for 7 days. Subsequently, cells were seeded at 0.3 cells per well in 96-well plates to allow selection of single-cell

clones. 45 clones were assessed, and PATU8902 pTetK (clone 18) was selected based on effectiveness of KRAS suppression upon doxycycline treatment.

Drug titration for cell counting and long-term proliferation assays

CALU1, HCC364, HCT116, and NCIH1299 cells were treated with at least 5 different concentrations of drug (trametinib, selumetinib, or vemurafenib) for 24 hours, and phospho-ERK levels were assessed by immunoblot analysis. The concentration of drug that fully inhibited phospho-ERK levels was used in subsequent assays. The trametinib concentration used for HT29 was guided by analogous titrations performed by Joseph Rosenbluh. The trametinib and vemurafenib doses used for A375 were guided by previously published IC50 values [427].

Short-term proliferation assays

NCIH1299 were seeded in white, opaque-bottom 96-well plates (Costar) and treated with DMSO or 1.5 μM trametinib. 5 days after seeding, cell viability was assessed by CellTiter-Glo (Promega) according to manufacturer's protocol.

Cell counting assay

Cells were seeded in 10 cm (1-2 x 10^6 cells) or 15 cm (1-3 x 10^6 cells) plates and treated with drug or DMSO as indicated. Cells were passaged or media was refreshed every 3-4 days. Cells were counted at each passage, and number of cell doublings was calculated.

Long-term proliferation assay

Cells were seeded in 12- or 24-well plates at a density of 5,000-20,000 cells per well and treated with drug or DMSO. Cells were exposed to DMSO for 6-9 days, and to drug or doxycycline (PATU8902 pTetK cells) for 9-18 days, with media changed every 3 days. Cells were fixed with 10% formalin and stained with 0.5% crystal violet in 10% ethanol for 20 minutes. After acquiring images, crystal violet uptake was extracted with 10% acetic acid and quantified by measuring absorbance at 565 nm using a SpectraMax M5 microplate reader (Molecular Devices).

***In vivo* xenografts**

For cell line xenograft experiments, approximately 1 x 10^6 cells were suspended in PBS (Corning), mixed 1:1 with Matrigel (BD Biosciences), and subcutaneously injected into the left and right flanks of female nude mice (Nu/Nu; Taconic) in a final volume of 100 µL. Mice with established tumors (average tumor volume > 100 mm^3) were randomized into cohorts (5 mice/group). Mice received daily oral vehicle (0.5% hydroxypropyl methyl cellulose and 0.4% Tween-80 in 0.05 N HCL; Sigma Aldrich) or 2 mg/kg trametinib treatment. Tumor volume was assessed via caliper measurement on days 0, 7, and 14, and calculated by the formula: volume = length x $width^2$ x 0.5. Body weight was recorded every 3 days. Mice were sacrificed when the tumor diameter reached 2 cm. All procedures were performed according to protocols approved by the Institutional Animal Care and Use Committees of the Dana-Farber Cancer Institute. Statistical significance of difference in tumor size between different groups was assessed by heteroscedastic paired two-tailed t-test.

RNA-sequencing

200,000 – 400,000 cells were seeded in 4 wells of a 6-well plate and allowed to adhere overnight. Subsequently, two wells were treated with DMSO and two wells were treated with trametinib (A375: 1 nM, CALU1: 50 nM, HCT116: 50 nM, PATU8902: 100 nM) for 24 hours. Total RNA was extracted using an RNeasy kit (Qiagen) according to manufacturer's recommendations. First strand cDNA was generated from 1.5 µg of total RNA using Oligo(dT)12-19 Primer (Invitrogen) and AfifinityScript Multiple Temperature Reverse Transcriptase (Agilent). Second strand cDNA was synthesized using an mRNA Second Strand Synthesis Module (#6111L) and washed with Agencourt AMPure XP beads (Beckman Coulter). Libraries were prepared by tagmentation (Nextera XT DNA Sample Preparation Kit, Illumina) according to the manufacturer's protocol, using index primers (Nextera XT Index kit, Illumina) to facilitate multiplexing. The concentration of each cDNA library was quantified with the KAPA Illumina ABI Quantification Kit (Kapa Biosystems). Libraries were normalized to 5 nM and pooled for sequencing using the HiSeq 2500 (50 base paired-end reads), yielding 3.55×10^6-14.1×10^6 reads per sample. Reads were mapped to the reference human genome (hg19) using Tophat 2.0.11. Transcript assembly, abundance estimation, and differential expression analysis were performed with Cufflinks 2.0.2. Two replicates for each cell line/genetic perturbation/treatment were grouped to derive significance of differential expression across experimental conditions. Data can be found in the NCBI Gene Expression Omnibus (GEO: GSE78519).

Quantitative PCR

RNA was isolated using an RNeasy kit (Qiagen). cDNA was synthesized using Superscript III First-Strand Synthesis Supermix for qRT-PCR (Invitrogen), and analyzed by quantitative PCR (q-PCR) using Power Sybr Green PCR Master Mix (Invitrogen) on a QuantStudio 6 Flex PCR system (Applied Biosystems) according to the manufacturer's recommendations. Target gene expression was normalized to GAPDH expression, and shown relative to control samples. Primer sequences used for q-PCR:

Table 4-1. q-PCR primer sequences

Gene	*Forward Primer*	*Reverse Primer*
ETV1	GGCCCCAGGCAGTTTTATGAT	GATCCTCGCCGTTGGTATGT
ETV4	GGACTTCGCCTACGACTCAG	GGGAATGGTCGCAGAGGTTT
ETV5	CACGGGTTCCAGTCACCAAT	TGACTGGCAGTTAGGCACTT
CIC	GGAAGAACTCCACGGACCTG	GTCCTCGGCTTCTGTACCTG
GAPDH	CCTGTTCGACAGTCAGCCG	CGACCAAATCCGTTGACTCC

Tracking of Indels by DEcomposition (TIDE)

Genomic DNA (2 x 10^6 cells) from PATU8988T sgLacZ-1, sgLacZ-2, sgATXN1L-1, and sgATXN1L-2 cells were harvested using the QIAamp DNA Blood Mini Kit (Qiagen) according to manufacturer's recommendation. PCR reactions were conducted with 500 ng genomic DNA in MyTaq Red mix (Bioline) according to manufacture instructions. PCR products were purified by gel extraction with the QIAquick Gel Extraction Kit (Qiagen) according to manufacturer's protocol. Purified PCR samples (~20 ng) were Sanger sequenced with the forward primer used in PCR amplification. Sequencing traces were analyzed as recommended[410] by the van Steensel laboratory

(https://tide.nki.nl/). Primer sequences spanning the indicated sgRNA target sites that were used in TIDE,

Table 4-2. TIDE primer sequences

sgRNA	*Forward Primer*	*Reverse Primer*
sgATXN1L-1	TCCAGGCATCCACTATCCTC	ATGAAATGGGAAGGCAAGTG
sgATXN1L-2	GAATGCCTTCCACCAAAGAA	AACTGTCCATCCACCACACA

Melanoma outcome data analysis

Data from 30 *BRAF*^{V600}-mutant melanoma metastases derived from 21 patients treated with dabrafenib or vemurafenib [314] and 9 patients treated with the combination of dabrafenib and trametinib [315] was analyzed. Patients were grouped by pre-treatment *ATXN1L* expression, where 'High *ATXN1L*' and 'Low ATXN1L' groups include the 10 patients with highest or lowest *ATXN1L* expression in the cohort of 30 patients, respectively. Statistical significance was calculated using the log-rank (Mantel-Cox) test.

Antibodies and immunoblots

ERK1/2, MEK1/2, AKT, Lamin A/C, and GAPDH immunoblots were performed by separating 10-50 µg cell lysate per sample on a 4%-12% Bis-Tris gel (Invitrogen NuPage) and transferring to nitrocellulose membrane using the iBlot system (Life Technologies); ETV1, ETV4, and ETV5 immunoblots were performed in the same way, using 40 µg cell lysate per sample. For CIC immunoblots, 40-80 µg of nuclear or cytoplasmic lysate (NE-PER Nuclear and Cytoplasmic Extraction Kit, Thermo Scientific) was separated on a 3-8% Tris-Acetate gel (Invitrogen NuPage) and transferred to PVDF

membrane (BioRad Trans-Blot). Primary antibodies were obtained from Cell Signaling (AKT #2920, phospho-AKT S473 #4060, p44/42 MAPK #9107, phospho-p44/42 MAPK #9101, MEK1/2 #9122, phospho-MEK1/2 #9154, GAPDH #2118, Lamin A/C #4777), Abcam (ETV1 ab81086, ETV5 ab54704), Proteintech (ETV4 10684-1-AP), and Bethyl (CIC A301-204A). Immunoblots were visualized by infrared imaging (LI-COR) with the exception of CIC, which was visualized by chemiluminescence.

Vectors

sgRNA and shRNA sequences are listed below. Cas9 in the pLX311 backbone (pXPR_BRD111), sgRNAs in the pXPR_BRD003 backbone, and shRNAs in the pLKO.1 (pLKO1) or pLKO_TRC005 (pLKO5) backbone were obtained from the Genetic Perturbation Platform at the Broad Institute unless otherwise specified. pLKO-Tet-On-shKRAS-509 was cloned into the pLKO-Tet-On backbone vector (Novartis) using EcoRI and AgeI restriction sites. sgATXN1L sgRNAs were cloned into the pXPR_BRD003 backbone using Bsmb1 restriction sites. sgLacZ sgRNAs in the pXPR_BRD003 backbone were acquired from Katherine Walsh. The shETV1-A (shETV1-3 [428]) shRNA in the pLKO.1 backbone was obtained from the Garraway laboratory. For the ETV1, 4, and 5 expression vectors, gBlocks gene fragments (Integrated DNA Technologies) containing ETV1 (GenBank: NM_004956), ETV4-L (NM_001079675), and ETV5 (NM_004454, codon optimized to facilitate cloning) coding sequences were cloned into the pLX311 lentiviral expression vector backbone (Genetic Perturbation Platform, Broad Institute) by LR cloning (Thermo Fisher Scientific). The pLX311-ETV4-S (GenBank:

NM_001261439) expression vector was obtained from the Genetic Perturbation Platform at the Broad institute, and contains a C-terminal V5 tag.

Table 4-3. sgRNA and shRNA sequences

Vector Name	*Sequence*
pXPR_BRD003_sgGFP-1	GGCGAGGGCGATGCCACCTA
pXPR_BRD003_sgGFP-2	GGTGCCCATCCTGGTCGAGC
pXPR_BRD003_sgGFP-3	GAAGGGCATCGACTTCAAGG
pXPR_BRD003_sgLacZ-1	AACGGCGGATTGACCGTAAT
pXPR_BRD003_sgLacZ-2	CTAACGCCTGGGTCGAACGC
pXPR_BRD003_sgCIC-1	CGCAGGGGCCCCATACCCCG
pXPR_BRD003_sgCIC-2	GCTCAGACACCAAGGCTCCG
pXPR_BRD003_sgCIC-3	CCGGACCGTCAGCAAGATCC
pXPR_BRD003_sgCIC-4	AGTGTATTCGGACAAGAAGT
pXPR_BRD003_sgCIC-5	CAGATTCCACCACCCCCAAA
pXPR_BRD003_sgCIC-6	GGTGCTGCCCCCAAACAAGG
pXPR_BRD003_sgCIC-7	GCAACCTGCCAGCCACCCAG
pXPR_BRD003_sgCIC-8	GCTACTGACCGAACATGCCG
pXPR_BRD003_sgCIC-9	AGATTGGAAGTGGTGCAACA
pXPR_BRD003_sgCIC-10	GGGCATACCACCACTCGCCC
pXPR_BRD003_sgCIC-11	TCTGTCTCACTGTCCAGCCG
pXPR_BRD003_sgATXN1L-1	GTAGCAGCACCAGCACACCG
pXPR_BRD003_sgATXN1L-2	AGACCCAATGAACTGCAGCG
pLKO1_shControl	ACACTCGAGCACTTTTTGAAT
pLKO1_shETV1-A	GACCCAGTGTATGAACACAA
pLKO1_ shETV1-B	GAGAGATATGTCTACAAGTTT
pLKO1_shETV4-A	CCCAACAAATGCCCATTTCAT
pLKO5_shETV4-B	AGCGTTACGTGTACAAGTTTG
pLKO5_shETV5-A	CACCTCCAACCAAGATCAAAC
pLKO1_shETV5-B	CCGTGACACTTAGTACATTAA
pLKO-Tet-On-shKRAS-509	CCTATGGTCCTAGTAGGAAAT

CHAPTER FIVE

CONCLUSION

The genomic view of cancer has introduced a fundamental shift in clinical oncology. Therapeutic principles, predominantly dictated by anatomic origin and stage of disease progression, are increasingly shaped by the underlying genetic changes that drive specific cancers. The phenomenon of "oncogene addiction," where a cancer cell is dependent on a single protein for continued proliferation/survival despite harboring many genetic alterations[178,429], has had major implications for the diagnosis and classification of tumors, patient selection for specific targeted therapies, and the mechanism by which therapeutic resistance develops and is treated. Indeed, oncogene addiction and resistance to targeted therapy are inextricably linked. For an oncogene-addicted cancer cell to be resistant to targeted therapy, it must either maintain activity of the oncogene in the presence of drug or, if the oncogene is successfully inhibited, activate other genes with redundant functional effects. Understanding mechanisms of resistance to oncogene inhibition can provide insights into oncogenic signaling pathways and important mediators of cancer cell survival and proliferation.

While most *RAS*-mutant cancers are addicted to RAS, direct RAS inhibitors have not yet been developed for clinical use. An alternative approach to therapeutically target *RAS*-mutant cancers is to inhibit RAS effector pathways, such as the MAPK pathway. BRAF and MEK inhibitors are currently being tested in clinical trials for *RAS*-mutant cancers. Findings from early phase clinical trials suggest that intrinsic and acquired resistance will limit the therapeutic efficacy of these inhibitors[248,249,359]. Identifying and characterizing potential mechanisms of resistance is important for patient stratification and for the design of combination therapies to prevent or combat resistance.

Recent advancements in large scale screening techniques have enabled the systematic identification of resistance mechanisms in human cancer cell lines using both GOF[298] and LOF[297,358] approaches. It is increasingly possible to identify a comprehensive cohort of genes that can promote resistance to a particular targeted therapy[301-303]. The ability to identify GOF and LOF resistance mechanisms at a genome scale broadens the scope of these studies and enables the detection of functional similarities among genes that are capable of conferring resistance. While some modulators of resistance identified from *in vitro* resistance studies may not be operant in the clinical setting, they may highlight functions or pathways that are important for clinically relevant mechanisms of resistance. Moreover, these studies can further our understanding of even well characterized oncogenic signaling pathways.

We performed pooled genome scale ORF and CRISPR-Cas9 screens and identified a variety of GOF and LOF mechanism that mediate resistance to MAPKi in *RAS*-mutant cancer cells. In the GOF spectrum, we found that the strongest resistance phenotypes were conferred by overexpression of members of the RTK-RAS-MAPK pathway. Indeed, in the pooled ORF screen, the resistant cell population had restored phospho-ERK signaling despite continued treatment with a MEK inhibitor. This suggests that the most robust GOF mechanisms of resistance to MAPKi are those that restore MAPK signaling.

Conversely, in the LOF resistance screens, the majority of genes identified were not immediately related to the MAPK pathway. Indeed, we found that deletion of many transcription factors, members of the Mediator complex, histone acetyltransferases, or components of E3 ubiquitin ligases conferred resistance. These LOF screening results

suggest that, in the context of continued MAPK pathway inhibition, resistance will arise from alterations in orthogonal pathways or downstream transcriptional networks. We focused our efforts studying the two most consistent and robust LOF resistance mechanisms identified from our screens, KEAP1 and CIC knockout. We found that KEAP1 deletion mediated resistance through mechanisms orthogonal to the MAPK pathway, such as reducing trametinib-induced ROS and promoting anabolic metabolism. On the other hand, CIC loss promoted resistance by partially restoring the transcriptional pathway downstream of ERK. In addition, we demonstrated that CIC is an important regulator of RAS/MAPK signaling downstream of ERK, highlighting the ability of systematic LOF screens to contribute novel insight to a well-studied pathway.

A major limitation of studying resistance *in vitro* is that the identified mechanisms of resistance may not be clinically operant. Currently, there are few pre-treatment and post-relapse specimens from ongoing clinical trials of BRAF and MEK inhibitor monotherapy in *RAS*- or *BRAF*-mutant non-melanoma cancers for molecular analysis of intrinsic and acquired resistance mechanisms. However, there is some evidence suggesting that some of the hits identified from our screens may be relevant in the clinical setting. Prior studies that identified mechanisms of resistance to BRAF or MEK inhibition in *BRAF*-mutant melanoma imply that some of the resistance mechanisms identified here, such as BRAF and CRAF overexpression or *NF1* deletion, may be clinically relevant. Genomic profiling of NSCLC samples have demonstrated that LOF *KEAP1* mutations or GOF *NFE2L2* mutations co-occur with *RAS* mutations, suggesting that dysregulation of the KEAP1/NRF2 axis may be a mechanism of intrinsic resistance to BRAF or MEK inhibitor therapy in a subset of tumors. In addition, we found that high

expression of ATXN1L, a CIC co-repressor, predicted poor overall survival in patients with *BRAF*-mutant melanoma treated with MAPKi. This suggests that dysregulation of the ATXN1L-CIC-ETS transcription factor axis may mediate intrinsic resistance to MAPKi. As samples from ongoing clinical trials become available, it will become more clear whether certain modules of resistance – such as restored ERK signaling; increased ETV1, 4, and 5 expression; or increased capacity to buffer ROS – are clinically operant. This knowledge could promote the rational design of therapeutic combinations to target or prevent resistance mechanisms.

Several questions emerge from these studies. First, while we investigated the mechanism by which CIC and KEAP1 deletion mediate resistance to MAPKi, we did not validate or study the other hits identified from the GOF or LOF screens. Several hits may have similar functional consequences as some of the validated mechanisms of resistance, such as MAPK pathway reactivation and CIC or KEAP1 deletion. This could be assessed by systematically testing all the hits from the GOF and LOF screens for their ability to confer resistance to MAPKi; reactivate ERK signaling; increase mRNA or protein levels of ETV1, 4, and 5; or reduce ROS levels in the context of MAPKi. In addition, as genes with similar functions scored as hits in the LOF screens – such as components of E3 ubiquitin ligases, members of the Mediator complex, and multiple histone acetyltransferases – it would be informative to investigate if altered function of these genes modulate MAPKi resistance. Second, in the genome scale CRISPR-Cas9 screens, certain genes, such as CIC and KEAP1, appeared to be broadly generalizable modifiers of sensitivity to MAPKi, whereas others mediated resistance in only a subset of cell lines. Unique hits are likely attributable to a combination of technical and

biological effects. Performing additional LOF screens using improved sgRNA libraries across a larger number of cell lines would enable the identification of mechanisms of resistance that may be associated with specific cell lineages or molecular characteristics. Third, given that *bona fide* mechanisms of intrinsic or acquired resistance must be observed in clinical specimens, it will be important to determine whether the various GOF and LOF mechanisms of resistance to MAPKi identified here are operant in the clinical setting as molecularly characterized specimens from ongoing clinical trials become available.

In summary, we have identified a group of genes that modulate resistance to MAPKi via GOF and LOF screening approaches. We found that the two most robust and generalizable LOF hits confer resistance by either activating orthogonal pathways unrelated to MAPK signaling or by activating the MAPK pathway downstream of ERK. Importantly, currently available clinical data suggests that at least one of the identified pathways may be a clinically operant mechanism of intrinsic pathways. Our studies highlight the ability of systematic and comprehensive *in vitro* functional screens to identify clinically relevant mediators of resistance and to provide novel insights into well-studied pathways.

REFERENCES

1. HARVEY, J. J. An unidentified virus which causes the rapid production of tumours in mice. (1964). doi:10.1038/2041104b0

2. Kirsten, W. H. & Mayer, L. A. Morphologic responses to a murine erythroblastosis virus. *J. Natl. Cancer Inst.* **39,** 311–335 (1967).

3. Scolnick, E. M. & Parks, W. P. Harvey sarcoma virus: a second murine type C sarcoma virus with rat genetic information. *J. Virol.* **13,** 1211–1219 (1974).

4. Scolnick, E. M., Rands, E., Williams, D. & Parks, W. P. Studies on the nucleic acid sequences of Kirsten sarcoma virus: a model for formation of a mammalian RNA-containing sarcoma virus. *J. Virol.* **12,** 458–463 (1973).

5. Shih, C., Padhy, L. C., Murray, M. & Weinberg, R. A. Transforming genes of carcinomas and neuroblastomas introduced into mouse fibroblasts. *Nature* **290,** 261–264 (1981).

6. Perucho, M. *et al.* Human-tumor-derived cell lines contain common and different transforming genes. *Cell* **27,** 467–476 (1981).

7. Shih, C. & Weinberg, R. A. Isolation of a transforming sequence from a human bladder carcinoma cell line. *Cell* **29,** 161–169 (1982).

8. Goldfarb, M., Shimizu, K., Perucho, M. & Wigler, M. Isolation and preliminary characterization of a human transforming gene from T24 bladder carcinoma cells. *Nature* **296,** 404–409 (1982).

9. Pulciani, S. *et al.* Oncogenes in human tumor cell lines: molecular cloning of a transforming gene from human bladder carcinoma cells. *Proc Natl Acad Sci USA* **79,** 2845–2849 (1982).

10. Santos, E., Tronick, S. R., Aaronson, S. A., Pulciani, S. & Barbacid, M. T24 human bladder carcinoma oncogene is an activated form of the normal human homologue of BALB- and Harvey-MSV transforming genes. *Nature* **298,** 343–347 (1982).

11. Der, C. J., Krontiris, T. G. & Cooper, G. M. Transforming genes of human bladder and lung carcinoma cell lines are homologous to the ras genes of Harvey and Kirsten sarcoma viruses. *Proc Natl Acad Sci USA* **79,** 3637–3640 (1982).

12. Parada, L. F., Tabin, C. J., Shih, C. & Weinberg, R. A. Human EJ bladder carcinoma oncogene is homologue of Harvey sarcoma virus ras gene. *Nature* **297,** 474–478 (1982).

13. Shimizu, K., Goldfarb, M., Perucho, M. & Wigler, M. Isolation and preliminary characterization of the transforming gene of a human neuroblastoma cell line.

Proc Natl Acad Sci USA **80,** 383–387 (1983).

14. Hall, A., Marshall, C. J., Spurr, N. K. & Weiss, R. A. Identification of transforming gene in two human sarcoma cell lines as a new member of the ras gene family located on chromosome 1. *Nature* **303,** 396–400 (1983).

15. Cox, A. D. & Der, C. J. Ras history: The saga continues. *Small GTPases* **1,** 2–27 (2010).

16. Kamata, T. & Feramisco, J. R. Epidermal growth factor stimulates guanine nucleotide binding activity and phosphorylation of ras oncogene proteins. *Nature* **310,** 147–150 (1984).

17. Mulcahy, L. S., Smith, M. R. & Stacey, D. W. Requirement for ras proto-oncogene function during serum-stimulated growth of NIH 3T3 cells. *Nature* **313,** 241–243 (1985).

18. Smith, M. R., DeGudicibus, S. J. & Stacey, D. W. Requirement for c-ras proteins during viral oncogene transformation. *Nature* **320,** 540–543 (1986).

19. Carpenter, G., King, L. & Cohen, S. Epidermal growth factor stimulates phosphorylation in membrane preparations in vitro. *Nature* **276,** 409–410 (1978).

20. Carpenter, G., Lembach, K. J., Morrison, M. M. & Cohen, S. Characterization of the binding of 125-I-labeled epidermal growth factor to human fibroblasts. *J. Biol. Chem.* **250,** 4297–4304 (1975).

21. Gschwind, A., Fischer, O. M. & Ullrich, A. Timeline: The discovery of receptor tyrosine kinases: targets for cancer therapy. *Nat Rev Cancer* **4,** 361–370 (2004).

22. Lowenstein, E. J. *et al.* The SH2 and SH3 domain-containing protein GRB2 links receptor tyrosine kinases to ras signaling. *Cell* **70,** 431–442 (1992).

23. Olivier, J. P. *et al.* A Drosophila SH2-SH3 adaptor protein implicated in coupling the sevenless tyrosine kinase to an activator of Ras guanine nucleotide exchange, Sos. *Cell* **73,** 179–191 (1993).

24. Simon, M. A., Dodson, G. S. & Rubin, G. M. An SH3-SH2-SH3 protein is required for p21Ras1 activation and binds to sevenless and Sos proteins in vitro. *Cell* **73,** 169–177 (1993).

25. Egan, S. E. *et al.* Association of Sos Ras exchange protein with Grb2 is implicated in tyrosine kinase signal transduction and transformation. *Nature* **363,** 45–51 (1993).

26. Gale, N. W., Kaplan, S., Lowenstein, E. J., Schlessinger, J. & Bar-Sagi, D. Grb2 mediates the EGF-dependent activation of guanine nucleotide exchange on Ras. *Nature* **363,** 88–92 (1993).

27. Li, N. *et al.* Guanine-nucleotide-releasing factor hSos1 binds to Grb2 and links receptor tyrosine kinases to Ras signalling. *Nature* **363,** 85–88 (1993).

28. Buday, L. & Downward, J. Epidermal growth factor regulates p21ras through the formation of a complex of receptor, Grb2 adapter protein, and Sos nucleotide exchange factor. *Cell* **73,** 611–620 (1993).

29. Chardin, P. *et al.* Human Sos1: a guanine nucleotide exchange factor for Ras that binds to GRB2. *Science* **260,** 1338–1343 (1993).

30. McCormick, F. How receptors turn Ras on. *Nature* **363,** 15–16 (1993).

31. Aronheim, A. *et al.* Membrane targeting of the nucleotide exchange factor Sos is sufficient for activating the Ras signaling pathway. *Cell* **78,** 949–961 (1994).

32. Quilliam, L. A. *et al.* Membrane-targeting potentiates guanine nucleotide exchange factor CDC25 and SOS1 activation of Ras transforming activity. *Proc Natl Acad Sci USA* **91,** 8512–8516 (1994).

33. Scolnick, E. M., Papageorge, A. G. & Shih, T. Y. Guanine nucleotide-binding activity as an assay for src protein of rat-derived murine sarcoma viruses. *Proc Natl Acad Sci USA* **76,** 5355–5359 (1979).

34. Shih, T. Y., Papageorge, A. G., Stokes, P. E., Weeks, M. O. & Scolnick, E. M. Guanine nucleotide-binding and autophosphorylating activities associated with the p21src protein of Harvey murine sarcoma virus. *Nature* **287,** 686–691 (1980).

35. Hurley, J. B., Simon, M. I., Teplow, D. B., Robishaw, J. D. & Gilman, A. G. Homologies between signal transducing G proteins and ras gene products. *Science* **226,** 860–862 (1984).

36. Stephen, A. G., Esposito, D., Bagni, R. K. & McCormick, F. Dragging ras back in the ring. *Cancer Cell* **25,** 272–281 (2014).

37. W Wei, R. D. M. P. S. E. G. D. M. C. D. P. L. B. X. L. D. B. Identification of a mammalian gene structurally and functionally related to the CDC25 gene of Saccharomyces cerevisiae. *Proc Natl Acad Sci USA* **89,** 7100 (1992).

38. Shou, C., Farnsworth, C. L., Neel, B. G. & Feig, L. A. Molecular cloning of cDNAs encoding a guanine-nucleotide-releasing factor for Ras p21. *Nature* **358,** 351–354 (1992).

39. Bowtell, D., Fu, P., Simon, M. & Senior, P. Identification of murine homologues of the Drosophila son of sevenless gene: potential activators of ras. *Proc Natl Acad Sci USA* **89,** 6511–6515 (1992).

40. Trahey, M. *et al.* Molecular cloning of two types of GAP complementary DNA

from human placenta. *Science* **242,** 1697–1700 (1988).

41. Vogel, U. S. *et al.* Cloning of bovine GAP and its interaction with oncogenic ras p21. *Nature* **335,** 90–93 (1988).

42. Xu, G. *et al.* The neurofibromatosis type 1 gene encodes a protein related to GAP. *Cell* **62,** 599–608 (1990).

43. Martin, G. A. *et al.* The GAP-related domain of the neurofibromatosis type 1 gene product interacts with ras p21. *Cell* **63,** 843–849 (1990).

44. Ballester, R. *et al.* The NF1 locus encodes a protein functionally related to mammalian GAP and yeast IRA proteins. *Cell* **63,** 851–859 (1990).

45. Wallace, M. R. *et al.* Type 1 neurofibromatosis gene: identification of a large transcript disrupted in three NF1 patients. *Science* **249,** 181–186 (1990).

46. Trahey, M. & McCormick, F. A cytoplasmic protein stimulates normal N-ras p21 GTPase, but does not affect oncogenic mutants. *Science* **238,** 542–545 (1987).

47. Scheffzek, K., Lautwein, A., Kabsch, W., Reza Ahmadian, M. & Wittinghofer, A. Crystal structure of the GTPase-activating domain of human p120GAP and implications for the interaction with Ras. *Nature* **384,** 591–596 (1996).

48. Gibbs, J. B. Mechanism-based target identification and drug discovery in cancer research. *Science* **287,** 1969–1973 (2000).

49. McGrath, J. P., Capon, D. J., Goeddel, D. V. & Levinson, A. D. Comparative biochemical properties of normal and activated human ras p21 protein. *Nature* **310,** 644–649 (1984).

50. Sweet, R. W. *et al.* The product of ras is a GTPase and the T24 oncogenic mutant is deficient in this activity. *Nature* **311,** 273–275 (1984).

51. Manne, V., Bekesi, E. & Kung, H. F. Ha-ras proteins exhibit GTPase activity: point mutations that activate Ha-ras gene products result in decreased GTPase activity. *Proc Natl Acad Sci USA* **82,** 376–380 (1985).

52. Wohlgemuth, S. *et al.* Recognizing and defining true Ras binding domains I: biochemical analysis. *Journal of Molecular Biology* **348,** 741–758 (2005).

53. Lim, K.-H. *et al.* Activation of RalA is critical for Ras-induced tumorigenesis of human cells. *Cancer Cell* **7,** 533–545 (2005).

54. Collisson, E. A. *et al.* A central role for RAF→MEK→ERK signaling in the genesis of pancreatic ductal adenocarcinoma. *Cancer Discovery* **2,** 685–693 (2012).

55. Eser, S. *et al.* Selective Requirement of PI3K/PDK1 Signaling for Kras Oncogene-Driven Pancreatic Cell Plasticity and Cancer. *Cancer Cell* **23,** 406–420 (2013).

56. Feldmann, G. *et al.* Inhibiting the Cyclin-Dependent Kinase CDK5 Blocks Pancreatic Cancer Formation and Progression through the Suppression of Ras-Ral Signaling. *Cancer Research* **70,** 4460–4469 (2010).

57. Shibatohge, M. *et al.* Identification of PLC210, a Caenorhabditis elegans phospholipase C, as a putative effector of Ras. *J. Biol. Chem.* **273,** 6218–6222 (1998).

58. Kelley, G. G., Reks, S. E., Ondrako, J. M. & Smrcka, A. V. Phospholipase C(epsilon): a novel Ras effector. *The EMBO Journal* **20,** 743–754 (2001).

59. Song, C. *et al.* Regulation of a Novel Human Phospholipase C, PLC , through Membrane Targeting by Ras. *Journal of Biological Chemistry* **276,** 2752–2757 (2001).

60. Lambert, J. M. *et al.* Tiam1 mediates Ras activation of Rac by a PI(3)K-independent mechanism. *Nat. Cell Biol.* **4,** 621–625 (2002).

61. Avruch, J. *et al.* Rassf Family of Tumor Suppressor Polypeptides. *Journal of Biological Chemistry* **284,** 11001–11005 (2009).

62. Moodie, S. A., Willumsen, B. M., Weber, M. J. & Wolfman, A. Complexes of Ras.GTP with Raf-1 and mitogen-activated protein kinase kinase. *Science* **260,** 1658–1661 (1993).

63. Warne, P. H., Viciana, P. R. & Downward, J. Direct interaction of Ras and the amino-terminal region of Raf-1 in vitro. *Nature* **364,** 352–355 (1993).

64. Zhang, X. F. *et al.* Normal and oncogenic p21ras proteins bind to the amino-terminal regulatory domain of c-Raf-1. *Nature* **364,** 308–313 (1993).

65. Vojtek, A. B., Hollenberg, S. M. & Cooper, J. A. Mammalian Ras interacts directly with the serine/threonine kinase Raf. *Cell* **74,** 205–214 (1993).

66. Van Aelst, L., Barr, M., Marcus, S., Polverino, A. & Wigler, M. Complex formation between RAS and RAF and other protein kinases. *Proc Natl Acad Sci USA* **90,** 6213–6217 (1993).

67. Marais, R., Light, Y., Paterson, H. F. & Marshall, C. J. Ras recruits Raf-1 to the plasma membrane for activation by tyrosine phosphorylation. *The EMBO Journal* **14,** 3136–3145 (1995).

68. Marais, R. *et al.* Requirement of Ras-GTP-Raf complexes for activation of Raf-1 by protein kinase C. *Science* **280,** 109–112 (1998).

69. Gallego, C., Gupta, S. K., Heasley, L. E., Qian, N. X. & Johnson, G. L. Mitogen-activated protein kinase activation resulting from selective oncogene expression in NIH 3T3 and rat 1a cells. *Proc Natl Acad Sci USA* **89,** 7355–7359 (1992).

70. Wood, K. W., Sarnecki, C., Roberts, T. M. & Blenis, J. ras mediates nerve growth factor receptor modulation of three signal-transducing protein kinases: MAP kinase, Raf-1, and RSK. *Cell* **68,** 1041–1050 (1992).

71. Howe, L. R. *et al.* Activation of the MAP kinase pathway by the protein kinase raf. *Cell* **71,** 335–342 (1992).

72. Dent, P. *et al.* Activation of mitogen-activated protein kinase kinase by v-Raf in NIH 3T3 cells and in vitro. *Science* **257,** 1404–1407 (1992).

73. Roux, P. P. & Blenis, J. ERK and p38 MAPK-Activated Protein Kinases: a Family of Protein Kinases with Diverse Biological Functions. *Microbiology and Molecular Biology Reviews* **68,** 320–344 (2004).

74. Sjölander, A., Yamamoto, K., Huber, B. E. & Lapetina, E. G. Association of p21ras with phosphatidylinositol 3-kinase. *Proc Natl Acad Sci USA* **88,** 7908–7912 (1991).

75. Rodriguez-Viciana, P. *et al.* Phosphatidylinositol-3-OH kinase direct target of Ras. *Nature* **370,** 527–532 (1994).

76. Ebi, H. *et al.* Receptor tyrosine kinases exert dominant control over PI3K signaling in human KRAS mutant colorectal cancers. *J. Clin. Invest.* **121,** 4311–4321 (2011).

77. Molina-Arcas, M., Hancock, D. C., Sheridan, C., Kumar, M. S. & Downward, J. Coordinate direct input of both KRAS and IGF1 receptor to activation of PI3 kinase in KRAS-mutant lung cancer. *Cancer Discovery* **3,** 548–563 (2013).

78. Kazlauskas, A. Receptor tyrosine kinases and their targets. *Curr. Opin. Genet. Dev.* **4,** 5–14 (1994).

79. Stephens, L. *et al.* A novel phosphoinositide 3 kinase activity in myeloid-derived cells is activated by G protein beta gamma subunits. *Cell* **77,** 83–93 (1994).

80. Stoyanov, B. *et al.* Cloning and characterization of a G protein-activated human phosphoinositide-3 kinase. *Science* **269,** 690–693 (1995).

81. Pacold, M. E. *et al.* Crystal structure and functional analysis of Ras binding to its effector phosphoinositide 3-kinase gamma. *Cell* **103,** 931–943 (2000).

82. Currie, R. A. *et al.* Role of phosphatidylinositol 3,4,5-trisphosphate in regulating the activity and localization of 3-phosphoinositide-dependent protein kinase-1. *Biochem. J.* **337 (Pt 3),** 575–583 (1999).

83. Alessi, D. R. *et al.* Characterization of a 3-phosphoinositide-dependent protein kinase which phosphorylates and activates protein kinase Balpha. *Curr. Biol.* **7,** 261–269 (1997).

84. Vanhaesebroeck, B., Stephens, L. & Hawkins, P. PI3K signalling: the path to discovery and understanding. *Nat Rev Mol Cell Biol* **13,** 195–203 (2012).

85. Hofer, F., Fields, S., Schneider, C. & Martin, G. S. Activated Ras interacts with the Ral guanine nucleotide dissociation stimulator. *Proc Natl Acad Sci USA* **91,** 11089–11093 (1994).

86. Spaargaren, M. & Bischoff, J. R. Identification of the guanine nucleotide dissociation stimulator for Ral as a putative effector molecule of R-ras, H-ras, K-ras, and Rap. *Proc Natl Acad Sci USA* **91,** 12609–12613 (1994).

87. Kikuchi, A., Demo, S. D., Ye, Z. H. & Chen, Y. W. ralGDS family members interact with the effector loop of ras p21. *Molecular and Cellular …* (1994). doi:10.1128/MCB.14.11.7483

88. Peterson, S. N., Trabalzini, L., Brtva, T. R. & Fischer, T. Identification of a novel RalGDS-related protein as a candidate effector for Ras and Rap1. *Journal of Biological …* (1996). doi:10.1074/jbc.271.47.29903

89. Shao, H. & Andres, D. A. A novel RalGEF-like protein, RGL3, as a candidate effector for rit and Ras. *J. Biol. Chem.* **275,** 26914–26924 (2000).

90. Xu, J., Shi, S., Matsumoto, N., Noda, M. & Kitayama, H. Identification of Rgl3 as a potential binding partner for Rap-family small G-proteins and profilin II. *Cellular Signalling* **19,** 1575–1582 (2007).

91. Lim, K.-H. *et al.* Divergent Roles for RalA and RalB in Malignant Growth of Human Pancreatic Carcinoma Cells. *Current Biology* **16,** 2385–2394 (2006).

92. Chien, Y. *et al.* RalB GTPase-mediated activation of the IkappaB family kinase TBK1 couples innate immune signaling to tumor cell survival. *Cell* **127,** 157–170 (2006).

93. Jullien-Flores, V. *et al.* Bridging Ral GTPase to Rho pathways. RLIP76, a Ral effector with CDC42/Rac GTPase-activating protein activity. *J. Biol. Chem.* **270,** 22473–22477 (1995).

94. Cantor, S. B., Urano, T. & Feig, L. A. Identification and characterization of Ral-binding protein 1, a potential downstream target of Ral GTPases. *Molecular and Cellular Biology* **15,** 4578–4584 (1995).

95. Nakashima, S. *et al.* Small G protein Ral and its downstream molecules regulate endocytosis of EGF and insulin receptors. *The EMBO Journal* **18,** 3629–3642 (1999).

96. Moskalenko, S. *et al.* The exocyst is a Ral effector complex. *Nat. Cell Biol.* **4,** 66–72 (2001).

97. Sugihara, K. *et al.* The exocyst complex binds the small GTPase RalA to mediate filopodia formation. *Nat. Cell Biol.* **4,** 73–78 (2002).

98. Moskalenko, S. *et al.* Ral GTPases Regulate Exocyst Assembly through Dual Subunit Interactions. *Journal of Biological Chemistry* **278,** 51743–51748 (2003).

99. Rosse, C. *et al.* RalB mobilizes the exocyst to drive cell migration. *Molecular and Cellular Biology* **26,** 727–734 (2006).

100. Chen, X. W., Inoue, M., Hsu, S. C. & Saltiel, A. R. RalA-exocyst-dependent Recycling Endosome Trafficking Is Required for the Completion of Cytokinesis. *Journal of Biological Chemistry* **281,** 38609–38616 (2006).

101. Gupta, S. *et al.* Binding of Ras to Phosphoinositide 3-Kinase p110α Is Required for Ras- Driven Tumorigenesis in Mice. *Cell* **129,** 957–968 (2007).

102. Blasco, R. B. *et al.* c-Raf, but not B-Raf, is essential for development of K-Ras oncogene-driven non-small cell lung carcinoma. *Cancer Cell* **19,** 652–663 (2011).

103. González-García, A. *et al.* RalGDS is required for tumor formation in a model of skin carcinogenesis. *CCELL* **7,** 219–226 (2005).

104. Ehrenreiter, K. *et al.* Raf-1 addiction in Ras-induced skin carcinogenesis. *Cancer Cell* **16,** 149–160 (2009).

105. Hamad, N. M. *et al.* Distinct requirements for Ras oncogenesis in human versus mouse cells. *Genes & Development* **16,** 2045–2057 (2002).

106. Eferl, R. & Wagner, E. F. AP-1: a double-edged sword in tumorigenesis. *Nat Rev Cancer* **3,** 859–868 (2003).

107. Yordy, J. S. & Muise-Helmericks, R. C. Signal transduction and the Ets family of transcription factors. *Oncogene* **19,** 6503–6513 (2000).

108. Hollenhorst, P. C. *et al.* Oncogenic ETS proteins mimic activated RAS/MAPK signaling in prostate cells. *Genes & Development* **25,** 2147–2157 (2011).

109. Filmus, J. *et al.* Induction of cyclin D1 overexpression by activated ras. *Oncogene* **9,** 3627–3633 (1994).

110. Yu, Q., Geng, Y. & Sicinski, P. Specific protection against breast cancers by cyclin D1 ablation. *Nature* **411,** 1017–1021 (2001).

111. Pylayeva-Gupta, Y., Grabocka, E. & Bar-Sagi, D. RAS oncogenes: weaving a

tumorigenic web. *Oncogene* **11,** 761–774 (2011).

112. Kimmelman, A. C. Metabolic Dependencies in RAS-Driven Cancers. *Clin. Cancer Res.* **21,** 1828–1834 (2015).

113. Horiguchi, K. *et al.* Role of Ras signaling in the induction of snail by transforming growth factor-beta. *J. Biol. Chem.* **284,** 245–253 (2009).

114. Giehl, K. Oncogenic Ras in tumour progression and metastasis. *Biological Chemistry* **386,** 193–205 (2005).

115. Campbell, P. M. & Der, C. J. Oncogenic Ras and its role in tumor cell invasion and metastasis. *Seminars in Cancer Biology* **14,** 105–114 (2004).

116. Willumsen, B. M., Christensen, A., Hubbert, N. L., Papageorge, A. G. & Lowy, D. R. The p21 ras C-terminus is required for transformation and membrane association. *Nature* **310,** 583–586 (1984).

117. Jackson, J. H. *et al.* Farnesol modification of Kirsten-ras exon 4B protein is essential for transformation. *Proc Natl Acad Sci USA* **87,** 3042–3046 (1990).

118. Hancock, J. F., Magee, A. I., Childs, J. E. & Marshall, C. J. All ras proteins are polyisoprenylated but only some are palmitoylated. *Current Biology* **57,** 1167–1177 (1989).

119. Schafer, W. R. *et al.* Genetic and pharmacological suppression of oncogenic mutations in ras genes of yeast and humans. *Science* **245,** 379–385 (1989).

120. Rowell, C. A., Kowalczyk, J. J., Lewis, M. D. & Garcia, A. M. Direct demonstration of geranylgeranylation and farnesylation of Ki-Ras in vivo. *J. Biol. Chem.* **272,** 14093–14097 (1997).

121. Whyte, D. B. *et al.* K- and N-Ras Are Geranylgeranylated in Cells Treated with Farnesyl Protein Transferase Inhibitors. *Journal of Biological Chemistry* **272,** 14459–14464 (1997).

122. Lerner, E. C. *et al.* Inhibition of the prenylation of K-Ras, but not H- or N-Ras, is highly resistant to CAAX peptidomimetics and requires both a farnesyltransferase and a geranylgeranyltransferase I inhibitor in human tumor cell lines. *Oncogene* **15,** 1283–1288 (1997).

123. Goldstein, J. L. Polylysine and CVIM Sequences of K-RasB Dictate Specificity of Prenylation and Confer Resistance to Benzodiazepine Peptidomimetic in Vitro. *Journal of Biological Chemistry* **270,** 6221–6226 (1995).

124. Willumsen, B. M., Norris, K., Papageorge, A. G., Hubbert, N. L. & Lowy, D. R. Harvey murine sarcoma virus p21 ras protein: biological and biochemical significance of the cysteine nearest the carboxy terminus. *The EMBO Journal* **3,**

2581–2585 (1984).

125. Fujiyama, A. & Tamanoi, F. RAS2 protein of Saccharomyces cerevisiae undergoes removal of methionine at N terminus and removal of three amino acids at C terminus. *J. Biol. Chem.* **265,** 3362–3368 (1990).

126. Clarke, S., Vogel, J. P., Deschenes, R. J. & Stock, J. Posttranslational modification of the Ha-ras oncogene protein: evidence for a third class of protein carboxyl methyltransferases. *Proc Natl Acad Sci USA* **85,** 4643–4647 (1988).

127. Gutierrez, L., Magee, A. I., Marshall, C. J. & Hancock, J. F. Post-translational processing of p21ras is two-step and involves carboxyl-methylation and carboxy-terminal proteolysis. *The EMBO Journal* **8,** 1093–1098 (1989).

128. Deschenes, R. J., Stimmel, J. B., Clarke, S., Stock, J. & Broach, J. R. RAS2 protein of Saccharomyces cerevisiae is methyl-esterified at its carboxyl terminus. *J. Biol. Chem.* **264,** 11865–11873 (1989).

129. Hancock, J. F., Paterson, H. & Marshall, C. J. A polybasic domain or palmitoylation is required in addition to the CAAX motif to localize p21ras to the plasma membrane. *Cell* **63,** 133–139 (1990).

130. Hancock, J. F., Cadwallader, K., Paterson, H. & Marshall, C. J. A CAAX or a CAAL motif and a second signal are sufficient for plasma membrane targeting of ras proteins. *The EMBO Journal* **10,** 4033–4039 (1991).

131. Cox, A. D., Fesik, S. W., Kimmelman, A. C., Luo, J. & Der, C. J. Drugging the undruggable RAS: Mission Possible? *Nature Publishing Group* **13,** 828–851 (2014).

132. Kandoth, C. *et al.* Mutational landscape and significance across 12 major cancer types. *Nature* **502,** 333–339 (2013).

133. Liu, P. *et al.* Oncogenic PIK3CA-driven mammary tumors frequently recur via PI3K pathway–dependent and PI3K pathway–independent mechanisms. *Nat Med* **17,** 1116–1120 (2011).

134. Forbes, S. A. *et al.* COSMIC: exploring the world's knowledge of somatic mutations in human cancer. *Nucleic Acids Research* **43,** D805–11 (2015).

135. Prior, I. A., Lewis, P. D. & Mattos, C. A Comprehensive Survey of Ras Mutations in Cancer. *Cancer Research* **72,** 2457–2467 (2012).

136. Cerami, E. *et al.* The cBio Cancer Genomics Portal: An Open Platform for Exploring Multidimensional Cancer Genomics Data. *Cancer Discovery* **2,** 401–404 (2012).

137. Gao, J. *et al.* Integrative analysis of complex cancer genomics and clinical

profiles using the cBioPortal. *Science Signaling* **6,** pl1 (2013).

138. Land, H., Parada, L. F. & Weinberg, R. A. Tumorigenic conversion of primary embryo fibroblasts requires at least two cooperating oncogenes. *Nature* **304,** 596–602 (1983).

139. Ruley, H. E. Adenovirus early region 1A enables viral and cellular transforming genes to transform primary cells in culture. *Nature* **304,** 602–606 (1983).

140. Hahn, W. C. *et al.* Creation of human tumour cells with defined genetic elements. *Nature* **400,** 464–468 (1999).

141. Hruban, R. H., Goggins, M., Parsons, J. & Kern, S. E. Progression model for pancreatic cancer. *Clin. Cancer Res.* **6,** 2969–2972 (2000).

142. Fearon, E. R. & Vogelstein, B. A genetic model for colorectal tumorigenesis. *Cell* **61,** 759–767 (1990).

143. Hingorani, S. R. *et al.* Trp53R172H and KrasG12D cooperate to promote chromosomal instability and widely metastatic pancreatic ductal adenocarcinoma in mice. *Cancer Cell* **7,** 469–483 (2005).

144. Haigis, K. M. *et al.* Differential effects of oncogenic K-Ras and N-Ras on proliferation, differentiation and tumor progression in the colon. *Nat Genet* **40,** 600–608 (2008).

145. Ji, H. *et al.* LKB1 modulates lung cancer differentiation and metastasis. *Nature* **448,** 807–810 (2007).

146. Vincent, A., Herman, J., Schulick, R., Hruban, R. H. & Goggins, M. Pancreatic cancer. *Lancet* **378,** 607–620 (2011).

147. Sansom, O. J. *et al.* Loss of Apc allows phenotypic manifestation of the transforming properties of an endogenous K-ras oncogene in vivo. *Proceedings of the National Academy of Sciences* **103,** 14122–14127 (2006).

148. Jakob, J. A. *et al.* NRAS mutation status is an independent prognostic factor in metastatic melanoma. *Cancer* **118,** 4014–4023 (2011).

149. Mascaux, C. *et al.* The role of RAS oncogene in survival of patients with lung cancer: a systematic review of the literature with meta-analysis. *Br. J. Cancer* **92,** 131–139 (2005).

150. Lampson, B. L. *et al.* Rare codons regulate KRas oncogenesis. *Curr. Biol.* **23,** 70–75 (2013).

151. Sarkisian, C. J. *et al.* Dose-dependent oncogene-induced senescence in vivo and its evasion during mammary tumorigenesis. *Oncogene* **9,** 493–505 (2007).

152. Potenza, N. *et al.* Replacement of K-Ras with H-Ras supports normal embryonic development despite inducing cardiovascular pathology in adult mice. *EMBO Rep* **6,** 432–437 (2005).

153. Ahrendt, S. A. *et al.* Cigarette smoking is strongly associated with mutation of the K-ras gene in patients with primary adenocarcinoma of the lung. *Cancer* **92,** 1525–1530 (2001).

154. Zarbl, H., Sukumar, S., Arthur, A. V., Martin-Zanca, D. & Barbacid, M. Direct mutagenesis of Ha-ras-1 oncogenes by N-nitroso-N-methylurea during initiation of mammary carcinogenesis in rats. *Nature* **315,** 382–385 (1985).

155. Westcott, P. M. K. *et al.* The mutational landscapes of genetic and chemical models of Kras-driven lung cancer. *Nature* **517,** 489–492 (2015).

156. Ihle, N. T. *et al.* Effect of KRAS oncogene substitutions on protein behavior: implications for signaling and clinical outcome. *J. Natl. Cancer Inst.* **104,** 228–239 (2012).

157. Hunter, J. C. *et al.* Biochemical and Structural Analysis of Common Cancer-Associated KRAS Mutations. *Molecular Cancer Research* **13,** 1325–1335 (2015).

158. Lau, K. S. & Haigis, K. M. Non-redundancy within the RAS oncogene family: Insights into mutational disparities in cancer. *Mol Cells* **28,** 315–320 (2009).

159. Quinlan, M. P., Quatela, S. E., Philips, M. R. & Settleman, J. Activated Kras, but Not Hras or Nras, May Initiate Tumors of Endodermal Origin via Stem Cell Expansion. *Molecular and Cellular Biology* **28,** 2659–2674 (2008).

160. Villalonga, P. *et al.* Calmodulin binds to K-Ras, but not to H- or N-Ras, and modulates its downstream signaling. *Molecular and Cellular Biology* **21,** 7345–7354 (2001).

161. Wang, M.-T. *et al.* K-Ras Promotes Tumorigenicity through Suppression of Non-canonical Wnt Signaling. *Cell* **163,** 1237–1251 (2015).

162. Rauen, K. A. The RASopathies. *Annu. Rev. Genom. Human Genet.* **14,** 355–369 (2013).

163. Johnson, L. *et al.* K-ras is an essential gene in the mouse with partial functional overlap with N-ras. *Genes & Development* **11,** 2468–2481 (1997).

164. Koera, K. *et al.* K-ras is essential for the development of the mouse embryo. *Oncogene* **15,** 1151–1159 (1997).

165. Plowman, S. J. *et al.* The K-Ras 4A isoform promotes apoptosis but does not affect either lifespan or spontaneous tumor incidence in aging mice. *Exp. Cell*

Res. **312,** 16–26 (2006).

166. Umanoff, H., Edelmann, W., Pellicer, A. & Kucherlapati, R. The murine N-ras gene is not essential for growth and development. *Proceedings of the National Academy of Sciences* **92,** 1709–1713 (1995).

167. Ise, K. *et al.* Targeted deletion of the H-ras gene decreases tumor formation in mouse skin carcinogenesis. *Oncogene* **19,** 2951–2956 (2000).

168. Esteban, L. M. *et al.* Targeted genomic disruption of H-ras and N-ras, individually or in combination, reveals the dispensability of both loci for mouse growth and development. *Molecular and Cellular Biology* **21,** 1444–1452 (2001).

169. To, M. D. *et al.* Kras regulatory elements and exon 4A determine mutation specificity in lung cancer. *Nat Genet* **40,** 1240–1244 (2008).

170. Cancer Genome Atlas Research Network. Comprehensive molecular profiling of lung adenocarcinoma. *Nature* **511,** 543–550 (2014).

171. Bazan, V. *et al.* Specific codon 13 K-ras mutations are predictive of clinical outcome in colorectal cancer patients, whereas codon 12 K-ras mutations are associated with mucinous histotype. *Ann. Oncol.* **13,** 1438–1446 (2002).

172. Villaruz, L. C. *et al.* The prognostic and predictive value of KRAS oncogene substitutions in lung adenocarcinoma. *Cancer* **119,** 2268–2274 (2013).

173. De Roock, W. *et al.* Association of KRAS p.G13D mutation with outcome in patients with chemotherapy-refractory metastatic colorectal cancer treated with cetuximab. *JAMA* **304,** 1812–1820 (2010).

174. Kim, E. S. *et al.* The BATTLE trial: personalizing therapy for lung cancer. *Cancer Discovery* **1,** 44–53 (2011).

175. Mao, C. *et al.* KRAS mutations and resistance to EGFR-TKIs treatment in patients with non-small cell lung cancer: a meta-analysis of 22 studies. *Lung Cancer* **69,** 272–278 (2010).

176. Karachaliou, N. *et al.* KRAS Mutations in Lung Cancer. *CLLC* **14,** 205–214 (2013).

177. Tejpar, S. *et al.* Association of KRAS G13D Tumor Mutations With Outcome in Patients With Metastatic Colorectal Cancer Treated With First-Line Chemotherapy With or Without Cetuximab. *Journal of Clinical Oncology* **30,** 3570–3577 (2012).

178. Weinstein, I. B. Cancer. Addiction to oncogenes--the Achilles heal of cancer. *Science* **297,** 63–64 (2002).

179. Weinstein, I. B. Disorders in cell circuitry during multistage carcinogenesis: the role of homeostasis. *Carcinogenesis* **21,** 857–864 (2000).

180. Haber, D. A., Gray, N. S. & Baselga, J. The Evolving War on Cancer. *Cell* **145,** 19–24 (2011).

181. Sharma, S. V. & Settleman, J. Oncogene addiction: setting the stage for molecularly targeted cancer therapy. *Genes & Development* **21,** 3214–3231 (2007).

182. Singh, A. *et al.* A Gene Expression Signature Associated with 'K-Ras Addiction' Reveals Regulators of EMT and Tumor Cell Survival. *Cancer Cell* **15,** 489–500 (2009).

183. Brummelkamp, T. R., Bernards, R. & Agami, R. Stable suppression of tumorigenicity by virus-mediated RNA interference. *Cancer Cell* **2,** 243–247 (2002).

184. Barbie, D. A. *et al.* Systematic RNA interference reveals that oncogenicKRAS-driven cancers require TBK1. *Nature* **461,** 108–112 (2009).

185. Chin, L. *et al.* Essential role for oncogenic Ras in tumour maintenance. *Nature Publishing Group* **400,** 468–472 (1999).

186. Fisher, G. H. *et al.* Induction and apoptotic regression of lung adenocarcinomas by regulation of a K-Ras transgene in the presence and absence of tumor suppressor genes. *Genes & Development* **15,** 3249–3262 (2001).

187. Hingorani, S. R. *et al.* Preinvasive and invasive ductal pancreatic cancer and its early detection in the mouse. *Cancer Cell* **4,** 437–450 (2003).

188. Ying, H. *et al.* Oncogenic Kras Maintains Pancreatic Tumors through Regulation of Anabolic Glucose Metabolism. *Cell* **149,** 656–670 (2012).

189. Collins, M. A. & Pasca di Magliano, M. Kras as a key oncogene and therapeutic target in pancreatic cancer. *Front. Physiol.* **4,** 407 (2013).

190. Collins, M. A. *et al.* Metastatic Pancreatic Cancer Is Dependent on Oncogenic Kras in Mice. *PLoS ONE* **7,** e49707 (2012).

191. Kwong, L. N. *et al.* Oncogenic NRAS signaling differentially regulates survival and proliferation in melanoma. *Nat Med* **18,** 1503–1510 (2012).

192. Luo, J., Solimini, N. L. & Elledge, S. J. Principles of cancer therapy: oncogene and non-oncogene addiction. *Cell* (2009).

193. Samatar, A. A. & Poulikakos, P. I. Targeting RAS-ERK signalling in cancer: promises and challenges. *Nature Publishing Group* **13,** 928–942 (2014).

194. Normanno, N., Bianco, C., De Luca, A. & Salomon, D. S. The role of EGF-related peptides in tumor growth. *Front. Biosci.* **6,** D685–707 (2001).

195. Sibilia, M. *et al.* The EGF receptor provides an essential survival signal for SOS-dependent skin tumor development. *Cell* **102,** 211–220 (2000).

196. Allegra, C. J. *et al.* American Society of Clinical Oncology Provisional Clinical Opinion: Testing for KRAS Gene Mutations in Patients With Metastatic Colorectal Carcinoma to Predict Response to Anti-Epidermal Growth Factor Receptor Monoclonal Antibody Therapy. *Journal of Clinical Oncology* **27,** 2091–2096 (2009).

197. Allegra, C. J. *et al.* Extended RAS Gene Mutation Testing in Metastatic Colorectal Carcinoma to Predict Response to Anti-Epidermal Growth Factor Receptor Monoclonal Antibody Therapy: American Society of Clinical Oncology Provisional Clinical Opinion Update 2015. *Journal of Clinical Oncology* (2015). doi:10.1200/JCO.2015.63.9674

198. Pao, W. *et al.* KRAS mutations and primary resistance of lung adenocarcinomas to gefitinib or erlotinib. *PLoS Med.* **2,** e17 (2005).

199. Zhu, C. Q. *et al.* Role of KRAS and EGFR as biomarkers of response to erlotinib in National Cancer Institute of Canada Clinical Trials Group Study BR.21. *Journal of Clinical Oncology* **26,** 4268–4275 (2008).

200. Morelli, M. P. & Kopetz, S. Hurdles and complexities of codon 13 KRAS mutations. *Journal of Clinical Oncology* **30,** 3565–3567 (2012).

201. Schirripa, M. *et al.* Phase II study of single-agent cetuximab in KRAS G13D mutant metastatic colorectal cancer. *Ann. Oncol.* **26,** 2503 (2015).

202. Goody, R. S., Frech, M. & Wittinghofer, A. Affinity of guanine nucleotide binding proteins for their ligands: facts and artefacts. *Trends Biochem. Sci.* **16,** 327–328 (1991).

203. Arkin, M. R. & Wells, J. A. Small-molecule inhibitors of protein-protein interactions: progressing towards the dream. *Nat Rev Drug Discov* **3,** 301–317 (2004).

204. Herrmann, C. *et al.* Sulindac sulfide inhibits Ras signaling. *Oncogene* **17,** 1769–1776 (1998).

205. Waldmann, H. *et al.* Sulindac-derived Ras pathway inhibitors target the Ras-Raf interaction and downstream effectors in the Ras pathway. *Angew. Chem. Int. Ed. Engl.* **43,** 454–458 (2004).

206. Karaguni, I.-M. *et al.* New indene-derivatives with anti-proliferative properties. *Bioorganic & Medicinal Chemistry Letters* **12,** 709–713 (2002).

207. Kato-Stankiewicz, J. *et al.* Inhibitors of Ras/Raf-1 interaction identified by two-hybrid screening revert Ras-dependent transformation phenotypes in human cancer cells. *Proc Natl Acad Sci USA* **99,** 14398–14403 (2002).

208. Shima, F. *et al.* In silico discovery of small-molecule Ras inhibitors that display antitumor activity by blocking the Ras-effector interaction. *Proceedings of the National Academy of Sciences* **110,** 8182–8187 (2013).

209. Hocker, H. J. *et al.* Andrographolide derivatives inhibit guanine nucleotide exchange and abrogate oncogenic Ras function. *Proceedings of the National Academy of Sciences* **110,** 10201–10206 (2013).

210. Maurer, T. *et al.* Small-molecule ligands bind to a distinct pocket in Ras and inhibit SOS-mediated nucleotide exchange activity. *Proceedings of the National Academy of Sciences* **109,** 5299–5304 (2012).

211. Patgiri, A., Yadav, K. K., Arora, P. S. & Bar-Sagi, D. An orthosteric inhibitor of the Ras-Sos interaction. *Nature Chemical Biology* **7,** 585–587 (2011).

212. Sacco, E. *et al.* Binding properties and biological characterization of new sugar-derived Ras ligands. *Med. Chem. Commun.* **2,** 396–401 (2011).

213. Sun, Q. *et al.* Discovery of small molecules that bind to K-Ras and inhibit Sos-mediated activation. *Angew. Chem. Int. Ed. Engl.* **51,** 6140–6143 (2012).

214. Taveras, A. G. *et al.* Ras oncoprotein inhibitors: the discovery of potent, ras nucleotide exchange inhibitors and the structural determination of a drug-protein complex. *Bioorganic & Medicinal Chemistry* **5,** 125–133 (1997).

215. Ostrem, J. M., Peters, U., Sos, M. L., Wells, J. A. & Shokat, K. M. K-Ras(G12C) inhibitors allosterically control GTP affinity and effector interactions. *Nature* – (2013). doi:10.1038/nature12796

216. Lim, S. M. *et al.* Therapeutic targeting of oncogenic K-Ras by a covalent catalytic site inhibitor. *Angew. Chem. Int. Ed. Engl.* **53,** 199–204 (2014).

217. Schafer, W. R. *et al.* Enzymatic coupling of cholesterol intermediates to a mating pheromone precursor and to the ras protein. *Science* **249,** 1133–1139 (1990).

218. Reiss, Y., Goldstein, J. L., Seabra, M. C., Casey, P. J. & Brown, M. S. Inhibition of purified p21ras farnesyl:protein transferase by Cys-AAX tetrapeptides. *Cell* **62,** 81–88 (1990).

219. Cox, A. D., Der, C. J. & Philips, M. R. Targeting RAS Membrane Association: Back to the Future for Anti-RAS Drug Discovery? *Clinical Cancer Research* **21,** 1819–1827 (2015).

220. Kohl, N. E. *et al.* Inhibition of farnesyltransferase induces regression of

mammary and salivary carcinomas in ras transgenic mice. *Nat Med* **1,** 792–797 (1995).

221. Nagasu, T., Yoshimatsu, K., Rowell, C., Lewis, M. D. & Garcia, A. M. Inhibition of human tumor xenograft growth by treatment with the farnesyl transferase inhibitor B956. *Cancer Research* **55,** 5310–5314 (1995).

222. Blumenschein, G., Ludwig, C., Thomas, G. & Tan, E. *O-082 A randomized phase III trial comparing ionafarnib/carboplatin/paclitaxel versus carboplatin/paclitaxel (CP) in chemotherapy-naive patients with ….* (Lung Cancer, 2005). doi:10.1016/S0169-5002(05)80215-6

223. Van Cutsem, E. *et al.* Phase III trial of gemcitabine plus tipifarnib compared with gemcitabine plus placebo in advanced pancreatic cancer. *J. Clin. Oncol.* **22,** 1430–1438 (2004).

224. Macdonald, J. S. *et al.* A phase II study of farnesyl transferase inhibitor R115777 in pancreatic cancer: a Southwest oncology group (SWOG 9924) study. *Invest New Drugs* **23,** 485–487 (2005).

225. Rao, S. *et al.* Phase III double-blind placebo-controlled study of farnesyl transferase inhibitor R115777 in patients with refractory advanced colorectal cancer. *J. Clin. Oncol.* **22,** 3950–3957 (2004).

226. Harousseau, J.-L. *et al.* A randomized phase 3 study of tipifarnib compared with best supportive care, including hydroxyurea, in the treatment of newly diagnosed acute myeloid leukemia in patients 70 years or older. *Blood* **114,** 1166–1173 (2009).

227. Sepp-Lorenzino, L. *et al.* A peptidomimetic inhibitor of farnesyl:protein transferase blocks the anchorage-dependent and -independent growth of human tumor cell lines. *Cancer Research* **55,** 5302–5309 (1995).

228. Kurzrock, R. *et al.* Farnesyltransferase inhibitor R115777 in myelodysplastic syndrome: clinical and biologic activities in the phase 1 setting. *Blood* **102,** 4527–4534 (2003).

229. End, D. W. *et al.* Characterization of the antitumor effects of the selective farnesyl protein transferase inhibitor R115777 in vivo and in vitro. *Cancer Research* **61,** 131–137 (2001).

230. Chen, X., Makarewicz, J. M., Knauf, J. A., Johnson, L. K. & Fagin, J. A. Transformation by HrasG12V is consistently associated with mutant allele copy gains and is reversed by farnesyl transferase inhibition. *Oncogene* **33,** 5442–5449 (2013).

231. Liu, M. *et al.* Targeting the protein prenyltransferases efficiently reduces tumor development in mice with K-RAS-induced lung cancer. *Proceedings of the*

National Academy of Sciences **107,** 6471–6476 (2010).

232. Desolms, S. J. *et al.* Dual Protein Farnesyltransferase−Geranylgeranyltransferase-I Inhibitors as Potential Cancer Chemotherapeutic Agents. *J. Med. Chem.* **46,** 2973–2984 (2003).

233. Lobell, R. B., Omer, C. A., Abrams, M. T. & Bhimnathwala, H. G. Evaluation of farnesyl: protein transferase and geranylgeranyl: protein transferase inhibitor combinations in preclinical models. *Cancer Research* (2001).

234. Lobell, R. B., Liu, D., Buser, C. A., Davide, J. P. & DePuy, E. Preclinical and clinical pharmacodynamic assessment of L-778,123, a dual inhibitor of farnesyl: protein transferase and geranylgeranyl: protein transferase type-I. *Mol. Cancer* (2002).

235. Zimmermann, G. *et al.* Small molecule inhibition of the KRAS–PDEδ interaction impairs oncogenic KRAS signalling. *Nature* **497,** 638–642 (2013).

236. Caunt, C. J., Sale, M. J., Smith, P. D. & Cook, S. J. MEK1 and MEK2 inhibitors and cancer therapy: the long and winding road. *Nat Rev Cancer* **15,** 577–592 (2015).

237. Lito, P., Rosen, N. & Solit, D. B. Tumor adaptation and resistance to RAF inhibitors. *Nat Med* **19,** 1401–1409 (2013).

238. Chapman, P. B. *et al.* Improved Survival with Vemurafenib in Melanoma with BRAF V600E Mutation. *N. Engl. J. Med.* **364,** 2507–2516 (2011).

239. Hauschild, A. *et al.* Dabrafenib in BRAF-mutated metastatic melanoma: a multicentre, open-label, phase 3 randomised controlled trial. *Lancet* **380,** 358–365 (2012).

240. Heidorn, S. J. *et al.* Kinase-dead BRAF and oncogenic RAS cooperate to drive tumor progression through CRAF. *Cell* **140,** 209–221 (2010).

241. Hatzivassiliou, G. *et al.* RAF inhibitors prime wild-type RAF to activate the MAPK pathway and enhance growth. *Nature* **464,** 431–435 (2010).

242. Poulikakos, P. I., Zhang, C., Bollag, G., Shokat, K. M. & Rosen, N. RAF inhibitors transactivate RAF dimers and ERK signalling in cells with wild-type BRAF. *Nature* **464,** 427–430 (2010).

243. Hall-Jackson, C. A. *et al.* Paradoxical activation of Raf by a novel Raf inhibitor. *Chem. Biol.* **6,** 559–568 (1999).

244. Zhang, C. *et al.* RAF inhibitors that evade paradoxical MAPK pathway activation. *Nature* **526,** 583–586 (2015).

245. Girotti, M. R. *et al.* Paradox-breaking RAF inhibitors that also target SRC are effective in drug-resistant BRAF mutant melanoma. *Cancer Cell* **27,** 85–96 (2015).

246. Flaherty, K. T. *et al.* Improved survival with MEK inhibition in BRAF-mutated melanoma. *N. Engl. J. Med.* **367,** 107–114 (2012).

247. Jänne, P. A. *et al.* Selumetinib plus docetaxel for KRAS-mutant advanced non-small-cell lung cancer: a randomised, multicentre, placebo-controlled, phase 2 study. *Lancet Oncol.* **14,** 38–47 (2013).

248. Infante, J. R. *et al.* Safety, pharmacokinetic, pharmacodynamic, and efficacy data for the oral MEK inhibitor trametinib: a phase 1 dose-escalation trial. *Lancet Oncol.* **13,** 773–781 (2012).

249. Blumenschein, G. *et al.* A randomized phase 2 study of the MEK1/MEK2 inhibitor trametinib (GSK1120212) compared with docetaxel in KRAS-mutant advanced non-small cell lung cancer (NSCLC). *Ann. Oncol.* (2015). doi:10.1093/annonc/mdv072

250. Ascierto, P. A. *et al.* MEK162 for patients with advanced melanoma harbouring NRAS or Val600 BRAF mutations: a non-randomised, open-label phase 2 study. *Lancet Oncol.* **14,** 249–256 (2013).

251. Carlino, M. S. *et al.* Differential activity of MEK and ERK inhibitors in BRAF inhibitor resistant melanoma. *Molecular Oncology* **8,** 544–554 (2014).

252. Castellano, E. *et al.* Requirement for Interaction of PI3-Kinase p110α with RAS in Lung Tumor Maintenance. *Cancer Cell* **24,** 617–630 (2013).

253. Lim, K.-H. & Counter, C. M. Reduction in the requirement of oncogenic Ras signaling to activation of PI3K/AKT pathway during tumor maintenance. *CCELL* **8,** 381–392 (2005).

254. Engelman, J. A. *et al.* Effective use of PI3K and MEK inhibitors to treat mutant Kras G12D and PIK3CA H1047R murine lung cancers. *Nat Med* **14,** 1351–1356 (2008).

255. Ihle, N. T. *et al.* Mutations in the phosphatidylinositol-3-kinase pathway predict for antitumor activity of the inhibitor PX-866 whereas oncogenic Ras is a dominant predictor for resistance. *Cancer Research* **69,** 143–150 (2009).

256. Shimizu, T. *et al.* The clinical effect of the dual-targeting strategy involving PI3K/AKT/mTOR and RAS/MEK/ERK pathways in patients with advanced cancer. *Clin. Cancer Res.* **18,** 2316–2325 (2012).

257. Do, K., Speranza, G., Bishop, R. & Khin, S. Biomarker-driven phase 2 study of MK-2206 and selumetinib (AZD6244, ARRY-142886) in patients with colorectal

cancer. *Investigational new …* (2015).

258. Kaelin, W. G. The Concept of Synthetic Lethality in the Context of Anticancer Therapy. *Nat Rev Cancer* **5,** 689–698 (2005).

259. Farmer, H. *et al.* Farmer et al. - 2005 - Targeting the DNA repair defect in BRCA mutant cells as a therapeutic strategy. *Oncogene* **434,** 917–921 (2005).

260. Bryant, H. E. *et al.* Specific killing of BRCA2-deficient tumours with inhibitors of poly(ADP-ribose) polymerase. *Nature* **434,** 913–917 (2005).

261. McCormick, F. KRAS as a Therapeutic Target. *Clin. Cancer Res.* **21,** 1797–1801 (2015).

262. Morgan-Lappe, S. E. *et al.* Identification of Ras-related nuclear protein, targeting protein for xenopus kinesin-like protein 2, and stearoyl-CoA desaturase 1 as promising cancer targets from an RNAi-based screen. *Cancer Research* **67,** 4390–4398 (2007).

263. Sarthy, A. V. *et al.* Survivin depletion preferentially reduces the survival of activated K-Ras-transformed cells. *Molecular Cancer Therapeutics* **6,** 269–276 (2007).

264. Luo, J. *et al.* A Genome-wide RNAi Screen Identifies Multiple Synthetic Lethal Interactions with the Ras Oncogene. *Cell* **137,** 835–848 (2009).

265. Fröhling, S. & Scholl, C. STK33 kinase is not essential in KRAS-dependent cells--letter. *Cancer Research* **71,** 7716–author reply 7717 (2011).

266. Babij, C. *et al.* STK33 Kinase Activity Is Nonessential in KRAS-Dependent Cancer Cells. *Cancer Research* **71,** 5818–5826 (2011).

267. Weïwer, M. *et al.* A Potent and Selective Quinoxalinone-Based STK33 Inhibitor Does Not Show Synthetic Lethality in KRAS-Dependent Cells. *ACS Med. Chem. Lett.* **3,** 1034–1038 (2012).

268. Scholl, C. *et al.* Synthetic lethal interaction between oncogenic KRAS dependency and STK33 suppression in human cancer cells. *Cell* **137,** 821–834 (2009).

269. Zhu, Z. *et al.* Inhibition of KRAS-driven tumorigenicity by interruption of an autocrine cytokine circuit. *Cancer Discovery* **4,** 452–465 (2014).

270. Vicent, S. *et al.* Wilms tumor 1 (WT1) regulates KRAS-driven oncogenesis and senescence in mouse and human models. *J. Clin. Invest.* **120,** 3940–3952 (2010).

271. Wang, Y. *et al.* Critical role for transcriptional repressor Snail2 in transformation

by oncogenic RAS in colorectal carcinoma cells. *Oncogene* **29,** 4658–4670 (2010).

272. Kumar, M. S. *et al.* The GATA2 Transcriptional Network Is Requisite for RAS Oncogene-Driven Non-Small Cell Lung Cancer. *Cell* **149,** 642–655 (2012).

273. Steckel, M. *et al.* Determination of synthetic lethal interactions in. *Cell Res* **22,** 1227–1245 (2012).

274. Singh, A. *et al.* TAK1 Inhibition Promotes Apoptosis in KRAS-Dependent Colon Cancers. *Cell* **148,** 639–650 (2012).

275. Beronja, S. *et al.* RNAi screens in mice identify physiological regulators of oncogenic growth. *Nature* **501,** 185–190 (2013).

276. Kim, H. S. *et al.* Systematic Identification of Molecular Subtype-Selective Vulnerabilities in Non-Small-Cell Lung Cancer. *Cell* **155,** 552–566 (2013).

277. Marcotte, R. *et al.* Essential Gene Profiles in Breast, Pancreatic, and Ovarian Cancer Cells. *Cancer Discovery* **2,** 172–189 (2012).

278. Cullis, J. *et al.* The RhoGEF GEF-H1 Is Required for Oncogenic RAS Signaling via KSR-1. *Cancer Cell* **25,** 181–195 (2014).

279. Corcoran, R. B. *et al.* Synthetic lethal interaction of combined BCL-XL and MEK inhibition promotes tumor regressions in KRAS mutant cancer models. *Cancer Cell* **23,** 121–128 (2013).

280. Gao, B. & Roux, P. P. Translational control by oncogenic signaling pathways. *Biochimica et Biophysica Acta (BBA) - Gene Regulatory Mechanisms* **1849,** 753–765 (2015).

281. Smith, D. *et al.* RAS mutation status and bortezomib therapy for relapsed multiple myeloma. *Br. J. Haematol.* **169,** 905–908 (2015).

282. Zhu, Z. *et al.* Inhibition of KRAS-driven tumorigenicity by interruption of an autocrine cytokine circuit. *Cancer Discovery* **4,** 452–465 (2014).

283. Druker, B. J. *et al.* Efficacy and safety of a specific inhibitor of the BCR-ABL tyrosine kinase in chronic myeloid leukemia. *N. Engl. J. Med.* **344,** 1031–1037 (2001).

284. Lynch, T. J. *et al.* Activating mutations in the epidermal growth factor receptor underlying responsiveness of non-small-cell lung cancer to gefitinib. *N. Engl. J. Med.* **350,** 2129–2139 (2004).

285. Baselga, J. *et al.* Phase II Trial of Pertuzumab and Trastuzumab in Patients With Human Epidermal Growth Factor Receptor 2-Positive Metastatic Breast Cancer

That Progressed During Prior Trastuzumab Therapy. *Journal of Clinical Oncology* **28,** 1138–1144 (2010).

286. Vogel, C. L. *et al.* Efficacy and safety of trastuzumab as a single agent in first-line treatment of HER2-overexpressing metastatic breast cancer. *J. Clin. Oncol.* **20,** 719–726 (2002).

287. Kwak, E. L. *et al.* Anaplastic lymphoma kinase inhibition in non-small-cell lung cancer. *N. Engl. J. Med.* **363,** 1693–1703 (2010).

288. Michor, F. *et al.* Dynamics of chronic myeloid leukaemia. *Oncogene* **435,** 1267–1270 (2005).

289. Garraway, L. A. & Janne, P. A. Circumventing Cancer Drug Resistance in the Era of Personalized Medicine. *Cancer Discovery* **2,** 214–226 (2012).

290. Daub, H., Specht, K. & Ullrich, A. Strategies to overcome resistance to targeted protein kinase inhibitors. *Nature Publishing Group* **3,** 1001–1010 (2004).

291. Azam, M., Latek, R. R. & Daley, G. Q. Mechanisms of autoinhibition and STI-571/imatinib resistance revealed by mutagenesis of BCR-ABL. *Cell* **112,** 831–843 (2003).

292. Bradeen, H. A. Comparison of imatinib mesylate, dasatinib (BMS-354825), and nilotinib (AMN107) in an N-ethyl-N-nitrosourea (ENU)-based mutagenesis screen: high efficacy of drug combinations. *Blood* **108,** 2332–2338 (2006).

293. Montagut, C. *et al.* Elevated CRAF as a potential mechanism of acquired resistance to BRAF inhibition in melanoma. *Cancer Research* **68,** 4853–4861 (2008).

294. Nazarian, R. *et al.* Melanomas acquire resistance to B-RAF(V600E) inhibition by RTK or N-RAS upregulation. *Nature* **468,** 973–977 (2010).

295. Villanueva, J. *et al.* Acquired Resistance to BRAF Inhibitors Mediated by a RAF Kinase Switch in Melanoma Can Be Overcome by Cotargeting MEK and IGF-1R/PI3K. *Cancer Cell* **18,** 683–695 (2010).

296. Poulikakos, P. I. *et al.* RAF inhibitor resistance is mediated by dimerization of aberrantly spliced BRAF(V600E). *Nature* **480,** 387–390 (2011).

297. Shalem, O. *et al.* Genome-scale CRISPR-Cas9 knockout screening in human cells. *Science* **343,** 84–87 (2014).

298. Yang, X. *et al.* A public genome-scale lentiviral expression library of human ORFs. *Nat Meth* **8,** 659–661 (2011).

299. Root, D. E., Hacohen, N., Hahn, W. C., Lander, E. S. & Sabatini, D. M. Genome-

scale loss-of-function screening with a lentiviral RNAi library. *Nat Meth* **3,** 715–719 (2006).

300. Konermann, S. *et al.* Genome-scale transcriptional activation by an engineered CRISPR-Cas9 complex. *Nature* **517,** 583–588 (2014).

301. Johannessen, C. M. *et al.* A melanocyte lineage program confers resistance to MAP kinase pathway inhibition. *Nature* **504,** 138–142 (2013).

302. Whittaker, S. R. *et al.* A genome-scale RNA interference screen implicates NF1 loss in resistance to RAF inhibition. *Cancer Discovery* **3,** 350–362 (2013).

303. Sharifnia, T. *et al.* Genetic modifiers of EGFR dependence in non-small cell lung cancer. *Proceedings of the National Academy of Sciences* **111,** 18661–18666 (2014).

304. Politi, K., Fan, P.-D., Shen, R., Zakowski, M. & Varmus, H. Erlotinib resistance in mouse models of epidermal growth factor receptor-induced lung adenocarcinoma. *Dis Model Mech* **3,** 111–119 (2010).

305. Lauchle, J. O. *et al.* Response and resistance to MEK inhibition in leukaemias initiated by hyperactive Ras. *Nature* **461,** 411–414 (2009).

306. Whittaker, S. *et al.* Gatekeeper Mutations Mediate Resistance to BRAF-Targeted Therapies. *Sci Transl Med* **2,** 35ra41–35ra41 (2010).

307. Johannessen, C. M. *et al.* COT drives resistance to RAF inhibition through MAP kinase pathway reactivation. *Nature* **468,** 968–972 (2010).

308. Wagle, N. *et al.* Dissecting therapeutic resistance to RAF inhibition in melanoma by tumor genomic profiling. *Journal of Clinical Oncology* **29,** 3085–3096 (2011).

309. Lin, L. *et al.* The Hippo effector YAP promotes resistance to RAF- and MEK-targeted cancer therapies. *Nat Genet* **47,** 250–256 (2015).

310. Sun, C. *et al.* Reversible and adaptive resistance to BRAF(V600E) inhibition in melanoma. *Nature* **508,** 118–122 (2014).

311. Corcoran, R. B. *et al.* EGFR-mediated re-activation of MAPK signaling contributes to insensitivity of BRAF mutant colorectal cancers to RAF inhibition with vemurafenib. *Cancer Discovery* **2,** 227–235 (2012).

312. Wagle, N. *et al.* MAP kinase pathway alterations in BRAF-mutant melanoma patients with acquired resistance to combined RAF/MEK inhibition. *Cancer Discovery* **4,** 61–68 (2014).

313. Van Allen, E. M. *et al.* The genetic landscape of clinical resistance to RAF inhibition in metastatic melanoma. *Cancer Discovery* **4,** 94–109 (2014).

314. Rizos, H. *et al.* BRAF Inhibitor Resistance Mechanisms in Metastatic Melanoma: Spectrum and Clinical Impact. *Clinical Cancer Research* **20,** 1965–1977 (2014).

315. Long, G. V. *et al.* Increased MAPK reactivation in early resistance to dabrafenib/trametinib combination therapy of BRAF-mutant metastatic melanoma. *Nat Commun* **5,** 5694 (2014).

316. Kobayashi, S. *et al.* EGFRMutation and Resistance of Non–Small-Cell Lung Cancer to Gefitinib. *N. Engl. J. Med.* **352,** 786–792 (2005).

317. Kosaka, T. *et al.* Analysis of epidermal growth factor receptor gene mutation in patients with non-small cell lung cancer and acquired resistance to gefitinib. *Clin. Cancer Res.* **12,** 5764–5769 (2006).

318. Engelman, J. A. *et al.* MET Amplification Leads to Gefitinib Resistance in Lung Cancer by Activating ERBB3 Signaling. *Science* **316,** 1039–1043 (2007).

319. Zhou, W. *et al.* Novel mutant-selective EGFR kinase inhibitors against EGFR T790M. *Nature* **462,** 1070–1074 (2009).

320. Engelman, J. A. *et al.* PF00299804, an Irreversible Pan-ERBB Inhibitor, Is Effective in Lung Cancer Models with EGFR and ERBB2 Mutations that Are Resistant to Gefitinib. *Cancer Research* **67,** 11924–11932 (2007).

321. Li, D. *et al.* BIBW2992, an irreversible EGFR/HER2 inhibitor highly effective in preclinical lung cancer models. *Oncogene* **27,** 4702–4711 (2008).

322. Nikolaev, S. I. *et al.* Exome sequencing identifies recurrent somatic MAP2K1 and MAP2K2 mutations in melanoma. *Nat Genet* **44,** 133–139 (2011).

323. Shi, H. *et al.* Melanoma whole-exome sequencing identifies (V600E)B-RAF amplification-mediated acquired B-RAF inhibitor resistance. *Nat Commun* **3,** 724 (2012).

324. Emery, C. M. *et al.* MEK1 mutations confer resistance to MEK and B-RAF inhibition. *Proceedings of the National Academy of Sciences* **106,** 20411–20416 (2009).

325. Hatzivassiliou, G. *et al.* ERK Inhibition Overcomes Acquired Resistance to MEK Inhibitors. *Molecular Cancer Therapeutics* **11,** 1143–1154 (2012).

326. Trunzer, K. *et al.* Pharmacodynamic Effects and Mechanisms of Resistance to Vemurafenib in Patients With Metastatic Melanoma. *Journal of Clinical Oncology* **31,** 1767–1774 (2013).

327. Morris, E. J. *et al.* Discovery of a novel ERK inhibitor with activity in models of acquired resistance to BRAF and MEK inhibitors. *Cancer Discovery* **3,** 742–750 (2013).

328. Villanueva, J. *et al.* Concurrent MEK2 Mutation and BRAF Amplification Confer Resistance to BRAF and MEK Inhibitors in Melanoma. *Cell Rep* **4,** 1090–1099 (2013).

329. Moriceau, G. *et al.* Tunable-combinatorial mechanisms of acquired resistance limit the efficacy of BRAF/MEK cotargeting but result in melanoma drug addiction. *Cancer Cell* **27,** 240–256 (2015).

330. Thakur, Das, M. *et al.* Modelling vemurafenib resistance in melanoma reveals a strategy to forestall drug resistance. *Nature* **494,** 251–255 (2013).

331. Shi, H. *et al.* Acquired resistance and clonal evolution in melanoma during BRAF inhibitor therapy. *Cancer Discovery* **4,** 80–93 (2014).

332. Antony, R., Emery, C. M., Sawyer, A. M. & Garraway, L. A. C-RAF mutations confer resistance to RAF inhibitors. *Cancer Research* **73,** 4840–4851 (2013).

333. Little, A. S. *et al.* Amplification of the driving oncogene, KRAS or BRAF, underpins acquired resistance to MEK1/2 inhibitors in colorectal cancer cells. *Science Signaling* **4,** ra17 (2011).

334. Corcoran, R. B. *et al.* BRAF Gene Amplification Can Promote Acquired Resistance to MEK Inhibitors in Cancer Cells Harboring the BRAF V600E Mutation. *Science Signaling* **3,** ra84–ra84 (2010).

335. Maertens, O. *et al.* Elucidating distinct roles for NF1 in melanomagenesis. *Cancer Discovery* **3,** 338–349 (2013).

336. Nissan, M. H. *et al.* Loss of NF1 in Cutaneous Melanoma Is Associated with RAS Activation and MEK Dependence. *Cancer Research* **74,** 2340–2350 (2014).

337. Lito, P. *et al.* Relief of Profound Feedback Inhibition of Mitogenic Signaling by RAF Inhibitors Attenuates Their Activity in BRAFV600E Melanomas. **22,** 668–682 (2012).

338. Hatzivassiliou, G. *et al.* Mechanism of MEK inhibition determines efficacy in mutant KRAS- versus BRAF-driven cancers. *Nature* **501,** 232–236 (2013).

339. Lito, P. *et al.* Disruption of CRAF-Mediated MEK Activation Is Required for Effective MEK Inhibition in KRAS Mutant Tumors. *Cancer Cell* **25,** 697–710 (2014).

340. Smalley, K. S. M. *et al.* Increased cyclin D1 expression can mediate BRAF inhibitor resistance in BRAF V600E-mutated melanomas. *Molecular Cancer Therapeutics* **7,** 2876–2883 (2008).

341. Franco, J., Witkiewicz, A. K. & Knudsen, E. S. CDK4/6 inhibitors have potent

activity in combination with pathway selective therapeutic agents in models of pancreatic cancer. *Oncotarget* **5,** 6512–6525 (2014).

342. Girotti, M. R. *et al.* Inhibiting EGF receptor or SRC family kinase signaling overcomes BRAF inhibitor resistance in melanoma. *Cancer Discovery* **3,** 158–167 (2013).

343. Duncan, J. S. *et al.* Dynamic reprogramming of the kinome in response to targeted MEK inhibition in triple-negative breast cancer. *Cell* **149,** 307–321 (2012).

344. Montero-Conde, C. *et al.* Relief of feedback inhibition of HER3 transcription by RAF and MEK inhibitors attenuates their antitumor effects in BRAF-mutant thyroid carcinomas. *Cancer Discovery* **3,** 520–533 (2013).

345. Straussman, R. *et al.* Tumour micro-environment elicits innate resistance to RAF inhibitors through HGF secretion. *Nature* **487,** 500–504 (2012).

346. Wilson, T. R. *et al.* Widespread potential for growth-factor-driven resistance to anticancer kinase inhibitors. *Nature* **487,** 505–509 (2012).

347. Prahallad, A. *et al.* Unresponsiveness of colon cancer to BRAF(V600E) inhibition through feedback activation of EGFR. *Oncogene* **483,** 100–103 (2012).

348. Mirzoeva, O. K. *et al.* Subtype-specific MEK-PI3 kinase feedback as a therapeutic target in pancreatic adenocarcinoma. *Molecular Cancer Therapeutics* **12,** 2213–2225 (2013).

349. Sun, C. *et al.* Intrinsic Resistance to MEK Inhibition in KRAS Mutant Lung and Colon Cancer through Transcriptional Induction of ERBB3. *Cell Rep* **7,** 86–93 (2014).

350. Marusiak, A. A. *et al.* Mixed lineage kinases activate MEK independently of RAF to mediate resistance to RAF inhibitors. *Nat Commun* **5,** – (2014).

351. Bid, H. K. *et al.* Development, Characterization, and Reversal of Acquired Resistance to the MEK1 Inhibitor Selumetinib (AZD6244) in an In Vivo Model of Childhood Astrocytoma. *Clinical Cancer Research* **19,** 6716–6729 (2013).

352. Halilovic, E. *et al.* PIK3CA Mutation Uncouples Tumor Growth and Cyclin D1 Regulation from MEK/ERK and Mutant KRAS Signaling. *Cancer Research* **70,** 6804–6814 (2010).

353. Paraiso, K. H. T. *et al.* PTEN Loss Confers BRAF Inhibitor Resistance to Melanoma Cells through the Suppression of BIM Expression. *Cancer Research* **71,** 2750–2760 (2011).

354. Xing, F. *et al.* Concurrent loss of the PTEN and RB1 tumor suppressors

attenuates RAF dependence in melanomas harboring (V600E)BRAF. *Oncogene* **31,** 446–457 (2012).

355. Lee, H.-J. *et al.* Drug resistance via feedback activation of Stat3 in oncogene-addicted cancer cells. *Cancer Cell* **26,** 207–221 (2014).

356. Konieczkowski, D. J. *et al.* A melanoma cell state distinction influences sensitivity to MAPK pathway inhibitors. *Cancer Discovery* **4,** 816–827 (2014).

357. Balmanno, K., Chell, S. D., Gillings, A. S., Hayat, S. & Cook, S. J. Intrinsic resistance to the MEK1/2 inhibitor AZD6244 (ARRY-142886) is associated with weak ERK1/2 signalling and/or strong PI3K signalling in colorectal cancer cell lines. *Int. J. Cancer* **125,** 2332–2341 (2009).

358. Doench, J. G. *et al.* Optimized sgRNA design to maximize activity and minimize off-target effects of CRISPR-Cas9. *Nature Biotechnology* (2016). doi:10.1038/nbt.3437

359. Hyman, D. M. *et al.* Vemurafenib in Multiple Nonmelanoma Cancers with BRAF V600 Mutations. *N. Engl. J. Med.* **373,** 726–736 (2015).

360. Shao, D. D. *et al.* KRAS and YAP1 Converge to Regulate EMT and Tumor Survival. *Cell* (2014). doi:10.1016/j.cell.2014.06.004

361. Kapoor, A. *et al.* Yap1 Activation Enables Bypass of Oncogenic Kras Addiction in Pancreatic Cancer. *Cell* (2014). doi:10.1016/j.cell.2014.06.003

362. Owens, D. M. & Keyse, S. M. Differential regulation of MAP kinase signalling by dual-specificity protein phosphatases. *Oncogene* **26,** 3203–3213 (2007).

363. Liu, X. *et al.* PTPN14 interacts with and negatively regulates the oncogenic function of YAP. *Oncogene* **32,** 1266–1273 (2013).

364. Levy, L. & Hill, C. S. Alterations in components of the TGF-beta superfamily signaling pathways in human cancer. *Cytokine Growth Factor Rev.* **17,** 41–58 (2006).

365. Uitdehaag, J. C. M. *et al.* Comparison of the Cancer Gene Targeting and Biochemical Selectivities of All Targeted Kinase Inhibitors Approved for Clinical Use. *PLoS ONE* **9,** e92146 (2014).

366. Doench, J. G. *et al.* Rational design of highly active sgRNAs for CRISPR-Cas9-mediated gene inactivation. *Nature Biotechnology* **32,** 1262–1267 (2014).

367. Paez, J. G. *et al.* EGFR mutations in lung cancer: correlation with clinical response to gefitinib therapy. *Science* **304,** 1497–1500 (2004).

368. Rosell, R. *et al.* Screening for Epidermal Growth Factor Receptor Mutations in

Lung Cancer. *N. Engl. J. Med.* **361,** 958–967 (2009).

369. Mok, T. S. *et al.* Gefitinib or Carboplatin–Paclitaxel in Pulmonary Adenocarcinoma. *N. Engl. J. Med.* **361,** 947–957 (2009).

370. Engelman, J. A. & Settleman, J. Acquired resistance to tyrosine kinase inhibitors during cancer therapy. *Curr. Opin. Genet. Dev.* **18,** 73–79 (2008).

371. Itoh, K., Mimura, J. & Yamamoto, M. Discovery of the negative regulator of Nrf2, Keap1: a historical overview. *Antioxid. Redox Signal.* **13,** 1665–1678 (2010).

372. Jaramillo, M. C. & Zhang, D. D. The emerging role of the Nrf2-Keap1 signaling pathway in cancer. *Genes & Development* **27,** 2179–2191 (2013).

373. Hayes, J. D. & Dinkova-Kostova, A. T. The Nrf2 regulatory network provides an interface between redox and intermediary metabolism. *Trends Biochem. Sci.* **39,** 199–218 (2014).

374. Mitsuishi, Y. *et al.* Nrf2 redirects glucose and glutamine into anabolic pathways in metabolic reprogramming. *Cancer Cell* **22,** 66–79 (2012).

375. DeNicola, G. M. *et al.* NRF2 regulates serine biosynthesis in non-small cell lung cancer. *Nat Genet* (2015). doi:10.1038/ng.3421

376. Sabharwal, S. S. & Schumacker, P. T. Mitochondrial ROS in cancer: initiators, amplifiers or an Achilles' heel? *Nat Rev Cancer* **14,** 709–721 (2014).

377. Trachootham, D. *et al.* Selective killing of oncogenically transformed cells through a ROS-mediated mechanism by beta-phenylethyl isothiocyanate. *CCELL* **10,** 241–252 (2006).

378. Trachootham, D., Alexandre, J. & Huang, P. Targeting cancer cells by ROS-mediated mechanisms: a radical therapeutic approach? *Nature Publishing Group* **8,** 579–591 (2009).

379. Schumacker, P. T. Reactive oxygen species in cancer cells: live by the sword, die by the sword. *CCELL* **10,** 175–176 (2006).

380. Hashemy, S. I., Ungerstedt, J. S., Avval, F. Z. & Holmgren, A. Motexafin Gadolinium, a Tumor-selective Drug Targeting Thioredoxin Reductase and Ribonucleotide Reductase. *Journal of Biological Chemistry* **281,** 10691–10697 (2006).

381. Conklin, K. A. Chemotherapy-associated oxidative stress: impact on chemotherapeutic effectiveness. *Integr Cancer Ther* **3,** 294–300 (2004).

382. Irani, K. *et al.* Mitogenic signaling mediated by oxidants in Ras-transformed fibroblasts. *Science* **275,** 1649–1652 (1997).

383. Kerr, E., Gaude, E., Turrell, F., Frezza, C. & Martins, C. P. Mutant Kras copy number defines metabolic reprogramming and therapeutic susceptibilities. (2016).

384. De Raedt, T. *et al.* Exploiting Cancer Cell Vulnerabilities to Develop a Combination Therapy for Ras-Driven Tumors. *Cancer Cell* **20,** 400–413 (2011).

385. Cancer Genome Atlas Research Network. Comprehensive genomic characterization of squamous cell lung cancers. *Nature* **489,** 519–525 (2012).

386. Mitsuishi, Y., Motohashi, H. & Yamamoto, M. The Keap1-Nrf2 system in cancers: stress response and anabolic metabolism. *Front Oncol* **2,** 200 (2012).

387. DeNicola, G. M. *et al.* Oncogene-induced Nrf2 transcription promotes ROS detoxification and tumorigenesis. *Nature* **475,** 106–109 (2011).

388. Rushworth, S. A. *et al.* The high Nrf2 expression in human acute myeloid leukemia is driven by NF-κB and underlies its chemo-resistance. *Blood* **120,** 5188–5198 (2012).

389. Solis, L. M. *et al.* Nrf2 and Keap1 Abnormalities in Non-Small Cell Lung Carcinoma and Association with Clinicopathologic Features. *Clinical Cancer Research* **16,** 3743–3753 (2010).

390. Wang, X.-J. *et al.* Nrf2 enhances resistance of cancer cells to chemotherapeutic drugs, the dark side of Nrf2. *Carcinogenesis* **29,** 1235–1243 (2008).

391. Jiang, T. *et al.* High levels of Nrf2 determine chemoresistance in type II endometrial cancer. *Cancer Research* **70,** 5486–5496 (2010).

392. Singh, A. *et al.* RNAi-mediated silencing of nuclear factor erythroid-2-related factor 2 gene expression in non-small cell lung cancer inhibits tumor growth and increases efficacy of chemotherapy. *Cancer Research* **68,** 7975–7984 (2008).

393. Kim, H.-R. *et al.* Suppression of Nrf2-driven heme oxygenase-1 enhances the chemosensitivity of lung cancer A549 cells toward cisplatin. *Lung Cancer* **60,** 47–56 (2008).

394. Ohta, T. *et al.* Loss of Keap1 function activates Nrf2 and provides advantages for lung cancer cell growth. *Cancer Research* **68,** 1303–1309 (2008).

395. Shibata, T. *et al.* Cancer related mutations in NRF2 impair its recognition by Keap1-Cul3 E3 ligase and promote malignancy. *Proceedings of the National Academy of Sciences* **105,** 13568–13573 (2008).

396. Nogueira, V. & Hay, N. Molecular pathways: reactive oxygen species homeostasis in cancer cells and implications for cancer therapy. *Clin. Cancer Res.* **19,** 4309–4314 (2013).

397. Schafer, F. Q. & Buettner, G. R. Redox environment of the cell as viewed through the redox state of the glutathione disulfide/glutathione couple. *Free Radic. Biol. Med.* **30,** 1191–1212 (2001).

398. Bailey, H. H. *et al.* Phase I clinical trial of intravenous L-buthionine sulfoximine and melphalan: an attempt at modulation of glutathione. *J. Clin. Oncol.* **12,** 194–205 (1994).

399. Bailey, H. H. *et al.* Phase I study of continuous-infusion L-S,R-buthionine sulfoximine with intravenous melphalan. *J. Natl. Cancer Inst.* **89,** 1789–1796 (1997).

400. O'Dwyer, P. J. *et al.* Phase I trial of buthionine sulfoximine in combination with melphalan in patients with cancer. *J. Clin. Oncol.* **14,** 249–256 (1996).

401. Hugo, W. *et al.* Non-genomic and Immune Evolution of Melanoma Acquiring MAPKi Resistance. *Cell* **162,** 1271–1285 (2015).

402. Jiménez, G., Guichet, A., Ephrussi, A. & Casanova, J. Relief of gene repression by torso RTK signaling: role of capicua in Drosophila terminal and dorsoventral patterning. *Genes & Development* **14,** 224–231 (2000).

403. Dissanayake, K. *et al.* ERK/p90(RSK)/14-3-3 signalling has an impact on expression of PEA3 Ets transcription factors via the transcriptional repressor capicúa. *Biochem. J.* **433,** 515–525 (2011).

404. Astigarraga, S. *et al.* A MAPK docking site is critical for downregulation of Capicua by Torso and EGFR RTK signaling. *The EMBO Journal* **26,** 668–677 (2007).

405. Lam, Y. C. *et al.* ATAXIN-1 interacts with the repressor Capicua in its native complex to cause SCA1 neuropathology. *Cell* **127,** 1335–1347 (2006).

406. Jiménez, G., Shvartsman, S. Y. & Paroush, Z. The Capicua repressor--a general sensor of RTK signaling in development and disease. *J. Cell. Sci.* **125,** 1383–1391 (2012).

407. Crespo-Barreto, J., Fryer, J. D., Shaw, C. A., Orr, H. T. & Zoghbi, H. Y. Partial loss of ataxin-1 function contributes to transcriptional dysregulation in spinocerebellar ataxia type 1 pathogenesis. *PLoS Genet* **6,** e1001021 (2010).

408. Lee, Y. *et al.* ATXN1 protein family and CIC regulate extracellular matrix remodeling and lung alveolarization. *Developmental Cell* **21,** 746–757 (2011).

409. Bowman, A. B. *et al.* Duplication of Atxn1l suppresses SCA1 neuropathology by decreasing incorporation of polyglutamine-expanded ataxin-1 into native complexes. *Nat Genet* **39,** 373–379 (2007).

410. Brinkman, E. K., Chen, T., Amendola, M. & van Steensel, B. Easy quantitative assessment of genome editing by sequence trace decomposition. *Nucleic Acids Research* **42,** e168 (2014).

411. Yoon, S. & Seger, R. The extracellular signal-regulated kinase: multiple substrates regulate diverse cellular functions. *Growth Factors* **24,** 21–44 (2006).

412. Porfiri, E. & McCormick, F. Regulation of epidermal growth factor receptor signaling by phosphorylation of the ras exchange factor hSOS1. *J. Biol. Chem.* **271,** 5871–5877 (1996).

413. Dougherty, M. K. *et al.* Regulation of Raf-1 by Direct Feedback Phosphorylation. *Molecular Cell* **17,** 215–224 (2005).

414. Ritt, D. A., Monson, D. M., Specht, S. I. & Morrison, D. K. Impact of feedback phosphorylation and Raf heterodimerization on normal and mutant B-Raf signaling. *Molecular and Cellular Biology* **30,** 806–819 (2010).

415. Li, X., Huang, Y., Jiang, J. & Frank, S. J. ERK-dependent threonine phosphorylation of EGF receptor modulates receptor downregulation and signaling. *Cellular Signalling* **20,** 2145–2155 (2008).

416. Buday, L., Warne, P. H. & Downward, J. Downregulation of the Ras activation pathway by MAP kinase phosphorylation of Sos. *Oncogene* **11,** 1327–1331 (1995).

417. Kim, H. J. & Bar-Sagi, D. Modulation of signalling by Sprouty: a developing story. *Nat Rev Mol Cell Biol* **5,** 441–450 (2004).

418. Jin, Y. *et al.* EGFR/Ras Signaling Controls Drosophila Intestinal Stem Cell Proliferation via Capicua-Regulated Genes. *PLoS Genet* **11,** e1005634 (2015).

419. Bettegowda, C. *et al.* Mutations in CIC and FUBP1 contribute to human oligodendroglioma. *Science* **333,** 1453–1455 (2011).

420. Padul, V., Epari, S., Moiyadi, A., Shetty, P. & Shirsat, N. V. ETV/Pea3 family transcription factor-encoding genes are overexpressed in CIC-mutant oligodendrogliomas. *Genes Chromosomes Cancer* (2015). doi:10.1002/gcc.22283

421. Kawamura-Saito, M. *et al.* Fusion between CIC and DUX4 up-regulates PEA3 family genes in Ewing-like sarcomas with t(4;19)(q35;q13) translocation. *Human Molecular Genetics* **15,** 2125–2137 (2006).

422. Wertz, I. E. *et al.* Human De-etiolated-1 regulates c-Jun by assembling a CUL4A ubiquitin ligase. *Science* **303,** 1371–1374 (2004).

423. Baert, J.-L. *et al.* The E3 ubiquitin ligase complex component COP1 regulates

PEA3 group member stability and transcriptional activity. *Oncogene* **29,** 1810–1820 (2010).

424. Vitari, A. C. *et al.* COP1 is a tumour suppressor that causes degradation of ETS transcription factors. *Nature* **474,** 403–406 (2011).

425. Bianchi, E. *et al.* Characterization of human constitutive photomorphogenesis protein 1, a RING finger ubiquitin ligase that interacts with Jun transcription factors and modulates their transcriptional activity. *J. Biol. Chem.* **278,** 19682–19690 (2003).

426. Tong, X. *et al.* Ataxin-1 and Brother of ataxin-1 are components of the Notch signalling pathway. *EMBO Rep* **12,** 428–435 (2011).

427. Boussemart, L. *et al.* eIF4F is a nexus of resistance to anti-BRAF and anti-MEK cancer therapies. *Nature* **513,** 105–109 (2014).

428. Pop, M. S. *et al.* A Small Molecule That Binds and Inhibits the ETV1 Transcription Factor Oncoprotein. *Molecular Cancer Therapeutics* **13,** 1492–1502 (2014).

429. Weinstein, I. B. & Joe, A. Oncogene addiction. *Cancer Research* **68,** 3077–80–discussion 3080 (2008).